frontiers | Research Topics

Local ablative therapies for the management of lung cancer

Edited by
Xin Ye, Yuliang Li and Roberto Iezzi

Published in
Frontiers in Oncology

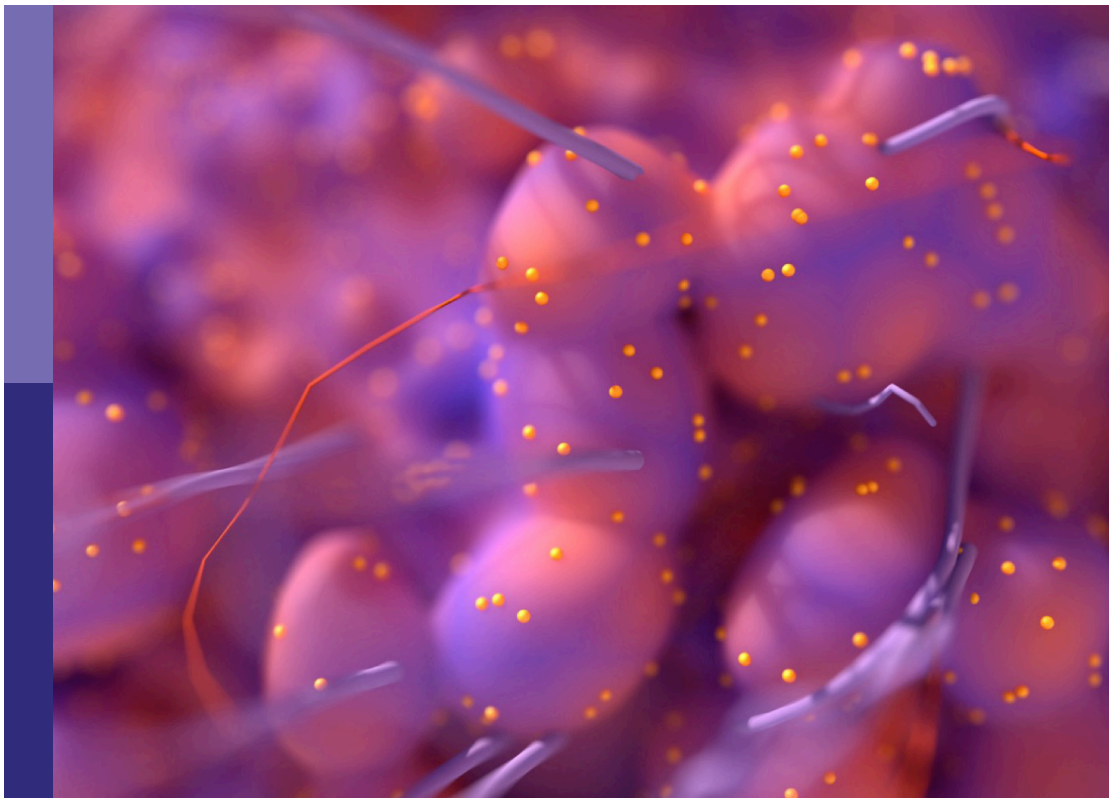

ISSN 1664-8714
ISBN 978-2-83251-811-3
DOI 10.3389/978-2-83251-811-3

About Frontiers

Frontiers is more than just an open access publisher of scholarly articles: it is a pioneering approach to the world of academia, radically improving the way scholarly research is managed. The grand vision of Frontiers is a world where all people have an equal opportunity to seek, share and generate knowledge. Frontiers provides immediate and permanent online open access to all its publications, but this alone is not enough to realize our grand goals.

Frontiers journal series

The Frontiers journal series is a multi-tier and interdisciplinary set of open-access, online journals, promising a paradigm shift from the current review, selection and dissemination processes in academic publishing. All Frontiers journals are driven by researchers for researchers; therefore, they constitute a service to the scholarly community. At the same time, the *Frontiers journal series* operates on a revolutionary invention, the tiered publishing system, initially addressing specific communities of scholars, and gradually climbing up to broader public understanding, thus serving the interests of the lay society, too.

Dedication to quality

Each Frontiers article is a landmark of the highest quality, thanks to genuinely collaborative interactions between authors and review editors, who include some of the world's best academicians. Research must be certified by peers before entering a stream of knowledge that may eventually reach the public - and shape society; therefore, Frontiers only applies the most rigorous and unbiased reviews. Frontiers revolutionizes research publishing by freely delivering the most outstanding research, evaluated with no bias from both the academic and social point of view. By applying the most advanced information technologies, Frontiers is catapulting scholarly publishing into a new generation.

What are Frontiers Research Topics?

Frontiers Research Topics are very popular trademarks of the *Frontiers journals series*: they are collections of at least ten articles, all centered on a particular subject. With their unique mix of varied contributions from Original Research to Review Articles, Frontiers Research Topics unify the most influential researchers, the latest key findings and historical advances in a hot research area.

Find out more on how to host your own Frontiers Research Topic or contribute to one as an author by contacting the Frontiers editorial office: frontiersin.org/about/contact

Local ablative therapies for the management of lung cancer

Topic editors

Xin Ye — Shandong Provincial Qianfoshan Hospital, China

Yuliang Li — The Second Hospital of Shandong University, China

Roberto Iezzi — Agostino Gemelli University Polyclinic (IRCCS), Italy

Citation

Ye, X., Li, Y., Iezzi, R., eds. (2023). *Local ablative therapies for the management of lung cancer*. Lausanne: Frontiers Media SA. doi: 10.3389/978-2-83251-811-3

Table of contents

frontiers | Frontiers in Oncology

TYPE Editorial
PUBLISHED 16 February 2023
DOI 10.3389/fonc.2023.1160932

OPEN ACCESS

EDITED AND REVIEWED BY
Lizza E. L. Hendriks,
Maastricht University Medical Centre,
Netherlands

*CORRESPONDENCE
Roberto Iezzi
roberto.iezzi.md@gmail.com
Xin Ye
yexintaian2020@163.com

SPECIALTY SECTION
This article was submitted to Thoracic Oncology, a section of the journal Frontiers in Oncology

RECEIVED 07 February 2023
ACCEPTED 09 February 2023
PUBLISHED 16 February 2023

CITATION
Wei Z, Iezzi R and Ye X (2023) Editorial: Local ablative therapies for the management of lung cancer. *Front. Oncol.* 13:1160932. doi: 10.3389/fonc.2023.1160932

Editorial: Local ablative therapies for the management of lung cancer

Zhigang Wei[1], Roberto Iezzi[2,3]* and Xin Ye[1]*

[1]Department of Oncology, The First Affiliated Hospital of Shandong First Medical University & Shandong Provincial Qianfoshan Hospital, Shandong Lung Cancer Institute, Shandong Key Laboratory of Rheumatic Disease and Translational Medicine, Jinan, China, [2]Department of Diagnostic Imaging, Oncologic Radiotherapy and Hematology-A. Gemelli University Hospital Foundation IRCCS, Rome, Italy, [3]Istituto di Radiodiagnostica, Università Cattolica del Sacro Cuore, Rome, Italy

KEYWORDS

lung cancer, metastases, ablation, MRI, combination

Editorial on the Research Topic
Local ablative therapies for the management of lung cancer

Lung cancer, the leading cause of cancer related death in China and worldwide (1, 2), were comprised of non-small cell lung cancer (NSCLC) and small cell lung cancer (SCLC), and the former account for nearly 85% (3). Furthermore, lungs have become the second most common metastatic site after liver, having a great impact on patient management and outcome (4). Therefore, the diagnosis and treatment of primary and secondary lung tumors deserves high emphasis.

For early-stage NSCLC and for some lung metastases, radical surgery usually represents the main treatment method; in unsurgical patients, percutaneous image-guided thermal ablation, such as radiofrequency ablation (RFA), microwave ablation (MWA) and cryoablation, has been increasingly applied as a safe, cost- effective, and precise minimally invasive alternative treatment methods (5).

Based on recent technical developments and new combinations of systemic and local therapy, we recognized the topic of "Local Ablative Therapies for The Management of Lung Cancer" in Frontiers of Oncology.

Primary lung cancer

Recently with application of low dose CT (LDCT), more patients with ground-glass nodules (GGNs) were identified and part GGNs progress to GGN-like lung adenocarcinoma. Although surgery was the main treatment regimen for those patients, MWA have being proved to be another radical treatment option (6, 7). However, up to date, no study explored the cost and effectiveness of microwave ablation versus video-assisted thoracoscopic surgical (VATS) resection for GGN-like lung adenocarcinoma. Han et al. verified that MWA had similar 3-year overall survival (OS) rate and a dramatically lower cost and shorter hospital stay compared with VATS. So based on efficacy and cost, MWA could provide an alternative treatment option for patients with GGN-like lung adenocarcinoma.

Although MWA was mainly applied in early-stage NSCLC, for locally advanced or metastatic NSCLC patients, MWA in combination with other treatments could also improve survival in the study. Based on the SEER database, Yang et al. verified that MWA improved both OS and cancer specific survival (CSS) for patients with stage II to III NSCLC, which indicating MWA maybe an alternative treatment for those unfit for radical surgery.

For advanced and standard treatments-refractory NSCLC patients, local treatment of drug-eluting beads bronchial arterial chemoembolization (DEB-BACE) could be an option (8, 9), also for treating complications. When DEB-BACE was combined with MWA, superior ORR and longer PFS were achieved as showed by Xu et al. Other combination treatment regimens such as DEB-BACE plus targeted therapy of anlotinb or iodine-125 brachytherapy also showed response and survival advantage (10, 11). The combination of systematic treatments of chemotherapy with local treatment such as radiotherapy and interventional embolization could achieve superior survival advantage. Zhou et al. reported a partial response after combined treatment in a squamous cell unresectable lung cancer was also achieved.

The treatments for advanced NSCLC range from routine chemotherapy to novel targeted therapy and immunotherapy (12). Immunotherapy targeting immune checkpoint (IC) especially anti-programmed death-1 (PD-1) and programmed death-ligand 1(PD-L1) antibodies have changed the treatment regimens of metastatic NSCLC. However, the relatively low response rate of immunotherapy monotherapy limits its application. Our previous study verified that PD-1 antibody combined with MWA could improve ORR (13). We further explored the MWA plus camrelizumab (a PD-1 inhibitor) monotherapy or camrelizumab combination therapy in NSCLC. The ORR was 29.9% and the PFS was 11.8 months. All these studies indicate the potential synergetic effect of MWA and PD-1 antibody.

New perspectives could also be focused on local drug injection, that could also be combined to locoregional treatments, highlighting apoptotic effects, as reported in early-stage NSCLC with the combination of RFA and intratumoral chemotherapy (14, 15). Huang et al. explored the combination of MWA and intratumoral chemotherapy and a median PFS of 8.1 months was achieved.

Pulmonary metastases

Pulmonary metastases from colorectal cancer (CRC) were commonly observed in clinical practice. Local treatments such as MWA was proved to be an effective treatment in oligometastases disease (16, 17). Han et al. conducted a long-term follow up of patients with CRC pulmonary metastases underwent MWA, the median OS was 76 months and the 5-year survival rate reached as high as 51.6%. The application of MWA provided long-term survival benefit for CRC pulmonary metastases.

Technical aspects

MWA is mainly performed under CT-guidance. In the last years, other image-guidance modalities were also explored. Cone-beam computed tomography (CBCT) has already been referred to several applications in interventional oncology such as renal cancer and osteoid osteoma (18, 19). It allows 3D images on a selected volume to be produced usually with a relatively small field of view (FOV). Wang et al. explored CBCT-assisted secondary pulmonary tumors ablation and verified that CBCT guided thermal ablation and helical tomotherapy provided comparable clinical effects and safety.

MR-guided MWA for lung malignant tumor could also be another option, just previously explored in rabbits (20, 21). Lin et al. firstly explored the efficacy and safety of MR-guided MWA for lung cancer and showed that the treatment was feasible and efficient. It could be a new guided method for lung cancer patients, even if its applications is limited by the longer procedural time and needed of dedicated devices. From a technical point of view, artificial pneumothorax and artificial hydrothorax were the common applied techniques to treat patients with tumors localized in the subpleural zone (22, 23). To show the effective puncture path and to obtain a sufficient safety margin, combination of artificial pneumothorax and artificial hydrothorax could improve the safety and the complete ablation rate, reducing procedural complications also in the treatment of lung cancer adjacent to vital organs.

Intraprocedural management

Besides assistance of artificial pneumothorax and artificial hydrothorax, another treatment regimen for patients with tumors localized in the subpleural those patients could be a local pleural anesthesia (24), that can also reduce the patient's pain and complications.

Thoracic Paravertebral Block (TPB) is generally used in thoracoscopic surgery as a major anesthesia method (25). When a single ultrasound-guided TPB with a large volume of anesthetic is applied during MWA procedure, an effective analgesia can be achieved. This technique allows to increase patient collaboration in order to reduce multiple lung punctures and consequent associated injury.

Image evaluation

A topic that could be interesting in the treatment of lung tumors with MWA is also represented by the ability to predict and evaluate the treatment efficacy. In detail, apparent diffusion coefficient (ADC) of MRI calculated 24 hours after MWA of lung cancer could be effectively used to predict the early treatment efficacy (20).

Furthermore, Chen et al. showed MRI manifestations of thermal ablation in VX2 tumor of rabbit lung have certain characteristics with strong pathological association. CT combined with MRI multimodal radiomics could also provide an effective new method for clinical evaluation of the immediate efficacy of thermal ablation of lung tumors.

Conclusions

Locoregional ablative therapies are minimally invasive procedures with an emerging and increasing role for the management of primary and secondary lung tumours.

Factors that could contribute to increase safety and efficacy include a thorough knowledge of new devices and techniques, as well as imaging-guiding modalities, assistive techniques for percutaneous treatment, and the role of prediction and follow-up. Furthermore, combination of percutaneous treatment option, as MWA, with other treatments could also allow a significant improvement of oncological outcomes in patients with both primary and secondary lung cancers.

Author contributions

All authors listed have made a substantial, direct, and intellectual contribution to the work and approved it for publication.

Conflict of interest

The authors declare that the research was conducted in the absence of any commercial or financial relationships that could be construed as a potential conflict of interest.

Publisher's note

References

1. Xia C, Dong X, Li H, Cao M, Sun D, He S, et al. Cancer statistics in China and united states, 2022: Profiles, trends, and determinants. *Chin Med J (Engl)* (2022) 135 (5):584–90. doi: 10.1097/CM9.0000000000002108

2. Oliver AL. Lung cancer: Epidemiology and screening. *Surg Clin North Am* (2022) 102(3):335–44. doi: 10.1016/j.suc.2021.12.001

3. Molina JR, Yang P, Cassivi SD, Schild SE, Adjei AA. Non-small cell lung cancer: Epidemiology, risk factors, treatment, and survivorship. *Mayo Clinic Proc* (2008) 83:584–94. doi: 10.4065/83.5.584

4. Zhang GQ, Taylor JP, Stem M, Almaazmi H, Efron JE, Atallah C, et al. Aggressive multimodal treatment and metastatic colorectal cancer survival. *J Am Coll Surgeons* (2020) 230(4):689–98. doi: 10.1016/j.jamcollsurg.2019.12.024

5. Ye X, Fan W, Wang Z, Wang J, Wang H, Niu L, et al. Clinical practice guidelines on image-guided thermal ablation of primary and metastatic lung tumors (2022 edition). *J Cancer Res Ther* (2022) 18(5):1213–30. doi: 10.4103/jcrt.jcrt_880_22

6. Huang G, Yang X, Li W, Wang J, Han X, Wei Z, et al. A feasibility and safety study of computed tomography-guided percutaneous microwave ablation: A novel therapy for multiple synchronous ground-glass opacities of the lung. *Int J Hyperthermia* (2020) 37(1):414–22. doi: 10.1080/02656736.2020.1756467

7. Yang X, Ye X, Lin Z, Jin Y, Zhang K, Dong Y, et al. Computed tomography-guided percutaneous microwave ablation for treatment of peripheral ground-glass opacity-lung adenocarcinoma: A pilot study. *J Cancer Res Ther* (2018) 14(4):764–71. doi: 10.4103/jcrt.JCRT_269_18

8. Bi Y, Li F, Ren J, Han X. The safety and efficacy of oxaliplatin-loaded drug-eluting beads transarterial chemoembolization for the treatment of unresectable or advanced lung cancer. *Front Pharmacol* (2022) 13:1079707. doi: 10.3389/fphar.2022.1079707

9. Ma X, Zheng D, Zhang J, Dong Y, Li L, Jie B, et al. Clinical outcomes of vinorelbine loading CalliSpheres beads in the treatment of previously treated advanced lung cancer with progressive refractory obstructive atelectasis. *Front Bioeng Biotechnol* (2022) 10:1088274. doi: 10.3389/fbioe.2022.1088274

10. Liu J, Zhang W, Ren J, Li Z, Lu H, Sun Z, et al. Efficacy and safety of drug-eluting bead bronchial arterial chemoembolization plus anlotinib in patients with advanced non-small-Cell lung cancer. *Front Cell Dev Biol* (2021) 9:768943. doi: 10.3389/fcell.2021.768943

11. Chen C, Wang W, Yu Z, Tian S, Li Y, Wang Y. Combination of computed tomography-guided iodine-125 brachytherapy and bronchial arterial chemoembolization for locally advanced stage III non-small cell lung cancer after failure of concurrent chemoradiotherapy. *Lung Cancer* (2020) 146:290–6. doi: 10.1016/j.lungcan.2020.06.010

12. Wang M, Herbst RS, Boshoff C. Toward personalized treatment approaches for non-small-cell lung cancer. *Nat Med* (2021) 27(8):1345–56. doi: 10.1038/s41591-021-01450-2

13. Wei Z, Yang X, Ye X, Huang G, Li W, Han X, et al. Camrelizumab combined with microwave ablation improves the objective response rate in advanced non-small cell lung cancer. *J Cancer Res Ther* (2019) 15(7):1629–34. doi: 10.4103/jcrt.JCRT_990_19

14. Hohenforst-Schmidt W, Zarogoulidis P, Stopek J, Kosmidis E, Vogl T, Linsmeier B. Enhancement of intratumoral chemotherapy with cisplatin with or without microwave ablation and lipiodol. future concept for local treatment in lung cancer. *J Cancer* (2015) 6(3):218–26. doi: 10.7150/jca.10970

15. Feng W, Li J, Han S, Tang J, Yao J, Cui Y, et al. CT guided radiofrequency ablation followed intratumoral chemotherapy in the treatment of early stage non-small cell lung cancer. *Zhongguo Fei Ai Za Zhi* (2016) 19(5):269–78. doi: 10.3779/j.issn.1009-3419.2016.05.04. Chinese.

16. Vogl TJ, Naguib NN, Gruber-Rouh T, Koitka K, Lehnert T, Nour-Eldin NE. Microwave ablation therapy: Clinical utility in treatment of pulmonary metastases. *Radiology* (2011) 261(2):643–51. doi: 10.1148/radiol.11101643

17. de Baere T, Tselikas L, Yevich S, Boige V, Deschamps F, Ducreux M, et al. The role of image-guided therapy in the management of colorectal cancer metastatic disease. *Eur J Cancer* (2017) 75:231–42. doi: 10.1016/j.ejca.2017.01.010

18. Monfardini L, Gennaro N, Della Vigna P, Bonomo G, Varano G, Maiettini D, et al. Cone-beam CT-assisted ablation of renal tumors: Preliminary results. *Cardiovasc Intervent Radiol* (2019) 42(12):1718–25. doi: 10.1007/s00270-019-02296-5

19. Perry BC, Monroe EJ, McKay T, Kanal KM, Shivaram G. Pediatric percutaneous osteoid osteoma ablation: Cone-beam CT with fluoroscopic overlay versus conventional CT guidance. *Cardiovasc Intervent Radiol* (2017) 40(10):1593–9. doi: 10.1007/s00270-017-1685-2

20. Vogl TJ, Emara EH, Elhawash E, Naguib NNN, Aboelezz MO, Abdelrahman HM, et al. Feasibility of diffusion-weighted magnetic resonance imaging in evaluation of early therapeutic response after CT-guided microwave ablation of inoperable lung neoplasms. *Eur Radiol* (2022) 32(5):3288–96. doi: 10.1007/s00330-021-08387-7

21. Chen J, Lin XN, Miao XH, Chen J, Lin RX, Su HY, et al. Evaluation of the correlation between infrared thermal imaging-magnetic resonance imaging-pathology of microwave ablation of lesions in rabbit lung tumors. *J Cancer Res Ther* (2020) 16 (5):1129–33. doi: 10.4103/0973-1482.296428

22. Jia H, Tian J, Liu B, Meng H, Pan F, Li C. Efficacy and safety of artificial pneumothorax with position adjustment for CT-guided percutaneous transthoracic microwave ablation of small subpleural lung tumors. *Thorac Cancer* (2019) 10(8):1710–6. doi: 10.1111/1759-7714.13137

23. Hou X, Zhuang X, Zhang H, Wang K, Zhang Y. Artificial pneumothorax: a safe and simple method to relieve pain during microwave ablation of subpleural lung malignancy. *Minim Invasive Ther Allied Technol* (2017) 26(4):220–6. doi: 10.1080/13645706.2017.1287089

24. Gorgos AB, Ferraro P, Chalaoui J, Prenovault J, Le SM, Chartrand-Lefebvre C. Percutaneous CT-guided lung interventions-local pleural anesthesia. *Clin Imaging* (2015) 39(6):1024–6. doi: 10.1016/j.clinimag.2015.07.029

25. Turhan ÖChecktae, Sivrikoz N, Sungur Z, Duman S, Özkan B, Şentürk M. Thoracic paravertebral block achieves better pain control than erector spinae plane block and intercostal nerve block in thoracoscopic surgery: A randomized study. *J Cardiothorac Vasc Anesth* (2021) 35(10):2920–7. doi: 10.1053/j.jvca.2020.11.034

frontiers in Oncology

ORIGINAL RESEARCH
published: 15 March 2022
doi: 10.3389/fonc.2022.851830

Drug-Eluting Bead Bronchial Arterial Chemoembolization With and Without Microwave Ablation for the Treatment of Advanced and Standard Treatment-Refractory/Ineligible Non-Small Cell Lung Cancer: A Comparative Study

*Sheng Xu[1,2], Zhi-Xin Bie[1], Yuan-Ming Li[1], Bin Li[1], Fan-Lei Kong[1,2], Jin-Zhao Peng[1,2] and Xiao-Guang Li[1,2]**

[1] Department of Minimally Invasive Tumor Therapies Center, Beijing Hospital, National Center of Gerontology, Institute of Geriatric Medicine, Chinese Academy of Medical Sciences, Beijing, China, [2] Graduate School of Peking Union Medical College, Chinese Academy of Medical Sciences, Beijing, China

OPEN ACCESS

Edited by:
Xin Ye,
Shandong University, China

Reviewed by:
Janaki Deepak,
University of Maryland, Baltimore, United States
Bin-Yan Zhong,
The First Affiliated Hospital of Soochow University, China

***Correspondence:**
Xiao-Guang Li
xglee88@126.com

Specialty section:
This article was submitted to Thoracic Oncology, a section of the journal Frontiers in Oncology

Received: 10 January 2022
Accepted: 17 February 2022
Published: 15 March 2022

Citation:
Xu S, Bie Z-X, Li Y-M, Li B, Kong F-L, Peng J-Z and Li X-G (2022) Drug-Eluting Bead Bronchial Arterial Chemoembolization With and Without Microwave Ablation for the Treatment of Advanced and Standard Treatment-Refractory/Ineligible Non-Small Cell Lung Cancer: A Comparative Study. Front. Oncol. 12:851830. doi: 10.3389/fonc.2022.851830

Purpose: To compare the outcomes of drug-eluting bead bronchial arterial chemoembolization (DEB-BACE) with and without microwave ablation (MWA) for the treatment of advanced and standard treatment-refractory/ineligible non-small cell lung cancer (ASTRI-NSCLC).

Materials and Methods: A total of 77 ASTRI-NSCLC patients who received DEB-BACE combined with MWA (group A; n = 28) or DEB-BACE alone (group B; n = 49) were included. Clinical outcomes were compared between groups A and B. Kaplan–Meier methods were used to compare the median progression-free survival (PFS) or overall survival (OS) between the two groups. Univariate and multivariate Cox proportional hazards analyses were used to investigate the predictors of OS for ASTRI-NSCLC treated with DEB-BACE.

Results: No severe adverse event was found in both groups. Pneumothorax was the predominant MWA-related complication in group A, with an incidence rate of 32.1% (9/28). Meanwhile, no significant difference was found in DEB-BACE-related complications between groups A and B. The overall disease control rate (DCR) was 61.0% (47/77), with a significantly higher DCR in group A (85.7% vs. 46.9%, $P = 0.002$). The median PFS in groups A and B was 7.0 and 4.0 months, respectively, with a significant difference ($P = 0.037$). The median OS in groups A and B was both 8.0 months, with no significant difference ($P = 0.318$). The 6-month PFS and OS rates in groups A and B were 75.0% and 78.6%, 22.4% and 59.2%, respectively, while the 12-month PFS and OS rates in groups A and B were 17.9% and 28.6%, 14.3% and 22.4%, respectively. Of these, a significantly higher 6-month PFS rate was found in group A (75.0% vs. 22.4%; $P < 0.001$). The cycles

of DEB-BACE/bronchial artery infusion chemotherapy [hazard ratio (HR): 0.363; 95% confidence interval (CI): 0.202–0.655; $P = 0.001$] and postoperative immunotherapy (HR: 0.219; 95% CI: 0.085–0.561; $P = 0.002$) were identified as the predictors of OS in ASTRI-NSCLC treated with DEB-BACE.

Conclusion: MWA sequentially combined with DEB-BACE was superior to DEB-BACE alone in the local control of ASTRI-NSCLC. Although the combination therapy reveals a trend of prolonging the OS, long-term prognosis warrants an investigation with a longer follow-up.

Keywords: microwave ablation, non-small cell lung cancer, drug-eluting beads, chemoembolization, complications, survival

INTRODUCTION

Primary lung cancer has an incidence and mortality of over 2.2 million and 1.79 million, respectively, estimated globally in 2020 (1). In China, non-small cell lung cancer (NSCLC) has a percentage over 85% in the diagnoses of lung cancer, and most of the patients are advanced when diagnosed (2, 3). The standard treatments for unresectable advanced NSCLC include chemoradiotherapy, molecular targeted therapy [such as tyrosine kinase inhibitors (TKIs)], and immunotherapy. However, it often develops refractoriness and almost 59% of unresectable stage III NSCLC patients are ineligible for chemoradiotherapy owing to the severe adverse events (4). In addition, TKIs are not available for a large proportion of patients without gene mutations. The prognosis of advanced NSCLC remains dismal, with a 5-year survival rate of 15% for stage III and that of less than 10% for stage IV (5). Furthermore, 30%–50% of NSCLC patients are diagnosed with poor performance status owing to cardiovascular and pulmonary diseases and are ineligible for systemic therapy (6). The therapeutic strategy for advanced and standard treatment-refractory/ineligible NSCLC (ASTRI-NSCLC) patients remains limited.

In recent decades, computed tomography (CT)-guided microwave ablation (MWA) has been recommended as a primary treatment option by several guidelines (7, 8), especially for early-stage NSCLC that is contraindicated to undergo surgery or radiotherapy, and has been presented as a part of combination therapy for advanced-stage NSCLC (9). Moreover, bronchial arterial chemoembolization (BACE) has been increasingly applied in NSCLC, which aims to embolize the tumor-feeding arteries, extend the action time of chemotherapeutic drugs, and increase drug concentration at tumor tissues (10). As a novel drug delivery and embolization system in transarterial chemoembolization (TACE), drug-eluting bead (DEB) microsphere can release the loaded chemotherapeutic drugs slowly, improve local drug concentration, and permanently embolize the tumor-feeding arteries (11). DEB-BACE was identified as an effective and safe approach for advanced standard treatment-ineligible/rejected NSCLC (12–16).

The optimal cutoff value of tumor diameter in predicting local recurrence after MWA was 3 cm, with the potential mechanisms for incomplete ablation in large tumors including the limited size and homogeneity of tumor necrosis achieved by MWA and the heat-sink effect caused by the blood vessels in ablated tumor (17). In theory, BACE could block the arterial blood flow and increase drug concentration at tumor sites, which may improve the prognosis of MWA. Similar effectiveness has already been shown and recommended in liver cancers treated with TACE and thermal ablation (18, 19). Liu et al. (20) indicate that combined treatment with DEB-TACE has advantages in improving the prognosis of early-stage liver cancer compared to MWA alone. However, few studies have focused on the outcomes of MWA combined with DEB-BACE for ASTRI-NSCLC. Therefore, a retrospective study was conducted to compare the outcomes of DEB-BACE with and without MWA in the treatment of ASTRI-NSCLC.

MATERIALS AND METHODS

Patient Criteria

This single-center case-control study included all ASTRI-NSCLC patients who underwent DEB-BACE at this institution. The institutional ethics review board approved this study. The study protocol was conducted per the Declaration of Helsinki. Informed consent was waived due to the retrospective nature of this study. ASTRI-NSCLC patients who received DEB-BACE between May 2017 and April 2021 were allocated to the combination therapy group (MWA+DEB-BACE, group A) and DEB-BACE alone group (group B). Informed consent of MWA or/and DEB-BACE was obtained before these procedures. Patient inclusion criteria were as follows: (a) age of 18–85 years; (b) advanced NSCLC that is ineligible for or is refractory to standard treatments; and (c) Eastern Cooperation Oncology Group score of 0–2. Patient exclusion criteria were as follows: (a) concomitant radioactive seed implantation was performed during MWA procedure; (b) incomplete data; (c) lost to follow-up; (d) MWA combined with bronchial artery infusion chemotherapy (BAI); and (e) period between MWA and DEB-BACE longer than 1.5 months.

The histopathological subtypes were confirmed *via* previous percutaneous needle aspiration biopsy or surgery or fiberoptic bronchoscopy. Positron emission tomography or CT was

performed to evaluate the tumor location, quantity, size, and local and distant metastases. The clinical TNM staging system of the Union for International Cancer Control (8th edition) was applied in identifying the tumor stage (5).

Microwave Ablation Procedure

The MWA indications and procedures followed the Society of Interventional Radiology (SIR) guidelines (21). As described previously (22), an MTC-3C MWA system (Vison Medical Inc., China) or an ECO-100A1 MWA system (ECO, China) was used, with a microwave emission frequency of 2,450 ± 50 MHz and an adjustable continuous wave output power of 20–80 W. The MWA antenna (Vison or ECO) was 15–18 cm in effective length and 15–17 G in outside diameter according to the tumor location and distance to the pleura, with a 15-mm active tip. Preprocedural CT was performed to inform the treatment plan and to clarify the suitable position, puncture site location, optimal puncture trajectory, and the number of MWA antennas. Local anesthesia was used for most patients, while intravenous anesthesia was used for selected patients requiring more pain control. Antennas were introduced into the planned site, and MWA was performed at the planned power and duration, with adjustments of suitable power and duration being carried out according to the intraprocedural location of MWA antennas as needed. The procedure was terminated when the tumor tissues were ablated and inactivated as much as possible. Finally, chest CT was repeated to evaluate the distribution of ablation zone and detect the potential complications.

DEB-BACE Procedure

As described previously (16), DEB-BACE procedures were performed under local anesthesia *via* a femoral artery approach. A 5-French pigtail catheter (PIG Impress; Merit Medical Systems, Inc., USA) was initially used for aortic arch angiography to detect the origins of tumor-feeding arteries. Then, a 5-French cobra (CB 1 Impress; Merit Medical Systems, Inc., USA) or left gastric catheter (Radifocus; Terumo Corporation, Japan) was used to select the bronchial arteries or non-bronchial systemic arteries. Super-selective catheterization with a 1.98-French microcatheter (Masters PARKWAY SOFT; Asahi Intec Co., Japan) was inserted coaxially. The chemotherapeutic regimen of paclitaxel (100–200 mg; Keaili, CSPC Pharmaceutical Group Co., China) was administered during BAI for patients who had already received systemic platinum-based chemotherapy, while nedaplatin (80–100 mg; Lubei, Qilu Pharmaceutical Co., China) was administered for patients who had not received systemic platinum-based chemotherapy. Gemcitabine (200–1,000 mg; Zefei, Hansoh Pharmaceutical Group Co., China) or endostatin (60-120 mg; Endu, Simcere Pharmaceutical Group, China) was infused on demand. BAI was followed by DEB-BACE, which was performed using 100–300 μm or 300–500 μm or 500–700 μm CalliSpheres microspheres (Jiangsu Hengrui Medical Co., China) loaded with gemcitabine (800 mg; Hansoh, China) or pirarubicin (30 mg; Adriamycin, Shenzhen Main Luck Pharmaceutical Inc., China). The CalliSpheres microspheres were first mixed with gemcitabine or pirarubicin at a temperature of 23°C–28°C for 30 min and vibrated every 5 min. Then, iodixanol (100 ml:65.2 g/32 g iodine; Hengrui, China) was added at a 1:1 ratio. The DEB-BACE was performed slowly and carefully in tumor-feeding arteries under fluoroscopic monitoring to avoid reflux into nontarget vessels. The technical endpoint of embolization was the absence of additional tumor staining or stasis/near stasis of the tumor-feeding arteries. For patients who received combination therapy, DEB-BACE was performed 2–45 days after MWA, followed by repeated DEB-BACE/BAI on demand. For the patients who received a repeated DEB-BACE/BAI, DEB-BACE was performed if abundant tumor staining was revealed in angiography, while BAI alone was performed for those patients without.

Follow-Up and Assessments

Short-term follow-up with CT was conducted 1–5 days after MWA during hospitalization and 3–4 weeks after MWA at an outpatient visit to detect postprocedural complications, including pneumothorax and pleural effusion. Chest tube placement was performed for patients with moderate and severe pneumothorax or pleural effusion (17). Immunotherapy was performed for patients who have not received and can tolerate programmed cell death ligand 1 (PD-L1) blockade and programmed cell death 1 (PD-1) blockade. PD-L1 blockade was administered for patients with high PD-L1 expression according to the previous testing.

MWA- or DEB-BACE-related complications were evaluated according to criteria from the SIR (21, 23). Enhanced CT was routinely performed every 3 months. Based on the Response Evaluation Criteria in Solid Tumors version 1.1 (24), treatment response was evaluated and classified as a complete response (CR), partial response (PR), stable disease (SD), or progressive disease (PD). The disease control rate (DCR) was defined as CR or PR or SD. Overall survival (OS) was defined as the interval from the start of MWA in group A or the first DEB-BACE in group B to death or the last follow-up (October 31, 2021). For patients who died during the follow-up period, OS was calculated as the interval from the MWA or DEB-BACE procedures to death. For patients who survived but were lost to follow-up, OS was calculated as the interval from the MWA or DEB-BACE procedures to the last follow-up. Progression-free survival (PFS) was defined as the interval from the MWA or DEB-BACE procedures to the time of objective progression, including local progression and/or distant metastases. For patients who did not die or progress, the censoring date was defined as the last clinical assessment date.

Statistical Analysis

Categorical variables are described as frequencies and percentages, and continuous variables are described as the mean ± SD. Statistical analyses were performed using SPSS 25.0 for Windows (IBM, Somers, New York). The clinical characteristics, complications, and prognostic data were compared by Student's t-test or Mann–Whitney U test for continuous variables and by chi-square test for categorical variables. Of these, Kaplan–Meier methods were used to

compare the median PFS or OS between the two groups. The OS for ASTRI-NSCLC treated with DEB-BACE was estimated using the Kaplan–Meier method. The possible predictors of OS included 21 parameters on demographics, treatment history, MWA or/and DEB-BACE factors, and radiological features. Variables with a *P*-value <0.05 in the univariate analyses were entered as candidate variables into a stepwise Cox proportional hazards analyses. The results of the multivariate analyses indicated the predictors for the OS. A *P*-value <0.05 was considered to indicate statistical significance in the univariate and multivariate Cox proportional hazards analyses.

RESULTS

Patient Characteristics

A total of 77 NSCLC patients (28 in group A and 49 in group B; **Figure 1**) were included. Of these, 41 patients (53.2%) were squamous cell carcinoma and 45 patients (58.4%) were stage III NSCLC. Detailed demographic characteristics are presented in **Table 1**; a significant difference was found in the incidence of hypertension ($P = 0.021$), whereas other variables revealed no differences. There were 21 patients (27.3%) who received immunotherapy after DEB-BACE, with PD-L1 blockade administered in six patients (7.8%) and PD-1 blockade administered in 15 patients (19.5%).

Complications

No severe adverse event was found in both groups. Detailed MWA-related complications in group A are presented in **Table 2**; pneumothorax was the predominant MWA-related complication, with an incidence rate of 32.1% (9/28). Detailed DEB-BACE-related complications between groups A and B are presented in **Table 3**, with no significant difference.

Clinical Outcomes

Detailed clinical outcomes between the two groups are presented in **Table 4**. In a mean follow-up of 21.7 ± 14.1 months, the median PFS in groups A and B was 7.0 and 4.0 months, respectively, with a significant difference ($P = 0.037$; **Figure 2A**). The median OS in groups A and B was both 8.0 months, with no significant difference ($P = 0.318$; **Figure 2B**). The 6-month PFS and OS rates in groups A and B were 75.0% and 78.6%, 22.4% and 59.2%, respectively, while the 12-month PFS and OS rates in groups A and B were 17.9% and 28.6%, 14.3% and 22.4%, respectively. Of these, a significantly higher 6-month PFS rate was found in group A (75.0% vs. 22.4%; $P < 0.001$). There were nine patients (11.7%) who achieved PR at 3 months after MWA or/and DEB-BACE (**Figure 3**). The overall DCR was 61.0% (47/77) at 3 months after MWA or DEB-BACE; of these, a significantly higher DCR was found in group A (85.7% vs. 46.9%, $P = 0.002$).

Predictors of Overall Survival for ASTRI-NSCLC Treated With DEB-BACE

Detailed results of univariate and multivariate analyses are presented in **Table 5**. The cycles of DEB-BACE/BAI [hazard ratio (HR): 0.363, 95% CI: 0.202–0.655, $P = 0.001$; **Figure 4A**] and postoperative immunotherapy (HR: 0.219, 95% CI: 0.085–0.561, $P = 0.002$; **Figure 4B**) were identified as the predictors of OS for ASTRI-NSCLC treated with DEB-BACE.

DISCUSSION

The first-line therapeutic strategy for unresectable advanced NSCLC is chemoradiotherapy, which can provide an objective response rate (ORR) of 23%–34% and a median OS of 11.6 months after systemic platinum-based chemotherapy, or an ORR of 51.5%, a median OS of 22.0 months, and a median PFS of 17.0 months after chemoradiotherapy (25–27). The incidence rate of adverse events was 62% as reported (26). Second-line systemic chemotherapy or TKIs were considered when the patients fail to respond to chemoradiotherapy and can provide a median OS of 12.2 months and a median PFS of 3.1 months for stage III NSCLC patients (28).

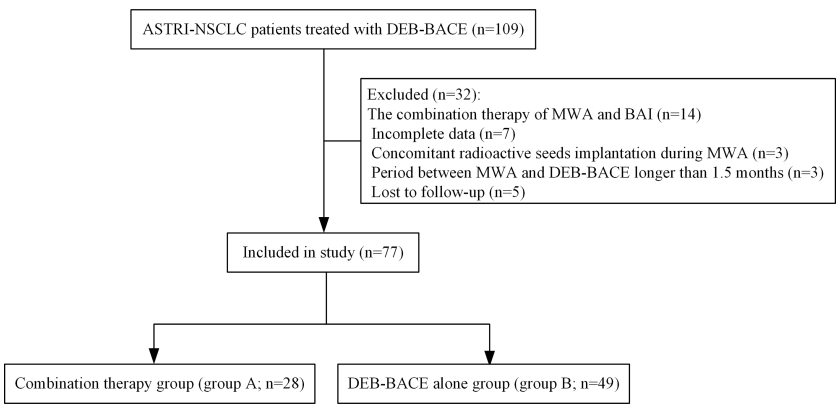

FIGURE 1 | Patient selection flowchart. ASTRI-NSCLC, advanced standard treatment-refractory/ineligible non-small cell lung cancer; DEB-BACE, drug-eluting bead bronchial artery chemoembolization; MWA, microwave ablation; BAI, bronchial artery infusion chemotherapy.

TABLE 1 | Clinical characteristics between ASTRI-NSCLC patients in groups A and B.

Variables	Overall (n = 77)	Group A (n = 28)	Group B (n = 49)	*P*-value
Age (years)	67.6 ± 9.8	66.9 ± 8.9	68.0 ± 10.4	0.637
Gender				0.219
Men	57 (74.0%)	23 (82.1%)	34 (69.4%)	
Women	20 (26.0%)	5 (17.9%)	15 (30.6%)	
Comorbidity				
Hypertension	26 (33.8%)	5 (17.9%)	21 (42.9%)	0.026
Diabetes	11 (14.3%)	3 (10.7%)	8 (16.3%)	0.735
Cardiocerebrovascular diseases	17 (22.1%)	6 (21.4%)	11 (22.4%)	0.917
Pulmonary diseases	6 (7.8%)	2 (7.1%)	4 (8.2%)	>0.999
Tumor subtypes				0.995
Adenocarcinoma	28 (36.4%)	10 (35.7%)	18 (36.7%)	
Squamous cell carcinoma	41 (53.2%)	15 (53.6%)	26 (53.1%)	
Others	8 (10.4%)	3 (10.7%)	5 (10.2%)	
Tumor stage				0.760
III	45 (58.4%)	17 (60.7%)	28 (57.1%)	
IV	32 (41.6%)	11 (39.3%)	21 (42.9%)	
Treatment history				
Previous surgery	5 (6.5%)	2 (7.1%)	3 (6.1%)	>0.999
Previous chemotherapy	24 (31.2%)	5 (17.9%)	19 (38.8%)	0.057
Previous radiotherapy	10 (13.0%)	3 (10.7%)	7 (14.3%)	0.654
Previous TKIs	15 (19.5%)	3 (10.7%)	12 (24.5%)	0.242
Radiological features				
Tumor diameter (cm)	6.3 ± 2.6	6.2 ± 2.4	6.4 ± 2.8	0.737
Location				0.208
Lower or middle lobe	34 (44.2%)	15 (53.6%)	19 (38.8%)	
Upper lobe	43 (55.8%)	13 (46.4%)	30 (61.2%)	
Emphysema	20 (26.0%)	10 (35.7%)	10 (20.4%)	0.141
Extrapulmonary metastases	20 (26.0%)	6 (21.4%)	14 (28.6%)	0.492
Tumor number				0.285
1	65 (84.4%)	22 (78.6%)	43 (87.8%)	
≥2	12 (15.6%)	6 (21.4%)	6 (12.2%)	
Laboratory examinations				
WBC (*10^9/L)	7.8 ± 2.6	8.2 ± 2.8	7.6 ± 2.5	0.294
Hb (g/L)	121.4 ± 18.4	125.9 ± 17.5	118.8 ± 18.5	0.107
PLT (*10^9/L)	265.2 ± 89.8	279.0 ± 89.1	257.4 ± 90.1	0.311
PT (s)	11.7 ± 1.6	11.5 ± 2.2	11.8 ± 1.1	0.377
Postoperative treatments				
TKIs	21 (27.3%)	5 (17.9%)	16 (32.7%)	0.161
Immunotherapy	21 (27.3%)	10 (35.7%)	11 (22.4%)	0.209
MWA-related factors				
Number of MWA antennas	/	1.4 ± 0.6	/	/
Maximum power (W)	/	51.8 ± 13.3	/	/
Ablation time (min)	/	12.6 ± 7.0	/	/
Number of pleural punctures	/	1.8 ± 0.8	/	/
Diameter of instruments				
15G	/	15 (53.6%)	/	/
17G	/	13 (46.4%)	/	/
DEB-BACE-related factors				
Diameter of microsphere (μm)				>0.999
100–300	13 (16.9%)	5 (17.9%)	8 (16.3%)	
300–500	62 (80.5%)	22 (78.6%)	40 (81.6%)	
500–700	2 (2.6%)	1 (3.6%)	1 (2.0%)	
Loaded drug				>0.999
Gemcitabine	69 (89.6%)	25 (89.3%)	44 (89.8%)	
Pirarubicin	8 (10.4%)	3 (10.7%)	5 (10.2%)	
BAI drugs				
Gemcitabine	34 (44.2%)	13 (46.4%)	21 (42.9%)	0.761
Platinum	52 (67.5%)	19 (67.9%)	33 (67.3%)	0.963
Endostatin	44 (57.1%)	20 (71.4%)	24 (49.0%)	0.056
Paclitaxel	21 (27.3%)	11 (39.3%)	10 (20.4%)	0.074
Embolized arteries				0.055
Bronchial artery	67 (87.0%)	27 (96.4%)	40 (81.6%)	
NBSA	6 (7.8%)	1 (3.6%)	5 (10.2%)	
Bronchial artery+NBSA	4 (5.2%)	0	4 (8.2%)	
Number	1.1 ± 0.4	1.1 ± 0.3	1.2 ± 0.4	0.137
DEB-BACE/BAI cycles	2.0 ± 1.3	1.9 ± 1.1	2.0 ± 1.4	0.722
Cycles of combination therapy	/	1.1 ± 0.4	/	/
Period between MWA and DEB-BACE (days)	/	15.5 ± 14.7	/	/

Frequencies and percentages are reported for categorical variables, and mean ± SD are reported for continuous variables.

ASTRI-NSCLC, advanced standard treatment-refractory/ineligible non-small cell lung cancer; MWA, microwave ablation; DEB-BACE, drug-eluting bead bronchial artery chemoembolization; WBC, white blood cell; Hb, hemoglobin; PLT, platelet; PT, prothrombin time; TKIs, tyrosine kinase inhibitors; MWA, microwave ablation; BAI, bronchial artery infusion chemotherapy; NBSA, non-bronchial systemic artery.

TABLE 2 | Details of MWA-related complications in group A.

Variables	Number	Percentage (%)
Major complications		
Pneumothorax	5	17.9
Pleural effusion	1	3.6
Bronchopleural fistula	0	0.0
Pneumonia	0	0.0
Minor complications		
Pneumothorax	4	14.3
Pneumonia	1	3.6
Side effects		
Chest pain	5	17.9
Pleural effusion	1	3.6
Post-ablation syndrome	6	21.4

MWA, microwave ablation.

In recent decades, BACE/BAI has been reported as an effective and safe approach for advanced NSCLC, especially for chemoradiotherapy-ineligible/rejected patients, with a median PFS of 6.5–14.0 months and a median OS of 13.1–25.0 months (29–31). NSCLC is mainly supplied by the bronchial artery (32), and the chemotherapeutic drug could be infused into the tumor-feeding arteries directly during BAI, which can improve the bioavailability of the drug without leading to severe adverse events (33). BAI has a local drug concentration 2–6 times higher than that of systemic chemotherapy and also has effects on lymph node metastases (34). Both local and systemic chemotherapy could be achieved in BACE/BAI, which attributes to the drugs entering the tumor again through the blood circulation, and tumor ischemia, necrosis, or shrinking caused by the embolization (35). In 2012, Nakanishi et al. (29) attempted BAI in 25 advanced chemotherapy-refractory/ineligible NSCLC patients and presented an ORR of 52% and a median PFS and OS of 6.5 months and 17.4 months, respectively. Similarly, another study performed 142 cycles of BAI in 40 advanced chemoradiotherapy-ineligible/rejected NSCLC patients and found an ORR of 32.5%, a DCR of 92.5%, and a median OS of 13.1 months (30). In 2017, Zhu et al. (31) analyzed 36 stage III squamous cell lung cancer patients treated with BAI and revealed a prolonged PFS or OS compared with systemic chemotherapy, with an effective rate, 1-year survival rate, and 2-year survival rate of 72.2%, 75.4%, and 52.1%, respectively.

DEB microspheres can provide a higher local drug concentration while reducing the systemic drug concentration and toxicity (11). Several studies have identified the efficacy and safety of DEB-BACE in advanced lung cancer and found a median PFS of 6.3–11.0 months and a median OS of 8.0–16.5

TABLE 3 | Details of DEB-BACE-related complications between ASTRI-NSCLC patients in groups A and B.

Variables	Overall (n = 77)	Group A (n = 28)	Group B (n = 49)	*P*-value
Mild adverse event				
Chest congestion or pain	8 (10.4%)	3 (10.7%)	5 (10.2%)	>0.999
Fever	5 (6.5%)	2 (7.1%)	3 (6.1%)	>0.999
Vomit	1 (1.3%)	1 (3.6%)	0	0.364
Moderate adverse event				
Chest congestion or pain	4 (5.2%)	1 (3.6%)	3 (6.1%)	>0.999
Fever	5 (6.5%)	1 (3.6%)	4 (8.2%)	0.760
Myelosuppression	3 (3.9%)	1 (3.6%)	2 (4.1%)	>0.999
Severe adverse event	/	/	/	/
Life-threatening or disabling event	/	/	/	/
Patient death or unexpected pregnancy abortion	/	/	/	/

DEB-BACE, drug-eluting bead bronchial artery chemoembolization.

TABLE 4 | Clinical outcomes between ASTRI-NSCLC patients in groups A and B.

Variables	Overall (n = 77)	Group A (n = 28)	Group B (n = 49)	*P*-value
Response				0.002
CR	/	/	/	
PR	9 (11.7%)	5 (17.9%)	4 (8.2%)	
SD	38 (49.4%)	19 (67.9%)	19 (38.8%)	
PD	30 (39.0%)	4 (14.3%)	26 (53.1%)	
DCR (%)	61.0 (47/77)	85.7 (24/28)	46.9 (23/49)	0.002
Status				0.279
Survival	27 (35.1%)	12 (42.9%)	15 (30.6%)	
Death	50 (64.9%)	16 (57.1%)	34 (69.4%)	
6-month PFS rate (%)	41.6 (32/77)	75.0 (21/28)	22.4 (11/49)	<0.001
12-month PFS rate (%)	15.6 (12/77)	17.9 (5/28)	14.3 (7/49)	0.678
6-month OS rate (%)	66.2 (51/77)	78.6 (22/28)	59.2 (29/49)	0.084
12-month OS rate (%)	24.7 (19/77)	28.6 (8/28)	22.4 (11/49)	0.549

ASTRI-NSCLC, advanced standard treatment-refractory/ineligible non-small cell lung cancer; MWA, microwave ablation; DEB-BACE, drug-eluting bead bronchial artery chemoembolization; CR, complete response; PR, partial response; SD, stable disease; PD, progression disease; DCR, disease control rate; PFS, progression-free survival; OS, overall survival.

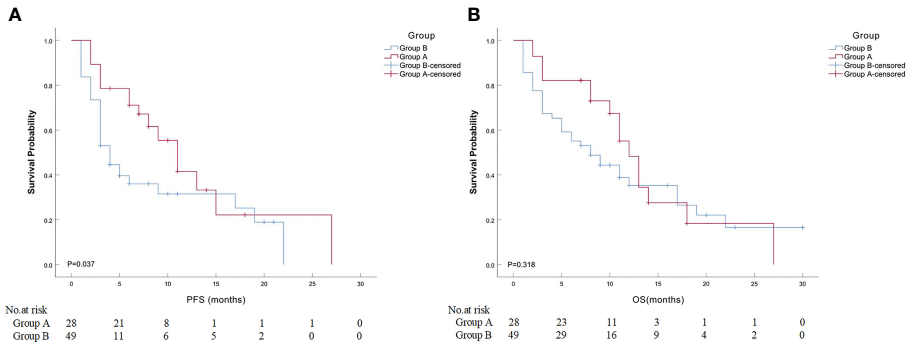

FIGURE 2 | Comparison of median PFS or OS between ASTRI-NSCLC patients in groups A and B. **(A)** The estimated median PFS was 11.0 months for patients in group A, while that was 4.0 months for patients in group B. **(B)** The estimated median OS was 12.0 months for patients in group A, while that was 8.0 months for patients in group **(B)** PFS, progression-free survival; OS, overall survival; ASTRI-NSCLC, advanced standard treatment-refractory/ineligible non-small cell lung cancer.

months (12–16). Gemcitabine-loaded DEB-BACE was first to be applied to NSCLC in 2019 (13). Although this study included only six patients, promising results with the median PFS of 8.0 months and median OS of 16.5 months were provided (13). Then, Shang et al. (12) compared the efficacy of pirarubicin-loaded DEB-BACE and BAI alone in 60 standard treatment-ineligible/rejected NSCLC patients; among them, over 85% of NSCLC patients were in advanced stage. Higher ORR, DCR, and 6-month PFS and OS rates were found in the DEB-BACE group, which indicated a superior efficacy than BAI alone (12). Sequentially, Zeng et al. (14) analyzed 23 advanced lung cancer patients treated with DEB-BACE and revealed an ORR of 78.3% and median OS of 15.6 months despite including four patients with small cell lung cancer or lung metastases. Another study from this institution showed median PFS and OS of 6.3 months and 10.2 months, respectively, for 29 advanced NSCLC patients treated with pirarubicin-loaded DEB-BACE (15). Nevertheless, there was no consensus on the optimal chemotherapeutic drug loaded in the DEB microsphere. The predominant chemotherapeutic drug loaded in the DEB microsphere was

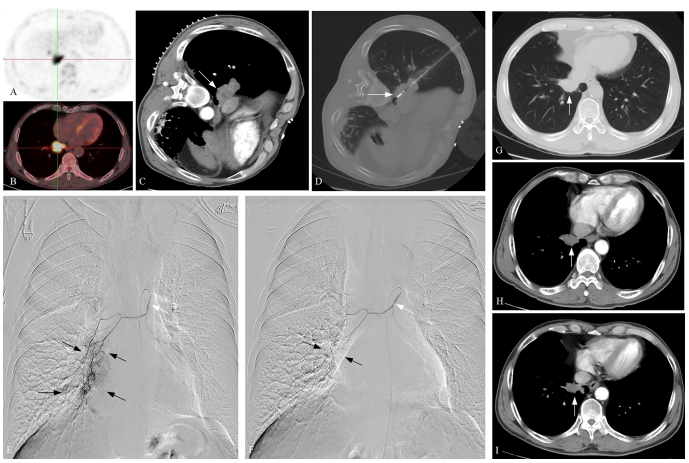

FIGURE 3 | A typical case of ASTRI-NSCLC treated with combination therapy. **(A–C)** A confirmed NSCLC patient with poor pulmonary function was admitted, with the tumor subtype of squamous cell carcinoma. Positron emission tomography revealed the presence of abnormal accumulation of the tracer in lung mass and enlarged hilar lymph nodes, and the maximum tumor diameter was 5.1 cm (white arrow), which showed T3N1M0 and stage III A for the patient. **(D)**. CT-guided MWA was performed (white arrow), with 40W of energy released and 10 minutes of ablation time. **(E)** DEB-BACE was performed 3 weeks after MWA, with the microcatheter being used for super-selective catheterization initially (white arrow). Sequential angiography revealed that the tumor was fed by the right bronchial artery, with the presence of abundant tumor staining (black arrow). **(F)** The 300–500-μm CalliSpheres microspheres loaded with gemcitabine (800 mg) were used for chemoembolization *via* the microcatheter (white arrow). The post-embolization angiography revealed the disappearance of tumor staining (black arrow). A total of four cycles of DEB-BACE/BAI were performed. **(G)** The 3-month CT scan after combination therapy revealed the tumor size decreases to 3.5 cm and showed a PR in response. **(H, I)** The 6-month and 9-month CT scans after combination therapy revealed a continued decrease in the tumor size. ASTRI-NSCLC, advanced standard treatment-refractory/ineligible non-small cell lung cancer; CT, computed tomography; MWA, microwave ablation; DEB-BACE, drug-eluting bead bronchial artery chemoembolization; BAI, bronchial artery infusion chemotherapy; PR, partial response.

TABLE 5 | Univariate and multivariate Cox proportional hazards analyses for OS in ASTRI-NSCLC treated with DEB-BACE.

Variables	Univariate analysis		Multivariate analysis	
	Median OS (95% CI)	*P*-value*	HR (95% CI)	*P*-value**
Tumor stage		0.030		
III	12.0 (8.863–15.137)			
IV	6.0 (1.067–10.933)			
Previous radiotherapy		0.048		
Yes	3.0 (0.000–7.132)			
No	11.0 (9.189–12.811)			
Tumor number		0.026		
1	11.0 (7.273–14.727)			
≥2	3.0 (0.000–9.365)			
DEB-BACE/BAI cycles		<0.001		0.001
1	3.0 (0.795–5.205)		1	
≥2	13.0 (8.443–17.557)		0.363(0.202–0.655)	
Postoperative immunotherapy		<0.001		0.002
Yes	27.0 (0.335–53.665)		0.219 (0.085–0.561)	
No	8.0 (3.626–12.374)		1	

**Log-rank test was used.*

***Cox proportional hazards regression analysis was used.*

OS, overall survival; ASTRI-NSCLC, advanced standard treatment-refractory/ineligible non-small cell lung cancer; DEB-BACE, drug-eluting bead bronchial artery chemoembolization; CI, confidence interval; HR, hazard ratio; BAI, bronchial artery infusion chemotherapy.

gemcitabine in this study. Although pirarubicin showed moderate anticancer activity, mild toxicity, and a high response rate for advanced NSCLC as reported (34), no superior efficacy of pirarubicin over gemcitabine was found in this study. The median PFS and OS of advanced NSCLC treated with DEB-BACE in this study were 5.0 and 8.0 months, which seem to be less than the reported results. Potential mechanisms were (a) over 40% of the patients were stage IV and over 50% of the patients were standard treatment-refractory, and (b) 35.1% of the patients survived until the last follow-up. In addition, the immune checkpoint inhibitors were identified as the second-line treatment for advanced NSCLC, and PD-1 blockade combined with systemic chemotherapy has been revealed as a promising approach (36). Identically, this study revealed that postoperative immunotherapy was one of the predictors to prolong the OS of ASTRI-NSCLC treated with DEB-BACE, which is per the additional immunotherapy that may improve the survival of advanced NSCLC after BAI/DEB-BACE, as reported (16).

The mechanisms of MWA are that microwaves can induce the oscillation of the water molecules that flip back and forth at a speed of 2–5 billion times a second depending on the frequency of the wave itself, allowing for a superior convection profile and causing coagulative necrosis conforming to the target sites (37). The optimal indication for thermal ablation is NSCLC with tumor <3 cm in diameter (8). Tumor diameter is a critical risk factor of local recurrence and OS after MWA in NSCLC as reported, especially for the tumor ≥3 cm in diameter (17, 38). Zhong et al. (39) indicated a local recurrence rate of 20.5% in advanced NSCLC treated with MWA; of these, 81.3% of relapse occurred in tumor size ≥3 cm, while Nelson et al. (40)

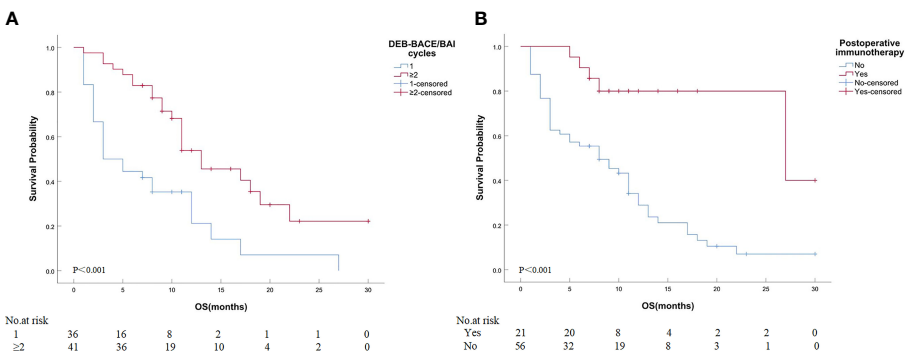

FIGURE 4 | Kaplan–Meier analyses of OS in ASTRI-NSCLC treated with DEB-BACE. **(A)** The estimated median OS was 3.0 months for patients treated with one cycle of DEB-BACE compared with 13.0 months for those patients with no less than two cycles of DEB-BACE/BAI. **(B)** The estimated median OS was 27.0 months for patients with postoperative immunotherapy compared with 8.0 months for those patients without. OS, overall survival; ASTRI-NSCLC, advanced standard treatment-refractory/ineligible non-small cell lung cancer; DEB-BACE, drug-eluting bead bronchial artery chemoembolization; BAI, bronchial artery infusion chemotherapy.

summarized a local recurrence rate of 5%–19% after MWA in NSCLC with tumor <4 cm in a systemic review. It has been reported that thermal ablation combined with TACE can decrease the recurrence rate and may improve the prognosis compared to ablation monotherapy for early-stage liver cancer (18, 19). Identical results were demonstrated in the combination therapy of DEB-TACE and MWA compared to MWA monotherapy for early-stage liver cancer (20). A study from China reviewed 138 advanced NSCLC patients and found that the 1-, 2-, and 3-year survival rates of the combination therapy group (BACE and radiofrequency ablation) were 90.7%, 58.1%, and 20.9%, respectively, which revealed a better prognosis than that of BACE or ablation monotherapy groups (41). In this study, the combination therapy of MWA and DEB-BACE revealed a superior local control, with a higher 6-month PFS rate and a longer PFS than DEB-BACE alone. The potential mechanisms were inactivating the majority of tumor tissues that can be achieved directly by MWA, and DEB-BACE leads to the continuous delivery of loaded chemotherapeutic drugs and the embolization of tumor-feeding arteries, thereby reducing the collateral circulation and enhancing the synergistic anticancer effects on residual tumor tissue. Although the combination therapy reveals a trend of prolonging the OS, no significant difference was found. The leading causes were that 42.9% of the patients in group A survived until the last follow-up and the limited mean follow-up of 21.7 ± 14.1 months in this study.

This study has several limitations. First, it was a retrospective study; patient selection bias may exist. Second, the sample size was still limited for patients treated with combination therapy. Third, this study consists of advanced patients who are ineligible for or are refractory to standard treatments, and heterogeneity may exist. Fourth, the sequence of MWA and DEB-BACE is required to be further investigated. Fifth, the follow-up period was still limited, and the long-term evaluation of OS for combination therapy should be further explored.

In conclusion, the combination therapy of MWA and DEB-BACE is an effective and safe approach for ASTRI-NSCLC. MWA sequentially combined with DEB-BACE was superior to DEB-BACE alone in the local control of ASTRI-NSCLC. Although the combination therapy reveals a trend of prolonging OS, long-term prognosis warrants an investigation with a longer follow-up.

DATA AVAILABILITY STATEMENT

The data used to support the findings of this study are available from the corresponding author upon request.

ETHICS STATEMENT

The studies involving human participants were reviewed and approved by Beijing Hospital, National Center of Gerontology, Institute of Geriatric Medicine, Chinese Academy of Medical Sciences. The ethics committee waived the requirement of written informed consent for participation. Written informed consent was obtained from the individual(s) for the publication of any potentially identifiable images or data included in this article.

AUTHOR CONTRIBUTIONS

SX: conceptualization, data curation, methodology, and writing—original draft. ZXB: data curation, methodology, resources, and writing—review and editing. YML: writing—review and editing. BL: resources and writing—review and editing. FLK: writing—review and editing. JZP: writing—review and editing. XGL: validation, supervision, and writing—review and editing. All authors contributed to the article and approved the submitted version.

FUNDING

This work was funded by the Clinical and Translational Medical Research Fund, Chinese Academy of Medical Sciences (no. 2020-I2M-C&T-A-021). Funding source had no involvement in the conduct of the research and preparation of the article.

REFERENCES

1. Sung H, Ferlay J, Siegel RL, Laversanne M, Soerjomataram I, Jemal A, et al. Global Cancer Statistics 2020: GLOBOCAN Estimates of Incidence and Mortality Worldwide for 36 Cancers in 185 Countries. *CA Cancer J Clin* (2021) 71(3):209–49. doi: 10.3322/caac.21660
2. Chen W, Zheng R, Baade PD, Zhang S, Zeng H, Bray F, et al. Cancer Statistics in China, 2015. *CA Cancer J Clin* (2016) 66(2):115–32. doi: 10.3322/caac.21338
3. Cao W, Chen HD, Yu YW, Li N, Chen WQ. Changing Profiles of Cancer Burden Worldwide and in China: A Secondary Analysis of the Global Cancer Statistics 2020. *Chin Med J (Engl)* (2021) 134(7):783–91. doi: 10.1097/CM9.0000000000001474
4. De Ruysscher D, Botterweck A, Dirx M, Pijls-Johannesma M, Wanders R, Hochstenbag M, et al. Eligibility for Concurrent Chemotherapy and Radiotherapy of Locally Advanced Lung Cancer Patients: A Prospective, Population-Based Study. *Ann Oncol* (2009) 20(1):98–102. doi: 10.1093/annonc/mdn559
5. Goldstraw P, Chansky K, Crowley J, Rami-Porta R, Asamura H, Eberhardt WE, et al. The IASLC Lung Cancer Staging Project: Proposals for Revision of the TNM Stage Groupings in the Forthcoming (Eighth) Edition of the TNM Classification for Lung Cancer. *J Thorac Oncol* (2016) 11(1):39–51. doi: 10.1016/j.jtho.2015.09.009
6. Lilenbaum RC, Cashy J, Hensing TA, Young S, Cella D. Prevalence of Poor Performance Status in Lung Cancer Patients: Implications for Research. *J Thorac Oncol* (2008) 3(2):125–9. doi: 10.1097/JTO.0b013e3181622c17
7. Postmus PE, Kerr KM, Oudkerk M, Senan S, Waller DA, Vansteenkiste J, et al. Early and Locally Advanced Non-Small-Cell Lung Cancer (NSCLC): ESMO Clinical Practice Guidelines for Diagnosis, Treatment and Follow-Up. *Ann Oncol* (2017) 28(suppl_4):iv1–21. doi: 10.1093/annonc/mdx222
8. Donington J, Ferguson M, Mazzone P, Handy JJ, Schuchert M, Fernando H, et al. American College of Chest Physicians and Society of Thoracic Surgeons

Consensus Statement for Evaluation and Management for High-Risk Patients With Stage I Non-Small Cell Lung Cancer. *Chest* (2012) 142(6):1620–35. doi: 10.1378/chest.12-0790

9. Wei Z, Yang X, Ye X, Feng Q, Xu Y, Zhang L, et al. Microwave Ablation Plus Chemotherapy Versus Chemotherapy in Advanced Non-Small Cell Lung Cancer: A Multicenter, Randomized, Controlled, Phase III Clinical Trial. *Eur Radiol* (2020) 30(5):2692–702. doi: 10.1007/s00330-019-06613-x
10. Lee WK, Lau EW, Chin K, Sedlaczek O, Steinke K. Modern Diagnostic and Therapeutic Interventional Radiology in Lung Cancer. *J Thorac Dis* (2013) 5 (Suppl 5):S511–23. doi: 10.3978/j.issn.2072-1439.2013.07.27
11. Melchiorre F, Patella F, Pescatori L, Pesapane F, Fumarola E, Biondetti P, et al. DEB-TACE: A Standard Review. *Future Oncol* (2018) 14(28):2969–84. doi: 10.2217/fon-2018-0136
12. Shang B, Li J, Wang X, Li D, Liang B, Wang Y, et al. Clinical Effect of Bronchial Arterial Infusion Chemotherapy and CalliSpheres Drug-Eluting Beads in Patients With Stage II-IV Lung Cancer: A Prospective Cohort Study. *Thorac Cancer* (2020) 11(8):2155–62. doi: 10.1111/1759-7714.13522
13. Bie Z, Li Y, Li B, Wang D, Li L, Li X. The Efficacy of Drug-Eluting Beads Bronchial Arterial Chemoembolization Loaded With Gemcitabine for Treatment of Non-Small Cell Lung Cancer. *Thorac Cancer* (2019) 10 (9):1770–8. doi: 10.1111/1759-7714.13139
14. Zeng Y, Yin M, Zhao Y, Liu Y, Li X, Qi Y, et al. Combination of Bronchial Arterial Infusion Chemotherapy Plus Drug-Eluting Embolic Transarterial Chemoembolization for Treatment of Advanced Lung Cancer-A Retrospective Analysis of 23 Patients. *J Vasc Interv Radiol* (2020) 31 (10):1645–53. doi: 10.1016/j.jvir.2020.06.007
15. Bi Y, Shi X, Yi M, Han X, Ren J. Pirarubicin-Loaded CalliSpheres(R) Drug-Eluting Beads for the Treatment of Patients With Stage III-IV Lung Cancer. *Acta Radiol* (2022) 63(3):311–8. doi: 10.1177/0284185121994298
16. Li YM, Guo RQ, Bie ZX, Li B, Li XG. Sintilimab Plus Bronchial Arterial Infusion Chemotherapy/Drug-Eluting Embolic Chemoembolization for Advanced Non-Small Cell Lung Cancer: A Preliminary Study of 10 Patients. *J Vasc Interv Radiol* (2021) 32(12):1679–87. doi: 10.1016/j.jvir.2021.08.019
17. Xu S, Qi J, Bie ZX, Li YM, Li B, Guo RQ, et al. Local Progression After Computed Tomography-Guided Microwave Ablation in Non-Small Cell Lung Cancer Patients: Prediction Using a Nomogram Model. *Int J Hyperthermia* (2021) 38(1):1366–74. doi: 10.1080/02656736.2021.1976852
18. Lu J, Zhao M, Arai Y, Zhong BY, Zhu HD, Qi XL, et al. Clinical Practice of Transarterial Chemoembolization for Hepatocellular Carcinoma: Consensus Statement From an International Expert Panel of International Society of Multidisciplinary Interventional Oncology (ISMIO). *Hepatobiliary Surg Nutr* (2021) 10(5):661–71. doi: 10.21037/hbsn-21-260
19. Peng ZW, Zhang YJ, Chen MS, Xu L, Liang HH, Lin XJ, et al. Radiofrequency Ablation With or Without Transcatheter Arterial Chemoembolization in the Treatment of Hepatocellular Carcinoma: A Prospective Randomized Trial. *J Clin Oncol* (2013) 31(4):426–32. doi: 10.1200/JCO.2012.42.9936
20. Liu J, Zhang W, Lu H, Li H, Zhou X, Li J, et al. Drug-Eluting Bead Trans-Arterial Chemoembolization Combined With Microwave Ablation Therapy vs. Microwave Ablation Alone for Early Stage Hepatocellular Carcinoma: A Preliminary Investigation of Clinical Value. *J Cancer Res Clin Oncol* (2021). doi: 10.1007/s00432-021-03760-x
21. Genshaft SJ, Suh RD, Abtin F, Baerlocher MO, Dariushnia SR, Devane AM, et al. Society of Interventional Radiology Quality Improvement Standards on Percutaneous Ablation of Non-Small Cell Lung Cancer and Metastatic Disease to the Lungs. *J Vasc Interv Radiol* (2021) 32(8):1242.e1–10. doi: 10.1016/j.jvir.2021.04.027
22. Xu S, Bie ZX, Li YM, Li B, Guo RQ, Li XG. A Comparative Study of Cavitary and Noncavitary Non-Small Cell Lung Cancer Patients Treated With CT-Guided Microwave Ablation. *J Vasc Interv Radiol* (2021) 32(8):1170–8. doi: 10.1016/j.jvir.2021.05.006
23. Dariushnia SR, Redstone EA, Heran M, Cramer HJ, Ganguli S, Gomes AS, et al. Society of Interventional Radiology Quality Improvement Standards for Percutaneous Transcatheter Embolization. *J Vasc Interv Radiol* (2021) 32 (3):476.e1–476.e33. doi: 10.1016/j.jvir.2020.10.022
24. Schwartz LH, Litiere S, de Vries E, Ford R, Gwyther S, Mandrekar S, et al. RECIST 1.1-Update and Clarification: From the RECIST Committee. *Eur J Cancer* (2016) 62:132–7. doi: 10.1016/j.ejca.2016.03.081
25. Noonan KL, Ho C, Laskin J, Murray N. The Influence of the Evolution of First-Line Chemotherapy on Steadily Improving Survival in Advanced Non-Small-Cell Lung Cancer Clinical Trials. *J Thorac Oncol* (2015) 10(11):1523–31. doi: 10.1097/JTO.0000000000000667
26. Thatcher N, Hirsch FR, Luft AV, Szczesna A, Ciuleanu TE, Dediu M, et al. Necitumumab Plus Gemcitabine and Cisplatin Versus Gemcitabine and Cisplatin Alone as First-Line Therapy in Patients With Stage IV Squamous Non-Small-Cell Lung Cancer (SQUIRE): An Open-Label, Randomised, Controlled Phase 3 Trial. *Lancet Oncol* (2015) 16(7):763–74. doi: 10.1016/S1470-2045(15)00021-2
27. Atagi S, Kawahara M, Yokoyama A, Okamoto H, Yamamoto N, Ohe Y, et al. Thoracic Radiotherapy With or Without Daily Low-Dose Carboplatin in Elderly Patients With Non-Small-Cell Lung Cancer: A Randomised, Controlled, Phase 3 Trial by the Japan Clinical Oncology Group (Jcog0301). *Lancet Oncol* (2012) 13(7):671–8. doi: 10.1016/S1470-2045(12)70139-0
28. Sun Y, Wu YL, Zhou CC, Zhang L, Zhang L, Liu XY, et al. Second-Line Pemetrexed Versus Docetaxel in Chinese Patients With Locally Advanced or Metastatic Non-Small Cell Lung Cancer: A Randomized, Open-Label Study. *Lung Cancer* (2013) 79(2):143–50. doi: 10.1016/j.lungcan.2012.10.015
29. Nakanishi M, Yoshida Y, Natazuka T. Prospective Study of Transarterial Infusion of Docetaxel and Cisplatin to Treat Non-Small-Cell Lung Cancer in Patients Contraindicated for Standard Chemotherapy. *Lung Cancer* (2012) 77 (2):353–8. doi: 10.1016/j.lungcan.2012.04.006
30. Fu YF, Li Y, Wei N, Xu H. Transcatheter Arterial Chemical Infusion for Advanced Non-Small-Cell Lung Cancer: Long-Term Outcome and Predictor of Survival. *Radiol Med* (2016) 121(7):605–10. doi: 10.1007/s11547-016-0629-2
31. Zhu J, Zhang HP, Jiang S, Ni J. Neoadjuvant Chemotherapy by Bronchial Arterial Infusion in Patients With Unresectable Stage III Squamous Cell Lung Cancer. *Ther Adv Respir Dis* (2017) 11(8):301–9. doi: 10.1177/1753465817717169
32. Du L, Morgensztern D. Chemotherapy for Advanced-Stage Non-Small Cell Lung Cancer. *Cancer J* (2015) 21(5):366–70. doi: 10.1097/PPO.0000000000000141
33. Huang J, Zhang T, Ma K, Fan P, Liu Y, Weng C, et al. Clinical Evaluation of Targeted Arterial Perfusion of Verapamil and Chemotherapeutic Drugs in Interventional Therapy of Advanced Lung Cancer. *Cancer Chemother Pharmacol* (2013) 72(4):889–96. doi: 10.1007/s00280-013-2271-1
34. Zhao G, Huang Y, Ye L, Duan L, Zhou Y, Yang K, et al. Therapeutic Efficacy of Traditional Vein Chemotherapy and Bronchial Arterial Infusion Combining With CIKs on III Stage Non-Small Cell Lung Cancer. *Zhongguo Fei Ai Za Zhi* (2009) 12(9):1000–4. doi: 10.3779/j.issn.1009-3419.2009.09.011
35. Chen C, Wang W, Yu Z, Tian S, Li Y, Wang Y. Combination of Computed Tomography-Guided Iodine-125 Brachytherapy and Bronchial Arterial Chemoembolization for Locally Advanced Stage III Non-Small Cell Lung Cancer After Failure of Concurrent Chemoradiotherapy. *Lung Cancer* (2020) 146:290–6. doi: 10.1016/j.lungcan.2020.06.010
36. Garcia-Gonzalez J, Ruiz-Banobre J, Afonso-Afonso FJ, Amenedo-Gancedo M, Areses-Manrique M, Campos-Balea B, et al. PD-(L)1 Inhibitors in Combination With Chemotherapy as First-Line Treatment for Non-Small-Cell Lung Cancer: A Pairwise Meta-Analysis. *J Clin Med* (2020) 9(7):2093. doi: 10.3390/jcm9072093
37. Duka E, Ierardi AM, Floridi C, Terrana A, Fontana F, Carrafiello G. The Role of Interventional Oncology in the Management of Lung Cancer. *Cardiovasc Intervent Radiol* (2017) 40(2):153–65. doi: 10.1007/s00270-016-1495-y
38. Xu S, Qi J, Li B, Li XG. Survival Prediction for Non-Small Cell Lung Cancer Patients Treated With CT-Guided Microwave Ablation: Development of a Prognostic Nomogram. *Int J Hyperthermia* (2021) 38(1):640–9. doi: 10.1080/02656736.2021.1914353
39. Zhong L, Sun S, Shi J, Cao F, Han X, Bao X, et al. Clinical Analysis on 113 Patients With Lung Cancer Treated by Percutaneous CT-Guided Microwave Ablation. *J Thorac Dis* (2017) 9(3):590–7. doi: 10.21037/jtd.2017.03.14
40. Nelson DB, Tam AL, Mitchell KG, Rice DC, Mehran RJ, Sepesi B, et al. Local Recurrence After Microwave Ablation of Lung Malignancies: A Systematic Review. *Ann Thorac Surg* (2019) 107(6):1876–83. doi: 10.1016/j.athoracsur.2018.10.049
41. Yang XG, Wu G, Li ZW, Wu H, Sun YY, Wen HH, et al. Efficacy for Artery Chemoembolization Combined With Radiofrequency Ablation in the

Treatment of Advanced Non-Small Cell Lung Cancer. *Zhonghua Yi Xue Za Zhi* (2016) 96(7):539–43. doi: 10.3760/cma.j.issn.0376-2491.2016.07.010

Conflict of Interest: The authors declare that the research was conducted in the absence of any commercial or financial relationships that could be construed as a potential conflict of interest.

Publisher's Note: All claims expressed in this article are solely those of the authors and do not necessarily represent those of their affiliated organizations, or those of the publisher, the editors and the reviewers. Any product that may be evaluated in this article, or claim that may be made by its manufacturer, is not guaranteed or endorsed by the publisher.

frontiers | Frontiers in Oncology

ORIGINAL RESEARCH
published: 27 April 2022
doi: 10.3389/fonc.2022.856340

MR-Guided Microwave Ablation for Lung Malignant Tumor: A Single Center Prospective Study

Ruixiang Lin[1†], Yan Fang[2†], Jin Chen[1], QingFeng Lin[1], Jian Chen[1], Yuan Yan[1], Jie Chen[3] and Zhengyu Lin[1]*

[1] Department of Interventional Radiology, First Affiliated Hospital of Fujian Medical University, Fuzhou, China, [2] Nursing Department, First Affiliated Hospital of Fujian Medical University, Fuzhou, China, [3] Department of Interventional Radiology, Sanming Second Hospital, Sanming, China

Objectives: To prospectively investigate the feasibility and efficacy of MRI-guided MWA for lung malignant tumor in our single center.

Materials and Methods: 22 patients [mean age, 56.86 ± 13.05(23–73)years] with 23 malignant lung tumors were enrolled in the study. 21 patients had a single lesion and 1 patient had 2 lesions in the ipsilateral lung. The average maximum diameter of the lesion was 1.26 ± 0.65 (0.50-2.58)cm. Percutaneous MWA was guided by 1.5T MRI scanner using a MR-compatible microwave antenna to the target the lung lesions and ablation area was monitored intraoperatively by using a shielded MR-compatible microwave device and then follow-up.

Results: All patients were successfully treated under MR-guided MWA for lung tumors. Average operation time was 72.21 ± 24.99 (36–158) mins. T2WI signal intensity of the lesion gradually decreased over the course of MWA. The center of the ablated zones showed a short T1 and short T2 signals with the ring-like of long T1 and long T2 signals surrounded after immediately evaluation. No serious complications occurred. The average follow-up period was 12.89 ± 4.33 (2.0-19.6) months. Local recurrence occurred in one patient, representing a technical efficacy of 95.5% (21/22).

Conclusion: Magnetic resonance-guided microwave ablation for lung malignant tumor was feasible and demonstrated unique advantages in efficacy evaluation.

Keywords: magnetic resonance imaging, lung neoplasms, microwave, ablation techniques, pneumothorax

OPEN ACCESS

Edited by:
Yuliang Li,
The Second Hospital of Shandong University, China

Reviewed by:
Kunal Bharat Gala,
Tata Memorial Hospital, India
Bilgin Kadri Aribas,
Bülent Ecevit University, Turkey

****Correspondence:***
Zhengyu Lin
linsinlan@aliyun.com

†These authors have contributed equally to this work and share first authorship

Specialty section:
This article was submitted to Thoracic Oncology, a section of the journal Frontiers in Oncology

Received: *17 January 2022*
Accepted: *23 March 2022*
Published: *27 April 2022*

Citation:
Lin R, Fang Y, Chen J, Lin Q, Chen J, Yan Y, Chen J and Lin Z (2022) MR-Guided Microwave Ablation for Lung Malignant Tumor: A Single Center Prospective Study. Front. Oncol. 12:856340. doi: 10.3389/fonc.2022.856340

INTRODUCTION

Primary lung cancer has the second highest incidence and highest mortality among all cancers, while lung also ranks the second most likely site of tumor metastasis (1). Although surgical resection is effective in treating lung cancer, only about 20% of lung lesions can be surgically removed due to various reasons, making effective alternative therapies for local treatment compulsory (2). Microwave ablation (MWA) is considered as an alternative treatment option for primary and metastatic lung cancers. Owing to its slight trauma and reliable efficacy, MWA has been widely used in cancer treatment in recent years (3, 4). As lung tissue contains air, MWA is predominantly guided

by computed tomography (CT) (5). As an alternative approach, magnetic resonance imaging (MRI) has the advantages such as free of ionizing radiation, scanning images in any orientation, sensitive to changes in moisture and temperature caused by MWA. Therefore, it has already been applied to guide tumor ablation in liver, kidney, bone, and soft tissues (6–8). The purpose of this study was to prospectively investigate the technical feasibility and short-term efficacy of MR-guided MWA for malignant lung tumor in our single center.

MATERIALS AND METHODS

Materials

Clinical Information

This prospective study was approved by the ethics committee of the institution, and all participating patients signed an informed consent. The inclusion criteria was as follows: (1) No presence of lesions other than the target(s); (2) Diameter of the solitary lung malignant lesion(0.5cm–3cm); (3) Distance between the lesion and hilar vessels or large bronchi >1 cm; (4) No presence of severe emphysema or pulmonary fibrosis; (5) Platelet count ≥50 x 10^9/L and prothrombin activity ≥40%; (6) ECOG score ≤2; and (7) No contraindications for MRI.

We prospectively analyzed 22 patients with 23 lesions who underwent MR-guided MWA for malignant lung tumors in our center between Jan 2020 and June 2020. Patients' general information is listed in **Table 1**. Of these cases, 9 were men and 13 were women, with an average age of 56.86 ± 13.05 (23–73) years. Ten cases had primary lung adenocarcinoma, and the remaining 12 had lung metastasis (4 cases of colorectal cancer metastasis, 2 cases of hepatocellular carcinoma metastasis, 2cases of lung cancer metastasis, and 1 case each of gastric, breast, tongue, and giant cell tumor of bone cancer metastasis). In addition, 21 cases only had a single lesion, while 1 case had 2 lesions on the ipsilateral lung. The pathological diagnoses of all cases were confirmed by needle biopsy. The average maximum diameter of the lesion was 1.26 ± 0.65 (0.50-2.58) cm. 11 lesions were located in the upper right lobe, 1 in the middle right lobe, 5 in the lower right lobe, 4 in the upper left lobe, and 2 in the lower left lobe.

TABLE 1 | Patient characteristics.

Characteristic	Value
Age	
Average age (years)	56.86 ± 13.05 (23-73)
Gender	
Male	9 (40.91%)
Female	13 (59.09%)
Pathological diagnosis	
Adenocarcinoma	10 (45.45%)
Lung metastasis	12 (54.55%)
Number of lesions	
Single leison	21
Two leisons	1
Location	
Left lung	6 (27.27%)
Right lung	16 (72.73%)
Lesion size (cm)	1.26 ± 0.65 (0.50-2.58)
Operation time (min)	71.77 ± 25.71 (36-158)
Ablation power (W)	81.32 ± 7.31 (60-90)
Ablation duration (min)	5.57 ± 1.71 (3.0-9.0)
Follow-up period (m)	12.89 ± 4.33 (2.0-19.6)

MRI

A 1.5T dual-gradient MRI scanner (GE Signa Infinity Twinspeed, USA) and a Torso coil with a rectangular operating hole were used in the study. Scan sequences and parameters were as follows:

1. Fat-suppressed fast-recovery fast spin echo (fs FRFSE) T2WI with repetition time (TR) of 8500.0 ms, echo time (TE) of 85.0 ms, 90°C flip angle (FA), 17 echo train length (ETL), 5.0 mm slice thickness (ST), 1.0 mm GAP, 280 × 380 field of view (FOV), 1 excitation (NEX), and 70 - 90 s scanning time (T).
2. Three-dimensional dynamic T1 weighted imaging (3D Dyn T1WI) with 4.8 ms TR, 1.1 ms TE, 45°C FA, 1 ETL, 3.0 mm ST, 280 × 380 FOV, 1 NEX, and 12 s T.

The 3D Dyn T1WI scan was acquired under breath-hold, whereas the fsFRFSE T2WI scan was acquired with respiratory gating.

MWA Device

A MR-compatible MWA device (MTC-3C, 2450 MHz, Vison Medical Co., Nanjing, China) was used in the study. Magnetic shielding was achieved by shielding the host with non-magnetic aluminum alloy plates and placing it outside the 0.5-mT line. In addition, a 2.5-m coaxial transmission cable equipped with a choke coil was used, so that MRI was not interfered during startup and tumor ablation. Lastly, a MR-compatible microwave antenna (14 G, 15 cm, Vison Medical Co., Nanjing, China) was adopted, which was made of copper alloy and ceramics and had a built-in water-cooling cycle.

Methods

Preoperative Preparation

One week before procedure, chest CT scans and chest MRI scans with contrast enhancement were performed to identify the lesion and surrounding tissues. Four hours before procedure, patients were instructed to fasting, and an intravenous indwelling needle was introduced. Subsequently, based on the needs of puncture, patients were placed either in the supine or the prone position, and were connected to the respiratory gating system, underwent training for their breathing patterns, and a skin marker was applied (cod liver oil matrix).

MWA Operation

FsFRFSE T2WI and 3D Dyn T1WI scans were first acquired to determine the puncture path and the puncture point on the skin. The puncture path was selected to pass through some normal lung tissue (≥ 2 cm) without touching important structures such as large blood vessels, heart, mediastinum and hilus. Before puncture, routine disinfection was performed and local anesthesia was induced with 2% lidocaine, followed by

application of a sterilized hole towel to the puncture point and a sterilized cover for the scanning coil.

A small incision was made at the puncture point by a surgical knife, through which the microwave antenna was inserted into the chest wall and gradually loaded under the guidance of MRI using the fsFRFSE T2WI sequence. During the procedure, efforts were made for the antenna to penetrate the center of the lesion so that its tip surpassed 0.5–1 cm beyond the tumor. Subsequently, once the microwave antenna was connected to the host using the coaxial cable, and the bed was moved to the scanning position, the ablation power and duration were set, the water-cooling cycle was initiated, and the air in the antenna was exhausted. MWA then started, during which fsFRFSE T2WI scans were continuously acquired to monitor the process. Ablation was terminated when its range covered at least 0.5–1.0 cm beyond the tumor. For incomplete ablations, the position of the microwave antenna was adjusted for supplemental ablation. Once the ablation was completed and the indwelling needle was removed, fsFRFSE T2WI and 3D Dyn T1WI scans of both lungs were acquired to evaluate the technical success rate and find any signs of complications. Last, chest radiographs were acquired one day after MWA, and chest CT scans were conducted three days after MWA to rule out perioperative complications.

COMPLICATION

Complications were evaluated based on the guidelines of the Society of Interventional Radiology. The description of complications follows the proposed standardization of terminology and reporting criteria in this study (9).

Follow-Up and Efficacy Evaluation

One month after MWA, chest MRI with contrast enhancement were performed to evaluate the technical efficacy (9). Subsequent follow-ups were conducted at an interval of 3–4 months using chest CT scans.

Statistical analysis

Parameters that were recorded included the operation time, power, and duration of MWA, incidence of complications, technical success rate, and technical efficacy. Statistical analysis was performed in the SPSS20.0 statistical software. Measurement data was expressed as average ± standard deviation.

RESULTS

MWA Results

All patients were successfully completed MR-guided MWA for lung malignant tumor with a technical success rate of 100%. The average operation time was 71.77 ± 25.71 (36-158) mins. Of all 23 lesions, 12 lesions were treated with single-site ablation and 11 lesions with 2-sites ablation, respectively. The average ablation power and duration were 81.32 ± 7.31 (60-90)W and 5.57 ± 1.71 (3.0-9.0) min, respectively. The average maximum ablation diameter was 3.61 ± 0.52cm(2.59-4.49cm) with the minimum ablation diameter of 2.67 ± 0.45cm(1.51-3.39cm), respectively.

Incidence of Complications

There were 3 cases of pneumothorax either during or after the ablation, with 1 case requiring management by catheterization. One patient had a small amount of hemorrhage during the procedure which stopped after ablation. Ten patients with mostly near pleural tumors experienced intraoperative and postoperative pain, which was alleviated after symptomatic treatment with analgesia. Two patients suffered from a small amount of pleural effusion without catheterization. Other complications included infection (2 patients), which was treated with antibiotics, and low-grade fever (4 patients) which was treated by physical cooling. No serious complications such as bronchopleural fistula and massive hemoptysis were observed in the study.

Follow-Up Results

The average follow-up period was 12.89 ± 4.33 (2.0-19.6) months. During the follow-up, one case colon cancer lung metastasis of local recurrences occurred 4 months after MWA. The resultant technical efficacy was 95.5% (21/22).

Intraoperative MRI Manifestations

Compared with the chest wall muscle, prior to ablation, lesions showed isointense or slightly low signals on T1WI images (**Figure 1A**). Alternatively, on T2WI images, all lesions showed high or slightly high signals (**Figure 1B**). During the intraoperative scan (**Figures 2A, B**), T2WI signal intensity of dynamic scan showed the zone of coagulative necrosis area with hypointense gradually expanded from the center to the outer periphery and covered the hyperintense lesion within time advances. Last, during the postoperative scan, tumors showed decreased T2WI signals surrounded by high signals (**Figures 3A, B**) and increased T1WI signals surrounded by isointense signal bands.

DISCUSSION

Microwave Ablation Guidance

The large amount of air in the lungs provides a natural contrast on computed tomography images. In addition, computed tomography can accurately evaluate ablation complications such as pneumothorax as well as clearly displaying the metal ablation antenna. Therefore, despite its ionization hazard, computed tomography remains the primary guidance method of microwave ablation for lung cancer, positron emission tomography-computed tomography and C-arm computed tomography are based on the same principles (10–12). Microwave ablation for lung cancer is considered successful if the ground glass opacity on the immediate post-ablation computed tomography covers 0.5–1.0 cm beyond the lesion (13). However, the boundary of the ground glass opacity

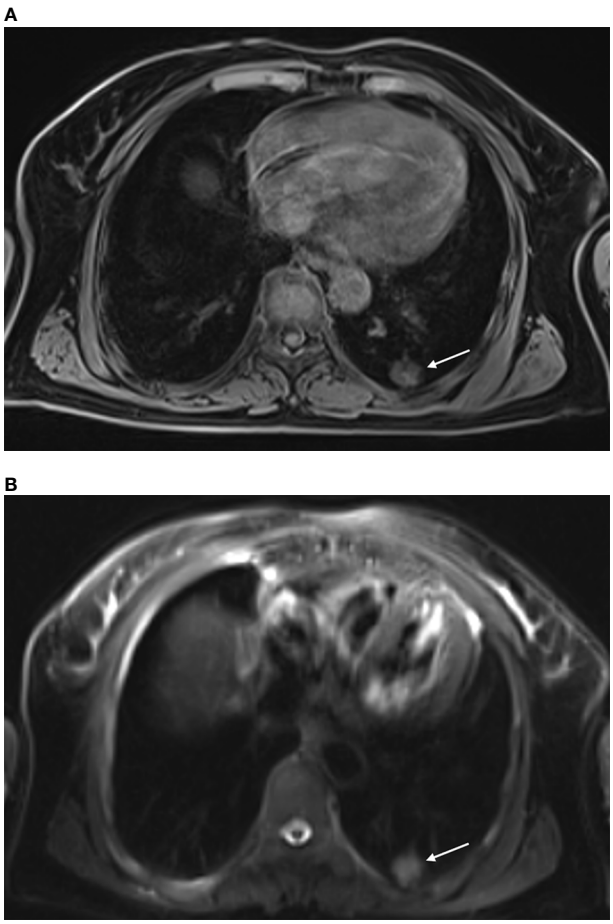

FIGURE 1 | MR-guided MWA for invasive adenocarcinoma of the left lower lobe for 72-year-old woman. Preoperative scan: Preoperative MRI showed a nodule in the left lower lobe, displayed as isointense signals on T1WI [**(A)** arrow] and high signals on fsFRFSE T2WI [**(B)** arrow].

is often unclear on computed tomography and can be covered by pulmonary hemorrhage as a result of puncture, and unobvious density changes in ablated tumor (14).

On the contrary,MR guided MWA has unique advantage including non-radiation especially at young patients, high solution of soft tissue, more precise efficacy assessment and can measure temperature changes non-invasively (14). In this prospective study, we select MR-guided for diameter of lung malignant lesion beyond 5mm and solitary nodule. Therefore, this study investigated the use of MRI to guide MWA for malignant lung tumors.

Feasibility of MR Guidance

Devices and Instruments

MR-guided MWA requires devices and instruments not only made of non-ferromagnetic, but also electromagnetic compatible materials, so that MRI can be acquired simultaneously during ablation without mutual interference. The MWA device and the microwave antenna adopted in this study were both made of non-ferromagnetic materials, allowing them to be placed in the MR scanning room. As a result, connecting cables did not need to be extended, thereby avoiding a substantially reduced ablation range due to microwave output loss. In addition, the MWA device was electromagnetically shielded, while the connecting cable was equipped with a choke coil according to the frequency of the MRI scanner's primary magnetic field (63.637 MHz). Consequently, ablation did not disrupt concurrent MRI, thereby making it possible to perform real-time monitoring of the ablation process to prevent excessive or insufficient ablation.

Microwave Antenna Display

Although the microwave antenna displays clearly in the soft tissue of the chest wall, once it enters the lung tissue with air, neither the antenna itself nor the lung tissue produces a signal on the MRI. Therefore, the fsFRFSE T2WI sequence was adopted in this study to guide the puncture, so that high signals generated by different degrees of pulmonary hemorrhage during puncture could be used to project the non-signal microwave antenna. It was possible to accurately guide the puncture process by comparing the *in vivo* depth of the microwave antenna with the depth measured on the MRI.

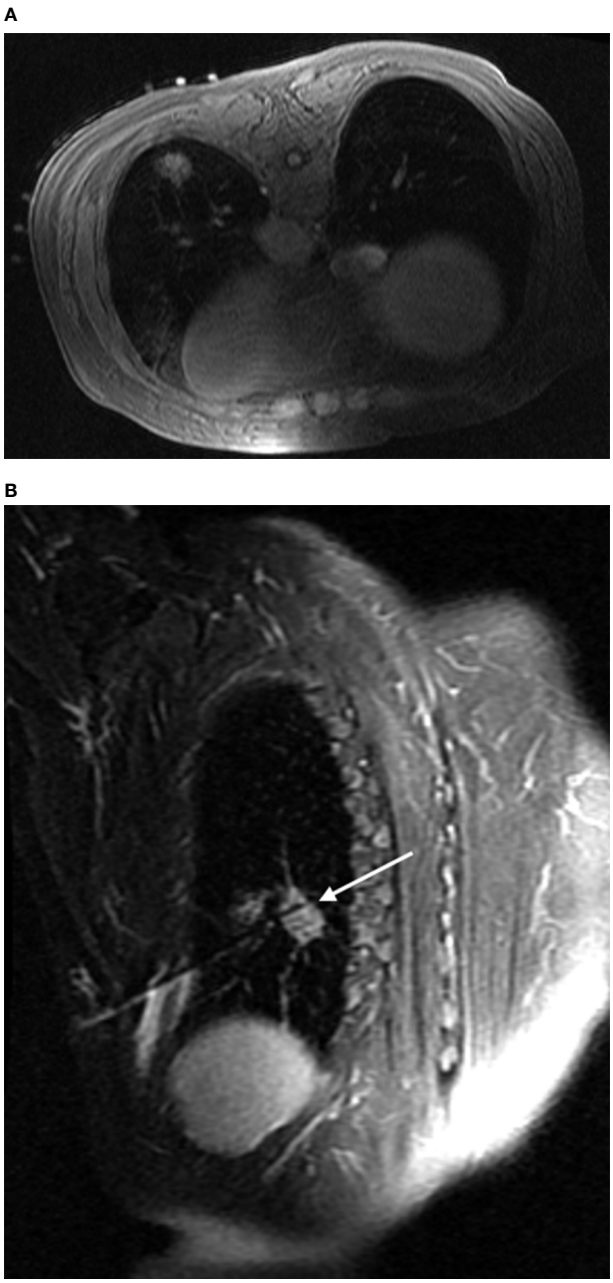

FIGURE 2 | Intraoperative scan: Intraoperative scan was acquired with the patient in the prone position. The lesion showed isointense signals on T1WI, and the hyperintensity marker (cod liver oil matrix) was visible on the patient's surface **(A)**. In the oblique sagittal fsFRFSE T2WI view with the microwave antenna as the long axis, the lesion was seen as high signals, while the microwave antenna displayed as a strip of low signals surrounded by a small amount of high signal due to hemorrhage [**(B)** arrow].

Efficacy and Complications

Among the 22 patients who underwent MR-guided MWA in this study, the technical success rate (100%), the technical efficacy (95.5%), and the incidence of complications were not inferior to those of CT-guided MWA (15–18). MR was also capable of indicating complications such as pneumothorax and hemorrhage and demonstrated unique advantages in efficacy evaluation. Studies have shown that MRI manifestations has a strong correlation with pathological findings (19, 20). In a study performing MWA on rabbit lung VX2 tumors, Chen Jian et al. found that lung VX2 tumors with high signals on T2WI and isointense or low signals on T1WI before MWA, showed significantly reduced T2WI signals and increased T1WI signals after MWA due to coagulation necrosis and dehydration. In contrary, due to inflammatory reaction after thermal injury, the surrounding lung tissue experienced an increase in water

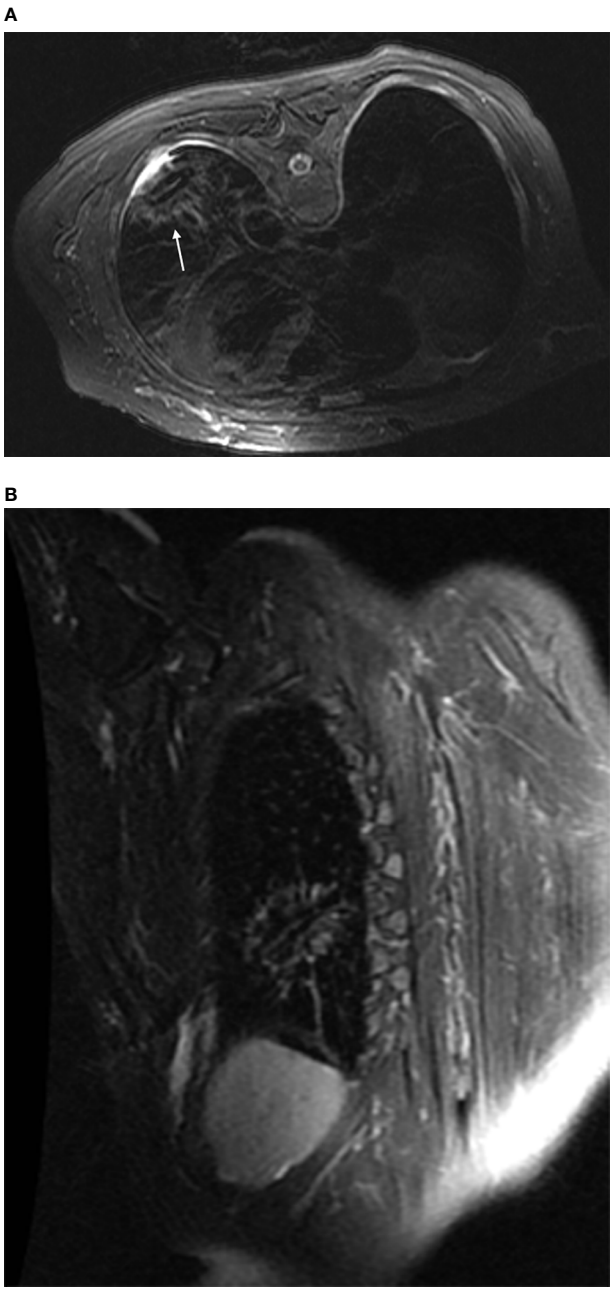

FIGURE 3 | Post-ablation scan: In both the transverse **(A)** and the oblique sagittal **(B)** views fsFRFSE T2WI scans, the ablation foci displayed as obvious low signals surrounded by ring-shaped high-signal shadows. In addition, the microwave antenna displayed as a strip of low signals, and a small amount of fluid was seen in the pleural cavity adjacent to the lesion.

content. This led to high signals on T2WI and isointense signals on T1WI that formed a clear contrast with the ablation foci, thereby facilitating a more accurate identification of the ablation boundary. Meanwhile, Chen Jin et al. (14) performed MR scans on 20 patients with lung cancer immediately after CT-guided radiofrequency ablation and found that MRI was accurate and reliable in the efficacy evaluation. In addition, they reported that bleeding during the puncture process displayed as low signals on T1WI, resulting in significant signal differences with the high signal of ablation foci and the isointense signal of thermal injuries that allowed MRI to provide a better efficacy evaluation than CT. In our study, as the study mention above, the center of the ablated zones showed a short T1 and short T2 signals with the ring-like of long T1 and long T2 signals surrounded by beyond 5mm after immediately evaluation considered as complete ablation.

This study has some shortcomings. First, only 22 cases were included in the study, most of them had a short follow-up period with small lesions, making studies with a larger sample size and a longer follow-up duration necessary. Second, after puncture into the lung, the display of the microwave antenna tract on MRI was not as clear as that on CT, causing a substantially longer operation time of the former. Third, due to the vascular flow effect of MRI, we could not determine the incidence of air embolism, a rare but serious complication.

In conclusion, magnetic resonance-guided microwave ablation for lung malignant tumor is feasible and has unique advantages in efficacy evaluation, making it suitable for guiding microwave ablation for lung lesions in the future.

DATA AVAILABILITY STATEMENT

The raw data supporting the conclusions of this article will be made available by the authors, without undue reservation.

ETHICS STATEMENT

The studies involving human participants were reviewed and approved by the ethics committee of first affiliated hospital of fujian medical univercity. The patients/participants provided their written informed consent to participate in this study

AUTHOR CONTRIBUTIONS

ZL conceptualized the study, prepared figures and tables.RL wrote the article and prepared figures and tables. YF collected the data, carried out the analysis, and prepared the figures and tables. JinC, QL and JiaC participated in drafting and editing the article and assisted in the preparation of figures and tables. YY and JieC participated in figure preparation and drafting and editing the article. All authors contributed to the article and approved the submitted version.

FUNDING

This study was funded by The key Research and Development Programs of Jiangsu,PRC(Social Development Clinical Frontier Technology)(BE2017758),and The Research and Develop Program of Focus Field of Guangdong Province, PRC (2019B110233001).

REFERENCES

1. Sung H, Ferlay J, Siegel RL, Laversanne M, Soerjomataram I, Jemal A, et al. Global Cancer Statistics 2020: GLOBOCAN Estimates of Incidence and Mortality Worldwide for 36 Cancers in 185 Countries. *CA Cancer J Clin* (2021) 71(3):209–49. doi: 10.3322/caac.21660
2. Scott WJ, Howington J, Feigenberg S, Movsas B, Pisters K. American College of Chest Physicians. Treatment of non-Small Cell Lung Cancer Stage I and Stage II: ACCP Evidence-Based Clinical Practice Guidelines (2nd Edition). *Chest* (2007) 132(3 Suppl):234S–42S. doi: 10.1378/chest.07-1378
3. Healey TT, March BT, Baird G, Dupuy DE. Microwave Ablation for Lung Neoplasms: A Retrospective Analysis of Long-Term Results. *J Vasc Interv Radiol* (2017) 28(2):206–11. doi: 10.1016/j.jvir.2016.10.030
4. Vogl TJ, Eckert R, Naguib NN, Beeres M, Gruber-Rouh T, Nour-Eldin NA. Thermal Ablation of Colorectal Lung Metastases: Retrospective Comparison Among Laser-Induced Thermotherapy, Radiofrequency Ablation, and Microwave Ablation. *AJR Am J Roentgenol* (2016) 207(6):1340–9. doi: 10.2214/AJR.15.14401
5. Han X, Yang X, Ye X, Liu Q, Huang G, Wang J, et al. Computed Tomography-Guided Percutaneous Microwave Ablation of Patients 75 Years of Age and Older With Early-Stage Nonsmall Cell Lung Cancer. *Indian J Cancer* (2015) 52 Suppl 2: e56–60. doi: 10.4103/0019-509X.172514
6. Lin Z, Chen J, Yan Y, Chen J, Li Y. Microwave Ablation of Hepatic Malignant Tumors Using 1.5T MRI Guidance and Monitoring: Feasibility and Preliminary Clinical Experience. *Int J Hyperthermia* (2019) 36(1):1216–22. doi: 10.1080/02656736.2019.1690166
7. Li H, Lin Z, Chen J, Guo R. Evaluation of the MR and Pathology Characteristics Immediately Following Percutaneous MR-Guided Microwave Ablation in a Rabbit Kidney VX2 Tumor Implantation Model. *Int J Hyperthermia* (2019) 36 (1):1197–206. doi: 10.1080/02656736.2019.1687944
8. Bing F, Garnon J, Tsoumakidou G, Enescu I, Ramamurthy N, Gangi A. Imaging-Guided Percutaneous Cryotherapy of Bone and Soft-Tissue Tumors: What is the Impact on the Muscles Around the Ablation Site? *AJR Am J Roentgenol* (2014) 202(6):1361–5. doi: 10.2214/AJR.13.11430
9. Ahmed M, Solbiati L, Brace CL, Breen DJ, Callstrom MR, Charboneau JW, et al. Image-Guided Tumor Ablation: Standardization of Terminology and Reporting Criteria–a 10-Year Update. *Radiol* (2014) 273(1):241–60. doi: 10.1148/radiol.14132958
10. Wei Z, Wang J, Ye X, Yang X, Huang G. Computed Tomography-Guided Percutaneous Microwave Ablation of Early Stage Non-Small Cell Lung Cancer in a Pneumonectomy Patient. *Thorac Cancer* (2016) 7(1):151–3. doi: 10.1111/1759-7714.12244
11. Cazzato RL, Battistuzzi JB, Catena V, Grasso RF, Zobel BB, Schena E, et al. Cone-Beam Computed Tomography (CBCT) Versus CT in Lung Ablation Procedure: Which is Faster? *Cardiovasc Intervent Radiol* (2015) 38:1231–6. doi: 10.1007/s00270-015-1078-3
12. Schoellnast H, Larson SM, Nehmeh SA, Carrasquillo JA, Thornton RH, Solomon SB. Radiofrequency Ablation of non-Small-Cell Carcinoma of the Lung Under Real-Time FDG PET CT Guidance. *Cardiovasc Intervent Radiol* (2011) 34 Suppl 2:S182–5. doi: 10.1007/s00270-010-9898-7
13. Pereira PL, Masala S. Cardiovascular and Interventional Radiological Society of Europe (CIRSE). Standards of Practice: Guidelines for Thermal Ablation of Primary and Secondary Lung Tumors. *Cardiovasc Intervent Radiol* (2012) 35 (2):247–54. doi: 10.1007/s00270-012-0340-1
14. Chen J, Lin ZY, Wu ZB, Chen ZW, Chen YP. Magnetic Resonance Imaging Evaluation After Radiofrequency Ablation for Malignant Lung Tumors. *J Cancer Res Ther* (2017) 13(4):669–75. doi: 10.4103/jcrt.JCRT-448-17
15. Welch BT, Brinjikji W, Schmit GD, Callstrom RM, Kurup AN, Cloft HJ, et al. A National Analysis of the Complications, Cost, and Mortality of Percutaneous Lung Ablation. *J Vasc Interv Radiol* (2015) 26(6):787–91. doi: 10.1016/j.jvir.2015.02.019
16. Zheng A, Wang X, Yang X, Wang W, Huang G, Gai Y, et al. Major Complications After Lung Microwave Ablation: A Single-Center Experience on 204 Sessions. *Ann Thorac Surg* (2014) 98(1):243–8. doi: 10.1016/j.athoracsur.2014.03.008
17. Carrafiello G, Mangini M, Fontana F, Massa A, Ierardi A, Cotta E, et al. Complications of Microwave and Radiofrequency Lung Ablation: Personal Experience and Review of the Literature. *Radiol Med* (2012) 117(2):201–13. doi: 10.1007/s11547-011-0741-2
18. Hiraki T, Gobara H, Fujiwara H, Ishii H, Tomita K, Uka M, et al. Lung Cancer Ablation: Complications. *Semin Intervent Radiol* (2013) 30(2):169–75. doi: 10.1055/s-0033-1342958

19. Chen J, Lin XN, Miao XH, Chen J, Lin ZY. Evaluation of the Correlation Between Infrared Thermal Imaging-Magnetic Resonance Imaging-Pathology of Microwave Ablation of Lesions in Rabbit Lung Tumors. *J Cancer Res Ther* (2020) 16(5):1129–33. doi: 10.4103/0973-1482.296428
20. Oyama Y, Nakamura K, Matsuoka T, Toyoshima M, Yamamoto A, Okuma T, et al. Radiofrequency Ablated Lesion in the Normal Porcine Lung: Long-Term Follow-Up With MRI and Pathology. *Cardiovasc Intervent Radiol* (2005) 28 (3):346–53. doi: 10.1007/s00270-004-0156-8

Conflict of Interest: The authors declare that the research was conducted in the absence of any commercial or financial relationships that could be construed as a potential conflict of interest.

Publisher's Note: All claims expressed in this article are solely those of the authors and do not necessarily represent those of their affiliated organizations, or those of the publisher, the editors and the reviewers. Any product that may be evaluated in this article, or claim that may be made by its manufacturer, is not guaranteed or endorsed by the publisher.

frontiers | Frontiers in Oncology

ORIGINAL RESEARCH
published: 15 July 2022
doi: 10.3389/fonc.2022.897329

Risk Prediction Model for Synchronous Oligometastatic Non-Small Cell Lung Cancer: Thoracic Radiotherapy May Not Prolong Survival in High-Risk patients

Chunliu Meng[1†], Fang Wang[1,2†], Jia Tian[1], Jia Wei[3], Xue Li[1], Kai Ren[1], Liming Xu[1], Lujun Zhao[1] and Ping Wang[1*]*

[1] Department of Radiation Oncology, Tianjin Medical University Cancer Institute and Hospital, National Clinical Research Center for Cancer, Tianjin Key Laboratory of Cancer Prevention and Therapy, Tianjin's Clinical Research Center for Cancer, Tianjin, China, [2] Department of Radiation Oncology, Affiliated Hospital of Hebei University, Baoding, China, [3] Department of Oncology, Shandong Provincial Third Hospital, Shandong University, Jinan, China

Background and Purpose: On the basis of the promising clinical study results, thoracic radiotherapy (TRT)[1] has become an integral part of treatment of synchronous oligometastatic non–small cell lung cancer (SOM-NSCLC). However, some of them experienced rapid disease progression after TRT and showed no significant survival benefit. How to screen out such patients is a more concerned problem at present. In this study, we developed a risk-prediction model by screening hematological and clinical data of patients with SOM-NSCLC and identified patients who would not benefit from TRT.

Materials and Methods: We investigated patients with SOM-NSCLC between 2011 and 2019. A formula named Risk-Total was constructed using factors screened by LASSO-Cox regression analysis. Stabilized inverse probability treatment weight analysis was used to match the clinical characteristics between TRT and non-TRT groups. The primary endpoint was overall survival (OS).

Results: We finally included 283 patients divided into two groups: 188 cases for the training cohort and 95 for the validation cohort. Ten prognostic factors included in the Risk-Total formula were age, N stage, T stage, adrenal metastasis, liver metastasis, sensitive mutation status, local treatment status to metastatic sites, systemic inflammatory index, CEA, and Cyfra211. Patients were divided into low- and high-risk groups based on risk scores, and TRT was found to have improved the OS of low-risk patients (46.4 vs. 31.7 months, $P = 0.083$; 34.1 vs. 25.9 months, $P = 0.078$) but not that of high-risk patients (14.9 vs. 11.7 months, $P = 0.663$; 19.4 vs. 18.6 months, $P = 0.811$) in the training and validation sets, respectively.

OPEN ACCESS

Edited by:
Xin Ye,
Qianfoshan Hospital, Shandong University, China

Reviewed by:
Maurizio Valeriani,
Sapienza University of Rome, Italy
Matthew Pierre Deek,
Johns Hopkins Medicine, United States

***Correspondence:**
Lujun Zhao
zhaolujun@tjmuch.com
Ping Wang
wangping@tjmuch.com

[†]These authors have contributed equally to this work

Specialty section:
This article was submitted to Thoracic Oncology, a section of the journal Frontiers in Oncology

Received: *16 March 2022*
Accepted: *16 June 2022*
Published: *15 July 2022*

Citation:
Meng C, Wang F, Tian J, Wei J, Li X, Ren K, Xu L, Zhao L and Wang P (2022) Risk Prediction Model for Synchronous Oligometastatic Non-Small Cell Lung Cancer: Thoracic Radiotherapy May Not Prolong Survival in High-risk Patients. Front. Oncol. 12:897329. doi: 10.3389/fonc.2022.897329

Conclusion: We developed a prediction model to help identify patients with SOM-NSCLC who would not benefit from TRT, and TRT could not improve the survival of high-risk patients.

Keywords: synchronous oligometastasis, non–small cell lung cancer, thoracic radiotherapy, risk prediction model, survival

INTRODUCTION

Non–small cell lung cancer (NSCLC)[2] is a common malignant tumor that accounts for 70%–80% of all lung cancer cases worldwide. NSCLC is associated with high morbidity and mortality rates (1). More than half of patients with NSCLC have stage IV disease at the time of diagnosis, and up to one-third of these patients have synchronous oligometastatic (SOM) disease (2, 3).

SOM disease has been described as a distinct disease entity characterized by reduced metastatic potential with a limited number of metastatic sites (4), which renders it amenable to local treatment (LT). There is no consensus on what specific criteria define SOM-NSCLC. Of note, inclusion criteria for previously cited studies were very different. Recently, the European Organization for Research and Treatment of cancer (EORTC) and the European Society of Radiotherapy & Oncology-American Society for Therapeutic Radiology and Oncology (ESTRO-ASTRO) conferences had attempted to standardize the definition of oligometastatic disease (2, 5). The documents showed that the definition of oligometastatic disease should base on safety of radical treatment rather than the number of metastases, and it would be better the number of metastatic lesions ≤ 5 and the number of metastatic sites ≤ 3, with or without primary sites, and mediastinal metastatic lymph nodes were included. Several clinical trials and multiple retrospectives series have reported favorable outcomes of thoracic radiotherapy (TRT) in highly selected patients with SOM-NSCLC (6–14). However, some of them experienced rapid disease progression after TRT and showed no significant survival benefit. And, to date, no effective predictive model has been developed to help identify patients with SOM-NSCLC who would not benefit from TRT. In this study, we sought to establish a risk prediction model to predict the mortality risk of these patients using baseline hematologic and clinical data and to identify patients who would not benefit from TRT.

Abbreviations: NSCLC, non–small cell lung cancer; LT, local treatment; TRT, thoracic radiotherapy; OS, overall survival; PFS, progression-free survival; TNM, tumor node metastasis; SM, sensitive mutations; EGFR, epidermal growth factor receptor; ALK, anaplastic lymphoma kinase; ROS1, ROS proto-oncogene 1, receptor tyrosine kinase; TPSA, tissue polypeptide–specific antigen; SCC, squamous cell carcinoma antigen; CEA, carcinoembryonic antigen; PLR, platelet-to-lymphocyte ratio; NLR, neutrophil-to-lymphocyte ratio; SII, systemic inflammatory index; LASSO, least absolute shrinkage and selection operator; MST, median survival time; ROC, receiver operator characteristic; AUC, area under the curve; KPS, Karnofsky performance status; SBRT, stereotactic body radiotherapy; IPTW, inverse probability treatment weight.

MATERIALS AND METHODS

Patient Selection

We retrospectively reviewed the medical records of consecutive patients who received a diagnosis of advanced NSCLC at our hospital between January 2011 and December 2019. Clinical staging of the disease at the time of presentation was again determined with reference to the eighth edition of tumor node metastasis classification (15). The inclusion criteria for this study were as follows: (1) confirmed diagnosis of NSCLC based on pathological or cytological specimens, or both; (2) patients were allowed to have up to five lesions of metastatic disease (do not include primary site and enlarged lymph nodes in the mediastinum and supraclavicular) with no more than three sites (2, 5); and (3) availability of gene mutation status information. To determine metastasis status, patients needed to undergo comprehensive imaging tests, including head contrast-enhanced MRI, neck ultrasound, chest–abdomen contrast-enhanced CT plus ECT, or PET-CT. If there was ambiguous metastatic lesion in the liver, then contrast-enhanced abdominal MRI was also necessary. Meanwhile, patients were excluded if they had second primary tumor, pleural or pericardial effusion, meningeal or peritoneal metastases, a metastatic site with ambiguous diagnosis, or incomplete medical records.

Definition of Special Concept

In this study, positively sensitive mutations (SM^+) included the following: *EGFR* (epidermal growth factor receptor) exon 19 deletion, *EGFR* exon 21 Leu858Arg mutation, *ROS* proto-oncogene 1, receptor tyrosine kinase (*ROS1*) fusion mutation, and *ALK* (anaplastic lymphoma kinase) mutation. *EGFR* uncommon mutations, such as exon 18 mutations, exon 20 insertion mutations, and so on, and other non-targeted therapeutic mutations or without any mutation, were defined as sensitive mutation negative (SM^-).

Hematological Markers

Laboratory examinations including routine blood tests, hepatic and renal function tests, and tumor markers of patients were collected before initial treatment. The calculation formulas of neutrophil-to-lymphocyte ratio (NLR), platelet-to-lymphocyte ratio (PLR), and systemic inflammatory index (SII) were as follows: NLR = neutrophil number (10^9/L)/lymphocyte count (10^9/L); PLR = number of platelets (10^9/L)/number of lymphocytes (10^9/L); SII = number of platelets (10^9/L) × number of neutrophils (10^9/L)/number of lymphocytes (10^9/L). The optimal cutoff levels for albumin, leukocyte, PLR, NLR, SII, tissue polypeptide–specific antigen (TPSA), squamous cell

carcinoma antigen (SCC), Ca19-9, carcinoembryonic antigen (CEA), and Cyfra211 were obtained according to overall survival (OS).

Thoracic Radiotherapy

In this study, 150 patients received TRT, and TRT could be carried out before, concomitant or after the systemic treatment. The specific radiotherapy target was determined by patient's attending physician. Generally, gross tumor volume (GTV) included primary lesions with or without mediastinal metastatic lymph nodes, and planning GTV (PGTV) extends 5 mm across the GTV margin. Radiation therapy technology could apply conventional fractionated radiotherapy, hypo-fractionated radiotherapy, and stereotactic body radiotherapy, and the radiation doses were 1.8–2.1 Gy/50–66 Gy, 3 Gy/36–45 Gy, and 9–17 Gy/50–60 Gy, respectively.

First-line Systemic Treatment Strategy

All patients with *EGFR* non-SMs, untargeted therapy mutations or without mutation, underwent first-line chemotherapy after confirmation of the initial NSCLC diagnosis. The treatment included platinum-based doublet chemotherapy such as pemetrexed, paclitaxel, docetaxel, or gemcitabine combined with cisplatin, carboplatin, or nedaplatin. Each chemotherapy session was separated by an interval of 3 to 4 weeks.

Patients with *EGFR*-SMs (exon 19 deletion, exon 21 Leu858Arg mutations) were administered first-line treatment with *EGFR* tyrosine kinase inhibitors (TKIs), such as gefitinib, erlotinib, and icotinib, or with chemotherapy mentioned above and then TKIs after disease progression. Patients with *ALK* and *ROS1* mutation were administered first-line treatment with crizotinib or with chemotherapy as aforesaid and then TKIs after disease progression.

Data Analysis and Statistical Considerations

The primary endpoint was OS defined as the time from the date of diagnosis until death or the most recent follow-up. The follow-up schedule began from the time of treatment to the final follow-up on December 17, 2021. The data on the date of death or at the final follow-up visit were acquired from hospital records or through direct correspondence with the family of the patient. R 4.1.1 and SPSS 24.0 software were used for statistical analyses. The Chi-squared test (or the Fisher's exact test as applicable) was used to compare the clinical characteristics between groups. OS was estimated using the Kaplan–Meier method, and between-group differences in OS were assessed using the log-rank test. The optimal cutoff values of hematological markers were determined using the package "survminer" based on OS. Using the "glmnet" and "survival" packages and a backward–forward stepwise method, LASSO-Cox regression analysis was performed to select the optimal prognostic factors. The "predict" function of package "survival" was used to calculate the risk score of each patient. Time-dependent receiver operator characteristic (ROC) analyses were conducted using the "timeROC" package. Package "IPWsurvival" was used for stabilized inverse probability treatment weight (IPTW) analyses.

RESULTS

Patient Characteristics

This study had been approved by the Ethics Committee of Tianjin Medical University Cancer Hospital (ab2022138). A total of 2,194 patients were diagnosed with advanced NSCLC at our hospital during the study reference period. Of these, 1,624, 23, 54, 76, and 134 patients were excluded due to extensive metastatic lesions, second primary tumors, pleural effusion, lack of gene sequencing results, and incomplete medical records, respectively.

Finally, 283 patients with SOM-NSCLC fulfilled the inclusion criteria for this study. The median OS was 23.4 months, and the 1-, 3-, and 5-year OS rates were 73.3%, 30.1%, and 11.5%, respectively. The entire cohort was randomly divided into two groups by a ratio of 2:1, 188 cases in the training set and 95 cases in the validation set, respectively. The median OS were 22.7 and 24.4 months, respectively; and 1-, 3-, and 5-year OS rates were 72.1%, 31.4%, and 12.7% and 75.6%, 27.0%, and 9.1%, respectively; and there was no difference in survival between sets (P = 0.655). The patient characteristics were summarized in **Table 1**.

Construction of Risk-Total Formula in the Training Set

In the training set, hematological markers, including albumin, leukocyte, PLR, NLR, SII, TPSA, SCC, Ca199, CEA, and Cyfra211, were divided into low and high groups according to the respective optimal cutoff levels (**Table 2**).

To assess the mortality risk of each patient in the training set, we established a prognostic scoring system named Risk-Total using LASSO-Cox regression model (**Figure A.1**). Hematological markers mentioned above and other clinical variables, such as age, sex, Karnofsky performance status (KPS), smoking, histopathology, T stage, N stage, brain metastasis, bone metastasis, adrenal metastasis, liver metastasis, SM status, and LT status to metastatic site status before progression disease (PD), were included in the analysis. In this model, low albumin, high leukocyte, high PLR, high NLR, high SII, high TPSA, high SCC, high Ca199, high CEA, high Cyfra211, age ≥ 65, male, KPS < 80, smoking, N1–3, T3–4, non-adenocarcinoma, presence of brain metastasis, bone metastasis, adrenal metastasis, liver metastasis, SM^-, and metastatic sites receiving partial or no LT before PD were assigned in level 2, and the corresponding alternatives were assigned in level 1.

Finally, 10 variables were included in the optimal model (AIC = 1,251.94, $P < 2.2 \times 10^{-16}$) as follows: Risk-Total = 1 × HR-value (age) × HR-value (N stage) × HR-value (T stage) × HR-value (adrenal metastasis) × HR-value (liver metastasis) × HR-value (SM status) × HR-value (LT status to metastatic sites

TABLE 1 | Clinical characteristics of patients.

Characteristics	Training set (N=188) No. of patients (%)	Validation set (N=95) No. of patients (%)	*P* value
Age			0.266
<65	116 (61.7)	65 (68.4)	
≥65	72 (38.3)	30 (31.6)	
Mean ± SD	61.2 ± 9.28	60.0 ± 8.11	0.282
Sex			0.082
Male	134 (71.3)	58 (61.1)	
Female	54 (28.7)	37 (38.9)	
KPS			0.773
<80	14 (7.4)	8 (8.4)	
≥80	174 (92.6)	87 (91.6)	
Smoking			0.017*
No	71 (37.8)	50 (52.6)	
Yes	117 (62.2)	45 (47.4)	
Histopathology			0.328
Adenocarcinoma	130 (69.1)	71 (74.7)	
Non-adenocarcinoma	58 (30.9)	24 (25.3)	
N stage			0.253
N0	47 (25.0)	18 (18.9)	
N1-3	141 (75.0)	77 (81.1)	
T stage			0.282
T1-2	125 (66.5)	57 (60.0)	
T3-4	63 (33.5)	38 (40.0)	
SM			0.153
Yes	61 (32.4)	39 (41.1)	
No	127 (67.6)	56 (8.9)	
LT status to metastatic sites before PD			0.764
All	60 (31.9)	32 (33.7)	
Partly or no	128 (68.1)	63 (66.3)	
Brain metastasis	38 (20.2)	13 (13.7)	0.177
Bone metastasis	82 (43.6)	48 (50.5)	0.271
Adrenal metastasis	22 (11.7)	9 (9.5)	0.571
Liver metastasis	5 (2.7)	1 (1.1)	0.653
TRT			0.968
CFR	49 (26.1)	23 (24.2)	
HFR	15 (8.0)	7 (7.4)	
SBRT	37(19.7)	19 (20.0)	
Albumin (g/L)	42.1 ± 4.19	41.1 ± 3.88	0.060
Leukocyte (10^9/L)	7.6 ± 2.46	7.3 ± 1.99	0.366
PLR	171.8 ± 92.61	165.3 ± 72.76	0.551
NLR	3.1 ± 2.05	3.2 ± 3.18	0.730
SII	888.0 ± 675.57	836.1 ± 572.67	0.522
TPSA (U/L)	114.2 ± 209.5	130.4 ± 222.36	0.548
SCC (μg/L)	2.5 ± 6.92	2.5 ± 6.95	0.926
Ca19-9 (U/mL)	40.1 ± 82.74	52.9 ± 153.82	0.366
CEA (μg/L)	39.6 ± 106.26	73.9 ± 183.17	0.094
Cyfra211 (μg/L)	6.6 ± 9.13	11.2 ± 23.00	0.064

*$P<0.05$.

KPS, Karnofsky performance status; SM, sensitive mutation; LT, local treatment; PD, progress disease; TRT, thoracic radiotherapy; CFR, conventional fractionated radiotherapy; HFR, hypo-fractionated radiotherapy; SBRT, stereotactic body radiotherapy; PLR, platelet to lymphocyte ratio; NLR, neutrophils to lymphocyte ratio; SII, systemic inflammatory index; TPSA, tissue polypeptide specific antigen; SCC, squamous cell carcinoma antigen; CEA, carcinoembryonic antigen.

before PD) × HR-value (SII) × HR-value (CEA) × HR-value (Cyfra211) (**Table 3**). According to the median Risk-Total value (10.0658), patients were divided into low-risk and high-risk groups, and the median survival time (MST) were 37.6 and 13.4 months, respectively ($P < 0.001$; **Figure 1A**). Meanwhile, the prognostic accuracy of Risk-Total was evaluated by time-dependent ROC analyses, with 2-, 3-, and 4-year AUC values of 0.873, 0.836, and 0.875, respectively, which confirmed the excellent prognostic power of it (**Figure 1B**). The patient characteristics between low- and high-risk groups were displayed in **Table 4**.

Validation of Risk-Total Formula in the Validation Set

In the validation set, patients' hematological markers were grouped on the basis of cutoff value, as shown in **Table 2**, and the risk score were calculated on the basis of Risk-Total formula, as shown in **Table 3**. Then, according to the median value

TABLE 2 | Cutoff level and univariate Cox analyses of hematological markers in the training set.

Characteristics	Cutoff	Categories	*P* value
Albumin	45.40	High (≥ 45.40) vs. Low (< 45.40)	0.014*
Leukocyte	7.82	High (≥ 7.82) vs. Low (< 7.82)	0.009*
PLR	112.24	High (≥112.24) vs. Low (<112.24)	0.096
NLR	1.63	High (≥ 1.63) vs. Low (< 1.63)	0.007*
SII	366.36	High (≥ 366.36) vs. Low (< 366.36)	0.001*
TPSA	95.56	High (≥ 95.56) vs. Low (< 95.56)	0.001*
SCC	1.60	High (≥ 1.60) vs. Low (< 1.60)	< 0.001*
Ca19-9	7.45	High (≥ 7.45) vs. Low (< 7.45)	0.197
CEA	2.00	High (≥ 2.00) vs. Low (< 2.00)	0.009*
Cyfra211	3.71	High (≥ 3.71) vs. Low (< 3.71)	< 0.001*

**P<0.05.*

PLR, platelet to lymphocyte ratio; NLR, neutrophils to lymphocyte ratio; SII, systemic inflammatory index; TPSA, tissue polypeptide specific antigen; SCC, squamous cell carcinoma antigen; CEA, carcinoembryonic antigen.

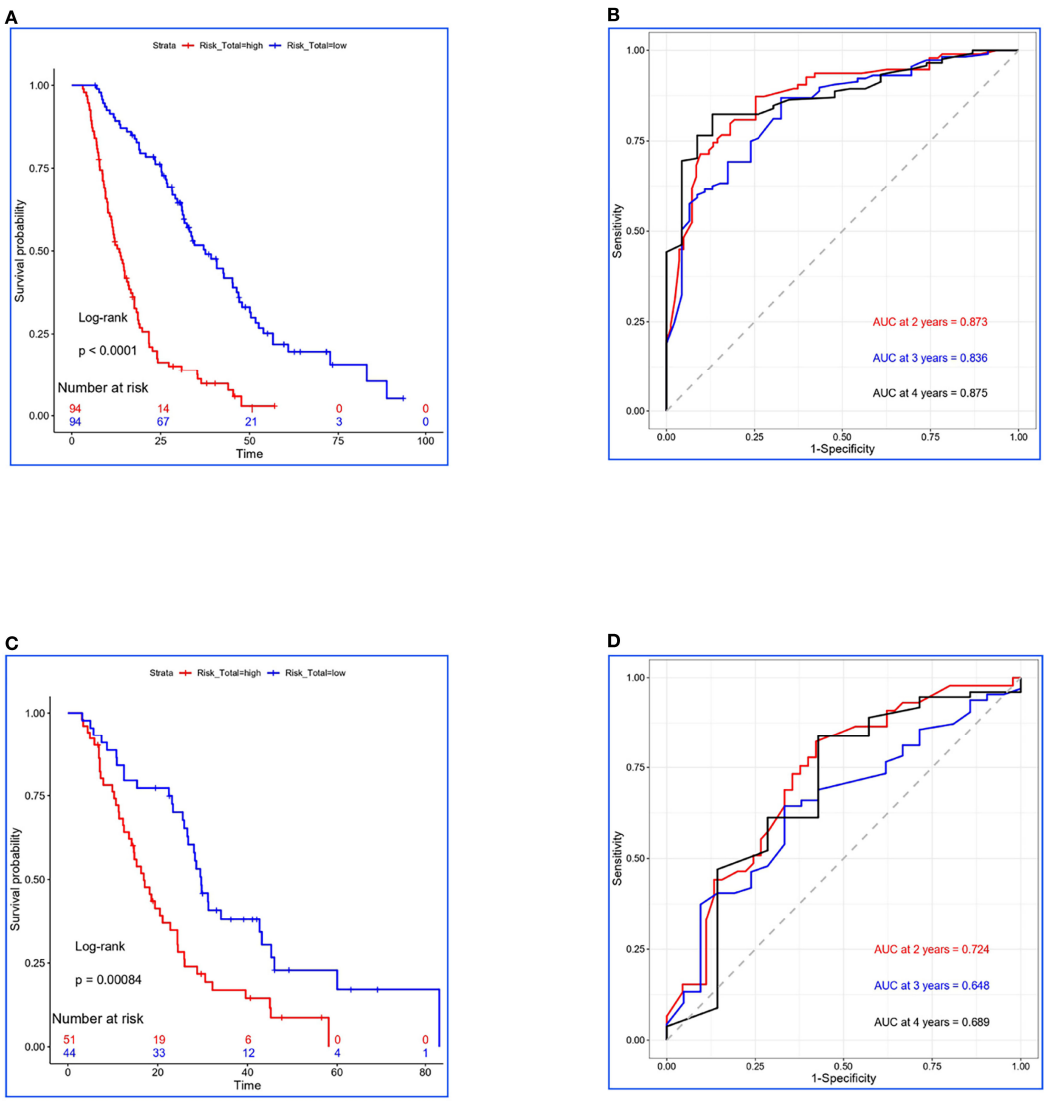

FIGURE 1 | Construction and validation for Risk-Total. **(A, C)** Kaplan–Meier survival analyses of Risk-Total in the training set and the validation set. **(B, D)** Risk-Total performance in time-dependent receiver operating characteristic (ROC) curves in the training set and the validation set.

TABLE 3 | Factors included in the Risk-Total formula.

Characteristics	Level	Coefficient	HR-value	*P* value
Age	1 = <65	0.3372	1	0.05597
	2 = ≥65		1.4010	
N stage	1 = N0	0.3463	1	0.08476
	2 = N1-3		1.4138	
T stage	1 = T1-2	0.4127	1	0.02272*
	2 = T3-4		1.5109	
Adrenal metastasis	1 = no	0.4580	1	0.06697
	2 = yes		1.5810	
Liver metastasis	1 = no	1.0923	1	0.02658*
	2 = yes		2.9811	
SM status	1 = SM^+	0.8548	1	9.09×e-06*
	2 = SM^-		2.3510	
LT status to metastatic sites before PD	1 = All	0.5407	1	0.00505*
	2 = Partly or no		1.7172	
SII	1 = low	0.9098	1	0.00348*
	2 = high		2.4838	
CEA	1 = low	-0.6275	1	0.01300*
	2 = high		0.5339	
Cyfra211	1 = low	0.8142	1	1.19×e-05*
	2 = high		2.2574	

**P<0.05.*

SM, sensitive mutation; PD, progress disease; SII, systemic inflammatory index; CEA, carcinoembryonic antigen.

*Risk-Total = 1*HR-value (age) *HR-value (N stage) *HR-value (T stage) *HR-value (adrenal metastasis) *HR-value (liver metastasis) *HR-value (SM status) *HR-value (LT to metastatic sites status before PD) *HR-value (SII) *HR-value (CEA) *HR-value (Cyfra211).*

TABLE 4 | Clinical characteristics of low- and high-risk patients in the training set.

Characteristics	Low risk (N=94) No. of patients (%)	High risk (N=94) No. of patients (%)	*P* value
Age			0.134
<65	63 (67.0)	53 (56.4)	
≥65	31 (33.0)	41 (43.6)	
Mean ± SD	59.6 ± 9.76	62.8 ± 8.53	0.017*
Sex			0.010*
Male	59 (62.8)	75 (79.8)	
Female	35 (37.2)	19 (20.2)	
KPS			0.578
<80	8 (8.5)	6 (6.4)	
≥80	86 (91.5)	88 (93.6)	
Smoking			0.001*
No	47 (50.0)	24 (25.5)	
Yes	47 (50.0)	70 (74.5)	
Histopathology			0.001*
Adenocarcinoma	76 (80.9)	54 (57.4)	
Non-adenocarcinoma	18 (19.1)	40 (42.6)	
N stage			0.029*
N0	30 (31.9)	17 (18.1)	
N1-3	64 (68.9)	77 (81.9)	
T stage			<0.001*
T1-2	77 (81.9)	48 (51.1)	
T3-4	17 (19.1)	46 (48.9)	
SM			<0.001*
Yes	50 (53.2)	11 (41.1)	
No	44 (46.8)	83 (8.9)	
LT status to metastatic sites before PD			0.001*
All	41 (43.6)	19 (20.2)	
Partly or no	53 (56.4)	75 (79.8)	
Brain metastasis	21 (22.3)	17 (18.1)	0.468
Bone metastasis	48 (51.1)	34 (36.2)	0.039*
Adrenal metastasis	4 (4.3)	18 (19.1)	0.001*
Liver metastasis	1 (1.1)	4 (4.3)	0.365

(Continued)

TABLE 4 | Continued

Characteristics	Low risk (N=94) No. of patients (%)	High risk (N=94) No. of patients (%)	*P* value
TRT			0.283
CFR	22 (23.4)	27 (28.7)	
HFR	8 (8.5)	7 (7.4)	
SBRT	23 (24.5)	14 (14.9)	
Albumin (g/L)	42.5 ± 4.64	41.7 ± 3.67	0.165
Leukocyte (10^9/L)	7.4 ± 2.74	7.8 ± 2.13	0.304
PLR	163.1 ± 63.81	180.5 ± 114.12	0.200
NLR	3.2 ± 2.45	3.0 ± 1.57	0.507
SII	838.4 ± 570.29	937.6 ± 766.49	0.316
TPSA (U/L)	91.7 ± 144.8	136.8 ± 257.35	0.140
SCC (μg/L)	1.8 ± 7.19	3.2 ± 6.61	0.165
Ca19-9 (U/mL)	30.8 ± 61.31	49.5 ± 99.15	0.122
CEA (μg/L)	39.6 ± 106.26	73.9 ± 183.17	0.130
Cyfra211 (μg/L)	5.1 ± 8.39	8.0 ± 9.64	0.027*

**P<0.05.*

KPS, Karnofsky performance status; SM, sensitive mutation; LT, local treatment; PD, progress disease; TRT, thoracic radiotherapy; CFR, conventional fractionated radiotherapy; HFR, hypo-fractionated radiotherapy; SBRT, stereotactic body radiotherapy; PLR, platelet to lymphocyte ratio; NLR, neutrophils to lymphocyte ratio; SII, systemic inflammatory index; TPSA, tissue polypeptide specific antigen; SCC, squamous cell carcinoma antigen; CEA, carcinoembryonic antigen.

(10.0658) mentioned above, patients were divided into low-risk and high-risk groups, and the MST were 29.7 and 16.9 months, respectively (P = 0.00084; **Figure 1C**). Similarly, the prognostic accuracy of Risk-Total was also evaluated by time-dependent ROC analyses, with 2-, 3-, and 4-year AUC values of 0.724, 0.648, and 0.689, respectively (**Figure 1D**). These results confirmed the super prognostic power of Risk-Total in another heterogeneous population. The patient characteristics between low- and high-risk groups are shown in **Table 5**.

Prognostic Value of TRT for Low- and High- risk Patients

In the training set, 54 of 94 patients with low-risk received TRT, and survival analysis showed improvement in OS (42.8 vs. 32.4 months, P = 0.070; **Figure 2A**). However, the inter-group clinical characteristics were very unbalanced, especially with respect to age, gender, LT status to metastatic sites, and PLR (**Table 6A**). Therefore, we applied the stabilized IPTW analysis to calculate the weights of clinical variables and match them. After matching,

TABLE 5 | Clinical characteristics of low- and high-risk patients in the validation set.

Characteristics	Low risk (N=44) No. of patients (%)	High risk (N=51) No. of patients (%)	*P* value
Age			0.085
<65	34 (77.3)	31 (60.8)	
≥65	10 (22.7)	20 (39.2)	
Mean ± SD	58.5 ± 7.47	61.3 ± 8.47	0.092
Sex			0.227
Male	24 (54.5)	34 (66.7)	
Female	20 (45.5)	17 (33.3)	
KPS			1.000
<80	4 (9.1)	4 (7.8)	
≥80	40 (90.9)	47 (92.2)	
Smoking			0.046*
No	28 (63.6)	22 (43.1)	
Yes	16 (36.4)	29 (56.9)	
Histopathology			0.051
Adenocarcinoma	37 (84.1)	34 (66.7)	
Non-adenocarcinoma	7 (15.9)	17 (33.3)	
N stage			0.054
N0	12 (27.3)	6 (11.8)	
N1-3	32 (72.7)	45 (88.2)	
T stage			<0.001*
T1-2	36 (81.8)	21 (41.2)	
T3-4	8 (18.2)	30 (58.8)	
SM			<0.001*
Yes	31 (70.5)	8 (15.7)	

(Continued)

TABLE 5 | Continued

Characteristics	Low risk (N=44) No. of patients (%)	High risk (N=51) No. of patients (%)	*P* value
No	13 (29.5)	43 (84.3)	
LT status to metastatic sites before PD			0.007*
All	21 (47.7)	11 (21.6)	
Partly or no	23 (52.3)	40 (78.4)	
Brain metastasis	7 (15.9)	6 (11.8)	0.558
Bone metastasis	29 (65.9)	19 (37.3)	0.005*
Adrenal metastasis	1 (2.3)	8 (15.7)	0.061
Liver metastasis	1 (2.3)	0 (0.0)	0.941
TRT			0.227
CFR	11 (25.0)	12 (23.5)	
HFR	4 (9.1)	3 (5.9)	
SBRT	11 (31.8)	5 (9.8)	
Albumin (g/L)	41.4 ± 3.75	40.8 ± 4.00	0.454
Leukocyte (10^9/L)	7.1 ± 2.08	7.6 ± 1.91	0.234
PLR	159.1 ± 70.64	170.7 ± 74.81	0.440
NLR	2.9 ± 2.18	3.5 ± 3.85	0.346
SII	790.2 ± 665.89	875.6 ± 481.41	0.472
TPSA (U/L)	81.9 ± 98.81	172.3 ± 284.07	0.037*
SCC (μg/L)	1.3 ± 1.79	3.5 ± 9.27	0.109
Ca19-9 (U/mL)	29.0 ± 61.30	52.9 ± 153.82	0.139
CEA (μg/L)	39.6 ± 106.26	73.4 ± 200.80	0.108
Cyfra211 (μg/L)	5.8 ± 9.64	15.8 ± 29.46	0.025*

**P<0.05.*

KPS, Karnofsky performance status; SM, sensitive mutation; LT, local treatment; PD, progress disease; TRT, thoracic radiotherapy; CFR, conventional fractionated radiotherapy; HFR, hypo-fractionated radiotherapy; SBRT, stereotactic body radiotherapy; PLR, platelet to lymphocyte ratio; NLR, neutrophils to lymphocyte ratio; SII, systemic inflammatory index; TPSA, tissue polypeptide specific antigen; SCC, squamous cell carcinoma antigen; CEA, carcinoembryonic antigen.

TRT was still found to improve the OS (46.4 vs. 31.7 months, P = 0.083; **Figure 2B**). Whereas, 47 of 94 patients with high-risk received TRT, but the OS was not prolonged (15.5 vs. 11.4 months, P = 0.300; **Figure 2C**). When the clinical variables were calculated weights and matched (**Table 6B**), the survival time was not improved all the same (14.9 vs. 11.7 months, P = 0.663; **Figure 2D**).

In the validation set, 29 of 44 low-risk patients received TRT, and the OS was prolonged 8.2 months (34.1 vs. 25.9 months, P = 0.080; **Figure 3A**). In addition, stabilized IPTW analysis was used to match the clinical characteristics (**Table 6C**), and the between-group differences in OS were close to statistical as ever (34.1 vs. 25.9 months, P = 0.078; **Figure 3B**). Meanwhile, 51 patients were divided into high-risk group, and 20 of them received TRT with no improvement in OS (17.1 vs. 14.7 months, P = 0.400; **Figure 3C**). On the basis of the clinical characteristics, the TRT group had more patients with no treatment to metastatic sites, which may have influenced the result (**Table 6D**). Similarly, we applied stabilized IPTW analysis to match the groups. After matching, TRT was not found to have improved survival as before (19.4 vs. 18.6 months, P = 0.811; **Figure 3D**).

DISCUSSION

In the current study, we established a risk prediction model to predict the mortality risk of patients with SOM-NSCLC and, further, to identify patients who would not benefit from TRT. Eventually, a total of 283 cases met the inclusion criteria and were divided into the training and validation sets. A Risk-Total formula constructed by 10 clinical prognostic factors was used to calculate each patient's risk score, and patients were divided into low- and high-risk groups according to the median value (10.0658) in the training set. Then, TRT was found to just have improved the survival of low-risk patients (P = 0.083) but not that of high-risk patients (P = 0.663) in the training set. Similarly, patients in the validation set were estimated risk-score on the basis of the Risk-Total formula, and were grouped into low- and high-risk groups basing on the median value (10.0658), and TRT only prolonged the OS of low-risk patients (P = 0.078) but not that of the high-risk patients (P = 0.811).

The biological characteristics of oligometastatic cancer are increasingly being defined, and the role of LT has evolved substantially during the past decade. In 2018, a prospective, multicenter, single-arm, phase 2 trial reported the long-term outcomes of consolidative radiation therapy (CRT) to the primary and metastatic sites from oligometastatic NSCLC, achieving a partial response or stable disease after three to six cycles of platinum-based chemotherapy. The median PFS and OS were 11.2 and 28.4 months, respectively, which met the primary endpoint and transcended the historical record (13). The first multicenter randomized trial of local consolidative therapy (LCT) for highly selected oligometastatic NSCLC (≤3 metastatic lesions, no progression after front-line systemic therapy) demonstrated significant PFS (14.2 vs. 4.4 months) and OS (41.2 vs. 17.0 months) benefit compared with patients

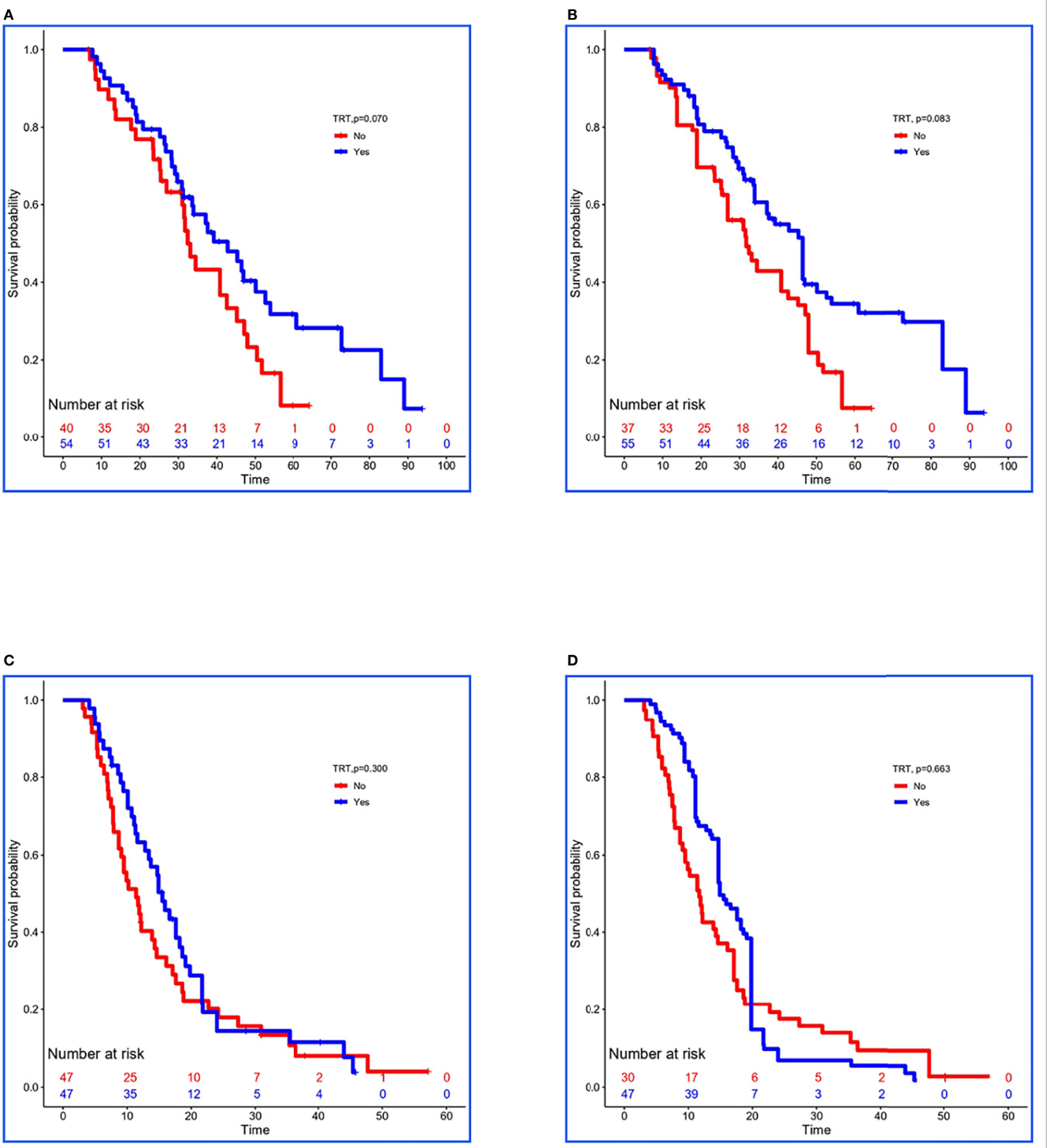

FIGURE 2 | Kaplan–Meier survival analyses for patients between groups. **(A, B)** Survival curves for low-risk patients between non-TRT and TRT groups when clinical characteristics were unmatched and matched using stabilized IPTW analysis in the training set. **(C, D)** Survival curves for high-risk patients between non-TRT and TRT groups when clinical characteristics were unmatched and matched using stabilized IPTW analysis in the training set.

TABLE 6 | Comparison of clinical characteristics of patients in no-TRT and TRT subgroups.

A

		Unmatched			Stabilized IPTW		
	Level	**no-TRT (%)**	**TRT (%)**	***P***	**no-TRT (%)**	**TRT (%)**	***P***
Number		40	54		36.8	55	
Age	<65	33 (82.5)	32 (59.3)	0.029	25.6 (69.6)	38.8 (70.5)	0.937
	>=65	7 (17.5)	22 (40.7)		11.2 (30.4)	16.2 (29.5)	
Gender	female	20 (50.0)	14 (25.9)	0.029	15.1 (41.1)	22.2 (40.3)	0.952
	male	20 (50.0)	40 (74.1)		21.7 (58.9)	32.8 (59.7)	
KPS	>=80	37 (92.5)	49 (90.7)	1.000	34.8 (94.5)	51.0 (92.8)	0.723
	<80	3 (7.5)	5 (9.3)		2.0 (5.5)	4.0 (7.2)	
Smoking	no	21 (52.5)	25 (46.3)	0.699	18.0 (48.8)	30.6 (55.7)	0.594
	yes	19 (47.5)	29 (53.7)		18.8 (51.2)	24.4 (44.3)	
Histopathology	adenocarcinoma	36 (90.0)	44 (81.5)	0.393	29.1 (79.0)	46.2 (84.0)	0.651
	non-adenocarcinoma	4 (10.0)	10 (18.5)		7.7 (21.0)	8.8 (16.0)	
N stage	N0	10 (25.0)	23 (42.6)	0.122	11.8 (32.1)	18.3 (33.3)	0.921
	N1-3	30 (75.0)	31 (57.4)		25.0 (67.9)	36.6 (66.7)	
T stage	T1-2	34 (85.0)	47 (87.0)	1.000	32.9 (89.4)	48.8 (88.7)	0.910
	T3-4	6 (15.0)	7 (13.0)		3.9 (10.6)	6.2 (11.3)	
Brain metastasis	no	31 (77.5)	39 (72.2)	0.733	29.4 (79.8)	43.0 (78.2)	0.869
	yes	9 (22.5)	15 (27.8)		7.4 (20.2)	12.0 (21.8)	
Bone metastasis	no	18 (45.0)	30 (55.6)	0.422	17.4 (47.3)	26.1 (47.5)	0.993
	yes	22 (55.0)	24 (44.4)		19.4 (52.7)	28.9 (52.5)	
Adrenal metastasis	no	37 (92.5)	52 (96.3)	0.729	35.1 (95.4)	52.8 (96.1)	0.882
	yes	3 (7.5)	2 (3.7)		1.7 (4.6)	2.2 (3.9)	
SM status	SM+	25 (62.5)	28 (51.9)	0.413	20.4 (55.6)	31.7 (57.7)	0.869
	SM-	15 (37.5)	26 (48.1)		16.4 (44.4)	23.3 (42.3)	
LT to metastatic sites before PD	all	13 (32.5)	31 (57.4)	0.029	13.5 (36.6)	23.3 (42.4)	0.641
	partly or no	27 (67.5)	23 (42.6)		23.3 (63.4)	31.7 (57.6)	
Albumin	high	8 (20.0)	14 (25.9)	0.671	6.5 (17.6)	10.9 (19.8)	0.790
	low	32 (80.0)	40 (74.1)		30.3 (82.4)	44.1 (80.2)	
Leukocyte	low	27 (67.5)	40 (74.1)	0.641	25.8 (70.0)	41.6 (75.7)	0.603
	high	13 (32.5)	14 (25.9)		11.1 (30.0)	13.3 (24.3)	
PLR	low	8 (20.0)	24 (44.4)	0.024	12.6 (34.2)	17.3 (31.4)	0.827
	high	32 (80.0)	30 (55.6)		24.2 (65.8)	37.7 (68.6)	
NLR	low	5 (12.5)	12 (22.2)	0.347	8.1 (22.1)	9.5 (17.2)	0.656
	high	35 (87.5)	42 (77.8)		28.7 (77.9)	45.5 (82.8)	
SII	low	6 (15.0)	16 (29.6)	0.159	9.5 (25.9)	13.4 (24.3)	0.901
	high	34 (85.0)	38 (70.4)		27.3 (74.1)	41.6 (75.7)	
TPSA	low	31 (77.5)	46 (85.2)	0.493	31.4 (85.4)	47.1 (85.7)	0.973
	high	9 (22.5)	8 (14.8)		5.4 (14.6)	7.9 (14.3)	
SCC	low	38 (95.0)	47 (87.0)	0.346	33.6 (91.4)	49.3 (89.8)	0.834
	high	2 (5.0)	7 (13.0)		3.2 (8.6)	5.6 (10.2)	
Ca199	low	11 (27.5)	13 (24.1)	0.891	7.4 (20.1)	10.1 (18.5)	0.846
	high	29 (72.5)	41 (75.9)		29.4 (79.9)	44.8 (81.5)	
CEA	low	0 (0.0)	4 (7.4)	0.214	0.0 (0.0)	2.3 (4.2)	0.135
	high	40 (100.0)	50 (92.6)		36.8 (100.0)	52.7 (95.8)	
Cyfra211	low	25 (62.5)	37 (68.5)	0.697	25.4 (69.1)	40.2 (73.1)	0.714
	high	15 (37.5)	17 (31.5)		11.4 (30.9)	14.8 (26.9)	

B

		Unmatched			Stabilized IPTW		
	Level	**no-TRT (%)**	**TRT (%)**	***P***	**no-TRT (%)**	**TRT (%)**	***P***
Number		47	47		30.4	47.2	
Age	<65	28 (59.6)	23 (48.9)	0.408	16.9 (55.5)	27.2 (57.6)	0.893
	>=65	19 (40.4)	24 (51.1)		13.5 (44.5)	20.0 (42.4)	
Gender	female	14 (29.8)	6 (12.8)	0.078	7.4 (24.3)	3.4 (7.3)	0.018
	male	33 (70.2)	41 (87.2)		23.0 (75.7)	43.7 (92.7)	
KPS	>=80	44 (93.6)	44 (93.6)	1.000	28.2 (92.7)	43.9 (93.1)	0.949
	<80	3 (6.4)	3 (6.4)		2.2 (7.3)	3.2 (6.9)	

(Continued)

Table 6 | Continued

B

		Unmatched			Stabilized IPTW		
	Level	**no-TRT (%)**	**TRT (%)**	***P***	**no-TRT (%)**	**TRT (%)**	***P***
Smoking	no	15 (31.9)	10 (21.3)	0.350	8.5 (27.8)	6.1 (13.0)	0.092
	yes	32 (68.1)	37 (78.7)		21.9 (72.2)	41.1 (87.0)	
Histopathology	adenocarcinoma	30 (63.8)	20 (42.6)	0.063	19.7 (64.9)	27.9 (59.1)	0.697
	non-adenocarcinoma	17 (36.2)	27 (57.4)		10.7 (35.1)	19.3 (40.9)	
N stage	N0	3 (6.4)	11 (23.4)	0.043	2.0 (6.4)	6.0 (12.6)	0.317
	N1-3	44 (93.6)	36 (76.6)		28.5 (93.6)	41.2 (87.4)	
T stage	T1-2	22 (46.8)	22 (46.8)	1.000	13.2 (43.5)	22.3 (47.2)	0.820
	T3-4	25 (53.2)	25 (53.2)		17.2 (56.5)	24.9 (52.8)	
Brain metastasis	no	40 (85.1)	40 (85.1)	1.000	26.3 (86.5)	41.9 (88.9)	0.757
	yes	7 (14.9)	7 (14.9)		4.1 (13.5)	5.3 (11.1)	
Bone metastasis	no	29 (61.7)	29 (61.7)	1.000	16.9 (55.7)	18.1 (38.3)	0.236
	yes	18 (38.3)	18 (38.3)		13.5 (44.3)	29.1 (61.7)	
Adrenal metastasis	no	40 (85.1)	37 (78.7)	0.592	26.0 (85.4)	40.2 (85.2)	0.987
	yes	7 (14.9)	10 (21.3)		4.5 (14.6)	7.0 (14.8)	
Liver metastasis	no	44 (93.6)	45 (95.7)	1.000	28.8 (94.5)	46.0 (97.5)	0.392
	yes	3 (6.4)	2 (4.3)		1.7 (5.5)	1.2 (2.5)	
SM status	SM+	7 (14.9)	1 (2.1)	0.065	3.5 (11.5)	0.5 (1.1)	0.007
	SM-	40 (85.1)	46 (97.9)		26.9 (88.5)	46.7 (98.9)	
LT to metastatic sites before PD	all	1 (2.1)	15 (31.9)	0.001	0.6 (1.9)	7.6 (16.0)	0.015
	partly or no	46 (97.9)	32 (68.1)		29.8 (98.1)	39.6 (84.0)	
Albumin	high	4 (8.5)	4 (8.5)	1.000	2.5 (8.4)	2.5 (5.2)	0.533
	low	43 (91.5)	43 (91.5)		27.9 (91.6)	44.7 (94.8)	
Leukocyte	low	22 (46.8)	24 (51.1)	0.837	14.2 (46.8)	22.6 (47.9)	0.946
	high	25 (53.2)	23 (48.9)		16.2 (53.2)	24.6 (52.1)	
PLR	low	6 (12.8)	8 (17.0)	0.772	3.4 (11.2)	4.5 (9.5)	0.774
	high	41 (87.2)	39 (83.0)		27.0 (88.8)	42.7 (90.5)	
NLR	low	1 (2.1)	3 (6.4)	0.609	0.8 (2.6)	1.8 (3.8)	0.744
	high	46 (97.9)	44 (93.6)		29.6 (97.4)	45.4 (96.2)	
SII	low	0 (0.0)	3 (6.4)	0.241	0.0 (0.0)	1.5 (3.2)	0.260
	high	47 (100.0)	44 (93.6)		30.4 (100.0)	45.7 (96.8)	
TPSA	low	26 (55.3)	28 (59.6)	0.835	17.4 (57.2)	27.3 (57.8)	0.971
	high	21 (44.7)	19 (40.4)		13.0 (42.8)	19.9 (42.2)	
SCC	low	31 (66.0)	29 (61.7)	0.830	20.7 (68.1)	32.7 (69.4)	0.925
	high	16 (34.0)	18 (38.3)		9.7 (31.9)	14.4 (30.6)	
Ca199	low	6 (12.8)	13 (27.7)	0.123	4.4 (14.5)	11.3 (24.0)	0.399
	high	41 (87.2)	34 (72.3)		26.0 (85.5)	35.9 (76.0)	
CEA	low	3 (6.4)	13 (27.7)	0.014	2.1 (7.0)	7.0 (14.9)	0.255
	high	44 (93.6)	34 (72.3)		28.3 (93.0)	40.2 (85.1)	
Cyfra211	low	4 (8.5)	14 (29.8)	0.018	4.4 (14.5)	8.3 (17.6)	0.759
	high	43 (91.5)	33 (70.2)		26.0 (85.5)	38.9 (82.4)	

C

		Unmatched			Stabilized IPTW		
	Level	**no-TRT (%)**	**TRT (%)**	***P***	**no-TRT (%)**	**TRT (%)**	***P***
Number		15	29		5.1	19.1	
Age	<65	14 (93.3)	21 (72.4)	0.216	4.8 (93.3)	13.8 (72.4)	0.111
	>=65	1 (6.7)	8 (27.6)		0.3 (6.7)	5.3 (27.6)	
Gender	female	8 (53.3)	13 (44.8)	0.828	2.7 (53.3)	8.6 (44.8)	0.599
	male	7 (46.7)	16 (55.2)		2.4 (46.7)	10.5 (55.2)	
KPS	>=80	13 (86.7)	27 (93.1)	0.880	4.4 (86.7)	17.8 (93.1)	0.490
	<80	2 (13.3)	2 (6.9)		0.7 (13.3)	1.3 (6.9)	
Smoking	no	10 (66.7)	19 (65.5)	1.000	3.4 (66.7)	12.5 (65.5)	0.940
	yes	5 (33.3)	10 (34.5)		1.7 (33.3)	6.6 (34.5)	
Histopathology	adenocarcinoma	13 (86.7)	25 (86.2)	1.000	4.4 (86.7)	16.5 (86.2)	0.967
	non-adenocarcinoma	2 (13.3)	4 (13.8)		0.7 (13.3)	2.6 (13.8)	
N stage	N0	2 (13.3)	10 (34.5)	0.256	0.7 (13.3)	6.6 (34.5)	0.144
	N1-3	13 (86.7)	19 (65.5)		4.4 (86.7)	12.5 (65.5)	

(Continued)

Table 6 | Continued

C

		Unmatched			Stabilized IPTW		
	Level	**no-TRT (%)**	**TRT (%)**	***P***	**no-TRT (%)**	**TRT (%)**	***P***
T stage	T1-2	11 (73.3)	25 (86.2)	0.524	3.8 (73.3)	16.5 (86.2)	0.304
	T3-4	4 (26.7)	4 (13.8)		1.4 (26.7)	2.6 (13.8)	
Brain metastasis	no	11 (73.3)	25 (86.2)	0.524	3.8 (73.3)	16.5 (86.2)	0.304
	yes	4 (26.7)	4 (13.8)		1.4 (26.7)	2.6 (13.8)	
Bone metastasis	no	4 (26.7)	12 (41.4)	0.528	1.4 (26.7)	7.9 (41.4)	0.346
	yes	11 (73.3)	17 (58.6)		3.8 (73.3)	11.2 (58.6)	
Adrenal metastasis	no	15 (100.0)	28 (96.6)	1.000	5.1 (100.0)	18.5 (96.6)	0.596
	yes	0 (0.0)	1 (3.4)		0.0 (0.0)	0.7 (3.4)	
Liver metastasis	no	14 (93.3)	29 (100.0)	0.734	4.8 (93.3)	19.1 (100.0)	0.059
	yes	1 (6.7)	0 (0.0)		0.3 (6.7)	0.0 (0.0)	
SM status	SM+	14 (93.3)	18 (62.1)	0.064	4.8 (93.3)	11.9 (62.1)	0.031
	SM-	1 (6.7)	11 (37.9)		0.3 (6.7)	7.3 (37.9)	
LT to metastatic sites before PD	all	5 (33.3)	17 (58.6)	0.203	1.7 (33.3)	11.2 (58.6)	0.120
	partly or no	10 (66.7)	12 (41.4)		3.4 (66.7)	7.9 (41.4)	
Albumin	high	0 (0.0)	5 (17.2)	0.227	0.0 (0.0)	3.3 (17.2)	0.182
	low	15 (100.0)	24 (82.8)		5.1 (100.0)	15.8 (82.8)	
Leukocyte	low	12 (80.0)	20 (69.0)	0.673	4.1 (80.0)	13.2 (69.0)	0.445
	high	3 (20.0)	9 (31.0)		1.0 (20.0)	5.9 (31.0)	
PLR	low	5 (33.3)	9 (31.0)	1.000	1.7 (33.3)	5.9 (31.0)	0.879
	high	10 (66.7)	20 (69.0)		3.4 (66.7)	13.2 (69.0)	
NLR	low	3 (20.0)	6 (20.7)	1.000	1.0 (20.0)	4.0 (20.7)	0.958
	high	12 (80.0)	23 (79.3)		4.1 (80.0)	15.2 (79.3)	
SII	low	3 (20.0)	5 (17.2)	1.000	1.0 (20.0)	3.3 (17.2)	0.825
	high	12 (80.0)	24 (82.8)		4.1 (80.0)	15.8 (82.8)	
TPSA	low	10 (66.7)	26 (89.7)	0.144	3.4 (66.7)	17.1 (89.7)	0.069
	high	5 (33.3)	3 (10.3)		1.7 (33.3)	2.0 (10.3)	
SCC	low	14 (93.3)	24 (82.8)	0.613	4.8 (93.3)	15.8 (82.8)	0.342
	high	1 (6.7)	5 (17.2)		0.3 (6.7)	3.3 (17.2)	
Ca199	low	4 (26.7)	10 (34.5)	0.852	1.4 (26.7)	6.6 (34.5)	0.604
	high	11 (73.3)	19 (65.5)		3.8 (73.3)	12.5 (65.5)	
CEA	low	2 (13.3)	4 (13.8)	1.000	0.7 (13.3)	2.6 (13.8)	0.967
	high	13 (86.7)	25 (86.2)		4.4 (86.7)	16.5 (86.2)	
Cyfra211	low	4 (26.7)	20 (69.0)	0.019	1.4 (26.7)	13.2 (69.0)	0.011
	high	11 (73.3)	9 (31.0)		3.8 (73.3)	5.9 (31.0)	

D

		Unmatched			Stabilized IPTW		
	Level	**no-TRT (%)**	**TRT (%)**	***P***	**no-TRT (%)**	**TRT (%)**	***P***
Number		31	20		27.8	16.2	
Age	<65	18 (58.1)	12 (60.0)	1.000	14.1 (50.8)	7.1 (43.6)	0.665
	>=65	13 (41.9)	8 (40.0)		13.7 (49.2)	9.1 (56.4)	
Gender	female	8 (25.8)	8 (40.0)	0.449	7.4 (26.5)	5.3 (32.4)	0.678
	male	23 (74.2)	12 (60.0)		20.4 (73.5)	11.0 (67.6)	
KPS	>=80	29 (93.5)	18 (90.0)	1.000	26.3 (94.7)	15.3 (94.2)	0.937
	<80	2 (6.5)	2 (10.0)		1.5 (5.3)	0.9 (5.8)	
Smoking	no	11 (35.5)	10 (50.0)	0.461	10.0 (36.2)	6.3 (38.7)	0.871
	yes	20 (64.5)	10 (50.0)		17.7 (63.8)	9.9 (61.3)	
Histopathology	adenocarcinoma	23 (74.2)	10 (50.0)	0.143	19.0 (68.5)	9.9 (60.9)	0.640
	non-adenocarcinoma	8 (25.8)	10 (50.0)		8.8 (31.5)	6.3 (39.1)	
N stage	N0	2 (6.5)	4 (20.0)	0.307	4.1 (14.6)	3.2 (19.5)	0.739
	N1-3	29 (93.5)	16 (80.0)		23.7 (85.4)	13.0 (80.5)	
T stage	T1-2	15 (48.4)	6 (30.0)	0.312	13.6 (48.8)	6.4 (39.6)	0.598
	T3-4	16 (51.6)	14 (70.0)		14.2 (51.2)	9.8 (60.4)	
Brain metastasis	no	28 (90.3)	18 (90.0)	1.000	25.6 (92.3)	15.2 (94.0)	0.788
	yes	3 (9.7)	2 (10.0)		2.1 (7.7)	1.0 (6.0)	
Bone metastasis	no	17 (54.8)	14 (70.0)	0.430	14.1 (50.7)	9.6 (59.2)	0.622
	yes	14 (45.2)	6 (30.0)		13.7 (49.3)	6.6 (40.8)	

(Continued)

Table 6 | Continued

D

	Level	Unmatched			Stabilized IPTW		
		no-TRT (%)	TRT (%)	*P*	no-TRT (%)	TRT (%)	*P*
Adrenal metastasis	no	25 (80.6)	18 (90.0)	0.615	23.1 (83.0)	13.2 (81.7)	0.928
	yes	6 (19.4)	2 (10.0)		4.7 (17.0)	3.0 (18.3)	
SM status	SM+	5 (16.1)	2 (10.0)	0.838	5.1 (18.2)	3.4 (21.1)	0.854
	SM-	26 (83.9)	18 (90.0)		22.7 (81.8)	12.8 (78.9)	
LT to metastatic sites before PD	all	2 (6.5)	8 (40.0)	0.010	1.9 (6.8)	3.5 (21.5)	0.124
	partly or no	29 (93.5)	12 (60.0)		25.9 (93.2)	12.7 (78.5)	
Albumin	high	5 (16.1)	3 (15.0)	1.000	5.0 (18.1)	3.7 (23.0)	0.750
	low	26 (83.9)	17 (85.0)		22.7 (81.9)	12.5 (77.0)	
Leukocyte	low	17 (54.8)	9 (45.0)	0.690	16.3 (58.6)	8.2 (50.9)	0.642
	high	14 (45.2)	11 (55.0)		11.5 (41.4)	8.0 (49.1)	
PLR	low	4 (12.9)	2 (10.0)	1.000	5.3 (19.0)	3.5 (21.6)	0.873
	high	27 (87.1)	18 (90.0)		22.5 (81.0)	12.7 (78.4)	
NLR	low	2 (6.5)	1 (5.0)	1.000	3.3 (12.1)	1.8 (11.2)	0.950
	high	29 (93.5)	19 (95.0)		24.4 (87.9)	14.4 (88.8)	
SII	low	2 (6.5)	1 (5.0)	1.000	3.3 (12.1)	1.8 (11.2)	0.950
	high	29 (93.5)	19 (95.0)		24.4 (87.9)	14.4 (88.8)	
TPSA	low	14 (45.2)	12 (60.0)	0.454	12.3 (44.2)	7.8 (48.4)	0.806
	high	17 (54.8)	8 (40.0)		15.5 (55.8)	8.4 (51.6)	
SCC	low	21 (67.7)	14 (70.0)	1.000	20.4 (73.3)	11.5 (71.1)	0.888
	high	10 (32.3)	6 (30.0)		7.4 (26.7)	4.7 (28.9)	
Ca199	low	7 (22.6)	8 (40.0)	0.309	7.5 (27.2)	4.7 (28.8)	0.912
	high	24 (77.4)	12 (60.0)		20.2 (72.8)	11.5 (71.2)	
CEA	low	4 (12.9)	5 (25.0)	0.465	4.8 (17.1)	2.5 (15.6)	0.899
	high	27 (87.1)	15 (75.0)		23.0 (82.9)	13.7 (84.4)	
Cyfra211	low	6 (19.4)	4 (20.0)	1.000	4.9 (17.8)	2.4 (15.1)	0.802
	high	25 (80.6)	16 (80.0)		22.8 (82.2)	13.8 (84.9)	

KPS, Karnofsky performance status; SM, sensitive mutation; LT, local treatment; PD, progress disease; TRT, thoracic radiotherapy; PLR, platelet to lymphocyte ratio; NLR, neutrophils to lymphocyte ratio; SII, systemic inflammatory index; TPSA, tissue polypeptide specific antigen; SCC, squamous cell carcinoma antigen; CEA, carcinoembryonic antigen.

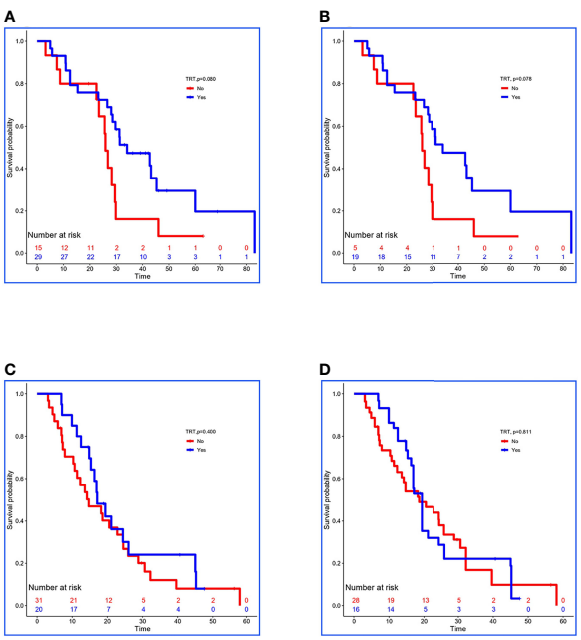

FIGURE 3 | Kaplan–Meier survival analyses for patients between groups. **(A, B)** Survival curves for low-risk patients between non-TRT and TRT groups when clinical characteristics were unmatched and matched using stabilized IPTW analysis in the validation set. **(C, D)** Survival curves for high-risk patients between non-TRT and TRT groups when clinical characteristics were unmatched and matched using stabilized IPTW analysis in the validation set.

who received maintenance therapy or observation (8). Another single-center randomized phase 2 study of maintenance chemotherapy alone versus stereotactic ablative radiotherapy followed by maintenance chemotherapy for patients with limited metastatic NSCLC (primary plus up to five metastatic sites) with no *EGFR*-targetable or *ALK*-targetable mutations but who did achieve a partial response or stable disease after induction chemotherapy also obtained gratifying results (7). Despite differences in the population inclusion criteria in these clinical trials, there was significant prolongation of OS (range of 28.4–41.2 months). However, some patients with SOM-NSCLC experienced rapid disease progression after TRT and showed no significant survival benefit. However, to date, no effective predictive model has been developed to help identify patients who would not benefit from TRT. Hence, in the present study, we established a risk prediction model to predict the mortality risk of patients with SOM-NSCLC and, further, to identify patients who would not benefit from TRT.

Several hematological and clinical factors have been shown to suggest a bad prognosis for lung cancer including hypoalbuminemia (16–18); increase of C-reactive protein (18, 19), lactate dehydrogenase (20), PLR (17, 21–23), NLR (17, 21–24), SII (17, 21), and tumor biomarkers (20, 25); abnormal coagulation and fibrinolysis (26, 27); high T and N stage; liver metastasis; adrenal metastasis (28, 29); absence of SMs; smoking history; male; and loss of weight (30). In the present study, 10 variables were included in the Risk-Total formula, and the level of risk score was associated with reduced survival of patients, which was consistent with previous studies. According to this model, we found that TRT just improve the survival of low-risk patients but not that of high-risk.

In recent years, immunotherapy has transformed the treatment approach for patients with advanced NSCLC. The combination of immunotherapy and LCT for these potentially curable patients is an area of active investigation. Bauml et al. (31) randomized 51 patients who had oligometastatic NSCLC (≤4 metastatic sites) and had completed LT to all known sites of disease to receive pembrolizumab. The median PFS was significantly greater than historical data (P = 0.005), and 1- and 2-year OS rates were 90.9% and 77.5%, respectively. Nevertheless, in our study, immunotherapy status was not included in the analysis, which may affect the practicality of this prediction model in the era of immunotherapy.

LIMITATIONS

Some limitations of our study should be considered. Most importantly, because of the retrospective study design, the diagnosis of metastatic sites was not based on homogenous imaging techniques. Next, local and systematic treatments were also inconsistent, which may have influenced survival. Finally, this study was based on the experience of a single institution, and the number of patients was limited. Future multicenter studies are required to verify this model and to refine the treatment method for primary lesion.

CONCLUSION

The prognosis of SOM-NSCLC is significantly influenced by many hematological and clinical factors. A prediction model was developed in this study to help identify patients who would not benefit from TRT, and we found that TRT improved the survival of low-risk patients but not that of the high-risk patients.

DATA AVAILABILITY STATEMENT

The original contributions presented in the study are included in the article/supplementary material. Further inquiries can be directed to the corresponding authors.

ETHICS STATEMENT

The studies involving human participants were reviewed and approved by Department of Ethics Committee, Tianjin Medical University Cancer Institute and Hospital. Written informed consent for participation was not required for this study in accordance with the national legislation and the institutional requirements.

AUTHOR CONTRIBUTIONS

CM: Conceptualization, Methodology, Formal analysis, Investigation, Writing - Original Draft. FW: Conceptualization, Methodology, Formal analysis, Investigation. JT, JW, and XL: Investigation. KR and LX: Methodology. LZ and PW: Writing - Review and Editing. All authors contributed to the article and approved the submitted version.

FUNDING

This work was supported by the Chinese National Key Research and Development Project (Grant No. 2018YFC1315601), and the National Natural Science Foundation of China (No.81903121).

REFERENCES

1. Sung H, Ferlay J, Siegel RL, Laversanne M, Soerjomataram I, Jemal A, et al. Global Cancer Statistics 2020: GLOBOCAN Estimates of Incidence and Mortality Worldwide for 36 Cancers in 185 Countries. *CA Cancer J Clin* (2021) 71(3):209–249. doi: 10.3322/caac.21660
2. Levy A, Hendriks LEL, Berghmans T, Faivre-Finn C, GiajLevra M, GiajLevra N, et al. EORTC Lung Cancer Group Survey on the Definition of NSCLC Synchronous Oligometastatic Disease. *Eur J Cancer* (2019) 122:109–14. doi: 10.1016/j.ejca.2019.09.012
3. Parikh RB, Cronin AM, Kozono DE, Oxnard GR, Mak RH, Jackman DM, et al. Definitive Primary Therapy in Patients Presenting With Oligometastatic

non-Small Cell Lung Cancer. *Int J Radiat Oncol Biol Phys* (2014) 89(4):880–7. doi: 10.1016/j.ijrobp.2014.04.007
4. Hellman S, Weichselbaum RR. Oligometastases. *J Clin Oncol* (1995) 13(1):8–10. doi: 10.1200/JCO.1995.13.1.8
5. Lievens Y, Guckenberger M, Gomez D, Hoyer M, Iyengar P, Kindts I, et al. Defining Oligometastatic Disease From a Radiation Oncology Perspective: An ESTRO-ASTRO Consensus Document. *Radiother Oncol* (2020) 148:157–66. doi: 10.1016/j.radonc.2020.04.003
6. Xu Q, Zhou F, Liu H, Jiang T, Li X, Xu Y, et al. Consolidative Local Ablative Therapy Improves the Survival of Patients With Synchronous Oligometastatic NSCLC Harboring EGFR Activating Mutation Treated With First-Line EGFR-TKIs. *J Thorac Oncol* (2018) 13(9):1383–92. doi: 10.1016/j.jtho.2018.05.019
7. Iyengar P, Wardak Z, Gerber DE, Tumati V, Ahn C, Hughes RS, et al. Consolidative Radiotherapy for Limited Metastatic Non-Small-Cell Lung Cancer: A Phase 2 Randomized Clinical Trial. *JAMA Oncol* (2018) 4(1): e173501. doi: 10.1001/jamaoncol.2017.3501
8. Gomez D, Tang C, Zhang J, Blumenschein G, Hernandez M, Lee J, et al. Local Consolidative Therapy Vs. Maintenance Therapy or Observation for Patients With Oligometastatic Non-Small-Cell Lung Cancer Long-Term Results of a Multi-Institutional, Phase II, Randomized Study. *J Clin Oncol* (2019) 37 (18):1558–65. doi: 10.1200/JCO.19.00201
9. Palma DA, Olson R, Harrow S, Gaede S, Louie AV, Haasbeek C, et al. Stereotactic Ablative Radiotherapy Versus Standard of Care Palliative Treatment in Patients With Oligometastatic Cancers (SABR-COMET): A Randomised, Phase 2, Open-Label Trial. *Lancet* (2019) 393(10185):2051–8. doi: 10.1016/S0140-6736(18)32487-5
10. Lopez Guerra JL, Gomez D, Zhuang Y, Hong DS, Heymach JV, Swisher SG, et al. Prognostic Impact of Radiation Therapy to the Primary Tumor in Patients With non-Small Cell Lung Cancer and Oligometastasis at Diagnosis. *Int J Radiat Oncol Biol Phys* (2012) 84(1):e61–7. doi: 10.1016/j.ijrobp.2012.02.054
11. Ashworth AB, Senan S, Palma DA, Riquet M, Ahn YC, Ricardi U, et al. An Individual Patient Data Metaanalysis of Outcomes and Prognostic Factors After Treatment of Oligometastatic non-Small-Cell Lung Cancer. *Clin Lung Cancer* (2014) 15(5):346–55. doi: 10.1016/j.cllc.2014.04.003
12. Collen C, Christian N, Schallier D, Meysman M, Duchateau M, Storme G, et al. Phase II Study of Stereotactic Body Radiotherapy to Primary Tumor and Metastatic Locations in Oligometastatic Nonsmall-Cell Lung Cancer Patients. *Ann Oncol* (2014) 25(10):1954–9. doi: 10.1093/annonc/mdu370
13. Petty WJ, Urbanic JJ, Ahmed T, Hughes R, Levine B, Rusthoven K, et al. Long-Term Outcomes of a Phase 2 Trial of Chemotherapy With Consolidative Radiation Therapy for Oligometastatic Non-Small Cell Lung Cancer. *Int J Radiat Oncol Biol Phys* (2018) 102(3):527–35. doi: 10.1016/j.ijrobp.2018.06.400
14. Farooqi A, Ludmir EB, Mitchell KG, Antonoff MB, Tang C, Lee P, et al. Increased Biologically Effective Dose (BED) to the Primary Tumor is Associated With Improved Survival in Patients With Oligometastatic NSCLC. *Radiother Oncol* (2021) 163:114–8. doi: 10.1016/j.radonc.2021.08.005
15. Chansky K, Detterbeck FC, Nicholson AG, Rusch VW, Vallieres E, Groome P, et al. The IASLC Lung Cancer Staging Project: External Validation of the Revision of the TNM Stage Groupings in the Eighth Edition of the TNM Classification of Lung Cancer. *J Thorac Oncol* (2017) 12(7):1109–21. doi: 10.1016/j.jtho.2017.04.011
16. Meng C, Wei J, Tian J, Ma J, Liu N, Yuan Z, et al. Estimating Survival and Clinical Outcome in Advanced non-Small Cell Lung Cancer With Bone-Only Metastasis Using Molecular Markers. *J Bone Oncol* (2021) 31:100394. doi: 10.1016/j.jbo.2021.100394
17. Qi J, Zhang J, Ge X, Wang X, Xu L, Liu N, et al. The Addition of Peripheral Blood Inflammatory Indexes to Nomogram Improves the Predictive Accuracy of Survival in Limited-Stage Small Cell Lung Cancer Patients. *Front Oncol* (2021) 11:713014. doi: 10.3389/fonc.2021.713014
18. Ni XF, Wu J, Ji M, Shao YJ, Xu B, Jiang JT, et al. Effect of C-Reactive Protein/Albumin Ratio on Prognosis in Advanced non-Small-Cell Lung Cancer. *Asia Pac J Clin Oncol* (2018) 14(6):402–9. doi: 10.1111/ajco.13055
19. Cetin K, Christiansen CF, Jacobsen JB, Norgaard M, Sorensen HT. Bone Metastasis, Skeletal-Related Events, and Mortality in Lung Cancer Patients: A Danish Population-Based Cohort Study. *Lung Cancer* (2014) 86(2):247–54. doi: 10.1016/j.lungcan.2014.08.022
20. Gu W, Hu M, Xu L, Ren Y, Mei J, Wang W, et al. The Ki-67 Proliferation Index-Related Nomogram to Predict the Response of First-Line Tyrosine Kinase Inhibitors or Chemotherapy in Non-Small Cell Lung Cancer Patients With Epidermal Growth Factor Receptor-Mutant Status. *Front Med (Lausanne)* (2021) 8:728575. doi: 10.3389/fmed.2021.728575
21. Tong YS, Tan J, Zhou XL, Song YQ, Song YJ. Systemic Immune-Inflammation Index Predicting Chemoradiation Resistance and Poor Outcome in Patients With Stage III non-Small Cell Lung Cancer. *J Transl Med* (2017) 15(1):221. doi: 10.1186/s12967-017-1326-1
22. Chen C, Yang H, Cai D, Xiang L, Fang W, Wang R. Preoperative Peripheral Blood Neutrophil-to-Lymphocyte Ratios (NLR) and Platelet-to-Lymphocyte Ratio (PLR) Related Nomograms Predict the Survival of Patients With Limited-Stage Small-Cell Lung Cancer. *Trans Lung Cancer Res* (2021) 10 (2):866–77. doi: 10.21037/tlcr-20-997
23. Zhang N, Jiang J, Tang S, Sun G. Predictive Value of Neutrophil-Lymphocyte Ratio and Platelet-Lymphocyte Ratio in Non-Small Cell Lung Cancer Patients Treated With Immune Checkpoint Inhibitors: A Meta-Analysis. *Int Immunopharmacol* (2020) 85:106677. doi: 10.1016/j.intimp.2020.106677
24. Huang W, Wang S, Zhang H, Zhang B, Wang C. Prognostic Significance of Combined Fibrinogen Concentration and Neutrophil-to-Lymphocyte Ratio in Patients With Resectable non-Small Cell Lung Cancer. *Cancer Biol Med* (2018) 15(1):88–96. doi: 10.20892/j.issn.2095-3941.2017.0124
25. Dall'Olio FG, Abbati F, Facchinetti F, Massucci M, Melotti B, Squadrilli A, et al. CEA and CYFRA 21-1 as Prognostic Biomarker and as a Tool for Treatment Monitoring in Advanced NSCLC Treated With Immune Checkpoint Inhibitors. *Ther Adv Med Oncol* (2020) 12:1758835920952994. doi: 10.1177/1758835920952994
26. Bharadwaj AG, Holloway RW, Miller VA, Waisman DM. Plasmin and Plasminogen System in the Tumor Microenvironment: Implications for Cancer Diagnosis, Prognosis, and Therapy, Cancers (Basel) 13(8):1838. (2021). doi: 10.3390/cancers13081838
27. Guo J, Gao Y, Gong Z, Dong P, Mao Y, Li F, et al. Plasma D-Dimer Level Correlates With Age, Metastasis, Recurrence, Tumor-Node-Metastasis Classification (TNM), and Treatment of Non-Small-Cell Lung Cancer (NSCLC) Patients. *BioMed Res Int* (2021) 2021:9623571. doi: 10.1155/2021/9623571
28. Nakazawa K, Kurishima K, Tamura T, Kagohashi K, Ishikawa H, Satoh H, et al. Specific Organ Metastases and Survival in Small Cell Lung Cancer. *Oncol Lett* (2012) 4(4):617–20. doi: 10.3892/ol.2012.792
29. Riihimäki M, Hemminki A, Fallah M, Thomsen H, Sundquist K, Sundquist J, et al. Metastatic Sites and Survival in Lung Cancer. *Lung Cancer* (2014) 86 (1):78–84. doi: 10.1016/j.lungcan.2014.07.020
30. Wang J, Zhao Y, Wang Q, Zhang L, Shi J, Wang Z, et al. Prognostic Factors of Refractory NSCLC Patients Receiving Anlotinib Hydrochloride as the Third- or Further-Line Treatment. *Cancer Biol Med* (2018) 15(4):443–51. doi: 10.20892/j.issn.2095-3941.2018.0158
31. Bauml JM, Mick R, Ciunci C, Aggarwal C, Davis C, Evans T, et al. Pembrolizumab After Completion of Locally Ablative Therapy for Oligometastatic Non-Small Cell Lung Cancer: A Phase 2 Trial. *JAMA Oncol* (2019) 5(9):1283–90. doi: 10.1001/jamaoncol.2019.1449

Conflict of Interest: The authors declare that the research was conducted in the absence of any commercial or financial relationships that could be construed as a potential conflict of interest.

Publisher's Note: All claims expressed in this article are solely those of the authors and do not necessarily represent those of their affiliated organizations, or those of the publisher, the editors and the reviewers. Any product that may be evaluated in this article, or claim that may be made by its manufacturer, is not guaranteed or endorsed by the publisher.

frontiers | Frontiers in Oncology

TYPE Clinical Trial
PUBLISHED 22 July 2022
DOI 10.3389/fonc.2022.943715

OPEN ACCESS

EDITED BY
Xin Ye,
Qianfoshan Hospital, Shandong University, China

REVIEWED BY
Xianqiang Wang,
PLA General Hospital, China
Zhigang Wei,
Qianfoshan Hospital, Shandong University, China

*CORRESPONDENCE
Yue Han
doctorhan@163.com

SPECIALTY SECTION
This article was submitted to Thoracic Oncology, a section of the journal Frontiers in Oncology

RECEIVED 14 May 2022
ACCEPTED 27 June 2022
PUBLISHED 22 July 2022

CITATION
Han Y, Yan X, Zhi W, Liu Y, Xu F and Yan D (2022) Long-term outcome following microwave ablation of lung metastases from colorectal cancer. *Front. Oncol.* 12:943715. doi: 10.3389/fonc.2022.943715

Long-term outcome following microwave ablation of lung metastases from colorectal cancer

Yue Han[1*], Xue Yan[2], Weihua Zhi[1], Ye Liu[3], Fei Xu[1] and Dong Yan[1]

[1]Department of Interventional Therapy, National Cancer Center/National Clinical Research Center for Cancer/Cancer Hospital, Chinese Academy of Medical Sciences and Peking Union Medical College, Beijing, China, [2]Department of General Surgery, Cancer Hospital of Huanxing, Beijing, China, [3]London School of Hygiene and Tropical Medicine, University of London, London, United Kingdom

Purpose: To retrospectively evaluate the safety and efficacy of percutaneous computed tomography (CT)-guided microwave ablation (MWA) in colorectal cancer (CRC) lung metastases, and to analyze prognostic factors.

Materials and methods: Data were collected from 31 patients with CRC lung metastases from May 2013 to September 2017. They had removed the CRC, no extrapulmonary metastases, no more than three metastases in the lung, the maximum diameter of the lesions was ≤3 cm, and all the lung metastases could be completely ablated. The ablation procedures were performed using a KY-2000 microwave multifunctional therapeutic apparatus. Efficacy is assessed two to four weeks after ablation, and follow-up are performed every three months for two years. The primary outcome was overall survival (OS). The secondary outcomes were progression-free survival (PFS), and complications. Cox regression analysis was used for the evaluation of the statistical significance of factors affecting the end result of MWA therapy. The Kaplan–Meier method was used for estimation of survival rates.

Results: A total of 45 metastatic lung lesions from CRC in 31 patients were treated with CT-guided MWA procedures. The median OS was 76 months. The one, two, three, and five-year survival rates were 93.5%, 80.6%, 61.3%, and 51.6%, respectively. Multivariate analysis showed that the primary tumor from the rectum (P = 0.009) and liver metastases at the diagnosis of lung metastases (P = 0.043) were risk factors affecting OS, while PFS was a protective factor. The median PFS was 13 months. The maximum diameter of lung metastases lesions (P = 0.004) was a risk factor. The interval between pulmonary metastases and MWA (P=0.031) was the protective factor. Pneumothorax was observed in 13 out of 36 procedures. Four patients developed pneumothorax requiring drainage tube insertion. No patient deaths occurred within 30 days of ablation. Three out of 31 patients (9.67%) were found to have local recurrence of the original lung metastatic ablation foci.

Conclusion: MWA therapy may be safely and effectively used as a therapeutic tool for the treatment of selected CRC pulmonary metastases, and the prognosis is better in patients without liver metastases at the diagnosis of lung metastases.

KEYWORDS

lung metastases, colon cancer, rectal cancer, microwave ablation, prognosis

1 Introduction

Colorectal cancer (CRC), with an increasing incidence in developing countries, ranks third among the most common malignant tumors in the world but second in terms of mortality, accounting for about 10% of all malignant tumor deaths (1). What's worse, about 20% to 25% of patients have distant metastases at initial diagnosis (2–4). Lungs have become the second most common metastatic site after liver, which makes it a severe threat to patients (5, 6). Long-term epidemiological research has shown that these patients have a poor prognosis unless effective treatment is taken (7). Therefore, the diagnosis and treatment of CRC with lung metastases deserves high emphasis.

Currently, a combination of systemic and local therapy is recommended in the management of CRC lung metastases, but for some patients, especially for those with primary lesions that can be controlled and those with a single metastasis in the lung or liver, appropriate local treatment can prolong their survival. Approximately 37.7%–44.5% of the initial lung metastasis population had isolated lung metastasis, of which only 21.1%–32.5% were suitable for radical therapy, while others were only eligible for palliative pharmacotherapy with or without local therapy (8–10). Besides, it is also demonstrated that stereotactic body radiation therapy can help yield better survival outcome (11–13).

Several modalities, including cryoablation, laser ablation, and radiofrequency ablation, have been used to eradicate tumors in a minimally invasive manner (14–20). Recently, as a safe, effective, and minimally invasive treatment, image-guided percutaneous local thermal ablation has been gradually applied to the therapy of lung metastases. Radiofrequency ablation and microwave ablation (MWA) are currently the two most widely used ablation methods (21). When compared to radiofrequency ablation, MWA has the advantage of producing a larger spherical ablation area in less time and having less influence from the heat sink effect, which is expected to improve the efficacy of thermal ablation on lung tumors (22–24). Furthermore, prior studies revealed the safety and efficacy of MWA in CRC pulmonary metastases with the median overall survival (OS) ranging from 31 to 32.8 months (25, 26), and MWA exhibited a potential benefit in local tumor management when compared to other ablation methods (26).

Our current study intends to retrospectively evaluate the safety and efficacy of computed tomography (CT)-guided percutaneous MWA in the management of patients with CRC lung metastasis as well as factors affecting these outcomes.

Abbreviations: CRC, Colorectal cancer; MWA, Microwave ablation; CT, Computed tomography; OS, Overall survival; PFS, Progression-free survival.

2 Materials and methods

2.1 Patients and tumor criteria

2.1.1 Patients

A total of 31 medical records of patients with CRC lung metastasis who were treated in the Department of Interventional Therapy, Cancer Hospital, Chinese Academy of Medical Sciences, from May 2013 to September 2017, were reviewed. This study was approved by the Hospital Ethics Committee (NCC3615). All procedures performed in studies involving human participants were in accordance with the ethical standards of the institutional and/or national research committee and with the 1964 Declaration of Helsinki and its later amendments or comparable ethical standards. The requirement for individual informed consent was waived by the Cancer Hospital Chinese Academy of Medical Sciences ethics committee.

2.1.2 Criteria

The inclusion criteria of the study are: (1) all patients had undergone surgical resection of their primary CRC with subsequent histopathological assessment, discovery of lung metastases during simultaneous or postoperative follow-up; (2) patients had to have three or fewer lesions, and the lesions had to be 3 cm or smaller in maximal axial diameter; (3) if liver metastases are concomitant, hepatic metastases are treated preferentially to obtain R0 efficacy; (4) patients were capable of tolerating MWA therapy for lung metastases and refused surgical resection; (5) Eastern Cooperative Oncology Group (ECOG) performance status score 0–1; (6) estimated survival ≥ 6 months. The exclusion criteria of the study are: (1) pulmonary metastases are adjacent to the hilar or lung segment bronchi and blood vessels; (2) concomitant primary tumors in other sites; (3) pulmonary insufficiency (PaO2 < 60

mmHg; PaCO2 > 50 mmHg); (4) concomitant of other chronic wasting diseases; (5) clinical data are incomplete.

2.2 Pretreatment assessment

A comprehensive clinical history was taken, a physical examination was performed, chest enhancement CT, pulmonary function test, and electrocardiography were also performed. The indications for, risks and benefits of the procedure were then discussed in detail by the multidisciplinary treatment. Preprocedural laboratory investigations, including a complete blood count, a coagulation profile, hepatorenal function, coagulation function, and tumor markers, were also completed. Anticoagulant or antiplatelet medications were stopped seven days before the procedure because of the risk of bleeding.

2.3 MWA procedure

All lung MWAs were performed by using CT guidance. Patients underwent CT scanning in the supine position immediately prior to treatment to confirm the location, number, and size of tumors. The ablation parameters, including applicator length and number, position of the patient, and site of puncture, were planned on the basis of tumor size and anatomic location. All ablation procedures were performed by using a KY-2000 microwave multifunctional therapeutic apparatus (Kangyou Medical Instruments, Nanjing, China) with power settings at 60–70 W and a mean ablation time of 10.8 minutes (range 4–24 minutes). Ablation times were recorded for all procedures. Multisite stacking therapy is performed according to the appropriate size. Treatment was performed in the CT suite under CT guidance. Conscious sedation was obtained using intraoperative local anesthesia combined with intravenous intensive anesthesia.

To prevent seeding of malignant cells in the needle track during removal of the needle electrode and to induce local hemostasis of the electrode track, needle track coagulation was routinely performed at the end of the procedure (17). At the end of every treatment, patients underwent a CT scan without contrast injection. Treatment was considered complete when densitometric decrease occurred in the lesion and a ground glass opacity developed around it. The patients' vital signs were monitored continuously during the procedure. Following MWA, electrocardiography was routinely monitored, with oxygen inhalation for 24 hours and fasting for 12 hours. Dissolving sputum, antibiotics, and supportive care are routinely taken for three to five days.

2.4 Postablation follow-up protocol

The assessment of the completeness of treatment was based on findings from a second spiral CT repeated two to four weeks later. The presence of enhancing tissue on the CT scan was thus regarded as indicative of incomplete treatment, whereas the presence at the tumor site of a nonenhancing area larger than the treated one was considered radiological evidence of complete tumor necrosis and therefore, of successful treatment. In the latter case, as planned previously by the multidisciplinary treatment, patients underwent clinical–radiological follow-up that included spiral CT scans every three months after MWA for the first two years and every six months thereafter. If preoperative tumor markers, such as CEA, are elevated, close dynamic observation is also required.

2.5 Study design and statistical analysis

All data was collected from the electronic health records, including age, gender, complications, number of pulmonary lesions, maximum lesion diameter, chemotherapy protocol, location of the primary tumor, extrapulmonary metastasis, disease-free interval, interval between pulmonary metastasis and MWA, and MWA procedure duration.

OS was defined as the time from the date of MWA to the date of death or the date of the final follow-up. Disease-free interval (DFI) was the period of time from the resection of the primary lesion of intestinal cancer to the first sign of pulmonary metastases. Progression-free survival (PFS) was the period of time from the date of MWA to the date of progression or the date of the final follow-up. Patients during this period are considered tumor-free survivors. The primary outcome was OS, the secondary outcome was PFS. Complications were observed and factors affecting the efficacy of MWA therapy were analyzed. The complications reported are based on the classifications of the American Society of Interventional Radiology (SIR) criteria (27).

The OS and PFS rates were evaluated with Kaplan–Meier analysis. A Cox regression analysis was performed to evaluate the prognosis factors for pulmonary metastases from CRC. $P < 0.05$ was considered to indicate a statistically significant difference for all analyses. IBM SPSS Statistics for Windows, version 25.0(IBM Corp., Armonk, N.Y., USA) was used to analyze all data.

3 Results

3.1 Baseline characteristics of patients

A total of 31 patients were included in the study. The mean age was 57.3 (range 38–78) years. There were 13 (41.9%) males and 18 (58.1%) females, respectively. There were 11 (35.5%) patients with primary tumors from the colon and 20 (64.5%) from the rectum. Patients and tumor characteristics are described in **Tables 1**, **2**.

TABLE 1 Baseline characteristics of patients.

Variable	Value
Gender	
Male	13 (41.9)
Female	18 (58.1)
Age (years)	
Mean ± standard deviation	57.3 ± 11.1
Range	38–78
<60	18 (58.1)
≥60	13 (41.9)
Location of the primary tumor	
Colon	11 (35.5)
Rectum	20 (64.5)
Chemotherapy before lung MWA	
Yes	26 (83.9)
No	5 (16.1)
Chemotherapy after lung MWA	
Yes	18 (58.1)
No	13 (41.9)
MWA procedure duration(min)	
Mean ± standard deviation	12.0 ± 5.7
Range	4.0–28.0
Interval between pulmonary metastases and MWA(m)	
Mean ± standard deviation	8.5 ± 12.7
Range	0–58
Disease-free Interval (m)	
Mean ± standard deviation	22.1 ± 17.2
Range	0–64
Liver metastases at the diagnosis of lung metastases	
Yes	7 (22.6)
No	24 (77.4)

Except where otherwise noted, data are in the form of numbers of participants or tumors, with percentages in parentheses. MWA, microwave ablation.

TABLE 2 Characteristics of lung metastases.

Variable	Value
Number of lung metastases	
Single	18(58.1)
Multiple	13(41.9)
Maximum tumor diameter (cm)	
Mean ± standard deviation	1.5 ± 0.8
Range	0.5–3.0
≤2 cm	23 (74.2)
>2 cm	8 (25.8)
Location of lung metastases	
Left	
Upper lobe	12 (26.7)
Lower lobe	9 (20.0)
Right	
Upper lobe	10 (22.2)
Middle lobe	6 (13.3)
Lower lobe	8 (17.8)
Synchronous	4 (12.9)
Metachronous	27 (87.1)

3.2 Safety and complications of percutaneous MWA

A total of 45 metastatic lung lesions from CRC in 31 patients were treated with CT-guided MWA procedures. Complications were in accordance with the standards of the society of interventional radiology (SIR). Major complications include pneumothorax, hemorrhage and infection. Pneumothorax was observed in 13 of 36 procedures, three of which were observed after the MWA procedure. Four patients developed a pneumothorax requiring drainage tube insertion, two patients had hemorrhage, only one patient with infection had a hospital stay more than 5 days. Delayed discharge happened in eight patients (hospital stay more than 5 days). Oncologic imaging showed that all lesions in the 31 patients were completely ablated at one-month follow-up after ablation. No patient deaths occurred within 30 days of ablation. Complications of percutaneous MWA (36 procedures) are described in Table 3.

3.3 Reablation of local recurrence lesions

During the follow-up period, three patients found local recurrence of the original lung metastatic ablation foci 9, 12, and 15 months after ablation. Reablation was performed for two of them after clinical justification and clinical exclusion of systemic tumor spread, while the other patient with recurrence was only eligible for systemic therapy for multiple metastases of lung and liver. Secondary tumor control after reablation revealed a success rate of 100% with no evidence of residual or recurrent tumor within the one to three months follow-up period. Unexpectedly, the one who refused postablation chemotherapy was found to have multiple lung metastases after six months of follow-up after reablation, and died of tumor progression 12 months later.

3.4 PFS

3.4.1

The median PFS was 13 months. The one, two, three, and five-year survival rates were 45.2%, 32.3%, 25.8%, and 22.6%, respectively. The survival curve of PFS is shown in Figure 1.

TABLE 3 Complications of percutaneous MWA.

Complications	N (%)
Major	
Pneumothorax, requiring drainage	4 (11.11)
Hemorrhage	2 (5.55)
Infection, with longer hospital stay	1 (3.2)
Minor	
Bloody sputum	10 (27.78)
Chest pain	21 (67.7)
Pneumothorax, asymptomatic	9 (25.0)
Infection, within mean hospital stay	1 (3.2)

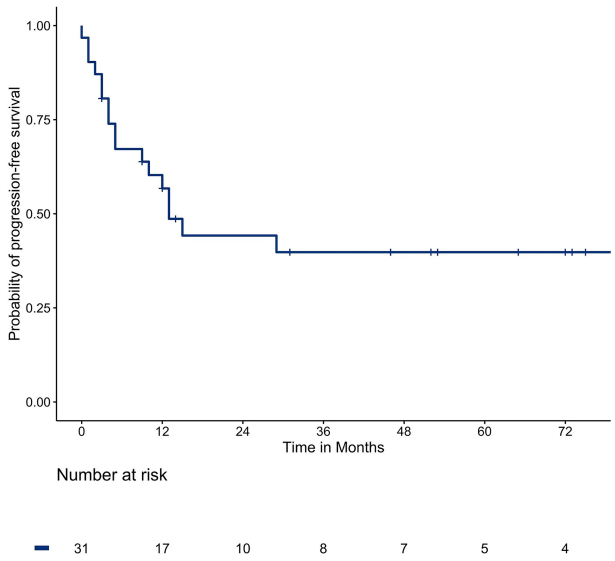

FIGURE 1
The PFS in the total population.

3.4.2

Multivariate analysis showed that the maximum diameter of lung metastases ($P = 0.004$) was a risk factor affecting PFS and the interval between pulmonary metastases and MWA ($P = 0.031$) was a protective factor. Multivariable analyses of prognostic factors for progression-free survival are described in Table 4.

3.5 Overall survival

3.5.1

The median OS was 76 months. The one, two, three, and five-year survival rates were 93.5%, 80.6%, 61.3%, and 51.6%, respectively. The survival curve of OS is shown in Figure 2.

3.5.2

Multivariate analysis showed that the primary tumor from the rectum ($P = 0.009$) and extrapulmonary metastases ($P = 0.043$) were risk factors affecting OS, while PFS was a protective factor. Multivariable analyses of prognostic factors for overall survival are described in Table 5.

4 Discussion

The lung is the second most common metastatic site of CRC, only after the liver. The main reason is that the blood supply to the lungs is sufficient and the blood flow is relatively slow, which is conducive to the implantation of metastatic cancer cells. Similar to

TABLE 4 Multivariable analyses of prognostic factors for progression-free survival.

Variable	Hazard Ratio	*P* Value
Gender	1.148	0.836
Age	1.011	0.683
Maximum tumor diameter	4.701	0.004*
Chemotherapy before lung MWA	0.169	0.051
Chemotherapy after lung MWA	1.515	0.467
Primary tumor from rectum	0.371	0.134
Liver metastases at the diagnosis of lung metastases	0.362	0.143
MWA procedure duration	0.940	0.381
Number of lung metastases	0.379	0.172
Disease-free interval	0.961	0.131
Interval between pulmonary metastases and MWA	0.952	0.031*

*means P<0.05.

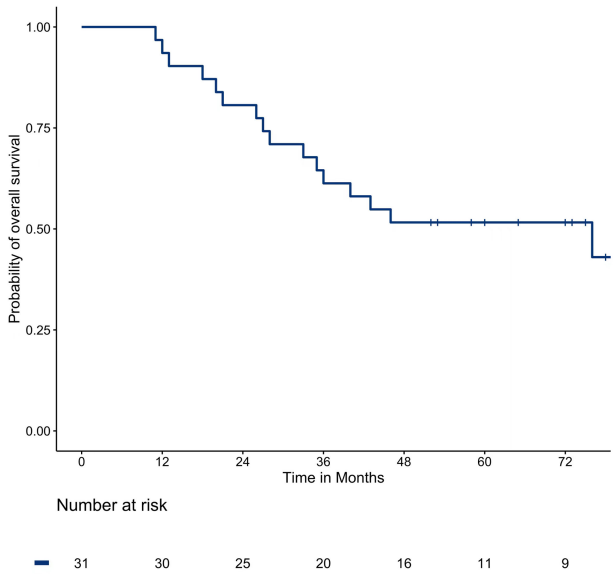

FIGURE 2
The OS in the total population.

TABLE 5 Multivariable analyses of prognostic factors for overall survival.

Variable	Hazard Ratio	*P* Value
Gender	0.211	0.153
Age	0.933	0.134
Maximum tumor diameter	0.183	0.155
Chemotherapy before lung MWA	10.933	0.171
Chemotherapy after lung MWA	0.667	0.626
Primary tumor from rectum	26.493	0.009*
Liver metastases at the diagnosis of lung metastases	5.254	0.043*
MWA procedure duration	1.124	0.499
Number of lung metastases	1.072	0.954
Progression-free survival	0.766	0.006*
Disease-free interval	1.043	0.278
Interval between pulmonary metastases and MWA	1.121	0.105

*means P<0.05.

the treatment strategy for CRC liver metastases, for patients with CRC lung metastases if the primary CRC has been resected with no extrapulmonary metastases, and the lung metastases can be completely resected, surgical resection is still the preferred option (28, 29). A clinical study of 378 patients with advanced CRC showed that patients with lung metastases had a 28% recurrence-free survival rate at three years and a 78% OS rate at three years after undergoing pulmonary metastasectomy (30). What's more, for patients under the premise of strict control of indications, combined pulmonary and hepatic resections of resectable metastatic disease have been implemented (31, 32).

For patients with advanced CRC where lung metastases have developed, lung metastasis resection is the standard practice of local treatment. However, surgical resection is traumatic and severely impairs lung function, and the majority of patients are unable to tolerate surgery due to poor general condition (33, 34). Such patients may be suitable candidates for percutaneous minimally invasive ablation. Commonly used ablation methods include radiofrequency ablation, MWA, and cryoablation (35–37).

For multiple lesions in both lungs, a staging ablation was adopted to avoid delayed pneumothorax, and a total of 36 ablation procedures were implemented among the 31 enrolled

patients in this study. The success rate of ablation was assessed at 100% at one month after MWA. There were no deaths in the perioperative period, 13 cases of pneumothorax occurred, and eight cases required thoracic drainage. There were eight cases of delayed discharge (hospital stay more than 5 days). What's mentioned before demonstrates the precision and minimal invasion of the ablation therapy of lung metastases. Under the guidance of CT, the ablation needles can be accurately punctured into the tumor area during the procedure. The complication rate is low, which can achieve complete ablation of bilateral, multiple lung metastases while preserving lung function as much as possible.

Only three out of 31 patients (9.67%) were found to have local recurrence of the original ablation foci 9–15 months after the first ablation, which is similar to what has been reported before (38, 39). Except for one patient who was converted to systemic therapy due to multiple metastases of the liver and lung, the other two were successfully treated with reablation, which revealed that ablation therapy is curative for metastases ≤3.0 cm in that the coagulating necrosis produced by ablation can completely inactivate the tumor, and that ablation can be performed again for recurrent metastases, which is crucially important for the management of metastases.

In this study, the median PFS was 13 months and the median survival was 76 months. The one, two, three, and five-year PFS rates and OS rates were 45.2%, 32.3%, 25.8%, 22.6%, and 93.5%, 80.6%, 61.3%, and 51.6%, respectively, which shows a slightly better survival outcome than other centers (40). A large prospective study enrolled 566 patients with CRC and a total of 1037 lung metastases underwent radiofrequency ablation, with PFS rates of 1–4 years at 40.2%, 23.3%, 16.4%, and 13.1%, respectively, and 40.7% to 67.5% of 5-year OS rates (40). The difference is that our study used MWA while they used radiofrequency ablation. MWA not only has better thermal conductivity, larger ablation zone, but it is less affected by blood flow and carbonization (23, 24, 41).

It has been reported that the OS rate at three years of surgical resection of lung metastases was 78%, which was 61.3% in this group. On the one hand, this may be related to different inclusion criteria, that is, the screening requirements for surgical resection are more stringent than for ablation therapy (30). On the other hand, lobectomy or lung segment resection of metastases resects the tumor and normal tissues around it compared with local ablation. Local ablation is still a safe and effective option for elderly patients with poor general condition, multiple comorbidities, and multiple lesions (26, 42).

The results of multivariate analysis suggest that lung metastases from rectal cancer are a risk factor for OS, which is similar to the results reported in the literature (43). For one thing, the chance of lung metastases may be increased due to the double venous drainage of the rectum from the portal vein and inferior vena cava (44, 45). On the other hand, the general prognosis of rectal cancer is also inferior to that of colon cancer (1, 46). Besides, liver metastases are the most important cause of death in patients with advanced CRC (47, 48). In our study population, seven patients had liver metastases at the diagnosis of lung metastases (22.6%), which turned out to be a risk factor for OS, which was in good agreement with the clinical epidemiological data. Therefore, in the face of patients with CRC and simultaneous metastases of the liver and lung, the importance of systemic therapy should be emphasized. It has been confirmed that the median chemotherapy-free survival of patients without extrapulmonary metastases is longer than that of patients with extrapulmonary metastases (20.9 months vs. 9.2 months) (49).

In the multivariate analysis of PFS, the maximum diameter of the lung metastasis lesion ($P = 0.004$) was the risk factor, and the interval between the time of lung metastasis detection and MWA ($P = 0.031$) was the protective factor. Consequently, regular follow-up of patients with CRC is critical to detect lung metastases as early as possible, and positive intervention at an early stage benefits patient more (7). The results of this study showed that gender, age, number of tumors, chemotherapy protocol, ablation duration, the interval between metastases and ablation, the disease-free interval, and the interval between primary cancer surgery and MWA were not related to survival.

In summary, for selected patients with CRC lung metastases, MWA therapy, which has the advantages of being minimally invasive, curative, and repeatable, is a safe and effective treatment option. However, this study is a single-center, small-sample retrospective study, which may have selective bias and still requires clinical validation of large-sample multicenter.

Data availability statement

The original contributions presented in the study are included in the article/supplementary material. Further inquiries can be directed to the corresponding author.

Ethics statement

The studies involving human participants were reviewed and approved by Hospital Ethics Committee of Cancer Hospital, Chinese Academy of Medical Sciences. Written informed consent for participation was not required for this study in accordance with the national legislation and the institutional requirements.

Author contributions

YH made contributions to the study design and manuscript writing; XY made contributions to the data collection and curation, literature search and manuscript writing; WZ made

contributions to the data analysis and manuscript writing; YL made contributions to the data analysis; FX was involved in literature search; DY was involved in figure preparation. All authors contributed to the article and approved the submitted version.

Acknowledgments

We express our deep thanks and gratitude to Tao Gong from Department of Interventional Therapy, National Cancer Center/ National Clinical Research Center for Cancer/Cancer Hospital, Chinese Academy of Medical Sciences and Peking Union Medical College, China, for his assistance with the figures of survival rate in the manuscript.

Conflict of interest

The authors declare that the research was conducted in the absence of any commercial or financial relationships that could be construed as a potential conflict of interest.

Publisher's note

References

1. Sung H, Ferlay J, Siegel RL, Laversanne M, Soerjomataram I, Jemal A, et al. Global cancer statistics 2020: Globocan estimates of incidence and mortality worldwide for 36 cancers in 185 countries. *CA: Cancer J Clin* (2021) 71(3):209–49. doi: 10.3322/caac.21660

2. Van Cutsem E, Nordlinger B, Adam R, Kohne CH, Pozzo C, Poston G, et al. Towards a pan-European consensus on the treatment of patients with colorectal liver metastases. *Eur J Cancer* (2006) 42(14):2212–21. doi: 10.1016/j.ejca.2006.04.012

3. Riihimaki M, Hemminki A, Sundquist J, Hemminki K. Patterns of metastasis in colon and rectal cancer. *Sci Rep* (2016) 6:29765. doi: 10.1038/srep29765

4. Siegel RL, Miller KD, Goding Sauer A, Fedewa SA, Butterly LF, Anderson JC, et al. Colorectal cancer statistics, 2020. *CA: Cancer J Clin* (2020) 70(3):145–64. doi: 10.3322/caac.21601

5. Watanabe K, Saito N, Sugito M, Ito M, Kobayashi A, Nishizawa Y. Incidence and predictive factors for pulmonary metastases after curative resection of colon cancer. *Ann Surg Oncol* (2013) 20(4):1374–80. doi: 10.1245/s10434-012-2747-y

6. Zhang GQ, Taylor JP, Stem M, Almaazmi H, Efron JE, Atallah C, et al. Aggressive multimodal treatment and metastatic colorectal cancer survival. *J Am Coll Surgeons* (2020) 230(4):689–98. doi: 10.1016/j.jamcollsurg.2019.12.024

7. Mitry E, Guiu B, Cosconea S, Jooste V, Faivre J, Bouvier AM. Epidemiology, management and prognosis of colorectal cancer with lung metastases: A 30-year population-based study. *Gut* (2010) 59(10):1383–8. doi: 10.1136/gut.2010.211557

8. Tampellini M, Ottone A, Bellini E, Alabiso I, Baratelli C, Bitossi R, et al. The role of lung metastasis resection in improving outcome of colorectal cancer patients: Results from a Large retrospective study. *Oncologist* (2012) 17 (11):1430–8. doi: 10.1634/theoncologist.2012-0142

9. Wang Z, Wang X, Yuan J, Zhang X, Zhou J, Lu M, et al. Survival benefit of palliative local treatments and efficacy of different pharmacotherapies in colorectal cancer with lung metastasis: Results from a Large retrospective study. *Clin Colorectal Cancer* (2018) 17(2):e233–e55. doi: 10.1016/j.clcc.2017.12.005

10. Li WH, Peng JJ, Xiang JQ, Chen W, Cai SJ, Zhang W. Oncological outcome of unresectable lung metastases without extrapulmonary metastases in colorectal cancer. *World J Gastroenterol* (2010) 16(26):3318–24. doi: 10.3748/wjg.v16.i26.3318

11. Agolli L, Bracci S, Nicosia L, Valeriani M, De Sanctis V, Osti MF. Lung metastases treated with stereotactic ablative radiation therapy in oligometastatic colorectal cancer patients: Outcomes and prognostic factors after long-term follow-up. *Clin Colorectal Cancer* (2017) 16(1):58–64. doi: 10.1016/j.clcc.2016.07.004

12. Rusthoven KE, Kavanagh BD, Burri SH, Chen C, Cardenes H, Chidel MA, et al. Multi-institutional phase I/Ii trial of stereotactic body radiation therapy for lung metastases. *J Clin Oncol Off J Am Soc Clin Oncol* (2009) 27(10):1579–84. doi: 10.1200/JCO.2008.19.6386

13. Li S, Dong D, Geng J, Zhu X, Shi C, Zhang Y, et al. Prognostic factors and optimal response interval for stereotactic body radiotherapy in patients with lung oligometastases or oligoprogression from colorectal cancer. *Front Oncol* (2019) 9:1080. doi: 10.3389/fonc.2019.01080

14. Dupuy DE, Zagoria RJ, Akerley W, Mayo-Smith WW, Kavanagh PV, Safran H. Percutaneous radiofrequency ablation of malignancies in the lung. *AJR Am J Roentgenol* (2000) 174(1):57–9. doi: 10.2214/ajr.174.1.1740057

15. Nahum Goldberg S, Dupuy DE. Image-guided radiofrequency tumor ablation: Challenges and opportunities–part I. *J Vasc Interventional Radiol JVIR* (2001) 12(9):1021–32. doi: 10.1016/s1051-0443(07)61587-5

16. Bojarski JD, Dupuy DE, Mayo-Smith WW. Ct imaging findings of pulmonary neoplasms after treatment with radiofrequency ablation: Results in 32 tumors. *AJR Am J Roentgenol* (2005) 185(2):466–71. doi: 10.2214/ajr.185.2.01850466

17. Wolf FJ, Grand DJ, Machan JT, Dipetrillo TA, Mayo-Smith WW, Dupuy DE. Microwave ablation of lung malignancies: Effectiveness, ct findings, and safety in 50 patients. *Radiology* (2008) 247(3):871–9. doi: 10.1148/radiol.2473070996

18. Hegenscheid K, Behrendt N, Rosenberg C, Kuehn JP, Ewert R, Hosten N, et al. Assessing early vascular changes and treatment response after laser-induced thermotherapy of pulmonary metastases with perfusion ct: Initial experience. *AJR Am J Roentgenol* (2010) 194(4):1116–23. doi: 10.2214/ajr.09.2810

19. Eradat J, Abtin F, Gutierrez A, Suh R. Evaluation of treatment response after nonoperative therapy for early-stage non-small cell lung carcinoma. *Cancer J (Sudbury Mass)* (2011) 17(1):38–48. doi: 10.1097/PPO.0b013e31820a0948

20. Simon CJ, Dupuy DE, DiPetrillo TA, Safran HP, Grieco CA, Ng T, et al. Pulmonary radiofrequency ablation: Long-term safety and efficacy in 153 patients. *Radiology* (2007) 243(1):268–75. doi: 10.1148/radiol.2431060088

21. Smith SL, Jennings PE. Lung radiofrequency and microwave ablation: A review of indications, techniques and post-procedural imaging appearances. *Br J Radiol* (2015) 88(1046):20140598. doi: 10.1259/bjr.20140598

22. Simon CJ, Dupuy DE, Mayo-Smith WW. Microwave ablation: Principles and applications. *Radiographics Rev Publ Radiological Soc North America Inc* (2005) 25 Suppl 1:S69–83. doi: 10.1148/rg.25si055501

23. Aufranc V, Farouil G, Abdel-Rehim M, Smadja P, Tardieu M, Aptel S, et al. Percutaneous thermal ablation of primary and secondary lung tumors: Comparison between microwave and radiofrequency ablation. *Diagn Interventional Imaging* (2019) 100(12):781–91. doi: 10.1016/j.diii.2019.07.008

24. Dupuy DE. Microwave ablation compared with radiofrequency ablation in lung tissue-is microwave not just for popcorn anymore? *Radiology* (2009) 251 (3):617–8. doi: 10.1148/radiol.2513090129

25. Cheng G, Shi L, Qiang W, Wu J, Ji M, Lu Q, et al. The safety and efficacy of microwave ablation for the treatment of crc pulmonary metastases. *Int J Hyperthermia Off J Eur Soc Hyperthermic Oncol North Am Hyperthermia Group* (2018) 34(4):486–91. doi: 10.1080/02656736.2017.1366553

26. Vogl TJ, Eckert R, Naguib NN, Beeres M, Gruber-Rouh T, Nour-Eldin NA. Thermal ablation of colorectal lung metastases: Retrospective comparison among laser-induced thermotherapy, radiofrequency ablation, and microwave ablation. *AJR Am J Roentgenol* (2016) 207(6):1340–9. doi: 10.2214/ajr.15.14401

27. Sacks D, McClenny TE, Cardella JF, Lewis CA. Society of interventional radiology clinical practice guidelines. *J Vasc Interventional Radiol JVIR* (2003) 14(9 Pt 2):S199–202. doi: 10.1097/01.rvi.0000094584.83406.3e

28. Gonzalez M, Gervaz P. Risk factors for survival after lung metastasectomy in colorectal cancer patients: Systematic review and meta-analysis. *Future Oncol* (2015) 11(2 Suppl):31–3. doi: 10.2217/fon.14.259

29. Gonzalez M, Poncet A, Combescure C, Robert J, Ris HB, Gervaz P. Risk factors for survival after lung metastasectomy in colorectal cancer patients: A systematic review and meta-analysis. *Ann Surg Oncol* (2013) 20(2):572–9. doi: 10.1245/s10434-012-2726-3

30. Onaitis MW, Petersen RP, Haney JC, Saltz L, Park B, Flores R, et al. Prognostic factors for recurrence after pulmonary resection of colorectal cancer metastases. *Ann Thorac Surg* (2009) 87(6):1684–8. doi: 10.1016/j.athoracsur.2009.03.034

31. Brouquet A, Vauthey JN, Contreras CM, Walsh GL, Vaporciyan AA, Swisher SG, et al. Improved survival after resection of liver and lung colorectal metastases compared with liver-only metastases: A study of 112 patients with limited lung metastatic disease. *J Am Coll Surgeons* (2011) 213(1):62–9; discussion 9-71. doi: 10.1016/j.jamcollsurg.2011.05.001

32. Hadden WJ, de Reuver PR, Brown K, Mittal A, Samra JS, Hugh TJ. Resection of colorectal liver metastases and extra-hepatic disease: A systematic review and proportional meta-analysis of survival outcomes. *HPB Off J Int Hepato Pancreato Biliary Assoc* (2016) 18(3):209–20. doi: 10.1016/j.hpb.2015.12.004

33. Bin Traiki TA, Fisher OM, Valle SJ, Parikh RN, Kozman MA, Glenn D, et al. Percutaneous lung ablation of pulmonary recurrence may improve survival in selected patients undergoing cytoreductive surgery for colorectal cancer with peritoneal carcinomatosis. *Eur J Surg Oncol J Eur Soc Surg Oncol Br Assoc Surg Oncol* (2017) 43(10):1939–48. doi: 10.1016/j.ejso.2017.08.005

34. Migliore M, Jakovic R, Hensens A, Klepetko W. Extending surgery for pulmonary metastasectomy: What are the limits? *J Thorac Oncol Off Publ Int Assoc Stud Lung Cancer* (2010) 5(6 Suppl 2):S155–60. doi: 10.1097/JTO.0b013e3181dcf7b1

35. Eiken PW, Welch BT. Cryoablation of lung metastases: Review of recent literature and ablation technique. *Semin Interventional Radiol* (2019) 36(4):319–25. doi: 10.1055/s-0039-1697002

36. Ghosn M, Solomon SB. Current management of oligometastatic lung cancer and future perspectives: Results of thermal ablation as a local ablative therapy. *Cancers* (2021) 13(20):5052. doi: 10.3390/cancers13205202

37. Pereira PL, Masala S. Standards of practice: Guidelines for thermal ablation of primary and secondary lung tumors. *Cardiovasc Interventional Radiol* (2012) 35 (2):247–54. doi: 10.1007/s00270-012-0340-1

38. Kurilova I, Gonzalez-Aguirre A, Beets-Tan RG, Erinjeri J, Petre EN, Gonen M, et al. Microwave ablation in the management of colorectal cancer pulmonary metastases. *Cardiovasc Interventional Radiol* (2018) 41(10):1530–44. doi: 10.1007/s00270-018-2000-6

39. Vogl TJ, Basten LM, Nour-Eldin NA, Kaltenbach B, Ackermann H, Naguib NNN. Microwave ablation (Mwa) of pulmonary neoplasms: Clinical performance of high-frequency mwa with spatial energy control versus conventional low-frequency mwa. *AJR Am J Roentgenol* (2019) 213(6):1388–96. doi: 10.2214/ajr.18.19856

40. de Baère T, Aupérin A, Deschamps F, Chevallier P, Gaubert Y, Boige V, et al. Radiofrequency ablation is a valid treatment option for lung metastases: Experience in 566 patients with 1037 metastases. *Ann Oncol Off J Eur Soc Med Oncol* (2015) 26 (5):987–91. doi: 10.1093/annonc/mdv037

41. Sonntag PD, Hinshaw JL, Lubner MG, Brace CL, Lee FTJr. Thermal ablation of lung tumors. *Surg Oncol Clinics North America* (2011) 20(2):369–87. doi: 10.1016/j.soc.2010.11.008

42. Hiyoshi Y, Miyamoto Y, Kiyozumi Y, Sawayama H, Eto K, Nagai Y, et al. Ct-guided percutaneous radiofrequency ablation for lung metastases from colorectal cancer. *Int J Clin Oncol* (2019) 24(3):288–95. doi: 10.1007/s10147-018-1357-5

43. Hasegawa T, Takaki H, Kodama H, Yamanaka T, Nakatsuka A, Sato Y, et al. Three-year survival rate after radiofrequency ablation for surgically resectable colorectal lung metastases: A prospective multicenter study. *Radiology* (2020) 294 (3):686–95. doi: 10.1148/radiol.2020191272

44. Bölükbas S, Sponholz S, Kudelin N, Eberlein M, Schirren J. Risk factors for lymph node metastases and prognosticators of survival in patients undergoing pulmonary metastasectomy for colorectal cancer. *Ann Thorac Surg* (2014) 97 (6):1926–32. doi: 10.1016/j.athoracsur.2014.02.026

45. Meimarakis G, Spelsberg F, Angele M, Preissler G, Fertmann J, Crispin A, et al. RResection of Pulmonary Metastases from Colon and Rectal Cancer: Factors to Predict Survival Differ Regarding to the Origin of the Primary Tumor. *Annals of surgical oncology* (2014) 21(8):2563–72. doi: 10.1245/s10434-014-3646-1

46. Lin A, Zhang X, Zhang RL, He XF, Zhang JG, Yan WH. Prognostic and risk stratification value of lesion Macc1 expression in colorectal cancer patients. *Front Oncol* (2019) 9:28. doi: 10.3389/fonc.2019.00028

47. van der Pool AE, Damhuis RA, Ijzermans JN, de Wilt JH, Eggermont AM, Kranse R, et al. Trends in incidence, treatment and survival of patients with stage iv colorectal cancer: A population-based series. *Colorectal Dis Off J Assoc Coloproctol Great Britain Ireland* (2012) 14(1):56–61. doi: 10.1111/j.1463-1318.2010.02539.x

48. Wei L, Lin Z, Xie S, Ruan D, Jiang W, Cui Y, et al. Complete response with cetuximab-based treatment of metastatic colorectal cancers: Two case reports and literature review. *Front Oncol* (2022) 12:798515. doi: 10.3389/fonc.2022.798515

49. Fonck M, Perez JT, Catena V, Becouarn Y, Cany L, Brudieux E, et al. Pulmonary thermal ablation enables long chemotherapy-free survival in metastatic colorectal cancer patients. *Cardiovasc Interventional Radiol* (2018) 41(11):1727–34. doi: 10.1007/s00270-018-1939-7

frontiers | Frontiers in Oncology

TYPE Original Research
PUBLISHED 28 July 2022
DOI 10.3389/fonc.2022.941752

OPEN ACCESS

EDITED BY
Xin Ye,
Shandong University, China

REVIEWED BY
Zhigang Wei,
The First Affiliated Hospital of Shandong First Medical University, China
Hong-Tao Hu,
Henan Provincial Cancer Hospital, China
Weijun Fan,
Sun Yat-sen University Cancer Center (SYSUCC), China

*CORRESPONDENCE
ZhengYu Lin
linsinlan@aliyun.com

SPECIALTY SECTION
This article was submitted to Thoracic Oncology, a section of the journal Frontiers in Oncology

RECEIVED 11 May 2022
ACCEPTED 27 June 2022
PUBLISHED 28 July 2022

CITATION
Chen J, Yan Y, Lin QF, Chen J, Chen J and Lin ZY (2022) The correlation between multimodal radiomics and pathology about thermal ablation lesion of rabbit lung VX2 tumor. *Front. Oncol.* 12:941752. doi: 10.3389/fonc.2022.941752

The correlation between multimodal radiomics and pathology about thermal ablation lesion of rabbit lung VX2 tumor

Jin Chen[1], Yuan Yan[1], QingFeng Lin[1], Jian Chen[1], Jie Chen[2] and ZhengYu Lin[1]*

[1]The Department of Interventional Radiology, First Affiliated Hospital of Fujian Medical University, Fujian Provincial Key Laboratory of Precision Medicine for Cancer, Fuzhou, China, [2]The Department of Interventional Radiology, Sanming Second Hospital, Sanming, China

Objective: To explore the correlation of CT-MRI pathology with lung tumor ablation lesions by comparing CT, MRI, and pathological performance of rabbit lung VX2 tumor after thermal ablation.

Methods: Thermal ablation including microwave ablation (MWA) and radiofrequency ablation (RFA) was carried out in 12 experimental rabbits with lung VX2 tumors under CT guidance. CT and MRI performance was observed immediately after ablation, and then the rabbits were killed and pathologically examined. The maximum diameter of tumors on CT before ablation, the central hypointense area on T2-weighted image (T2WI) after ablation, and the central hyperintense area on T1-weighted image (T1WI) after ablation and pathological necrosis were measured. Simultaneously, the maximum diameter of ground-glass opacity (GGO) around the lesion on CT after ablation, the surrounding hyperintense area on T2WI after ablation, the surrounding isointense area on T1WI after ablation, and the pathological ablation area were measured, and then the results were compared and analyzed.

Results: Ablation zones showed GGO surrounding the original lesion on CT, with a central hypointense and peripheral hyperintense zone on T2WI as well as a central hyperintense and peripheral isointense zone on T1WI. There was statistical significance in the comparison of the maximum diameter of the tumor before ablation with a central hyperintense zone on T1WI after ablation and pathological necrosis. There was also statistical significance in the comparison of the maximum diameter of GGO around the lesion on CT with the surrounding hyperintense zone on T2WI and isointense on T1WI after ablation and pathological ablation zone. There was only one residual tumor abutting the vessel in the RFA group.

Conclusions: MRI manifestations of thermal ablation of VX2 tumors in rabbit lungs have certain characteristics with a strong pathological association. CT combined with MRI multimodal radiomics is expected to provide an effective new method for clinical evaluation of the immediate efficacy of thermal ablation of lung tumors.

10.3389/fonc.2022.941752

KEYWORDS

VX2 tumor, lung cancer, Thermal ablation, Magnetic Resonance Imaging, multimodal radiomics

Introduction

Lung cancer is the second most common malignant tumor in terms of morbidity and has the highest death rate in the world (1), and the lung is one of the most common metastatic target organs of malignant tumors. Lung metastases appear in 30%–40% of malignant tumor patients with advanced stage (2). Thermal ablation can effectively prolong the survival time of patients in the treatment of pulmonary malignant tumors, and the treatment efficacy of smaller lung tumors is close to the efficacy of surgery (3, 4). Currently, thermal ablation of lung tumors is mainly represented by radiofrequency and microwave. However, the lung tissue is poorer in heat conduction with the singleness post-ablation evaluation method, and the therapeutic efficacy is lower than that of liver tumor ablation. Therefore, the immediate efficacy assessment of post-ablation is extremely important.

This study aims to compare and analyze the multimodal radiomics, pathological manifestations, and the correlation between the acute thermal injury after radiofrequency ablation (RFA) and microwave ablation (MWA) in rabbit lung VX2 tumors, so as to provide more information for the precise evaluation of the efficacy of thermal ablation of lung tumors.

Materials and methods

Establishment of rabbit lung VX2 tumor model

Three New Zealand male rabbits (weight 2.0–2.5 kg) were inoculated with VX2 tumor strain (gifted by the First Affiliated Hospital of Fujian Medical University) after general anesthesia with ketamine 1 ml/kg and chlorpromazine 0.5 ml/kg. Tumors formed on the inner musculature of the hind legs of the rabbits. About 2–3 weeks after tumor formation, fish sarcoid tumor tissue with vigorous growth at the edge of the tumor block was excised, and the tumor tissue was cut into tumor blocks of about 1-mm^3 size.

Cultivation of tumor strains in rabbit lungs

Fifteen New Zealand male rabbits (weight 2.0–2.5 kg), were fasted for 12 h before the operation, their skin was prepared after general anesthesia, and they were fixed in a prone position on a CT (Somatom Emotion, Siemens) scan table. The appropriate puncture path was determined after the CT scan. After the rabbits were positioned, disinfected, and draped, a 17G coaxial needle was used to puncture the lower lung under CT guidance. Then the tissue block was inserted into the lung parenchyma through the coaxial needle. CT was reexamined to observe the growth of the tumor in the rabbit lung 2–4 weeks after implantation. When the tumor grew to about 10 mm in diameter, it was used for ablation.

Thirteen experimental rabbits were successfully implanted with a VX2 tumor in the lung, showing a single nodule with soft tissue density in the lung by CT, and no tumor was found in 2 experimental rabbits. One tumor-bearing rabbit was killed and confirmed by pathological examination. There were 12 rabbits with VX2 tumors in the remaining lungs enrolled in our study (Figure 1). The tumor foci were located in the right lower lung in 6 rabbits and in the left lower lung in 6 rabbits. The average diameter of the tumor was 11.6 ± 2.9 mm (range 9.1–15.1 mm, median 11.3 mm).

Pre-ablation MRI scan

After general anesthesia, 12 tumor-bearing rabbits underwent a 1.5-T MRI plain scan (Magnet Espree, Siemens, Germany) of the lung using the surface coil. The MRI scan sequence and parameters are shown in Table 1.

CT-guided thermal ablation of VX2 tumor in rabbit lung

Twelve tumor-forming rabbits were divided into 2 groups, 6 in each group. All tumor-bearing rabbits were placed in the prone position, and a CT scan was performed to select the appropriate puncture point. In the RFA group, a 17G needle with a 20-mm working radiofrequency electrode (star RF Electrode-Fixed, Starmed, Korea) with water cooling was gradually inserted under CT guidance. Through the water cooling cycle, the automatic pulse mode and the output power were set to 40–70 W; the continuous treatment time was 5–10 min.

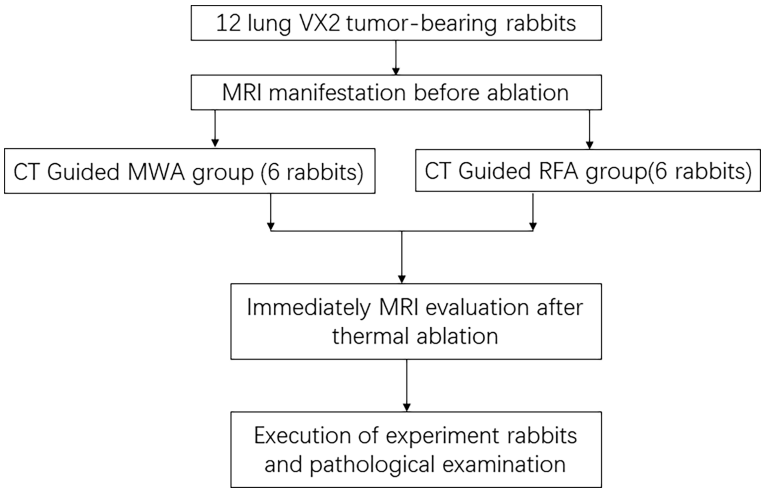

FIGURE 1
CONSORT flow diagram summarizes the process in this study. CONSORT, Consolidated Standards of Reporting Trials.

In the MWA group, a microwave ablation antenna (15G, 150 mm, VISON Medical Equipment Co., Nanjing, China) with an outer diameter of 1.8 mm was gradually inserted into the distal end of the tumor under CT guidance, and the output power was set to 40–50 W with treating time of 4–6 min. The repeat CT scan showed that the surrounding ground-glass opacity (GGO) of the lesion exceeded 5–10 mm after ablation, which was considered complete ablation.

The needle was withdrawn after ablation, and a CT scan was performed again to observe whether there were complications such as pneumothorax, hemorrhage, and pleural effusion. If there was a pneumothorax and the lung was compressed by more than 20%, lung recruitment maneuver was performed by aspiration of the thoracic cavity.

All rabbit lung VX2 tumor ablation treatments were performed by physicians with more than 5 years of experience in tumor ablation.

Post-ablation MRI scan

MRI was performed to observe the VX2 tumor in the rabbit lung immediately after ablation. The MRI sequences were the same as those before ablation. The experimental rabbits were killed and pathologically examined after an MRI scan.

TABLE 1 MRI sequences and parameters.

Sequence	3D-VIBE-T1WI	FS-TSE-T2WI	DWI
Scan mode	Breath-free	Diaphragm trigger	Diaphragm trigger
TR	5.1 ms	4,000 ms	4,900 ms
TE	2.4 ms	80 ms	91 ms
FA	14°	90°	N/A
FOV	200 × 280 mm	200 × 210 mm	220 × 300 mm
NEX	1	2	2
Slice thickness	3 mm	3 mm	3 mm
Fat suppression	Yes	Yes	Yes
Gap	N/A	0.6 mm	0.6 mm
B value	N/A	N/A	50/800 mm^2/s
Scan time	10–12 s	130–150 s	120–160 s

T1WI, T1-weighted image; T2WI, T2-weighted image; DWI, diffusion-weighted imaging; TR, repetition time; TE, echo time; FA, fractional anisotropy; FOV, field of view. VIBE, volumetric interpolated body examination; FS-TSE, fat saturation-turbo spin echo; NEX, number of excitation. N/A, not applicable.

Statistical analysis

The maximum diameter of the tumor on CT before ablation, the central hypointense area on MRI T2-weighted image (T2WI) after ablation, the central hyperintense area on T1-weighted image (T1WI) after ablation, and the maximum diameter of coagulative necrosis on pathology were measured and compared. At the same time, the maximum diameter of the GGO around the tumor on CT after ablation, the peripheral hyperintense area on T2WI after ablation, the peripheral isointense area on T1WI after ablation, and the maximum diameter of the thermal injury area on pathology were also measured and compared. All indicators are expressed as mean ± SD. Statistical analysis was performed using the t-test of the SPSS software (version 22.0; IBM, Chicago, IL, USA), and $p < 0.05$ was considered statistically significant.

Results

MRI findings before ablation

All rabbit lung VX2 tumors before ablation showed a round or slightly round-like hyperintense zone on T2WI and an isointense zone on T1WI compared with chest wall muscle (Figures 2, 3), as well as a hyperintense zone on diffusion-weighted imaging (DWI) with clear boundaries.

Procedure and CT/MRI findings after ablation

Thermal ablation was accomplished in all 12 rabbits' lung VX2 tumors. CT showed GGO surrounding the original tumor in the lungs of 11 rabbits immediately after ablation (Figure 2E). In the remaining 1 rabbit, a blood vessel was injured during the RF electrode puncture into the target, resulting in patchy hemorrhage in the lung. The margin of the ablative zone was relatively unclear after the procedure.

In an MR scan immediately after ablation, the ablative areas showed a hypointense zone in the center surrounded by a ring-like hyperintense zone on T2WI. Meanwhile, the ablative areas showed a hyperintense zone in the center surrounded by a ring-like isointense zone on T1WI (Figure 2F). There was a hypointense zone in the center with a slightly ring-like hyperintense zone surrounding the ablated area, and the signal of original lesions was significantly reduced after ablation as observed on DWI.

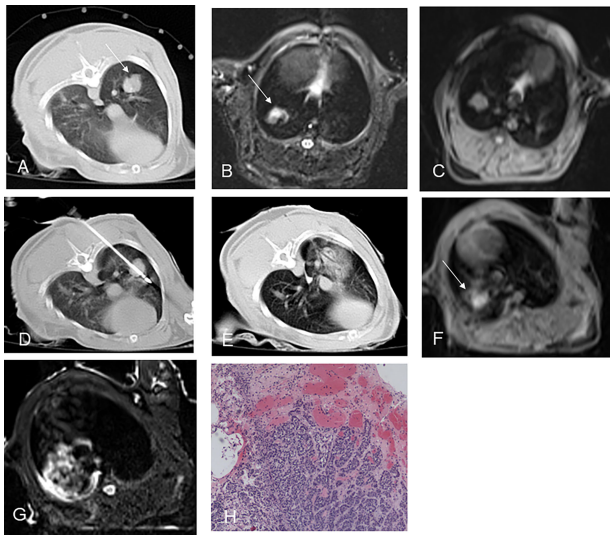

FIGURE 2
CT-guided RFA for rabbit lung VX2 tumor with MR and pathological findings. CT showed a VX2 tumor located in right lower lobe with 12 mm in diameter (**A**, arrow). The pre-ablation MR scan of the tumor showed hyperintensity on T2WI and isointensity on T1WI before RFA (**B, C**, arrow). Radiofrequency electrode was gradually punctured into the tumor under CT guidance **(D)**. GGO surrounding the lesion with 5 mm beyond was displayed immediately after RFA on CT **(E)**. Immediately after RFA, MR showed short T1 and short T2 signals in the central area and patchy iso-T1 and long T2 signals in the periphery (**F, G** arrow). Pathology showed coagulative necrosis of the ablation foci, with peripheral hemorrhage and inflammatory reaction zone **(H)**. RFA, radiofrequency ablation; T2WI, T2-weighted image; T1WI, T1-weighted image; GGO, ground-glass opacity.

10.3389/fonc.2022.941752

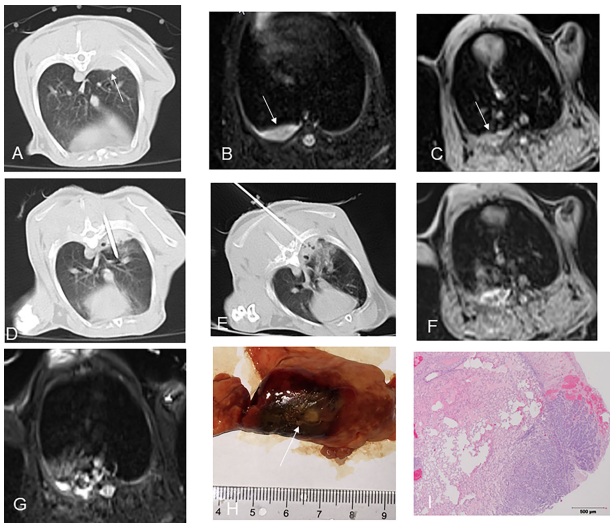

FIGURE 3
CT-guided MWA for rabbit lung VX2 tumor with MR and pathological findings. CT showed a VX2 tumor located in right lower lobe with 13 mm in diameter and invasion of adjacent pleura (**A**, arrow). The pre-ablation MR scan of the tumor showed hyperintensity on T2WI and isointense zone on T1WI before MWA (**B, C**, arrow). MW antenna was gradually punctured into the tumor under CT guidance **(D)**. GGO surrounding the lesion was displayed immediately after MWA on CT **(E)**. Immediately after MWA, MR showed short T1 and short T2 signals in the central area with patchy iso-T1 and long T2 signals in the periphery including adjacent pleura and chest wall **(F, G)**. Pathology showed coagulative necrosis of the ablation area including invasion of adjacent pleura, with peripheral hemorrhage and inflammatory reaction zone (**H, I** arrow). MWA, microwave ablation; T2WI, T2-weighted image; T1WI, T1-weighted image; GGO, ground-glass opacity. .

Pathology

The gross specimens of rabbit lung VX2 tumors after thermal ablation showed that the tumor tissues had a gray-white coagulation necrosis area after ablation, and the needle track area in the center of the ablation area was a fissure-like carbonization center, which was seen more in the MWA group than the RFA group. The lung tissue had a reddish-brown coagulation necrosis area, the coagulation necrosis areas were surrounded by a hemorrhagic zone, and a large area of congestion and edema was seen around the hemorrhage zone (Figures 2H and 3H, I). One case showed residual VX2 tumor tissue in the RFA group confirmed by pathological examination. The remaining 11 cases showed complete ablation confirmed by pathological examination.

Statistical results

There was statistical significance in the comparison of the maximum diameter of the tumor before ablation with a central hypointense zone on T2WI, a central hyperintense zone on T1WI after ablation, and pathological necrosis in both the RFA and MWA groups ($p < 0.002$, Table 2). There was no significant difference between the maximum diameter of the central hypointense zone on T2WI after ablation, the central hyperintense zone on T1WI after RFA, and the maximum diameter of coagulative necrosis on pathology in both the RFA and MWA groups ($p > 0.05$, Tables 2, 3).

There was no significant difference between the maximum diameter of the peripheral hyperintense area on T2WI after ablation and the maximum diameter of the peripheral isointense

TABLE 2 Comparison of MD of tumor on CT pre-ablation, central hypointense zone on T2WI, central hyperintense zone on T1WI, and MD of coagulative necrosis on pathology post-ablation (mm).

	Pre-ablation (CT)	Central hypointense (T2)	Central hyperintense (T1)	Necrosis (pathology)
MD (RFA)	11.4 ± 3.2	13.6 ± 4.5	13.8 ± 6.3	15.0 ± 4.8
MD (MWA)	11.8 ± 2.9	14.2 ± 5.5	14.9 ± 3.3	15.2 ± 5.5

MD, maximum diameter; T2WI, T2-weighted image; T1WI, T1-weighted image; RFA, radiofrequency ablation; MWA, microwave ablation.

TABLE 3 Comparison of MD of MR performance and pathology after thermal ablation (mm).

	Central hypointense (T2) and central hyperintense (T1)	Necrosis (pathology)	p-Value
MD	14.5 ± 4.8	15.1 ± 2.8	0.07
	Peripheral hyperintense (T2) and peripheral isointense (T1)	Thermal injury (pathology)	
MD	23.8 ± 3.8	25.2 ± 6.3	0.004

MD, maximum diameter.

area on T1WI after ablation ($p > 0.05$, Table 4). There was statistical significance in the comparison of the maximum diameter of GGO around the lesion on CT with a peripheral hyperintense zone on T2WI, peripheral isointense on T1WI after ablation, and thermal injury on pathology ($p < 0.005$, Tables 3, 4).

Discussion

At present, CT is commonly used to guide thermal ablation for lung tumors and evaluate the ablative efficacy immediately (3–5). GGO of the lung tissue covering the original tumor and exceeding 5–10 mm is usually considered a sign of successful ablation (6, 7). However, the GGO after ablation is sometimes confused with the hemorrhage of mechanical damage to the lung tissue during the puncture process, and the density of the tumors does not significantly change during the CT scan. Therefore, it is not accurate to use CT alone to evaluate the immediate effect of lung tumor ablation, especially when combined with postoperative puncture bleeding (8).

Miao et al. (9) performed RFA for rabbit VX2 lung tumor models and found that five typical isocenter areas formed around the radiofrequency needle after RFA: needle tract area, tumor coagulated necrosis area, lung parenchyma coagulated necrosis area, peripheral hemorrhage, and inflammatory area. In this study, the pathological changes of the rabbit lung VX2 tumor after thermal ablation were similar to those reported in the literature. MRI findings have certain characteristics after ablation due to MRI's sensitivity to changes in tissue temperature and water content (10–12). Oyama (13) conducted a comparison study of MRI manifestations and pathology after RFA of normal pig lungs. After RFA of normal pig lungs, there was an inner zone of equal T1 short T2 signals with an outer zone of long T2 signal surrounding. The analysis with confirmation by pathological examination showed that the inner zone with equal T1 short T2 signal was a coagulated necrosis area, and the outer zone with long T2 signal showed pulmonary heat injury area including neutrophil infiltration, alveolar effusion, and pulmonary congestion. In this study, short T1 and short T2 signals were observed in the center of the thermal ablated zone on MRI. The maximum diameters of the central short T2 signal area and the central short T1 signal area after ablation are similar to those of the pathological coagulated necrosis area, which included tumor coagulated necrosis and lung coagulated necrosis area. Meanwhile, the maximum diameter of the pathological coagulated necrosis area was larger than that of the tumor before ablation but smaller than the maximum diameter of the GGO on the CT after ablation. The peripheral equal T1 long T2 signal area on MRI was considered to correspond to the pathological peripheral hemorrhage area and inflammatory layer area, both of which were larger than the peripheral GGO range on CT after ablation. It was indicated that MRI was more sensitive to the changes of intra-alveolar exudation than CT.

In this study, there was 1 case of needle tract bleeding during puncture in the RFA group, which affected the judgment of CT curative effect. Immediate post-ablation MRI could clearly distinguish the coagulation necrosis area from the bleeding area according to the characteristic changes, which showed a more objective evaluation of the ablation curative effect.

According to reports, MWA is less affected by the heat sink effect compared to RFA (14, 15). In this study, all 6 cases of rabbit lung VX2 tumors in the MWA group showed complete ablation by pathology. In the RFA group, 1 case showed residual tumor after ablation, which was located next to the blood vessel in the right lower lobe. Residual tumor was displayed as slightly equal T1 long T2 signal and considered to be related to the heat sink effect.

This study had certain limitations. First, the sample size of experimental animals was small. Second, contrast-enhanced MRI and CT scans were not used to further evaluate the

TABLE 4 Comparison of MD of GGO around tumor on CT, peripheral hyperintense zone on T2WI, peripheral isointense on T1WI, and thermal injury on pathology post-ablation (mm).

	GGO (CT)	Peripheral hyperintense (T2)	Peripheral isointense (T1)	Thermal injury (pathology)
MD (RFA)	20.8 ± 4.5	23.7 ± 5.4	23.5 ± 6.2	24.9 ± 6.9
MD (MWA)	21.6 ± 6.5	24.2 ± 4.7	24.0 ± 3.8	25.2 ± 5.8

MD, maximum diameter; GGO, ground-glass opacity; T2WI, T2-weighted image; T1WI, T1-weighted image; RFA, radiofrequency ablation; MWA, microwave ablation.

efficacy of ablation. Third, only acute thermal ablation injury was observed immediately without dynamic observation for imaging and pathological evolution of ablated lesions. The shortcomings need to be improved in future research.

In conclusion, MRI manifestations of thermal ablation zones for rabbit lung VX2 tumors have certain characteristics and better corresponded with pathology than CT. CT combined with MRI multimodal radiomics is expected to provide an effective new method for clinical evaluation of the immediate efficacy of thermal ablation of lung tumors and to improve the complete tumor ablation rate.

Data availability statement

The raw data supporting the conclusions of this article will be made available by the authors, without undue reservation.

Ethics statement

The animal study was reviewed and approved by First Affiliated Hospital of Fujian Medical University.

Author contributions

ZL conceptualized the study, prepared figures and tables. JinC wrote the article and prepared figures and tables. YY collected the data, carried out the analysis, and prepared the figures and tables. QL, JiaC, and JieC participated in drafting and editing the article and assisted in the preparation of figures and tables. All authors contributed to the article and approved the submitted version.

Funding

This study was funded by Develop Program of Focus Field of Guangdong Province, PRC (2019B110233001).

Conflict of interest

The authors declare that the research was conducted in the absence of any commercial or financial relationships that could be construed as a potential conflict of interest.

Publisher's note

All claims expressed in this article are solely those of the authors and do not necessarily represent those of their affiliated organizations, or those of the publisher, the editors and the reviewers. Any product that may be evaluated in this article, or claim that may be made by its manufacturer, is not guaranteed or endorsed by the publisher.

References

1. Sung H, Ferlay J, Siegel RL, Laversanne M, Soerjomataram I, Jemal A, et al. Global cancer statistics 2020: GLOBOCAN estimates of incidence and mortality worldwide for 36 cancers in 185 countries. *CA Cancer J Clin* (2021) 71(3):209–49. doi: 10.3322/caac.21660

2. Baère TD, Aupérin A, Deschamps F, Chevallier P, Gaubert Y, Boige V, et al. Radiofrequency ablation is a valid treatment option for lung metastases: experience in 566 patients with 1037 metastases. *Ann Oncol* (2015) 26(5):987–91. doi: 10.1093/annonc/mdv037

3. Hasegawa T, Takaki H, Kodama H, Yamanaka T, Nakatsuka A, Sato Y, et al, et al. Three-year survival rate after radiofrequency ablation for surgically resectable colorectal lung metastases: A prospective multicenter study. *Radiology* (2020) 294 (3):686–95. doi: 10.1148/radiol.2020191272

4. Ni Y, Hui X, Xin Y. Image-guided percutaneous microwave ablation of early-stage non-small cell lung cancer[J]. *Asia-Pacific J Clin Oncol* (2020) 16(6):320–5. doi: 10.1111/ajco.13419

5. Uhlig J, Ludwig JM, Goldberg SB, Chiang A, Blasberg JD, Kim HS., et al. Survival rates after thermal ablation versus stereotactic radiation therapy for stage 1 non-small cell lung cancer: A national cancer database Study. *Radiology* (2018) 289 (3):862–70. doi: 10.1148/radiol.2018180979

6. Iguchi T, Hiraki T, Gobara H, Fujiwara H, Matsui Y, Soh J, et al. Percutaneous radiofrequency ablation of lung cancer presenting as ground-glass opacity. *Cardiovasc Intervent Radiol* (2014). doi: 10.1007/s00270-014-0926-x

7. Abtin FG, Eradat J, Gutierrez AJ, Lee C, Fishbein MC, Suh RD, et al. Radiofrequency ablation of lung tumors: imaging features of the postablation zone. *Radiographics* (2012) 32(4):947–69. doi: 10.1148/rg.324105181

8. Jin C, Lin Z-Y, Wu Z-B, Chen Z-W, Chen Y-P. Magnetic resonance imaging evaluation after radiofrequency ablation for malignant lung tumors. *J Cancer Res Ther* (2017) 13(4):669–75. doi: 10.4103/jcrt.JCRT_448_17

9. Miao Y, Ni Y, Bosmans H, Yu J, Vaninbroukx J, Dymarkowski S, et al. Radiofrequency ablation for eradication of pulmonary tumor in rabbits. *J Surg Res* (2001) 99(2):265–271. doi: 10.1006/jsre.2001.6208

10. Stephan C, Pereira PL. Magnetic resonance guidance for radiofrequency ablation of liver tumors. *J Magn Reson Imaging.* (2010) 27(2):421–33. doi: 10.1002/jmri.21264

11. Lazebnik RS, Breen MS, Fitzmaurice M, Nour SG, Lewin JS, Wilson DL. Radio-frequency-induced thermal lesions: Subacute magnetic resonance appearance and histological correlation. *J Magn Reson Imaging.* (2003) 18 (4):487–95. doi: 10.1002/jmri.10382

12. Weiss J, Hoffmann R, Rempp H, Keβler DE, Pereira PL, Nikolaou K, et al. Feasibility, efficacy, and safety of percutaneous MR-guided ablation of small (≤12 mm) hepatic malignancies. *J Magn Reson Imaging.* (2019) 49(2):374–81. doi: 10.1002/jmri.26252

13. Oyama Y, Nakamura K, Matsuoka T, Toyoshima M, Yamamoto A, Okuma T, et al. Radiofrequency ablated lesion in the normal porcine lung: Long-term follow-up with MRI and pathology. *Cardiovasc Intervent Radiol* (2005) 28:346–53. doi: 10.1007/s00270-004-0156-8

14. Vogl TJ, Eckert R, Naguib NN, Beeres M, Gruber-Rouh T, Nour-Eldin NA. Thermal ablation of colorectal lung metastases: Retrospective comparison among laser-induced thermotherapy, radiofrequency ablation, and microwave ablation. *AJR Am J Roentgenol.* (2016) 207(6):1340–9. doi: 10.2214/AJR.15.14401

15. Lu DS, Raman SS, Vodopich DJ, Wang M, Sayre J, Lassman C. Effect of vessel size on creation of hepatic radiofrequency lesion in pig: Assessment of the "heat sink" effect. *AJR Am J Roentgenol* (2002) 178(1):47–51. doi: 10.2214/ajr.178.1.1780047

frontiers | Frontiers in Oncology

ORIGINAL RESEARCH
published: 28 July 2022
doi: 10.3389/fonc.2022.955545

Synchronous Microwave Ablation Combined With Cisplatin Intratumoral Chemotherapy for Large Non-Small Cell Lung Cancer

Guanghui Huang[1], Wenhong Li[1], Min Meng[1], Yang Ni[1], Xiaoying Han[1], Jiao Wang[1], Zhigeng Zou[1], Tiehong Zhang[1], Jianjian Dai[1], Zhigang Wei[2], Xia Yang[1]* and Xin Ye[2]**

[1] Department of Oncology, Shandong Provincial Hospital Affiliated to Shandong First Medical University, Jinan, China, [2] Shandong Key Laboratory of Rheumatic Disease and Translational Medicine, Department of Oncology, The First Affiliated Hospital of Shandong First Medical University & Shandong Provincial Qianfoshan Hospital, Shandong Lung Cancer Institute, Jinan, China

OPEN ACCESS

Edited by:
Edouard Auclin,
Hôpital Européen
Georges-Pompidou, France

Reviewed by:
Frank Aboubakar Nana,
Catholic University of Louvain, Belgium
Mattia Falchetto Osti,
Sapienza University of Rome, Italy
Xin Li,
People's Liberation Army General
Hospital, China

***Correspondence:**
Guanghui Huang
hgh3612@163.com
Xia Yang
yangxjinan@163.com
Xin Ye
yexintaian2014@163.com

Specialty section:
This article was submitted to
Thoracic Oncology,
a section of the journal
Frontiers in Oncology

Received: 28 May 2022
Accepted: 22 June 2022
Published: 28 July 2022

Citation:
Huang G, Li W, Meng M, Ni Y, Han X, Wang J, Zou Z, Zhang T, Dai J, Wei Z, Yang X and Ye X (2022) Synchronous Microwave Ablation Combined With Cisplatin Intratumoral Chemotherapy for Large Non-Small Cell Lung Cancer. Front. Oncol. 12:955545. doi: 10.3389/fonc.2022.955545

Background: Microwave ablation (MWA) and intratumoral chemotherapy (ITC) are useful for treating tumors in animal models; however, their clinical use in patients with large non–small cell lung cancer (NSCLC) remains unknown. This retrospective study aimed to evaluate preliminary outcomes of MWA + ITC for large NSCLC.

Methods: From November 2015 to April 2020, a total of 44 NSCLC patients with a mean lesion diameter of 6.1 ± 1.5 cm were enrolled and underwent synchronous MWA + ITC procedures. The primary endpoint was local progression-free survival (LPFS); secondary endpoints were progression-free survival (PFS), complications, overall survival (OS), and associated prognostic factors.

Results: The median follow-up time was 19.0 months. At the 1-month CT scan, complete tumor ablation was observed in 47.7% of cases. Median LPFS was 12.1 months; 1-, 2-, and 3-year LPFS rates were 51.2%, 27.9%, and 13.6%, respectively. A shorter LPFS was significantly associated with large lesions (HR 1.23, 95% CI 1.02–1.49; p = 0.032). Median PFS was 8.1 months; 1-, 2-, and 3-year PFS rates were 29.5%, 18.2%, and 9.1%, respectively. LPFS was significantly superior to PFS (p = 0.046). Median OS was 18.8 months. The 1-, 2-, 3-, and 5-year OS rates were 65.9%, 43.2%, 26.4%, and 10.0%, respectively. In univariate comparisons, high performance status (PS) score, smoking, and larger lesions were significantly correlated with poor survival. In multivariate analysis, advanced age, higher PS score, higher stage, larger lesion, and prior systematic treatment were independent prognostic factors for shorter OS. Adverse events were well tolerated and all patients recovered after appropriate intervention.

Conclusions: MWA + ITC is a safe and effective new modality of local treatment for large NSCLC and can significantly prolong LPFS.

Keywords: microwave ablation, intratumoral chemotherapy, non-small cell lung cancer, cisplatin, local progression-free survival

INTRODUCTION

Lung cancer is the second most frequently occurring malignancy with an estimated 2.2 million new cases, constituting 11.4% of all diagnosed cancers in 2020, and as the leading cause of cancer-related mortality with an estimated 1.8 million deaths making up 18% of total cancer deaths worldwide (1). Non-small cell lung cancer (NSCLC) accounts for approximately 85% of all lung cancer patients. Despite advances in treatment and prognosis in the last decade, NSCLC presents a poor 5-year overall survival rate, ranging from 68% at clinical stage IB to 0%–10% at clinical stage IVA-IVB (2, 3).

Over the last decade, percutaneous image-guided thermal ablation (IGTA) has been increasingly applied as a safe, cost-effective, and precise minimally invasive alternative therapy for patients not qualified for surgery. Radiofrequency ablation (RFA), microwave ablation (MWA), and cryoablation are the most frequently used modalities. In contrast to RFA, MWA utilizes the dielectric hysteresis effect of polar molecules under a high-frequency electromagnetic field (915 or 2450 MHz) to generate heat >60°C and achieve cellular coagulation necrosis (4). Microwaves can propagate effectively through air-filled lungs, which are special organs characterized by a high impedance, low electrical conductivity, and low thermal transfer. Furthermore, MWA is more advantageous than RFA as it has a larger ablation zone, shorter ablation duration, lower heat-sinking effect, and combines the synergistic action of multiple antennae (5). Therefore, MWA either alone or in combination with systemic treatment has been progressively used for the treatment of early-stage and advanced NSCLC stage I to IV (6–8).

Despite the theoretical superiority of MWA, as it is unlimited by impedance, unsatisfactory long-term effects in lesions >3 cm, particularly those of 5 cm diameter, or adjacent to large vessels, has decreased the confidence in expanding MWA's scope of clinical application (9). Therefore, a new strategy for MWA treatment of large tumors capable of persistently enhancing local control or strongly debulk tumor burden by maximizing the area of coagulation necrosis is needed. One very promising modality surmounting the current limitations of MWA alone is its combination with intratumoral chemotherapy (ITC) (10). Results from animal models have provided evidence supporting a positive role for synchronous thermal ablation plus ITC with cisplatin, paclitaxel, or doxorubicin (11–13). This retrospective study aimed to investigate the feasibility, safety, and preliminary outcomes of patients with large advanced NSCLC undergoing synchronous MWA plus ITC (hereinafter referred to as MWA + ITC) under computed tomography (CT) guidance as a local palliative treatment.

MATERIAL AND METHODS

Patient's Selection

This study was approved by the Ethics Committee of Shandong Provincial Hospital Affiliated to Shandong First Medical University and followed the tenets of the Declaration of Helsinki. Informed consent was waived due to the retrospective nature of this study. However, written informed consent was obtained before MWA + ITC. For the purposes of this study, 44 NSCLC patients who received MWA + ITC were recruited and retrospectively analyzed between November 2015 and April 2020. The integral course of treatment for each patient was accomplished by a comprehensive medical team including interventional radiology, thoracic surgery, medical oncology, and radiotherapy experts. In this study, the chemotherapeutic agent administered directly into the lesions of all NSCLC patients was a cisplatin aqueous solution with iodixanol.

Patient inclusion criteria were as follows: (a) Eastern Cooperative Oncology Group performance status (ECOG PS) score 0–2, (b) age ≥18 years, and non-pregnant if female, (c) pathologically confirmed NSCLC, (d) newly diagnosed patients unsuitable for or refusing surgery and radiotherapy, or patients with progressive disease after or refractory to standard treatments, (e) the maximum diameter of primary lung lesions to be ablated >4 cm, (f) life expectancy ≥6 months. Exclusion criteria included: (a) primary lung tumors other than NSCLC (e.g., small cell lung cancer and neuroendocrine tumors), (b) untreatable coagulopathies and/or platelet count $< 50 \times 10^9$/L, (c) brain metastasis with compression symptoms, (d) incomplete clinical and radiological data, and (e) loss of follow-up.

The clinical database collected from the entire study population before and after MWA + ITC procedures consisted of (a) age, (b) sex, (c) initial staging for new patients or re-staging for treated patients, (d) tumor characteristics including size, location, pathological type, and anatomical structures nearby (such as large vessels, pleura, or chest wall), (e) previous treatment modality including surgery, radiotherapy, chemotherapy, molecular targeted therapy, and/or immunotherapy, (f) follow-up data including the occurrence of local and systemic tumor progression, survival time, and cause of mortality.

Pretreatment Preparation and Instruments

Before treatment, chest and abdomen contrast-enhanced CT scan and brain magnetic resonance imaging (MRI) within 2 weeks were implemented for each patient in addition to a routine examination of complete blood count, coagulation function, electrocardiogram, and cardiopulmonary function. If necessary and economically feasible, PET-CT and E-BUS were highly recommended for accurate staging. The decision to perform MWA + ITC was ultimately reached after a comprehensive discussion by a multi-disciplinary team comprised of at least a medical oncologist, thoracic surgeon, respiratory physician, radiologist, and pathologist. All patients were nonsurgical candidates due to poor cardiopulmonary function, advanced age, other medical comorbidities, or refusal of surgery and radiation therapy. The patients or their legal representatives were fully informed of disease severity, treatment risks, possible complications, and benefits of the combination treatment. Patients should be fasted for >4 h and not routinely prescribed antibiotics for prophylaxis during the peri-procedural period.

CT (Lightspeed 64 V, GE General Electric or NeuViz64, Neusoft Co., Ltd. or uCT 760, United Imaging Healthcare Co., Ltd.) was used to guide procedures. MWA was performed with

an MTC-3C microwave ablation system (Vison-China Medical Devices R&D Center), ECO-100A1 microwave ablation system (ECO Medical Instrument Co., Ltd.), or KY-2450B microwave ablation system (CANYOU Medical Inc.), with a frequency of 2450 ± 50 MHz; the adjustable continuous-wave output power ranged from 0 to 100 W. For the microwave antenna, the effective length was 100–180 mm and the outside diameter was 19 G (a 19G antenna has the advantages of high puncture accuracy and few complications), with a 1.5 cm radiating tip (tapered end). The surface temperature of the antennae was cooled with a water circulation cooling system. ITC was performed *via* ≥1 21 gage Chiba needles (Hakko Co., LTD. Chikuma-Shi, Japan) directly inserted into the tumors. Cisplatin (Qilu Medical Co., Jinan, China) was diluted into an aqueous solution at 2–4 mg/mL (14, 15), then mixed with iodixanol (Jiangsu Hengrui Medical Co., LTD. China) at a ratio of 10:1. Iodixanol was used to aid local drug visualization for tracking the dispersion of the cisplatin solution.

MWA + ITC Procedure

Detailed MWA procedures were as we previously described. For tumors contiguous to or involving the chest wall, intercostal nerve block plus intravenous conscious sedation was applied to relieve the patients' discomfort as much as possible during the procedures. The entire procedure was conducted by simultaneously placing the antenna and Chiba needles into the pre-planned tumor sites. Once proper positioning of the antenna and Chiba needles was ascertained *via* CT, ITC was performed immediately followed by MWA. The procedure of ITC was similar to that of the MWA procedure (6–8). Given the remarkably larger size of the lesions in this study, MWA + ITC were accomplished by a flexible pattern of multiple antenna/needles placed at multiple sites to maximize the treatment area (example cases shown in **Figures 1**, **2**). Based on the lesion size, cisplatin doses administration was as follows: (a) 20–40 mg for tumors with a diameter ≤4.5 cm; (b) 40–60 mg for those between 4.5–6.5 cm; (c) 60–80 mg for those ≥6.5 cm. Ablation parameters such as power and time referred to the recommendations of the device manufacturer. Depending on the stage, histology, genetic alterations, prior treatment regime, and patient's condition, administration of systemic chemotherapy, molecularly targeted therapy, and immunotherapy either alone or in combination was allowed after MWA + ITC if necessary and feasible. The general interval between MWA + ITC and systemic therapy was <7 days.

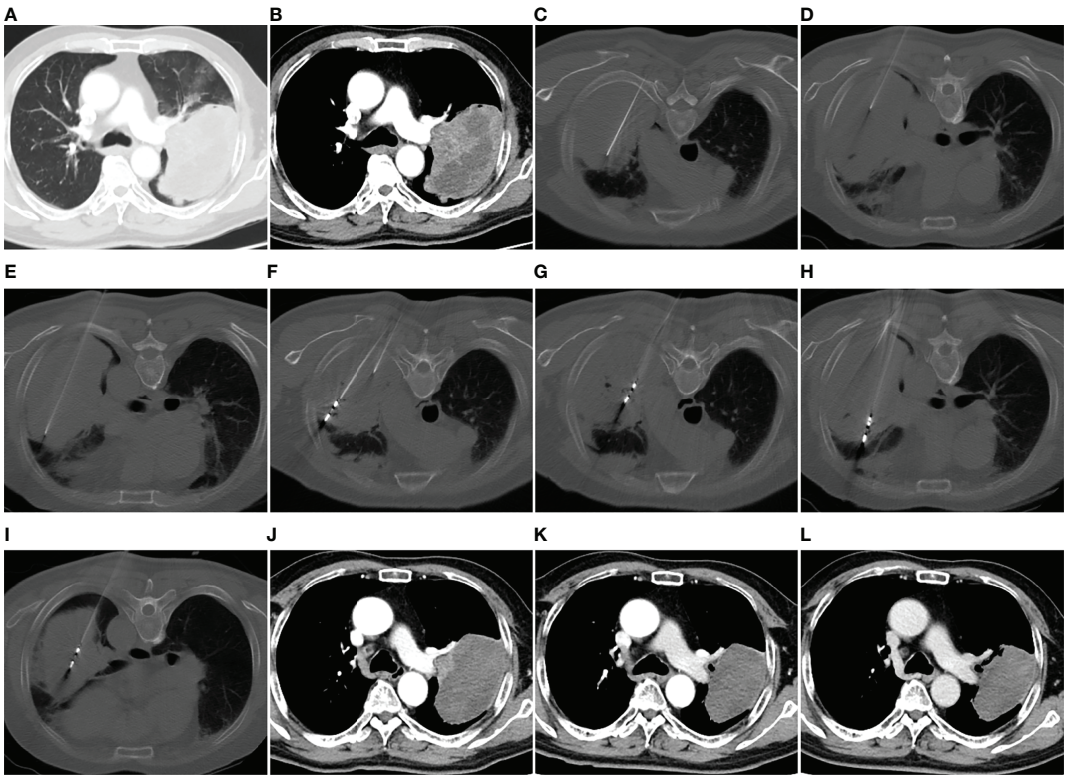

FIGURE 1 | MWA + ITC treatment of a large squamous cell lung cancer in the left upper lobe of a 69-year-old man. Enhanced CT scan in the pulmonary window **(A)** and mediastinal window **(B)** showing a mass with a maximum diameter of 11.5 cm adjacent to the left pulmonary artery. **(C–E)** Direct injection of 40 mL aqueous solution containing 80 mg cisplatin into the mass *via* three 21-gage Chiba needles at a multisite. **(F–I)** MWA using four antennae at multisite and multisession with an ablation power of 60 W and a cumulative ablation time of 52 min. **(J)** Enhanced CT scan at 1-month follow-up after MWA + ITC showing an almost complete necrosis of the ablation zone. **(K, L)** Enhanced CT scan at 3- and 9-month follow-up after MWA + ITC showing gradually involuting fibrosis of the necrotic zone and no local residue. MWA, microwave ablation; ITC, intratumoral chemotherapy; CT, computed tomography.

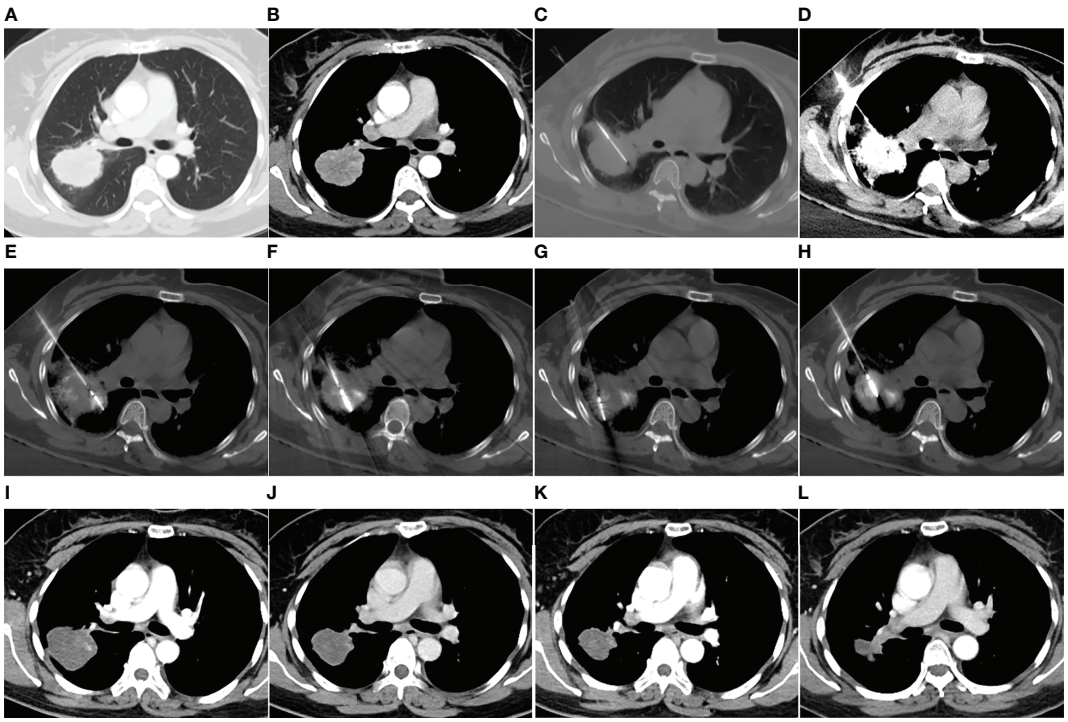

FIGURE 2 | MWA + ITC treatment of a large lung adenocarcinoma in the right upper lobe of a 48-year-old woman. Enhanced CT scan in the pulmonary **(A)** and mediastinal window **(B)** showing a nearly round mass with a diameter of 5.0 cm close to a large hilar vessel. **(C)** Insertion of a 21-gage Chiba needle into the side of the tumor near the hilar vessel. **(D)** Injection of 40 mg cisplatin aqueous solution containing 2 mL iodixanol into the mass, and diffusion of the agent over the entire tumor displayed by high-density iodixanol. **(E–H)** MWA using two antennae with multisite and multisession insertions. **(I)** Enhanced CT scan at 1-month follow-up showing complete necrosis. **(J–L)** Enhanced CT scan at 3-, 9-, and 18-month follow-up after MWA + ITC showing gradually involuting fibrosis of the necrotic zone and no local recurrence. MWA, microwave ablation; ITC, intratumoral chemotherapy; CT, computed tomography.

Follow-Up

A non-contrast chest CT scan was performed 24 h post-procedure for all patients to assess potential complications, such as massive pneumothorax, pleural effusion, or hemorrhage, which needed prompt interventions. Contrast-enhanced whole-body CT scans were performed at 1, 3, 6, 9, and 12 months for the first year, and every 6 months thereafter, or at any time attributable to sudden aggravation of the patient's condition. The size of the ablation zone measured at the 1-month CT scan was used as a baseline reference to which subsequent follow-up images were compared. According to expert consensus for thermal ablation of lung tumors (2018 Edition), the local effect of ablative responses involves complete and incomplete ablation, and local progression (16). No abnormal contrast enhancement in the arterial phase of the follow-up CT scan at 1 month was considered complete ablation, whereas irregular or nodular enhancement signs at the margin of the ablation zone were considered incomplete. Local progression was defined as increases >10 mm in size with irregular or nodular enhancement signs in the ablation field at the later CT scan compared with the 1-month CT scan. When necessary, PET-CT was also used for assessment of the uncertainty of viable tumors 3 months after the procedure. In the case of locally progressive foci, ≥2 MWA ± ITC sessions were performed if feasible, but these subsequent procedures were not included in the analysis.

The primary endpoint was local progression-free survival (LPFS), defined as the interval from MWA + ITC treatment to local progression, or death. Secondary endpoints included progression-free survival (PFS), complications, overall survival (OS), and predictive factors associated with prognosis. PFS was defined as the interval from MWA + ITC treatment to disease objective progression, including local progression and/or distant progression, or death. OS was defined as the interval from MWA + ITC treatment to death or last follow-up. In this study, the cause of death for all patients was cancer-related.

Statistical Analysis

Continuous data are presented as mean/median, range, and standard deviation and categorical data are described as frequencies and percentages. The Kaplan–Meier log-rank test was used for univariate survival curve comparisons, if no additional statement was attached. When variables had a $P< 0.2$ in univariate analysis, they were included in multivariate analysis. Multivariate Cox proportional hazard models were

performed to screen prognostic factors and the corresponding hazard ratios (HR) for different factors with 95% confidence intervals (CI). P-values were two-sided and considered significant if <0.05. Statistical analysis was performed using SPSS for Windows Version 26.0 (IBM, Chicago, IL, USA).

RESULTS

Patients and Tumors Characteristics

Based on our inclusion and exclusion criteria, 44 patients (34 males and 10 females; mean age: 65.9 ± 10.4 years, range: 44–86 years) with primary NSCLC lesions (mean size: 6.1 ± 1.5 cm, range: 4.1–11.5 cm) underwent percutaneous MWA + ITC treatment under CT guidance from November 2015 to April 2020 in this study. The clinical characteristics of patients and tumors are summarized in **Table 1**. Adenocarcinoma was the most common pathologic type (23, 52.3%), followed by squamous cell carcinoma (SCC, 16, 36.4%) and undefined NSCLC (5, 11.4%). The clinical staging in all patients covered stage IIA in one (2.3%) case, stage IIB in six (13.6%) cases, stage IIIA in seven (15.9%) cases, stage IIIB in six (13.6%) cases, stage IIIC in six (13.6%) cases, stage IVA in 10 (22.7%) cases, and stage IVB in eight (18.2%) cases. Stratification by lesion size manifested as 10 (22.7%) cases ranging between 4.0–5.0 cm, 16 (36.4%) cases between 5.1–6.0 cm, 10 (22.7%) cases between 6.1–7.0 cm, and eight (18.2%) cases >7.0 cm. Of 44 lesions to be

TABLE 1 | Clinical characteristics of 44 patients (44 tumors) and univariate analysis of OS.

Variables	N (%)	mOS (95% CI) m	*p*-value
Age (years)	65.9 ± 10.4 (44-86)		
≤ 65	18 (40.9)	21.9 (9.5-34.4)	0.159
> 65	26 (59.1)	16.9 (8.6-25.2)	
Gender			
Male	34 (77.3)	16.9 (7.6-26.3)	0.123
Female	10 (22.7)	25.2 (11.0-39.4)	
Smoking history			
Smoking	31 (70.5)	12.23 (3.5-21.0)	0.035
Non-smoking	13 (29.5)	31.1 (3.3-58.9)	
ECOG PS score			
0-1	27 (61.4)	24.1 (14.1-34.1)	0.029
2	17 (38.6)	9.1 (4.3-13.8)	
Chronic comorbidities			
Yes	23 (52.3)	19.3 (11.5-27.1)	0.901
No	21 (47.7)	18.8 (8.4-29.1)	
Pathology			
SCC	16 (36.4)	18.6 (15.0-22.2)	0.792
Non-SCC	28 (63.6)	21.9 (5.2-38.7)	
Stage at treatment			
IIA-IIIB	20 (45.5)	21.9 (10.9-43.3)	0.16
IIIC-IVB	24 (54.5)	12 (2.4-21.7)	
Lesion size (cm)	6.1 ± 1.5 (4.1-11.5)		
≤5.5 cm	23 (52.3)	31.1 (18.7-43.5)	0.032
>5.5 cm	21 (47.7)	12.2 (4.9-19.6)	
EGFR status			
Wild type	35 (79.5)	18.6 (10.5-26.8)	0.28
Mutant	9 (20.5)	31.1 (13.8-48.4)	
Prior antitumor therapy			
No	28 (63.6)	21.9 (9.15-34.7)	0.174
Yes	16 (36.4)	11.9 (9.1-14.7)	
Prior systematic treatment			
Yes	13 (29.5)	11.9 (8.5-15.4)	0.058
No	31 (70.5)	25.2 (13.2-37.1)	
Site of onset occurrence			
Peripheral	27 (61.4)	21.9 (13.6-30.3)	0.283
Central	17 (38.6)	12.8 (4.3-21.3)	
Closer to hilar large vessels			
Yes	24 (54.5)	16.9 (9.0-24.9)	0.722
No	20 (45.5)	19.3 (13.3-25.3)	
Involvement of pleura/chest wall			
Yes	17 (38.6)	12.2 (3.2-21.2)	0.139
No	27 (61.4)	25.2 (8.5-41.9)	

Continuous data are presented as mean ± SD (range). Numbers in the parentheses represent percentages or ranges.
OS, overall survival; CI, confidence interval; ECOG PS, Eastern Cooperative Oncology Group performance status; SCC, squamous cell carcinoma; EGFR, epidermal growth factor receptor.

treated locally, 12 (27.3%), one (2.3%), seven (15.9%), 13 (29.5%), and 11 (25.0%) cases were located in the right upper lobe, right middle lobe, right lower lobe, left upper lobe, and left lower lobe, respectively. Of all enrolled patients, 16 (36.4%) received prior antitumor therapy including surgery alone in one case, MWA alone in two cases, and systematic treatment (≥1 chemotherapy, molecularly targeted therapy, and immunotherapy) in 13 cases. Over half (23, 52.3%) of the patients suffered from ≥1 coexisting chronic comorbidities involving cardio-cerebrovascular disease (14 cases), chronic obstructive pulmonary disease (six cases), diabetes (six cases), cirrhosis (two cases), and autoimmune disease (one case).

Side Effects and Complications

No death occurred during the procedures or within 30 days after MWA + ITC. Side effects mainly included pain and postablation syndrome (**Table 2**). A total of 13 (29.5%) patients suffered intra- or post-procedural pain including 10 cases of mild and five cases of moderate pain and were positively treated with non-opioid analgesics. Postablation syndrome, mainly characterized by low-grade fever (<38.5°C), nausea, vomiting, and/or general malaise, occurred in 11 (25.0%) cases and was managed through low-dose dexamethasone or non-steroidal anti-inflammatory drugs. Major complications (**Table 2**) included massive pneumothorax or pleural effusion requiring chest tube drainage, as well as severe pulmonary infection or bronchopleural fistula lengthening the hospital stay. Minor complications (**Table 2**) included mild pneumothorax, small amounts of pleural effusion, pulmonary hemorrhage/hemoptysis, and subcutaneous emphysema, all asymptomatic or self-limiting and not requiring invasive intervention (17). Pneumothorax developed in 23 cases (52.3%), of which 10 (22.7%) cases required chest tube drainage. Pleural effusions occurred in 34 (77.3%) patients, only five (11.4%) of which required chest tube drainage. Pulmonary hemorrhage/hemoptysis was observed in nine (20.5%) cases and was effectively alleviated by the application of conventional hemostatic drugs such as reptilase and etamsylate. Slight subcutaneous emphysema appeared in four (9.1%) cases with spontaneous recovery. In addition, three (6.8%) patients showed pulmonary infection, including two cases of bacterial infection and one of Aspergillus infection; appropriate antibiotics were administered according to a drug susceptibility test. A bronchopleural fistula caused by pulmonary Aspergillus infection occurred in one (2.3%) patient for whom thoracic intubation for continuous drainage and regular flushing was required.

TABLE 2 | Parameters, side effects, and complications of MWA + ITC in 44 patients.

Variables	N (%)
Power of MWA (W)	
40	2 (4.5)
50	5 (11.4)
60	34 (77.3)
65	3 (6.8)
Number of antennae	
2	69 (88.6)
3	3 (6.8)
4	2 (4.5)
Ablation time (min)	26.82 ± 7.03 (12-52)
Dosage of cisplatin (mg)	
20	4 (9.1)
30	2 (4.5)
40	27 (61.4)
50	1 (2.3)
60	9(20.5)
80	1 (2.3)
Pain	13 (29.5)
Postablation syndrome	11 (25.0)
Pneumothorax	23 (52.3)
Chest tube drainage	10 (22.7)
Pleural effusion	34 (77.3)
Chest tube drainage	5 (11.4)
Subcutaneous emphysema	4 (9.1)
Pulmonary hemorrhage/hemoptysis	9 (20.5)
Infection	3 (6.8)
Bronchopleural fistula	1 (2.3)

Continuous data are presented as mean ± SD (range). Numbers in parentheses represent percentages or ranges.
MWA, microwave ablation; ITC, intratumoral chemotherapy.

Follow-Up

All procedures were technically successful and generally well tolerated. Detailed MWA + ITC parameters, including ablation power, ablation time, number of ablation antennae, and cisplatin dosage are listed in **Table 2**. Of all patients, 34 (77.3%) received systematic therapy after MWA + ITC, specifically presented as the application of chemotherapy, targeted therapy, and immunotherapy combined or alone in concurrent or sequential patterns. In addition, eight (18.2%) patients received local retreatment owing to local progression after MWA + ITC, including two cases with MWA, two cases with ^{125}I seed implantation, two cases with radiotherapy, one case with surgery, and another with MWA + ITC. At the 1-month enhanced CT scan, complete ablation was observed after 21 (47.7%) MWA + ITC procedures, and incomplete ablation after 25 (56.8%). The mean follow-up time was 24.3 ± 18.4 months with a median duration of 19.0 months (range, 3.4–76.3 months); no patients were lost to follow-up. Median PFS was 8.1 months, and 1-, 2-, and 3-year PFS rates were 29.5%, 18.2%, and 9.1%, respectively. Median LPFS was 12.1 months, and 1-, 2-, and 3-year LPFS rates were 51.2%, 27.9%, and 13.6%, respectively (**Table 3**). LPFS was significantly superior to PFS ($p = 0.046$), as shown in **Figure 3**. A shorter LPFS was significantly associated with large lesion size in Cox regression univariate analysis (HR 1.23, 95% CI 1.02–1.49; $p = 0.032$). A total of 36 (81.8%) patients succumbed to cancer in the follow-up period. Median OS was 18.8 months (95% CI, 8.8–28.7). The 1-, 2-, 3-, and 5-year OS rates were 65.9%, 43.2%, 26.4%, and 10.0%, respectively (**Table 3**, **Figure 4**). In univariate analysis, smoking, high ECOG PS score, and larger lesions were significantly correlated with poor survival (**Table 1**, **Figures 5**, **6**). In multivariate analysis, age, ECOG PS score, stage at treatment, lesion size, and prior systematic treatment were independent prognostic factors for OS (**Table 4**), while the impact of smoking on OS was not obvious.

TABLE 3 | Probability of survival in 44 patients undergoing MWA + ITC.

Variables	1-year (%)	2-year (%)	3-year (%)	5-year (%)
LPFS	51.2	27.9	13.6	ND
PFS	29.5	18.2	9.1	ND
OS	65.9	43.2	26.4	10.0

LPFS, local progression-free survival; PFS, progression-free survival; OS, overall survival; ND, no data.

DISCUSSION

MWA is increasingly used for radical treatment of inoperable early-stage NSCLC or refusal of surgery and has comparable therapeutic effects to SBRT (18). Generally, most patients are clearly defined as stage I with lesions ≤4 cm, while the remaining few cases were stage T2b-3N0M0 with lesions > 4 cm (7, 19, 20). In this study, the lesions of seven patients at stages IIA and IIB were confined to the lungs and could not be surgically removed due to chronic comorbidities. For patients with advanced NSCLC, the addition of local MWA as a local palliative treatment can significantly prolong PFS and OS based on systemic therapies such as chemotherapy, molecularly targeted therapy, or immunotherapy. However, in these patient groups, the mean diameter of ablated lesions is generally <5 cm (8, 21, 22). In this study, the average size of ablation lesions was 6.1 cm (4.1–11.5 cm); 34 (78.3%), 18 (40.9%), and eight (18.2%) of them were >5, 6, and 7 cm in diameter, respectively. Hence, both the average size of lesions and the proportion of lesions >4 cm in this study were far higher than described in a previous report focusing on MWA in large tumors (6 vs. 5 cm, 100% vs. 60%) (23, 24). Furthermore, our study did not exclude tumors abutting hilar large vessels, involving the visceral pleura, or transgressing the parietal pleura into the chest wall. Unfortunately, clinical evidence on the use of MWA for large NSCLC lesions is scarce, since very large tumors are extremely difficult to completely ablate. Here we hypothesize that tumor debulking may be of benefit in the following situations: (1) refractory pain caused by tumor infiltration of the parietal pleural nerve, (2) airway obstruction resulting from tumor compression near the center, (3) local rapid progression after systemic therapy, and (4) excessive tumor burden and unresectability.

In the past, ITC of primary NSCLC, a remarkably effective local intervention by direct injection or delivery of various cytotoxic agents into the tumor *via* an ordinary needle-catheter under the guidance of bronchoscopy, was mainly used for rapid re-canalization of central airway obstruction, commonly life-threatening and frequently resulting in death from suffocation if untreated (25). ITC has more unique advantages than conventional intravenous chemotherapy, including: (1) accuracy in local drug delivery, (2) complete drug permeation inside and around the target tumor, (3) achievement of dramatically higher tumor tissue concentrations, (4) marked reduction of systemic toxic and side effects, (5) synergistic effect in combination with surgery, radiotherapy, thermal ablation, and immunotherapy (11–15, 26), and (6) the potential for a tumor-specific immune response (27). In this study, a cisplatin aqueous solution injected *via* multisite Chiba needles was uniformly dispersed, completely encompassing the tumor mass and the surrounding margin, and could be visually displayed by incorporated iodixanol. As mentioned, despite the larger lesions undergoing MWA in this study, our complete ablation rate at 1 month was better than in

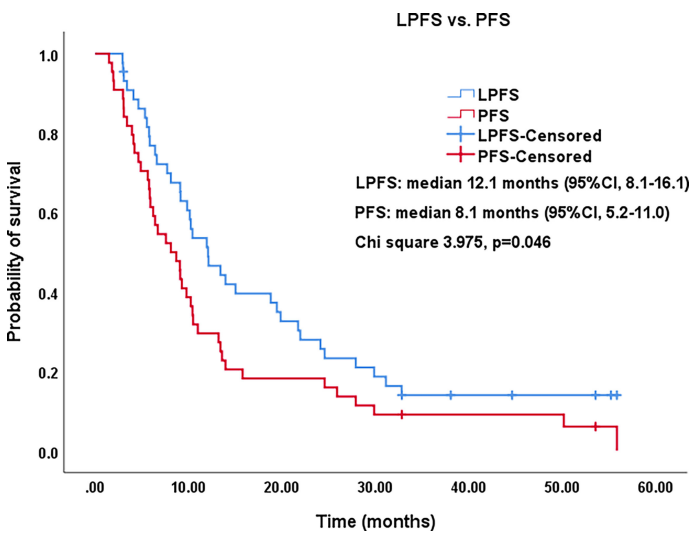

FIGURE 3 | Kaplan–Meier survival curves of LPFS versus PFS. The 1-,2-, and 3-year PFS rates were 29.5%, 18.2%, and 9.1%, respectively. The 1-,2-, and 3-year LPFS rates were 51.2%, 27.9%, and 13.6%, respectively. LPFS, local progression-free survival; PFS, progression-free survival; CI, confidence intervals.

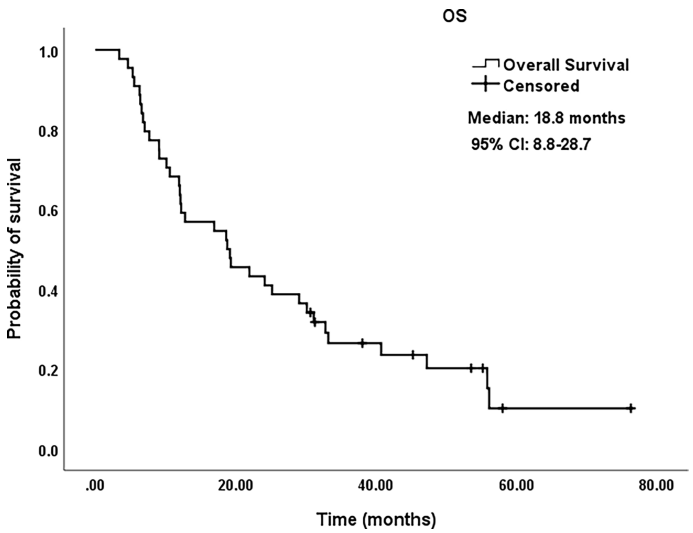

FIGURE 4 | Kaplan–Meier survival curves of OS for patients. OS rate was 65.9% at 1 year, 43.2% at 2 years, 26.4% at 3 years, and 10.0% at 5 years, respectively. OS, overall survival; CI, confidence intervals.

previous studies (47.7% vs. 44.6%) (23). Hence, we explicitly conclude that MWA + ITC could greatly expand the scope of coagulative necrosis than either alone, showing stronger synergy or additive effects and confirmed in the transplanted tumor animal model (12, 13, 28). In addition, barely any patients had toxic side effects related to the local application of cytotoxic drugs in this study.

Feng et al. published one of the earliest papers on early-stage NSCLC treated with RFA + ITC showing better survival, less complications, and small damage; a sequence of ablation followed by immediate ITC was adopted, which was a reversal of our order (29). The most beneficial paradigm to the patients is currently unclear. Irreversible thermal injury, triggering cellular death, occurs when cells are heated >46°C; coagulation necrosis can be induced in focal tissue when heated to 50°C for 4–6 min (30). Although lower temperature hyperthermia (42–45°C) merely results in reversible cellular injury, this can enhance cellular susceptibility to additional chemotherapeutics (28). In this study, more than half (54.5%) of lesions were close to hilar large vessels where a steep thermal descent due to heat sink effect was observed, which likely led to the inability of completely encompassing the tumor tissue with the 50°C isotherm even if multiple antennae were simultaneously used.

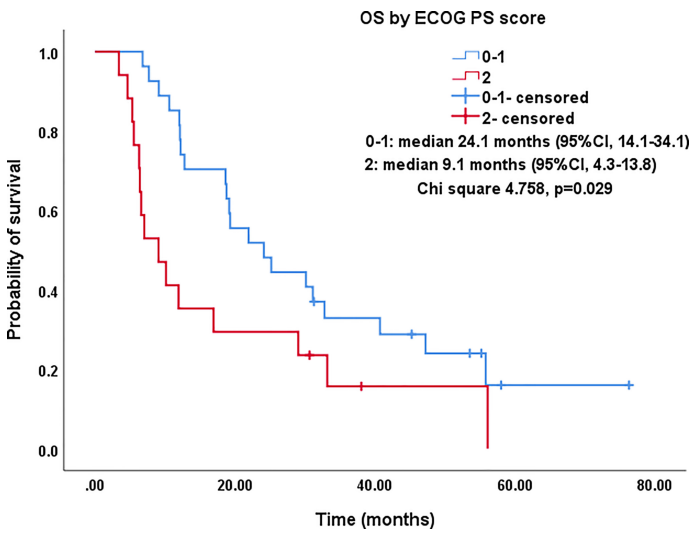

FIGURE 5 | Kaplan–Meier survival curves of OS by ECOG PS score for all patients. The OS of PS score of 0-1 was significantly better than that of PS=2 (median: 24.1 months vs. 9.1 months; P=0.029). OS, overall survival; ECOG PS, Eastern Cooperative Oncology Group performance status; CI, confidence intervals.

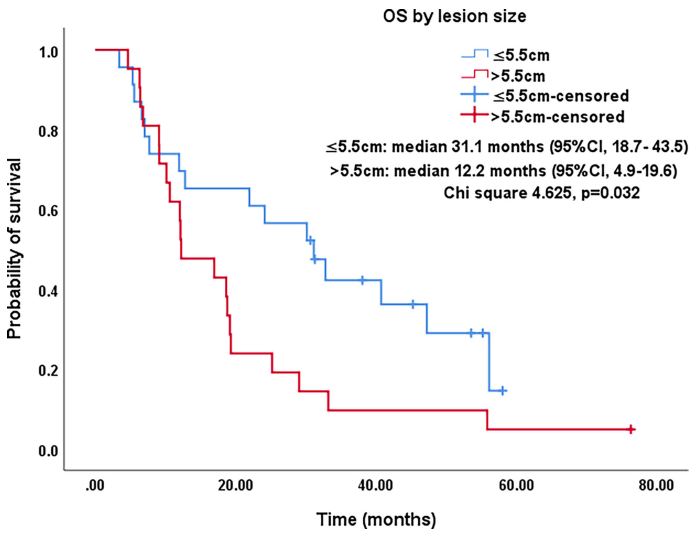

FIGURE 6 | Kaplan–Meier survival curves of OS by lesion size for all patients. The OS of lesions ≤5.5 cm was significantly better than that for lesions >5.5 cm (median: 31.1 months vs. 12.2 months; P=0.032). OS, overall survival; CI, confidence intervals.

Under such circumstances, a combination of MWA + ITC was innovatively used in this study, obtaining a larger necrosis volume and a more complete tumor destruction area, as reflected in the superiority of LPFS over PFS at follow-up (p = 0.046). The rationale for this optimized combination therapy may be explained by a "two-hit" exposure of sublethal hyperthermia and high concentration cisplatin, and by filling the cisplatin aqueous solution in untreated gaps within the ablation zone.

In this study, side effects and complications were mainly related to MWA. Possibly, they were aggravated in terms of incidence and severity by the introduction of ITC. Given the unprecedented large lesions to be ablated and the combined utility of MWA with ITC in this study, ≥2 ablation antennae and ≥1 Chiba needles were used to cause multiple punctures through the pleura, which could slightly increase the incidence (52.3% vs. 31.9%) and severity (chest tube: 22.7% vs. 11.5%) of pneumothorax (7). Likewise, the incidence (77.3% vs. 68.2%) and severity (chest tube: 11.4% vs. 3.0%) of pleural effusion in this study were modestly higher than in our previous report, which was associated with severe thermal injury to the pleura due to a higher proportion (38.6%) of lesions involving the pleura or chest wall and a longer ablation time (mean 26.8 min) (6). The incidence (6.8%) of pulmonary infections, including bacterial (4.5%) and fungal (2.3%) infections corresponded with previously reported rates of 1%–6% (16). Particularly, the fungal infection was a deep invasive Aspergillosis which resulted in one case of bronchopleural fistula with hemoptysis, resulting from the potent erosive ability of Aspergillus to surround normal lung tissue (31). The pulmonary hemorrhage/hemoptysis (20.5%) and slight subcutaneous emphysema (9.1%) recovered spontaneously after conservative treatment. In addition, almost no patients had toxic side effects related to the local application of cytotoxic drugs. In general, these

TABLE 4 | Cox regression multivariate analysis of survival predictors for OS.

Variables	HR	95% CI	*p*-value
Age	1.065	1.016-1.117	0.010
ECOG PS score			
0-1	1		
2	3.815	1.591-9.149	0.003
Stage at treatment			
IIA - IIIB	1		
IIIC - IVB	4.057	1.606-10.253	0.003
Lesion size	1.314	1.044-1.654	0.020
Prior systematic treatment			
Yes	1		
No	0.436	0.200-0.951	0.037

OS, overall survival; CI, confidence interval; ECOG PS, Eastern Cooperative Oncology Group performance status.

data reinforce the concept that MWA + ITC of NSCLC is a relatively safe and tolerable procedure.

In this study, in a comparison with 8.1 months at median PFS and 29.5%, 18.2%, and 9.1% at 1-, 2–, and 3-year PFS rates, median LPFS under MWA + ITC treatment was further extended to 12.1 months, and 1-, 2–, and 3-year LPFS rates were further raised to 51.2%, 27.9%, and 13.6%. Hence, sites undergoing additional MWA + ITC displayed slower progression than others undergoing subsequent systemic therapy alone. We speculate that the partial gain is due to increased intratumoral drug accumulation in the larger peripheral periablative zone after subsequent systematic treatment. Studies in animal models have demonstrated up to a 5.6-fold increase in intratumoral agent accumulation after RFA; most of the agents are concentrated in the immediate periphery of the area coagulated by radiofrequency heating and within the region with non-lethal hyperthermia (32, 33). Similarly, this study was no exception in that lesion size was still a significant prognostic factor for LPFS. Further, the larger the tumor mass, the lower the chance of obtaining complete necrosis (23).

Studies on IIIA-IVB NSCLC cases not receiving MWA have shown a 5-year OS range between 0%–36% (3). A preliminary study on MWA for large NSCLC showed 5-year OS and CCS rates of 18.3% and 30.0%, respectively; NSCLC at stage IIIB-IIIC was the main indication that at stage IV was excluded (23). In this study, there was a large proportion of cases at stage IV NSCLC (18/44, 40.9%), which was responsible for the relatively lower 5-year OS and CCS rates of only 10%. As expected in univariate analysis, the OS in patients with smoking, PS score of 2, and lesions >5.5 cm was significantly lower than in patients with non-smoking, PS score of 0-1, and lesions ≤5.5 cm (P-value: 0.035, 0.029, 0.032, respectively). Similarly, in multivariate comparisons, besides advanced age, higher PS score, higher stage, and larger lesion, receiving systematic treatment prior to MWA+ITC also indicated a poorer prognosis characterized by shorter survival probably due to the worse response to second- or third-line therapy.

This study had some limitations. First, it was a retrospective single-arm study comprising a small number of patients. Second, multiple NSCLC stages were included in the study, which limits the ability to reflect the real survival benefit at each stage. Third, it was difficult to achieve uniform diffusion of the directly injected cisplatin over larger tumors. Last, it was uncertain whether the gains of local treatment helped prolong OS in advanced NSCLC patients. Nonetheless, the preliminary results support the utility of MWA + ITC as a palliative modality in patients with advanced NSCLC. Particularly, to our knowledge, this is the first clinical study showing MWA + ITC application for the treatment of large, advanced NSCLC lesions. In the future, a prospective, preferably multi-center, controlled study with a larger sample size is needed to better evaluate the role of MWA + ITC in local tumor control, evaluate survival outcomes, and improve its application as part of a comprehensive multimodality treatment.

In conclusion, this study supports MWA + ITC as a safe and effective new modality of local treatment for large, advanced NSCLC. MWA + ITC was successfully applied to large NSCLC and could significantly prolong LPFS. Nevertheless, further large-scale, multi-center, prospective clinical trials are needed to evaluate long-term survival benefits.

DATA AVAILABILITY STATEMENT

The raw data supporting the conclusions of this article will be made available by the authors, without undue reservation.

ETHICS STATEMENT

The studies involving human participants were reviewed and approved by Ethics Committee of Shandong Provincial Hospital Affiliated to Shandong First Medical University. Written informed consent for participation was not required for this study in accordance with the national legislation and the institutional requirements.

AUTHOR CONTRIBUTIONS

GH, XYa, and XYe performed MWA + ITC and reviewed the patients' images. GH, WL, MM, YN, and XH helped to collect the data and follow-up. GH, JW, ZZ, and TZ wrote the draft version of the manuscript and analyzed the data. JD and ZW revised the manuscript and gave some important opinions. The scientific guarantor of this publication is Xin Ye. All authors have read and approved the final manuscript.

FUNDING

This study has received funding from the National Natural Science Foundation of China (81502610 and 82072028) and Shandong Provincial Natural Science Foundation, China (ZR2021MH143 and ZR2020MH294).

REFERENCES

1. Sung H, Ferlay J, Siegel RL, Laversanne M, Soerjomataram I, Jemal A, et al. Global Cancer Statistics 2020: GLOBOCAN Estimates of Incidence and Mortality Worldwide for 36 Cancers in 185 Countries. *CA Cancer J Clin* (2021) 71(3):209–49. doi: 10.3322/caac.21660
2. Fidler MM, Bray F, Soerjomataram I. The Global Cancer Burden and Human Development: A Review. *Scand J Public Health* (2018) 46(1):27–36. doi: 10.1177/1403494817715400
3. Goldstraw P, Chansky K, Crowley J, Rami-Porta R, Asamura H, Eberhardt WE, et al. The Iaslc Lung Cancer Staging Project: Proposals for Revision of the TNM Stage Groupings in the Forthcoming (Eighth) Edition of the TNM

Classification for Lung Cancer. *J Thorac Oncol* (2016) 11(1):39–51. doi: 10.1016/j.jtho.2015.09.009
4. Ye X, Fan W, Wang Z, Wang J, Wang H, Wang J, et al. Expert Consensus on Thermal Ablation Therapy of Pulmonary Subsolid Nodules (2021 Edition). *J Cancer Res Ther* (2021) 17(5):1141–56. doi: 10.4103/jcrt.jcrt_1485_21
5. Lubner MG, Brace CL, Hinshaw JL, Lee FTJr. Microwave Tumor Ablation: Mechanism of Action, Clinical Results, and Devices. *J Vasc Interv Radiol* (2010) 21(8 Suppl):S192–203. doi: 10.1016/j.jvir.2010.04.007
6. Huang G, Yang X, Li W, Wang J, Han X, Wei Z, et al. A Feasibility and Safety Study of Computed Tomography-Guided Percutaneous Microwave Ablation: A Novel Therapy for Multiple Synchronous Ground-Glass Opacities of the Lung. *Int J Hyperthermia* (2020) 37(1):414–22. doi: 10.1080/02656736.2020.1756467
7. Ni Y, Huang G, Yang X, Ye X, Li X, Feng Q, et al. Microwave Ablation Treatment for Medically Inoperable Stage I Non-Small Cell Lung Cancers: Long-Term Results. *Eur Radiol* (2022). doi: 10.1007/s00330-022-08615-8
8. Wei Z, Yang X, Ye X, Feng Q, Xu Y, Zhang L, et al. Microwave Ablation Plus Chemotherapy Versus Chemotherapy in Advanced non-Small Cell Lung Cancer: A Multicenter, Randomized, Controlled, Phase III Clinical Trial. *Eur Radiol* (2020) 30(5):2692–702. doi: 10.1007/s00330-019-06613-x
9. Aufranc V, Farouil G, Abdel-Rehim M, Smadja P, Tardieu M, Aptel S, et al. Percutaneous Thermal Ablation of Primary and Secondary Lung Tumors: Comparison Between Microwave and Radiofrequency Ablation. *Diagn Interv Imaging* (2019) 100(12):781–91. doi: 10.1016/j.diii.2019.07.008
10. Páez-Carpio A, Gómez FM, Isus Olivé G, Paredes P, Baetens T, Carrero E, et al. Image-Guided Percutaneous Ablation for the Treatment of Lung Malignancies: Current State of the Art. *Insights Imaging* (2021) 12(1):57. doi: 10.1186/s13244-021-00997-5
11. Wu H, Fan ZP, Jiang AN, Di XS, He B, Wang S, et al. Combination of Intratumoural Micellar Paclitaxel With Radiofrequency Ablation: Efficacy and Toxicity in Rodents. *Eur Radiol* (2019) 29(11):6202–10. doi: 10.1007/s00330-019-06207-7
12. Ahmed M, Liu Z, Lukyanov AN, Signoretti S, Horkan C, Monsky WL, et al. Combination Radiofrequency Ablation With Intratumoral Liposomal Doxorubicin: Effect on Drug Accumulation and Coagulation in Multiple Tissues and Tumor Types in Animals. *Radiology* (2005) 235(2):469–77. doi: 10.1148/radiol.2352031856
13. Hohenforst-Schmidt W, Zarogoulidis P, Stopek J, Kosmidis E, Vogl T, Linsmeier B, et al. Enhancement of Intratumoral Chemotherapy With Cisplatin With or Without Microwave Ablation and Lipiodol. Future Concept for Local Treatment in Lung Cancer. *J Cancer* (2015) 6(3):218–26. doi: 10.7150/jca.10970
14. Celikoglu SI, Celikoglu F, Goldberg EP. Endobronchial Intratumoral Chemotherapy (EITC) Followed by Surgery in Early non-Small Cell Lung Cancer With Polypoid Growth Causing Erroneous Impression of Advanced Disease. *Lung Cancer* (2006) 54(3):339–46. doi: 10.1016/j.lungcan.2006.09.004
15. Celikoglu F, Celikoglu SI, York AM, Goldberg EP. Intratumoral Administration of Cisplatin Through a Bronchoscope Followed by Irradiation for Treatment of Inoperable non-Small Cell Obstructive Lung Cancer. *Lung Cancer* (2006) 51(2):225–36. doi: 10.1016/j.lungcan.2005.10.012
16. Ye X, Fan W, Wang H, Wang J, Wang Z, Gu S, et al. Expert Consensus Workshop Report: Guidelines for Thermal Ablation of Primary and Metastatic Lung Tumors (2018 Edition). *J Cancer Res Ther* (2018) 14 (4):730–44. doi: 10.4103/jcrt.JCRT_221_18
17. Ahmed M, Solbiati L, Brace CL, Breen DJ, Callstrom MR, Charboneau JW, et al. Image-Guided Tumor Ablation: Standardization of Terminology and Reporting Criteria–a 10-Year Update. *Radiology* (2014) 273(1):241–60. doi: 10.1148/radiol.14132958
18. Watson RA, Tol I, Gunawardana S, Tsakok MT. Is Microwave Ablation an Alternative to Stereotactic Ablative Body Radiotherapy in Patients With Inoperable Early-Stage Primary Lung Cancer? *Interact Cardiovasc Thorac Surg* (2019) 29(4):539–43. doi: 10.1093/icvts/ivz123
19. Uhlig J, Ludwig JM, Goldberg SB, Chiang A, Blasberg JD, Kim HS. Survival Rates After Thermal Ablation Versus Stereotactic Radiation Therapy for Stage 1 non-Small Cell Lung Cancer: A National Cancer Database Study. *Radiology* (2018) 289(3):862–70. doi: 10.1148/radiol.2018180979
20. Zhao H, Steinke K. Long-Term Outcome Following Microwave Ablation of Early-Stage non-Small Cell Lung Cancer. *J Med Imaging Radiat Oncol* (2020) 64(6):787–93. doi: 10.1111/1754-9485.13091
21. Nian-Long L, Bo Y, Tian-Ming C, Guo-Dong F, Na Y, Yu-Huang W, et al. The Application of Magnetic Resonance Imaging-Guided Microwave Ablation for Lung Cancer. *J Cancer Res Ther* (2020) 16(5):1014–9. doi: 10.4103/jcrt.JCRT_354_20
22. Ni Y, Peng J, Yang X, Wei Z, Zhai B, Chi J, et al. Multicentre Study of Microwave Ablation for Pulmonary Oligorecurrence After Radical Resection of non-Small-Cell Lung Cancer. *Br J Cancer* (2021) 125(5):672–8. doi: 10.1038/s41416-021-01404-y
23. Pusceddu C, Melis L, Sotgia B, Guerzoni D, Porcu A, Fancellu A. Usefulness of Percutaneous Microwave Ablation for Large non-Small Cell Lung Cancer: A Preliminary Report. *Oncol Lett* (2019) 18(1):659–66. doi: 10.3892/ol.2019.10375
24. Palussière J, Catena V, Buy X. Percutaneous Thermal Ablation of Lung Tumors-Radiofrequency, Microwave and Cryotherapy: Where are We Going? *Diagn Interv Imaging* (2017) 98(9):619–25. doi: 10.1016/j.diii.2017.07.003
25. Celikoglu F, Celikoglu SI, Goldberg EP. Bronchoscopic Intratumoral Chemotherapy of Lung Cancer. *Lung Cancer* (2008) 61(1):1–12. doi: 10.1016/j.lungcan.2008.03.009
26. Song P, Sun W, Pang M, He W, Zhang W, Sheng L. Efficacy Comparison Between Microwave Ablation Combined With Radiation Therapy and Radiation Therapy Alone for Locally Advanced Nonsmall-Cell Lung Cancer. *J Cancer Res Ther* (2021) 17(3):715–9. doi: 10.4103/jcrt.JCRT_633_20
27. Goldberg EP, Hadba AR, Almond BA, Marotta JS. Intratumoral Cancer Chemotherapy and Immunotherapy: Opportunities for Nonsystemic Preoperative Drug Delivery. *J Pharm Pharmacol* (2002) 54(2):159–80. doi: 10.1211/0022357021778268
28. Ahmed M, Moussa M, Goldberg SN. Synergy in Cancer Treatment Between Liposomal Chemotherapeutics and Thermal Ablation. *Chem Phys Lipids* (2012) 165(4):424–37. doi: 10.1016/j.chemphyslip.2011.12.002
29. Feng W, Li J, Han S, Tang J, Yao J, Cui Y, et al. CT Guided Radiofrequency Ablation Followed Intratumoral Chemotherapy in the Treatment of Early Stage non-Small Cell Lung Cancer. *Zhongguo Fei Ai Za Zhi* (2016) 19(5):269–78. doi: 10.3779/j.issn.1009-3419.2016.05.04
30. Larson TR, Bostwick DG, Corica A. Temperature-Correlated Histopathologic Changes Following Microwave Thermoablation of Obstructive Tissue in Patients With Benign Prostatic Hyperplasia. *Urology* (1996) 47(4):463–9. doi: 10.1016/S0090-4295(99)80478-6
31. Huang G, Ye X, Yang X, Wang C, Zhang L, Ji G, et al. Invasive Pulmonary Aspergillosis Secondary to Microwave Ablation: A Multicenter Retrospective Study. *Int J Hyperthermia* (2018) 35(1):71–8. doi: 10.1080/02656736.2018.1476738
32. Ahmed M, Monsky WE, Girnun G, Lukyanov A, D'Ippolito G, Kruskal JB, et al. Radiofrequency Thermal Ablation Sharply Increases Intratumoral Liposomal Doxorubicin Accumulation and Tumor Coagulation. *Cancer Res* (2003) 63(19):6327–33.
33. Monsky WL, Kruskal JB, Lukyanov AN, Girnun GD, Ahmed M, Gazelle GS, et al. Radio-Frequency Ablation Increases Intratumoral Liposomal Doxorubicin Accumulation in a Rat Breast Tumor Model. *Radiology* (2002) 224(3):823–9. doi: 10.1148/radiol.2243011421

Conflict of Interest: The authors declare that the research was conducted in the absence of any commercial or financial relationships that could be construed as a potential conflict of interest.

frontiers | Frontiers in Oncology

TYPE Original Research
PUBLISHED 11 August 2022
DOI 10.3389/fonc.2022.957138

OPEN ACCESS

EDITED BY
Xin Ye,
Shandong University, China

REVIEWED BY
Zhengyu Lin,
First Affiliated Hospital of Fujian Medical University, China
Hong-Tao Hu,
Henan Provincial Cancer Hospital, China
Xiaoguang Li,
Peking University, China
Chengli Li,
Shandong Provincial Hospital, China

*CORRESPONDENCE
Yueyong Xiao
yueyongxiao@yahoo.com

†These authors share first authorship

SPECIALTY SECTION
This article was submitted to Thoracic Oncology, a section of the journal Frontiers in Oncology

RECEIVED 30 May 2022
ACCEPTED 25 July 2022
PUBLISHED 11 August 2022

CITATION
Meng L, Wu B, Zhang X, Zhang X, Wei Y, Xue X, Zhang Z, Zhang X, Li J, He X, Ma L and Xiao Y (2022) Microwave ablation with local pleural anesthesia for subpleural pulmonary nodules: our experience. *Front. Oncol.* 12:957138. doi: 10.3389/fonc.2022.957138

Microwave ablation with local pleural anesthesia for subpleural pulmonary nodules: our experience

Liangliang Meng[1,2†], Bin Wu[1,2†], Xiao Zhang[1], Xiaobo Zhang[1], Yingtian Wei[1], Xiaodong Xue[1], Zhongliang Zhang[1], Xin Zhang[1], Jing Li[3], Xiaofeng He[1], Li Ma[1,4] and Yueyong Xiao[1*]

[1]Department of Radiology, the First Medical Center, Chinese PLA General Hospital, Beijing, China, [2]Department of Radiology, Chinese PAP Beijing Corps Hospital, Beijing, China, [3]Department of MRI, Affiliated Hospital, Logistics University of Chinese Peoples Armed Police Forces, Tianjin, China, [4]Department of Anesthesia and Surgery, the First Medical Center, Chinese PLA General Hospital, Beijing, China

Objectives: To explore the efficacy and safety of local pleural anesthesia (LPA) for relieving pain during microwave ablation (MWA) of pulmonary nodules in the subpleural regions.

Materials and Methods: From June 2019 to December 2021, 88 patients with 97 subpleural nodules underwent percutaneous CT-guided MWA. Patients were divided into two groups according to whether LPA was applied; 53 patients with local pleural anesthesia during MWA; and 35 patients with MWA without LPA. The differences in technical success, pre-and post- and intra-operative visual analog scale (VAS) pain scores, complications of the procedure, and local progression-free survival (LPFS) between the two groups were assessed. Thus, to evaluate the efficacy and safety of MWA combined with LPA for treating subpleural nodules.

Results: In this study, the procedures in all patients of both groups achieved technical success according to pre-operative planning. There was no statistically significant difference in the pre-operative VAS pain scores between the two groups. Intra-operative VAS scores were significantly higher in the non-LPA (NLPA) group than in the LPA group. They remained significantly higher in the NLPA group than in the LPA group during the short postoperative period. Analgesics were used more in the NLPA group than in the LPA group intra- and postoperatively, with a statistically significant difference, especially during the MWA procedures. The overall LPFS rates were 100%, 98.333%, 98.333%, and 98.333% at 1, 3, 6, and 12 months postoperatively in the LPA group and 100%, 97.297%, 94.595%, and 94.595% postoperatively in the NLPA group, respectively. Tumor recurrence occurred in one and two patients with lung adenocarcinoma in the LPA and NLPA groups. The incidence of pneumothorax was significantly higher in the NLPA group (25,714%, 9/35) than in the LPA group (15.094%, 8/53), and there were three cases of pleural

10.3389/fonc.2022.957138

effusion (blood collection) and one case of pulmonary hemorrhage in the NLPA group.

Conclusion: Percutaneous CT-guided MWA is a safe and effective treatment for subpleural pulmonary nodules. Applying a combined LPA technique can reduce the patient's pain and complications during and after the MWA. The long-term efficacy must be verified in more patients and a longer follow-up.

KEYWORDS

microwave ablation (MWA), lung cancer, anesthesia, pleural, pain

1 Introduction

Lung cancer is one of the most prevalent malignancies worldwide, with the highest morbidity and mortality in males in China (1, 2). For a long time, surgical resection was the preferred or even the only treatment for early-stage lung cancer (3). According to the latest clinical guideline, radical surgical resection is the preferred local treatment for stage I and II non-small cell lung cancer (NSCLC) (4). However, the most obvious limitation of surgery is the damage to the patient's pulmonary function reserve, especially in older patients with poor underlying lung function (5). In addition, the surgery is more costly and the recovery time for patients is usually long. The popularity of thoracoscopy has reduced the damage to patients, but there are still some shortcomings (6). However, for patients who are inoperable or unwilling to have a surgical resection, CT-guided percutaneous thermal ablation plays an increasingly crucial role in treating lung tumors. It has comparable treatment efficacy to surgical procedures, but the overall damage to the patient is minimal, and the cost is significantly less than conventional surgery (7).

Recently, numerous studies confirming the effectiveness and safety of minimally invasive percutaneous ablations in the treatment of lung tumors (8). However, the efficacy of minimally invasive CT-guided treatment is closely related to the surgeon's procedure plan and requires more skill and experience from the surgeon. Incomplete ablation of the tumor leads to recurrence or even recoil. Heavy pain during thermal ablation, which seriously affects the procedure, is the most reason for incomplete ablation and the most common postoperatively complication (9). The pleura is rich in nerves, and a slight irritation can lead to a severe pleural reaction. Therefore, the most serious difficulty in thermal ablation of subpleural nodules is achieving complete inactivation of the tumor safely and comfortably. Okuma reported that patients were more likely to undergo pain during radiofrequency ablation (RFA) when the distance between the tumor nodule and the thoracic wall was <1 cm (10). Pleuritic pain is the most common complication during thermal ablation (9). Some patients experience intolerable pain during local anesthetic ablation, which can usually be relieved by reducing the treatment power or shortening the ablation time. Still, this management may lead to incomplete ablation and increase the risk of tumor recurrence. Intravenous anesthesia can adversely affect pulmonary ventilation and increase the chance of infection (9). Microwave ablation (MWA) is more likely to cause pain in patients than RFA due to the difference in the underlying mechanism of thermogenesis (11).

The nerves that innervate the parietal pleura are the intercostal and phrenic nerves, which are somatosensory (12, 13). Stimulating the nerves on the parietal pleura can cause significant pain, radiating along the intercostal nerve to the chest and abdominal wall and the phrenic nerve to the neck and shoulder (13). The nerves in the visceral pleura come from the pulmonary plexus and enter the lung surface *via* the pulmonary hilum along the outer membrane of the pulmonary artery, peribronchial and lobular septa visceral sensory nerves with a high threshold for pain. Due to the proximity to the pleura, heat conduction will involve the pleura during radiofrequency ablation, which will cause pain in milder cases and partially cause a pleural reaction, leading to the failure of the procedure (13).

Our institution has performed many thermal ablations of pulmonary nodules in recent years, including MWAand radiofrequency ablation. It has accumulated considerable unique experience, including in the thermal ablation of pulmonary nodules in the adjacent pleural area. Our team has gradually worked out a method of local pleural anesthesia for the difficult treatment of subpleural pulmonary nodules, ensuring complete tumor ablation while minimizing the patient's pain and damage to the pleura. This study aimed to evaluate the efficacy and safety of local pleural anesthesia in the MWA treatment of subpleural pulmonary nodules.

2 Materials and methods

2.1 Patients enrollment

This retrospective study was approved by the Ethics Committee of the Chinese PLA general hospital. Fifty-three patients with subpleural pulmonary nodules who underwent CT-guided percutaneous MWA with local pleural anesthesia in our hospital from June 1, 2019, to December 31, 2021, were retrospectively analyzed, and another 35 patients with subpleural pulmonary nodules who underwent MWA without local pleural anesthesia during this period were also recruited in this study as a control group. Because of the study's retrospective nature, informed consent was waived by the Ethics Committee of our institution. This paper does not contain any person's data in any form. We reviewed the hospital records and radiographic data of these patients.

Based on our prior knowledge, we defined subpleural nodules as pulmonary nodules at any distance within 1.0 cm from the pleura (10, 14). The specific inclusion criteria for patients were: (1) tumor margin within 1 cm from the pleura, including pleural apex, cribriform pleura, diaphragmatic pleura and mediastinal pleura. The distance of the lesion from the skin puncture point should be less than 15 cm to ensure that the antenna can reach the center of the lesion; (2) single pulmonary nodule less than 3.0 cm; (3) number of pulmonary malignancies three or less; (4) patients who refused or were not suitable for surgical resection. Exclusion criteria included severe lung infection, coagulation dysfunction, severe pulmonary failure, uncontrollable angina pectoris, cardiac arrhythmia, congestive heart failure, or a history of implantable cardiac devices. After screening, a total of 88 patients (51 male and 37 female, 42-90 years) were enrolled in the study. The baseline and tumor characteristics of the patients are summarized in Table 1. These 88 patients had 97 subpleural pulmonary nodules and were treated with MWA. Patients were divided into groups LPA and NLPA according to whether they applied local pleural anesthesia.

The vast majority of nodules had definite pathology by percutaneous biopsy before the MWA procedures, while some patients' pathology was obtained during the ablation. Only 13 nodules could not have definite pathology. For patients without definite pathology before surgery, we performed the MWA procedure at the patients' strong request and with the ethics committee's consent because the imaging signs suggested a high possibility of malignancy.

TABLE 1 Patient clinical information and demographics for all patients.

	Group LPA	Group NLPA	p-value
Age (years) (range)	66.04±10.427 (42-86)	67.00±10.350 (51-90)	0.672
Gender			0.449
Male	29	22	
Female	24	13	
Nodule size (mm) (range)	18.50±5.625 (9-30)	16.43±5.928 (6-30)	0.088
≤10	4	7	
10<d≤20	35	21	
20<d≤30	21	9	
Nidus location			0.288
Left upper lung lobe	14	10	
Left lower lung lobe	6	8	
Right upper lung lobe	20	9	
Right middle lung lobe	2	3	
Right lower lung lobe	18	7	
Body position			
Supine	18	13	
Left lateral	24	16	
Right lateral	18	8	
Type of lesion			0.017
Solid	45	19	
Sub-solid	15	18	
Pathology			0.210
Squamous cell carcinoma	4	1	
Adenocarcinoma	25	21	
Pulmonary metastases	22	7	
Unknown	6	7	
Other	3	1	
Preoperative VAS score	0.83±0.753 (0-3)	1.06±0.906 (0-3)	0.260
0-2	52	33	
3-5	1	2	
6-10	0	0	
Distance from tumor to pleura (mm)	2.92±2.999 (0-9)	4.68±2.819 (0-9)	0.004
0-4	45	18	
5-10	15	19	
Ablation parameters (range)			
Power (W)	30.75±6.163 (20-40)	28.784±6.056 (20-40)	0.164
Duration (min)	7.409±2.653 (3-16.5)	7.526±2.351 (4.33-14)	0.695

LPA, local pleural anesthesia, NLPA, non-local pleural anesthesia, VAS, visual analog scale.

2.2 Local pleural anesthesia adjuvant MWA procedure

2.2.1 MWA procedure

The procedures were performed with a spiral computed tomography (CT) Scanner (Philips Brilliance Big Bore 16-layer, Philips, USA) for pre-operative localization, pre-operative planning, intraoperative monitoring of ablation procedures, assessment of treatment response, and observation of complications. MWA of pulmonary nodules was performed using the "Tumor Microwave Ablation Therapy System" and

the matched sterile disposable MWAantennas from Cannyon Medical Technology Co. The ablation antennas were selected according to the position, the size of the lesion, and the distance of the lesion from the skin. The procedures were usually performed by three experienced interventionalists with at least five years of experience in MWA treatment at our institution. There were also two permanent CT technicians and two surgical nurses who cooperated with the procedures. The patient's position during the procedure was determined according to the tumor's location. The patient's position was fixed using shaped pads, pads, and baffles to ensure that the patient could remain comfortably in the same position for a long period.

Before the procedure, intravenous access was first established by the operating nurse to facilitate intraoperative emergency or therapeutic drug administration; the patients were kept on continuous low-flow oxygen (3-5L/min) through a nasal tube. The procedure monitored patients with cardiac monitoring, oxygen saturation, and heart rate. The patient's blood pressure was measured every 5 minutes. All the above actions were taken to monitor the patient's status during the procedure and provide timely intervention and treatment.

All patients included in this study underwent MWAunder local anesthesia. After local disinfection of the skin of the puncture point, 10-20ml of 1% lidocaine would be applied for local anesthesia. Local anesthesia before antenna entry acts primarily subcutaneously at the entry point and at the point where the microwave antenna would soon pass through the pleura. Lidocaine was usually mixed with 0.9% saline at a ratio of 1:1.

After local anesthesia, the ablation applicators should be placed in a predefined position using a stepwise method. The ablation parameters were selected according to the tumor size, location, morphology, adjacent structures, and the approach. The gauge size of the MWAapplicator was 17G, and the antenna length was 10cm or 15cm. Double-antenna clamping was usually chosen for the treatment when the tumor was larger than 2 cm, or the lesion was dense and difficult to penetrate. The power and duration of ablation vary according to the lesion's density and size. Complete ablation refers to complete necrotic lesions of the local tumor tissue and a possible cure through thermal ablation. The complete ablation in the MWA procedure was usually indicated by the appearance of the halo sign around the lesion (15). When the ground-glass opacity around the lesion exceeded the nodule border by more than 5 mm, the tumor could be considered completely covered by the ablation area, complete ablation should be achieved, the procedure could be stopped, and the antennas should be removed. CT scan or enhanced imaging observed complete ablation of the tumor, and the ablated area appeared as a clear non-enhanced area (15). If the patient experienced significant pain during or after the procedure, analgesics should be given intravenously, usually 50 mg of flurbiprofen axetil injection.

2.2.2 Application of local pleural anesthesia

To reduce the damage to the pleura after microwave ablation, we creatively applied the method of local pleural anesthesia. Select an appropriate syringe or percutaneous puncture to anesthetize the pleura adjacent to the lesion according to the positional relationship between the lesion and the pleura. Specifically, the site of administration of local pleural anesthesia should be in the pleura closest to the subpleural nodule. When the length of the anesthesia needle was less than 3 cm, a 5ml syringe and needle could be used directly for anesthesia, and when it was longer than 3 cm, a 20G or 21G puncture needle (PTC needle) should be used for anesthesia. The specific method was first to measure the distance from the skin of the puncture site to the target pleura on the CT image and to use a 20G or 21G puncture needle to lay the needle after anesthesia for the subcutaneous and puncture access, and to place the needle tip outside the pleura. All MWAprocedures in this study was done under local anesthesia, and patients were kept awake throughout the procedure. The local pleura is adequately anesthetized before the start of microwave ablation. If the patient felt any painful stimuli during the ablation procedure, regional lidocaine analgesia should be administered immediately until the patient achieved complete pain-free. During administration, local CT images should be used to confirm adequate infiltration of the pleura by the anesthetic. When the amount of lidocaine reached 20ml, ropivacaine was usually used to avoid the toxic side effects of the patient due to an overdose of anesthesia. In addition, lidocaine is a short-acting local anesthetic with faster dispersion by local injection, whereas ropivacaine has better analgesia and lasts longer than lidocaine, so ropivacaine was also given to some patients who were not satisfied with lidocaine analgesia.

2.2.3 Pain assessment

All patients were evaluated before, during, and after the MWA procedure using a visual analog scale (VAS) system, which was applied in previous literature (16–18). The patients were scored and recorded on the VAS scale before, during, and 24 hours after the procedure to compare the differences in pain degrees between the two groups. Depending on the score, they were graded as mild (VAS 0-2 points), moderate (VAS 3-5 points), or severe (VAS 6-10 points). We obtained the above information through in-patient records and follow-up records. We compared the differences in pain levels between the two groups preoperatively, intraoperatively and postoperatively. In addition, since some patients used two antennas during ablation, we also compared the differences in pain levels between single- and double-antennas patients within each group separately to analyze the effect of the number of MWA antennas on pain levels.

2.3 Treatment efficacy

Local efficacy after MWAtreatment was assessed according to the criteria drafted by Ye et al. (15). Post-treatment follow-up imaging by CT was performed to evaluate the ablation outcome. Follow-up CT observed the efficacy of treatment and the presence of residual or recurrent lesions. Chest-enhanced CT was usually used to assess the outcome of the procedure. A complete lack of enhancement in the ablation zone is defined as technical success. Complete ablation of the tumor was observed by CT scan or enhanced imaging, and the ablated area appeared as a clear non-enhanced area. Incomplete ablation was observed as a nodular enhancement at the tumor margin or enlargement of the lesion in some areas around the tumor. Irregular nodal enhancement in the ablation zone was considered a recurrence or residual tumor. CT scan can also be used to observe the size and morphological changes of the tumor ablation area. Local progression-free survival (LPFS) was used to describe the absence of disease progression after treatment. The incidence of LPFS at different follow-up times was assessed according to the modified solid tumor response evaluation criteria. Due to the various tumors included in this study, the efficacy evaluation was only validated using LPFS. The time of LPFS was calculated from the day of the MWA procedure.

2.4 Complications

CT scan would be performed intra- and postoperatively to exclude complications. Common complications of MWA include pneumothorax, hemorrhage, and pleural effusion. Complications should be reported using the updated SIR classification criteria table so they can be consistently classified according to severity. Major complications result in severe morbidity and disability (e.g., resulting in unexpected organ loss), which increase the level of care or result in prolonged hospitalization (SIR C-E). This includes any condition requiring blood transfusion or interventional drainage. All other complications are considered to be minor.

2.5 Statistical analysis

Statistical analysis was performed using SPSS software version 26.0 (Chicago, IL, USA). Pearson chi-square and Fisher's exact tests were used for categorical variables and Mann–Whitney U tests for continuous variables. A Paired two-sample T-test was used to compare the differences in VAS scores before and after MWA in each group separately. Two independent samples t-tests were used to compare differences in clinical information and outcomes related to patients in the two groups (LPA vs. NLPA). If the data did not conform to a normal distribution, then a non-parametric test was used. The statistical threshold was set at a *P*-value of less than 0.05.

3 Results

3.1 Patient clinical information and demographics

Eighty-eight patients with 97 subpleural pulmonary lesions were included in this study, and all patients underwent CT-guided microwave ablation. There were 53 patients in the LPA group and 35 in the NLPA group. The mean patient age was 66.04 ± 10.43 in the LPA group and 67.00 ± 10.27 mm in the NLPA group. The mean tumor size was 18.50 ± 5.63 mm in the LPA group and 16.43 ± 5.93 mm in the NLPA group. Both groups had the highest proportion of pathological types of lung adenocarcinoma (Group LPA: 24/53, Group NLPA: 21/35), followed by lung metastases. Thirty-one patients were placed in the supine position, and 66 were placed in the lateral position during the MWA procedure.

The detailed clinical information of all patients is shown in Table 1.

3.2 Technical success rate

This study performed CT-guided MWA on 97 subpleural pulmonary nodules in 88 patients. All 88 patients were treated according to the protocol, and ablation was performed by single- or double-antenna, and intra- and post-operative enhanced CT assessment of the ablated tumor area showed complete coverage of the tumor without significant enhancement of the tumor area, suggesting the technical success of MWA. In the LPA group, local pleural anesthesia was applied, and the anesthetic needle reached the designated position and worked in all patients (Figures 1A–C). In the NLPA group, no local pleural anesthesia was used during MWAin all patients (Figures 1D–F). The technical success rate of the LPA group was 100%; the technical success rate of the NLPA group was also 100%. (Table 2)

3.3 Treatment efficacy

We observed the efficacy of the treatment through post-operative CT follow-up. The postoperative outcomes were followed up at one day, one month, three months, six months, and 12 months after the MWA procedure. In both groups, most patients experienced complete ablation of the lesions after microwave ablation, which gradually shrank or even disappeared over time (Figure 2). Only one patient in the LPA group showed abnormal internal enhancement three months after

10.3389/fonc.2022.957138

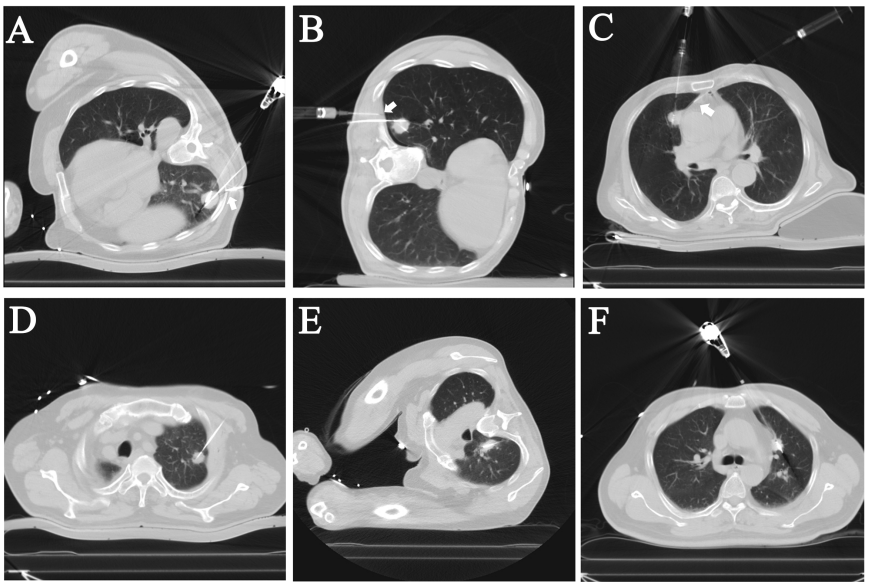

FIGURE 1
Intraoperative CT images of patients who underwent local pleural anesthesia (LPA) or not during the microwave ablation (MWA) procedures. **(A–C)** In the LPA group, the needle and syringe used for local pleural anesthesia can be seen on the CT images. The tips of the anesthesia needles (Arrows) were visualized on the CT as reaching the subpleural and used to administer the anesthesia. **(D–F)** The NLPA group's ablation antennas were located in the center of the nodules without local pleural anesthesia.

TABLE 2 Technique efficacy and follow-up of LPFS.

Group	Characteristics	Patients	Technical success	Technique efficacy (LPFS)		
				≥3 Months	≥6 Months	≥12 Months
Group LPA n=60	Pathology					
	Adenocarcinoma	25	25	24	24	24
	Squamous cell carcinoma	4	4	4	4	4
	Pulmonary metastases	22	22	22	22	22
	Nodule size (mm)					
	0<d≤10	4	4	4	4	4
	10<d≤20	35	35	34	34	34
	20<d≤30	21	21	21	21	21
	Distance to pleura (mm)					
	0-4	45	45	44	44	44
	5-10	15	15	15	15	15
Group NLPA n=37	Pathology					
	Adenocarcinoma	22	22	21	20	20
	Squamous cell carcinoma	1	1	1	1	1
	Pulmonary metastases	7	7	7	7	7
	Nodule size (mm)					
	0<d≤10	7	7	7	7	7
	10<d≤20	21	21	21	20	20
	20<d≤30	9	9	8	8	8
	Distance to pleura (mm)					
	0-4	18	18	17	16	16
	5-10	19	19	19	19	19

LPFS, Local Progress Free Survival; LPA, local pleural anesthesia; NLPA, non-local pleural anesthesia.

treatment, which was considered an incomplete ablation, and a second MWA operation was performed electively (Figure 3). In the NLPA group, two lesions showed inhomogeneous enhancement 3 and 6 months after the procedure, and incomplete tumor ablation and recurrence were considered. Each of these patients underwent secondary ablation.

The technical outcomes and short-term follow-up of the two groups are shown in Table 2, in which the overall LPFS rates were 100%, 98.333%, 98.333%, and 98.333% at 1, 3, 6, and 12 months postoperatively in the LPA group and 100%, 97.297%, 94.595%, and 94.595% postoperatively in the NLPA group, respectively (Table 2).

3.4 Pain degree assessment

We applied only a small amount of ropivacaine (less than 10 ml) after 20 ml of lidocaine in only three patients in the study, and the postoperative VAS score was performed 24 h after the MWA, so our anesthetist considered that this would not have an impact on the accuracy of the VAS score.

Since the data of each group did not satisfy a normal distribution, the Mann-Whitney U test was used to determine whether there was a difference in VAS scores between the two groups at pre-, intra-, and post-operative periods. The shape of the VAS score distribution was not consistent between the two groups as judged by the histogram. The mean rank order of VAS in the pre-operative LPA group was 42.17, and the mean rank order of VAS in the NLPA group was 48.03. The Mann-Whitney U test showed that the difference in VAS between the pre-operative LPA and NLPA groups was not statistically significant (U=804.000, P=0.260). The mean rank order of VAS was 35.12 in the LPA group and 58.7 in the NLPA group, and the Mann-Whitney U test showed that there was a statistically significant difference between the VAS of the LPA (2.36 ± 1.039) and NLPA (3.86 ± 1.574) groups during the procedure (U=430.500, P<0.001). The mean rank order of VAS in the post-operative LPA group was 40.04, and the mean rank order of VAS in the NLPA group was 51.26. The Mann-Whitney U test showed a statistically significant difference between the VAS in the post-operative LPA and NLPA groups (U=691.000, P<0.031) (Table 3).

The Mann-Whitney U test was also used to determine whether there were differences in VAS scores in each group at the time points, respectively. The analysis showed statistically significant differences in VAS between the LPA group preoperatively, intraoperatively, and postoperatively (P<0.05). The intraoperative VAS was the highest, while the postoperative score was slightly higher than the pre-operative score (P=0.027). Similar to the results of the LPA group, there were statistically significant differences in VAS between the two groups in the NLPA group preoperatively, intraoperatively, and postoperatively (P<0.05) (Supplementary Table 1).

In addition, some patients used analgesics during and after the MWA procedure, and statistics revealed that the use frequency of intraoperative analgesics in the NLPA group was significantly higher than that in the LPA group (P=0.036) (Table 4).

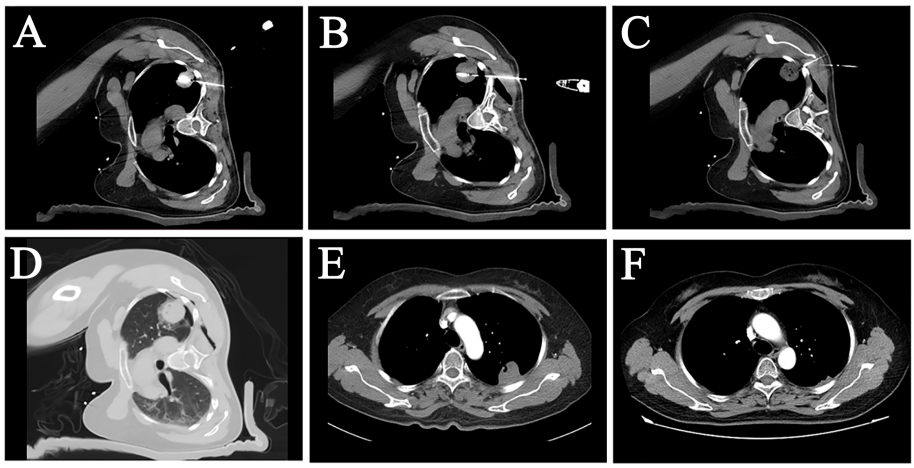

FIGURE 2
A female patient, 50 years old, with pulmonary metastasis from osteosarcoma, which was eradicated with an MWA procedure with LPA. **(A, B)** CT image showed a sizeable subpleural metastasis in the upper lobe of the patient's left lung. Two MWA antennas were used on the patient at different layers to perform MWAof this metastatic tumor. **(C)** Local pleural anesthesia was used on the patient during the treatment. The tip of the anesthesia needle was placed in the subpleural area near the tumor. **(D)** An immediate postoperative CT scan showed a "halo sign" surrounded by a ground-glass density around the lesion. **(E)** A follow-up examination three months after surgery showed that the lesion was smaller than before, and no abnormal enhancement was seen inside the lesion. **(F)** Twelve months later, the tumor largely disappeared, suggesting that the pulmonary metastasis had achieved radical ablation.

10.3389/fonc.2022.957138

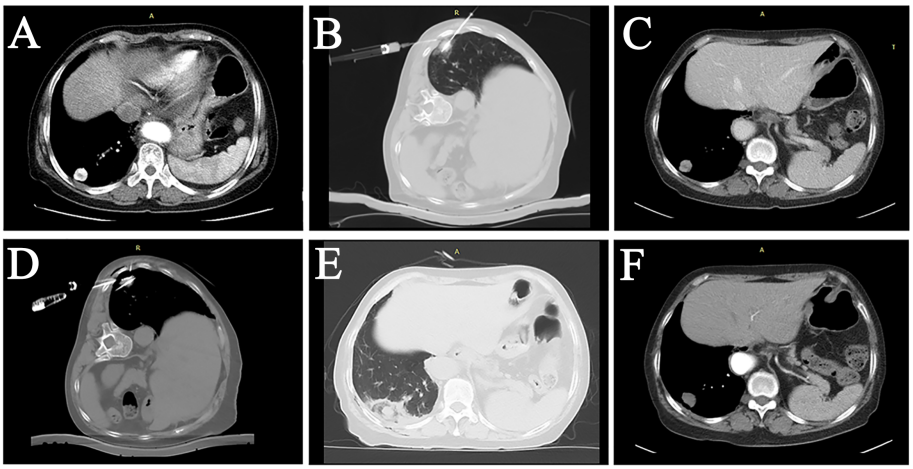

FIGURE 3
A female patient, 72 years old, with lung adenocarcinoma in the right lower lung lobe, underwent secondary ablation after the first incomplete ablation. **(A)** The tumor was located in the subpleural area with significant enhancement. **(B)** First MWA treatment combined with LPA. **(C)** Follow-up CT three months after the intervention showed significant inhomogeneous enhancement within the tumor. **(D)** Re-ablation of the tumor was performed using two MWA antennas combined with LPA. **(E)** Postoperative CT showed a "halo sign" surrounding the tumor. **(F)** 3-month follow-up after the secondary ablation indicated complete tumor ablation.

TABLE 3 Differences of VAS scores between the two groups.

Period	Group	Number	Mean	Std. Deviation	Median	Mann-Whitney U	*P*-value
Pre-operation	LPA	53	0.83	0.753	1	804.000	**0.260**
	NLPA	35	1.06	0.906	1		
Intra-operation	LPA	53	2.36	1.039	2	430.500	**0.000**
	NLPA	35	3.86	1.574	4		
Post-operation	LPA	53	1.21	0.906	1	691.000	**0.031**
	NLPA	35	1.51	0.818	2		

LPA, local pleural anesthesia; NLPA, non-local pleural anesthesia; VAS, visual analog scale.

We also analyzed the effect of the number of antennas on the pain degree. Given that the data did not conform to a normal distribution, we used the Mann-Whitney U test to conduct the analyses in the LPA and NLPA groups separately. The Mann-Whitney U test showed no statistically significant difference in pain levels between single and dual antenna patients in the LPA group intraoperatively (U=310, *P*=0.511). The NLPA group showed the same results, with no statistically significant difference in pain levels between single and dual antenna patients intraoperatively (U=142.5, *P*=0.756). No statistically significant differences were also found between both groups in the postoperative analysis (*P*>0.05) (Supplementary Table 2).

3.5 Adverse events/complications

The SIR scoring system was used to assess the complications of MWA surgery (17). All 88 patients had no severe complications. In the LPA group, pneumothorax occurred in 8 patients (15.094%, 8/53), 4 of whom were evaluated for large pneumothorax volume and underwent tube drainage; 2 patients had Pleural effusion, and one patient underwent bleeding around the lesion, and the related complications were effectively controlled after the application of hemostatic drugs and other medical treatments (Supplementary Figure 1).

In the NLPA group, nine patients had a pneumothorax (25.714%, 9/35), 6 of whom were evaluated and underwent tube drainage due to the large volume of pneumothorax; 3 patients had different amounts of pleural effusion, and the related complications were effectively controlled after the application of hemostatic drugs and other medical treatments. The relevant results are detailed in Table 4.

4 Discussion

The subpleural pulmonary nodule itself was not precisely defined. Okuma et al. reported that when the distance between

10.3389/fonc.2022.957138

TABLE 4 Efficacy and complications of microwave ablation in the two groups.

	Group LPA (n=53)	Group NLPA (n=35)	*P*-value
Days of hospitalization	6.00±1.373	6.60±1.594	0.51
Technical success			
Yes	53	35	
No	0	0	
Technique Efficacy			
Yes	52	33	
No	1	2	
Intra-operative analgesics			0.036
Yes	8	12	
No	45	23	
Post-operative analgesics			0.082
Yes	5	8	
No	48	27	
Post-procedure VAS score (range)	1.21±0.906 (0-4)	1.51±0.818 (0-3)	0.031
Follow-up duration (months) (range)	12.19±3.157	13.43±3.509	0.104
Recurrences			
Yes	1	2	
No	52	33	
Complications			
Pleurodynia	0	1	
Pneumothorax	8	9	
Pleural effusion	2	3	
Pulmonary hemorrhage	1	1	
Pneumonia	0	0	
Others	0	0	

LPA, local pleural anesthesia; NLPA, non-local pleural anesthesia; VAS, visual analog scale.

the tumor and the chest wall was less than 1 cm, patients may feel severe pain from heat transfer from the target area to the pleura during thermal ablation therapy (10). Local pleural anesthesia can protect adjacent structures and reduce pain without affecting the patient's respiratory function. This study defined nodules less than 1 cm from the pleura as subpleural nodules, and subpleural nodules were ablated using MWA. To explore the safety and efficacy of local pleural anesthesia in the MWA of subpleural nodules, we grouped patients with subpleural nodules treated by MWA for nearly two years into group LPA and group NLPA. In this study, 88 patients with 97 subpleural nodules were treated with MWA, and local pleural anesthesia was used to address the pain during the ablation process. The use of local pleural anesthesia significantly reduced intraoperative and postoperative pain compared to a small number of patients who did not have local pleural anesthesia. All patients tolerated the entire procedure better. In addition, we routinely applied a mixture of lidocaine and saline to increase the diffusion thickness and extent of local pleural anesthesia within the range of safe anesthetic doses and provided better protection to the pleura. The results showed that local pleural anesthesia significantly reduced the intraoperative pain of patients, and the patients' post-operative pain got to be alleviated accordingly. In addition, the use of intra- and post-operative intravenous analgesics was also less in the LPA group than in the NLPA group, suggesting that LPA played a promising analgesic role in the intra- and post-operative periods. Painkillers such as flurbiprofen have substantial side effects such as neurotoxicity and are contraindicated in patients with digestive tract ulcers or bleeding (19).

We are the first to report the use of local pleural anesthesia in MWA. The local pleural anesthesia mentioned here differs from the anesthesia for puncture procedures such as biopsy. Because of the short biopsy time and the absence of distance pain caused by thermal stimulation, the local anesthesia done during the biopsy is sometimes acceptable for less than complete pleural anesthesia. However, the pain caused by thermal ablation is very intense, and the analgesic effect is not good enough during microwave ablation treatment. The present study is thorough and continuous anesthesia of the local pleura adjacent to the lesion during ablation using local anesthetics lidocaine or ropivacaine, which is an innovation in pain management of microwave ablation and has been reported very rarely in the literature before. Most of the related literature has focused on the use of artificial pneumothorax and has not explicitly reported the use of local pleural anesthesia. Artificial pneumothorax was considered an effective pain relief and tissue protection method during thermal ablation and tumor biopsy (9, 20, 21). Previously, artificial pneumothorax was used in RFA of pulmonary adjacent mediastinal lesions, and effective therapeutic results and effective protection of proximal mediastinal structures could be achieved using artificial pneumothorax (9). Yang et al. compared MWA in 17 patients with and 20 without artificial pneumothorax and reported that artificial pneumothorax significantly reduced pain during and after the procedure (17). However, in some cases, including patients with pleural adhesions and severe respiratory insufficiency, artificial pneumothorax may not be effective or may not be tolerated by the patient. In addition, excessive compression of the lung parenchyma can alter the RF's electrical conductivity and thermal conductivity, affecting the ablation efficiency and leading to increased lung tissue damage (22). In particular, the excessive collapse of lung tissue can lead to subpleural lesions closer to the pleura, and ultimately thermal ablation may lead to complications such as pleural fistula. In addition, the application of artificial pneumothorax requires a high level of technical skill, and improper operations can lead to severe complications such as respiratory distress and subcutaneous emphysema; in addition, for some specific lesions, the adjustment of position and gas pushing are not effective in forming an ideal gas isolation zone. An excessive amount of artificial pneumothorax may also lead to lung

collapse, increase the difficulty of antenna transfer, produce more damage to lung tissue during treatment, and even lead to severe complications such as pleural fistula. In addition, a small amount of gas does not eliminate the pain caused by MWA due to the preferable conductivity of the gas to heat. The application of artificial pneumothorax in the treatment of subpleural lung cancer has a considerable limitation.

Pneumothorax is the most common complication of RFAand MWA (23, 24). Rika Yoshimatsu et al. suggested that delayed and recurrent pneumothorax occurs more likely when the GGO around the lesion adheres to the pleura (24). A small amount of pneumothorax can usually resolve independently, while a larger amount may require chest tube drainage. In this study, the incidence of pneumothorax was significantly lower in the LPA group than in the NLPA group. We believe this may be due to the better compliance and tolerance of local pleural anesthesia patients, who are less prone to violent coughing and excessive respiratory dynamics that may lead to pneumothorax. In addition, very few patients in both groups had thoracic bleeding and a small amount of intrapulmonary hemorrhage. Local pleural anesthesia also did not increase the chance of intercostal artery injury or bleeding, indicating the safety of local pleural anesthesia.

MWA is an effective minimally invasive treatment for eradicating pulmonary nodules (25, 26) and has achieved better outcomes in treating subpleural nodules (14, 17). Previously, for subpleural lesions, ablation was usually performed at lower power for a longer period to protect the pleura and reduce pain as much as possible. This may result in incomplete tumor ablation for larger lesions and affect the ablation outcome. The higher power usually leads to pain and the inability to tolerate the procedure. The duration of MWA depends mainly on the changes in lung tissue density around the lesion of ablation (27). Usually, we use the halo sign of ground-glass density around the lesion and the range of ground-glass density beyond the edge of the lesion by more than 5 mm as the sign of complete ablation. Although there was no significant difference in the duration of ablation between the two groups in this study, the mean treatment power was somewhat higher in the LPA group than in the NLPA group, suggesting that patients who underwent local pleural anesthesia were more tolerant of the higher MWA power to achieve complete ablation. This study again demonstrated the efficacy of MWAin primary and metastatic subpleural pulmonary nodules. Only 3 of all 88 patients had a postoperative recurrence, and all were eradicated after repeated MWA. Due to the different pathology of subpleural nodules, only LPFS was used in this study to observe the efficacy of local lesion ablation. The LPFS rate was slightly higher in the LPA group than in the NLPA group, suggesting that LPA combined with MWA may produce better efficacy. And this needs to be validated with more patients and longer follow-ups in the future.

There are some limitations of this study. First, the degree of pain was assessed using the VAS score, a highly subjective score system that may affect the accuracy of the results. Second, this study was a retrospective analysis. More confounding factors such as the application of ropivacaine in a few patients in this study brought bias to the results; Second, because of the different pathologies of pulmonary nodules, we only observed the short-term efficacy of MWA by comparing the LPFS of the patients. The long-term efficacy of MWA needs to be validated further; Third, Due to the limitation of patients, the control group was not selected using the more scientific propensity score matching method, and the relevant results need to be further validated in a larger sample in the future.

5 Conclusion

In conclusion, CT-guided MWA is a safe and effective minimally invasive treatment for subpleural pulmonary nodules. Local pleural anesthesia can significantly reduce patients' intra- and postoperative pain during MWA, facilitate the implementation of the surgical plan, complete ablation of the lesion, and reduce the occurrence of complications such as pneumothorax. The long-term efficacy must be verified in more patients and a longer follow-up.

Data availability statement

The raw data supporting the conclusions of this article will be made available by the authors, without undue reservation.

Ethics statement

The studies involving human participants were reviewed and approved by Ethics Committee of the Chinese PLA general hospital. Written informed consent for participation was not required for this study in accordance with the national legislation and the institutional requirements.

Author contributions

LM, WB and YYX conceived and designed the study. LM and BW drafted the entire manuscript. XZ and XBZ are responsible for patient information acquisition and post-operative follow-up. XDX and XFH are responsible for imaging and image processing. YTW and XNZ reviewed and revised the manuscript. LMA and ZLZ participated in figures and table preparation. JL and YYX guided the article revision and the selection of statistical methods. All authors

contributed to the manuscript revision and approved the submitted version.

Conflict of interest

The authors declare that the research was conducted in the absence of any commercial or financial relationships that could be construed as a potential conflict of interest.

Publisher's note

Supplementary material

The Supplementary Material for this article can be found online at: https://www.frontiersin.org/articles/10.3389/fonc.2022.957138/full#supplementary-material

SUPPLEMENTARY FIGURE 1
Complications of MWA for subpleural pulmonary nodules. **(A)** After ablation of the tumor in the right lung, a CT scan revealed a large pneumothorax with decreased oxygen saturation in the patient. **(B)** The patient was placed on a chest tube for drainage. **(C)** A slight intraoperative intrathoracic bleeding was found in the patient's right lower lobe lung lesion. **(D)** After treatment was completed, the scan after antenna removal revealed an increase in pleural blood accumulation compared to the previous one, and symptomatic therapies such as hemostatic drugs were given, and the patient was closely monitored.

SUPPLEMENTARY TABLE 1
Differences of VAS in the peri-operative periods in each group.

SUPPLEMENTARY TABLE 2
Differences in VAS between single and dual antennas in each group.

References

1. Zheng R, Zhang S, Zeng H, Wang S, Sun K, Chen R, et al. Cancer incidence and mortality in China, 2016. *J Natl Cancer Center* (2022) 2(1):1–9. doi: 10.1016/j.jncc.2022.02.002

2. Sung H, Ferlay J, Siegel RL, Laversanne M, Soerjomataram I, Jemal A, et al. Global cancer statistics 2020: Globocan estimates of incidence and mortality worldwide for 36 cancers in 185 countries. *CA Cancer J Clin* (2021) 71(3):209–49. doi: 10.3322/caac.21660

3. De Ruysscher D, Nakagawa K, Asamura H. Surgical and nonsurgical approaches to small-size nonsmall cell lung cancer. *Eur Respir J* (2014) 44 (2):483–94. doi: 10.1183/09031936.00020214

4. Ettinger DS, Wood DE, Aisner DL, Akerley W, Bauman JR, Bharat A, et al. Non-small cell lung cancer, version 3.2022, nccn clinical practice guidelines in oncology. *J Natl Compr Canc Netw* (2022) 20(5):497–530. doi: 10.6004/jnccn.2022.0025

5. McDonald F, De Waele M, Hendriks LE, Faivre-Finn C, Dingemans AC, Van Schil PE. Management of stage I and ii nonsmall cell lung cancer. *Eur Respir J* (2017) 49(1):1600764. doi: 10.1183/13993003.00764-2016

6. Deboever N, Mitchell KG, Feldman HA, Cascone T, Sepesi B. Current surgical indications for non-Small-Cell lung cancer. *Cancers (Basel)* (2022) 14 (5):1263. doi: 10.3390/cancers14051263

7. Páez-Carpio A, Gómez FM, Isus Olivé G, Paredes P, Baetens T, Carrero E, et al. Image-guided percutaneous ablation for the treatment of lung malignancies: Current state of the art. *Insights Imaging* (2021) 12(1):57. doi: 10.1186/s13244-021-00997-5

8. Kong Y, Xu H, Huang Y, Wei Z, Ye X. Local thermal ablative therapies for extracranial oligometastatic disease of non-Small-Cell lung cancer. *Asia Pac J Clin Oncol* (2022). doi: 10.1111/ajco.13766

9. Hou X, Zhuang X, Zhang H, Wang K, Zhang Y. Artificial pneumothorax: A safe and simple method to relieve pain during microwave ablation of subpleural lung malignancy. *Minim Invasive Ther Allied Technol* (2017) 26(4):220–6. doi: 10.1080/13645706.2017.1287089

10. Okuma T, Matsuoka T, Yamamoto A, Oyama Y, Toyoshima M, Nakamura K, et al. Frequency and risk factors of various complications after computed tomography-guided radiofrequency ablation of lung tumors. *Cardiovasc Intervent Radiol* (2008) 31(1):122–30. doi: 10.1007/s00270-007-9225-0

11. Singh S, Melnik R. Thermal ablation of biological tissues in disease treatment: A review of computational models and future directions. *Electromagn Biol Med* (2020) 39(2):49–88. doi: 10.1080/15368378.2020.1741383

12. Charalampidis C, Youroukou A, Lazaridis G, Baka S, Mpoukovinas I, Karavasilis V, et al. Pleura space anatomy. *J Thorac Dis* (2015) 7(Suppl 1):S27–32. doi: 10.3978/j.issn.2072-1439.2015.01.48

13. Gulati A, Shah R, Puttanniah V, Hung JC, Malhotra V. A retrospective review and treatment paradigm of interventional therapies for patients suffering from intractable thoracic chest wall pain in the oncologic population. *Pain Med* (2015) 16(4):802–10. doi: 10.1111/pme.12558

14. Cao F, Xie L, Qi H, Chen S, Shen L, Song Z, et al. Safety and efficacy of thermal ablation for subpleural lung cancers. *Thorac Cancer* (2019) 10(6):1340–7. doi: 10.1111/1759-7714.13068

15. Ye X, Fan W, Chen JH, Feng WJ, Gu SZ, Han Y, et al. Chinese Expert consensus workshop report: Guidelines for thermal ablation of primary and metastatic lung tumors. *Thorac Cancer* (2015) 6(1):112–21. doi: 10.1111/1759-7714.12152

16. Jia H, Tian J, Liu B, Meng H, Pan F, Li C. Efficacy and safety of artificial pneumothorax with position adjustment for ct-guided percutaneous transthoracic microwave ablation of small subpleural lung tumors. *Thorac Cancer* (2019) 10 (8):1710–6. doi: 10.1111/1759-7714.13137

17. Yang X, Zhang K, Ye X, Zheng A, Huang G, Li W, et al. Artificial pneumothorax for pain relief during microwave ablation of subpleural lung tumors. *Indian J Cancer* (2015) 52 Suppl 2:e80–3. doi: 10.4103/0019-509x.172519

18. Li W, Ye X, Yang X, Li Y, Huang G, Wang J, et al. Microwave ablation as palliative treatment of locally recurrent colorectal cancer. *Indian J Cancer* (2015) 52 Suppl 2:e61–3. doi: 10.4103/0019-509x.172515

19. Wu H, Chen Z, Sun G, Gu K, Pan Y, Hao J, et al. Intravenous flurbiprofen axetil can increase analgesic effect in refractory cancer pain. *J Exp Clin Cancer Res* (2009) 28(1):33. doi: 10.1186/1756-9966-28-33

20. Solomon SB, Thornton RH, Dupuy DE, Downey RJ. Protection of the mediastinum and chest wall with an artificial pneumothorax during lung ablations. *J Vasc Interv Radiol* (2008) 19(4):610–5. doi: 10.1016/j.jvir.2008.01.004

21. Hiraki T, Gobara H, Shibamoto K, Mimura H, Soda Y, Uka M, et al. Technique for creation of artificial pneumothorax for pain relief during radiofrequency ablation of peripheral lung tumors: Report of seven cases. *J Vasc Interv Radiol* (2011) 22(4):503–6. doi: 10.1016/j.jvir.2010.12.018

22. de Baere T, Dromain C, Lapeyre M, Briggs P, Duret JS, Hakime A, et al. Artificially induced pneumothorax for percutaneous transthoracic radiofrequency ablation of tumors in the hepatic dome: Initial experience. *Radiology* (2005) 236 (2):666–70. doi: 10.1148/radiol.2362040992

23. Xu S, Qi J, Li B, Bie ZX, Li YM, Li XG. Risk prediction of pneumothorax in lung malignancy patients treated with percutaneous microwave ablation: Development of nomogram model. *Int J Hyperthermia* (2021) 38(1):488–97. doi: 10.1080/02656736.2021.1902000

24. Yoshimatsu R, Yamagami T, Terayama K, Matsumoto T, Miura H, Nishimura T. Delayed and recurrent pneumothorax after radiofrequency ablation of lung tumors. *Chest* (2009) 135(4):1002–9. doi: 10.1378/chest.08-1499

25. Wei Z, Wang Q, Ye X, Yang X, Huang G, Li W, et al. Microwave ablation followed by immediate biopsy in the treatment of non-small cell lung cancer. *Int J Hyperthermia* (2018) 35(1):262–8. doi: 10.1080/02656736.2018.1494856

26. Aufranc V, Farouil G, Abdel-Rehim M, Smadja P, Tardieu M, Aptel S, et al. Percutaneous thermal ablation of primary and secondary lung tumors: Comparison between microwave and radiofrequency ablation. *Diagn Interv Imaging* (2019) 100(12):781–91. doi: 10.1016/j.diii.2019.07.008

27. Vogl TJ, Nour-Eldin NA, Albrecht MH, Kaltenbach B, Hohenforst-Schmidt W, Lin H, et al. Thermal ablation of lung tumors: Focus on microwave ablation. *Rofo* (2017) 189(9):828–43. doi: 10.1055/s-0043-109010

frontiers | Frontiers in Oncology

TYPE Original Research
PUBLISHED 17 August 2022
DOI 10.3389/fonc.2022.947284

OPEN ACCESS

EDITED BY
Xin Ye,
Qianfoshan Hospital, Shandong University, China

REVIEWED BY
Xinshuang Yu,
The First Affiliated Hospital of Shandong First Medical University, China
Hongtao Zhang,
Hebei General Hospital, China
Bin Liu,
The Second Hospital of Shandong University, China
Yong Jin,
The Second Affiliated Hospital of Soochow University, China

*CORRESPONDENCE
Jian He
hejian62@163.com
Lingxiao Liu
liulingxiao2022@163.com

†These authors have contributed equally to this work and share first authorship

SPECIALTY SECTION
This article was submitted to Thoracic Oncology, a section of the journal Frontiers in Oncology

RECEIVED 18 May 2022
ACCEPTED 25 July 2022
PUBLISHED 17 August 2022

CITATION
Wang F, Fan S, Shi Q, Zhao D, Sun H, Sothea Y, Wu M, Song H, Chen Y, Cheng J, Zeng Z, Yan Z, He J and Liu L (2022) Comparison of clinical outcomes between cone beam CT-guided thermal ablation and helical tomotherapy in pulmonary metastases from hepatocellular carcinoma. *Front. Oncol.* 12:947284. doi: 10.3389/fonc.2022.947284

Comparison of clinical outcomes between cone beam CT-guided thermal ablation and helical tomotherapy in pulmonary metastases from hepatocellular carcinoma

Feihang Wang[1,2,3†], Shaonan Fan[4†], Qin Shi[1,2,3†], Danyang Zhao[1,2,3], Huiyi Sun[5], Yav Sothea[1,2,3], Mengfei Wu[6], Huadan Song[7], Yi Chen[1,2,3], Jiemin Cheng[1,2,3], Zhaochong Zeng[4], Zhiping Yan[1,2,3], Jian He[4*] and Lingxiao Liu[1,2,3*]

[1]Department of Interventional Radiology, Zhongshan Hospital, Fudan University, Shanghai, China, [2]Shanghai Institute of Medical Imaging, Fudan University, Shanghai, China, [3]National Clinical Research Center for Interventional Medicine, Zhongshan Hospital, Fudan University, Shanghai, China, [4]Department of Radiation Oncology, Zhongshan Hospital, Fudan University, Shanghai, China, [5]Shanghai Medical College, Fudan University, Shanghai, China, [6]Department of Computed Tomography (CT) and Magnetic Resonance Imaging (MRI), Third Hospital of Hebei Medical University, Shijiazhuang, China, [7]Department of Radiology, Xinhua Hospital, Shanghai Jiao Tong University School of Medicine, Shanghai, China

Objective: This retrospective study compares the clinical results of cone beam CT (CBCT)-guided thermal ablation with those of helical tomotherapy in hepatocellular carcinoma (HCC) patients with pulmonary metastases.

Methods: A total of 110 patients undergoing thermal ablation or helical tomotherapy for pulmonary metastases from April 2014 to December 2020 were included in the study. The endpoints were local tumor progression-free survival (LTPFS), overall survival (OS), and complications. Univariate and multivariate analyses using the Cox proportional hazard model were conducted to identify independent factors (univariate: $P < 0.1$; multivariate: $P < 0.05$). The Kaplan–Meier method was used to calculate the LTPFS and OS rates.

Results: The results of 106 patients were taken into the final analysis. The 1- and 3-year LTPFS rates were 50 and 19% for the thermal ablation group and 65 and 25% for the helical tomotherapy group. The median LTPFS in the thermal ablation group was 12.1 months, while it was 18.8 months in the helical tomotherapy group ($P = 0.25$). The 1- and 3-year OS rates were 75 and 26% for the thermal ablation group and 77 and 37% for the helical tomotherapy group. The median OS was 18.0 months in the thermal ablation group and 23.4 months in the helical tomotherapy group ($P = 0.38$). The multivariate analyses found that α-fetoprotein (AFP) at <400 ng/ml ($P = 0.003$) was significantly associated with better LTPFS. Tumor number <3 and AFP <400 ng/ml were

favorable prognostic factors for OS. There were no grades 3–5 adverse events in both groups. Grade 2 was recorded in three patients (4.8%) in the thermal ablation group and two patients (4.7%) in the helical tomotherapy group.

Conclusions: For pulmonary metastases from HCC, CBCT-guided thermal ablation and helical tomotherapy provided comparable clinical effects and safety.

KEYWORDS

pulmonary metastases, hepatocellular carcinoma, thermal ablation, helical tomotherapy, comparison

Introduction

The lung is the most common site of extrahepatic metastases in patients with hepatocellular carcinoma (HCC) (1). Systemic therapy is the mainstream treatment for HCC patients with extrahepatic metastases (2). Sorafenib is recommended as the first-line therapy, and its median overall survival (OS) was 7.13–9.6 months for HCC patients with extrahepatic metastases (3, 4). However, a phase 2 trial revealed that pulmonary metastases had a poor response to sorafenib in advanced HCC patients (5). Surgery is the mainstream of locoregional treatment for pulmonary metastases (6). In 2018, a meta-analysis reported that the median OS of patients with pulmonary metastases from colorectal carcinoma undergoing pulmonary metastasectomy was 43 months (7). The 5-year survival rate for pulmonary metastasectomy of HCC was 66.9 ± 10% (8). However, most patients are not suitable for surgery due to poor liver function that is unable to tolerate surgery, surgical trauma, and multiple or bilateral metastases of pulmonary metastases (9, 10).

Noninvasive or minimally invasive locoregional treatments, such as thermal ablation and radiotherapy, have gained increasing acceptance (11). In China, guidelines and expert consensus demonstrated that thermal ablation and radiotherapy could be used as curative or palliative therapy for treating pulmonary metastases from hepatocellular carcinoma (12–14). A previous study compared the effectiveness of thermal ablation and stereotactic radiotherapy in lung cancer and reported no significant overall survival difference between the two therapies ($P = 0.13$) (15). In HCC patients with pulmonary metastases, thermal ablation could acquire 79.8% 1-year OS and 58% 3-year OS (16), and radiotherapy could achieve 65.5% 1-year OS (17). Nevertheless, there is a lack of direct comparisons of clinical outcomes between thermal ablation and radiotherapy. This retrospective study directly compares the clinical outcomes between thermal ablation and helical tomotherapy in HCC patients with pulmonary metastases.

Materials and methods

Patients

This retrospective study was approved by the institutional review boards of Zhongshan Hospital, Fudan University. Informed consent was waived. From April 2014 to December 2020, 110 patients with lung metastasis from liver cancer, who underwent thermal ablation or helical tomotherapy for lung metastasis, were selected for this study. The inclusion criteria were as follows: (a) age between 18 and 80 years, (b) clinical or histological diagnosis of lung metastasis from liver cancer, (c) controlled intrahepatic tumors, and (d) patients refused or were not suitable for lung metastasectomy. The exclusion criteria were as follows: (a) liver cancer was diagnosed as intrahepatic cholangiocarcinoma (ICC), (b) uncorrectable coagulopathy, and (c) loss to follow-up after treatment or incomplete medical records.

Chest computed tomography (CT) or ^{18}F-fluorodeoxyglucose positron emission tomography-CT was used for pretreatment evaluation. Laboratory tests including blood routine, coagulation function, liver function, and alpha-fetoprotein were also performed.

Cone beam CT-guided thermal ablation

The patients were scanned by cone beam CT (CBCT) to determine the puncture angles, depths, and appropriate positions. After the scan, local anesthesia was administrated with 1% lidocaine at the selected puncture point. Then, a 17-gauge trocar was inserted into the target tumor to guide the core-needle biopsy, antenna, or electrode to the target. For microwave ablation (MWA), the antenna was advanced into the target tumor, and the power was set at 40-60W (Figure 1A). For radiofrequency ablation (RFA), the electrode was inserted into the target lesion, and radiofrequency energy was applied with an

impedance control algorithm for 8-14 minutes. At the end of the MWA or RFA procedure, CBCT scans were performed to confirm that the ablation margin around the tumor was more than 5 mm and to evaluate complications. The needle track was also ablated to avoid bleeding and tumor seeding along the electrode route.

Helical tomotherapy

All treatments were administered using Helical Tomotherapy (HT) Hi-Art Treatment System (Accuray, Madison, WI, USA). Radiation therapy (RT) was delivered using either intensity-modulated radiation therapy (IMRT) or SBRT based on tumor location, tumor size, and physician/patient preference. Radiotherapy simulation was done in the supine position with both arms overhead using a vacuum bag. All patients were simulated with the application of respiration-correlated helical four-dimensional CT (4D-CT) (Siemens Somatom Sensation, Siemens Healthineers Corporation, Germany) scans with a slice thickness of 3 mm (Figure 1B).

The gross tumor volume (GTV) was delineated as a lesion observed at the lung window level on the enhanced CT and/or PET/CT. The clinical target volume was equal to gross tumor volume. The internal target volume (ITV) was contoured based on the extension of GTVs at all phases (five inspiratory, five expiratory, and one resting) of the respiratory cycle on the 4D-CT scanning to include the full movement of the tumor. To compensate for uncertainty of the tumor position and changes of the tumor motion caused by breathing, the planning target volume extended a margin of 0.5 cm from the ITV. Cone beam CT was implemented before each treatment to confirm that the position of the target was achieved.

The HT-SBRT technique and treatment planning were performed as previously described according to our institutional protocol (1): In general, the fractionation regimes primarily depended on the treating physicians' preference, based on tumor location, tumor size, and lung function parameters. Typically, 5.0 to 10.0 Gy per fraction for three to 10 fractions and a total dose of 30–60 Gy were adopted in our institution. According to the experience of the Radiation Therapy Oncology Group 0236 guidelines, the dose constraints for the organs at risk (OAR) were implemented (2); When patients in the study received IMRT radiotherapy, the CT images and contours were directly transferred onto the 3D planning system (CMS XiO Treatment Planning System), and the total RT doses ranged from 30 to 60 Gy, while the daily doses ranged from 2.0 to 3.0 Gy. The OARs included the lungs, esophagus, heart, and spinal cord.

Follow-up and evaluation

All patients were followed until death or December 2021. The patients were followed up every month for the first 3 months after their treatments and at 3-month intervals thereafter.

Local tumor progression-free survival (LTPFS) was defined as the interval from initial thermal ablation or helical tomotherapy to radiologic evidence of local tumor progression or the last follow-up date. OS was defined as the interval from initial ablation to death or the last follow-up date. Complications were recorded based on the Common Terminology Criteria for

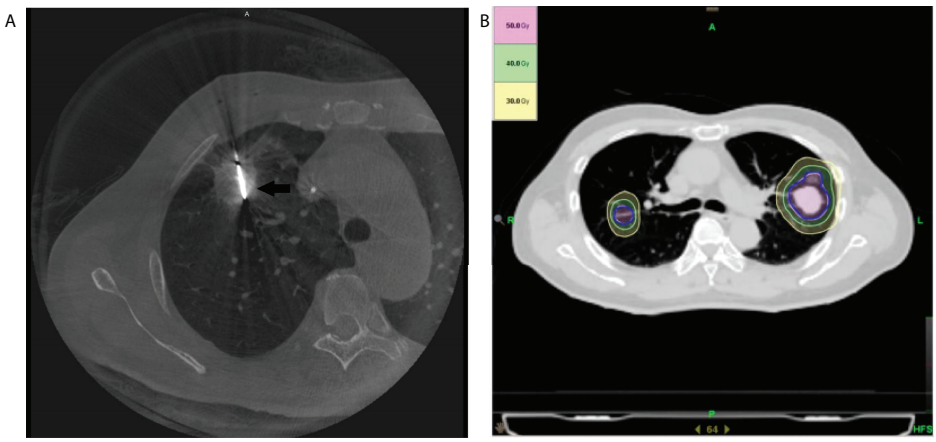

FIGURE 1
Illustration of the treatment plan. **(A)** The axial cone beam CT image obtained during microwave ablation shows a microwave antenna positioned in the tumor (arrow). **(B)** An SBRT treatment plan with isodose curve distribution for a patient with bilateral pulmonary metastasis of hepatocellular carcinoma is displayed.

Adverse Events, v5.0. The major complications of the two groups [grade 3 or higher adverse event (AEs)] were compared.

Statistical analysis

The baseline characteristics of the two groups were compared using chi-square test or *T*-test. Local tumor progression-free survival and overall survival rates were calculated using the Kaplan–Meier method with R (version 4.1.0). SPSS statistical software (version 24.0) was used for data analysis. The Cox proportional hazard model was used for univariate and multivariate analyses to determine the prognostic factors. Factors in the univariate analysis with P <0.1 were included in the multivariate analysis. The statistical significance of the multivariate analysis was defined as a P-value <0.05.

Results

There were 106 out of the 110 patients included in the study at the end (63 patients in the ablation group and 43 patients in the helical tomotherapy group). Four patients were excluded from the final analysis (two due to ICC and two due to loss to follow-up). The mean follow-up time was 21.6 months (ranging from 1.3 to 87.8 months). The mean age was 55 years (ranging from 19 to 78 years). For treatments of primary liver cancer, 46 patients were treated with surgery, 52 patients had locoregional treatment, and 13 patients accepted systemic therapy in the thermal ablation group, and for the helical tomotherapy group, there were 41 patients who received surgery, 32 patients who went through locoregional treatment, and 15 patients who had systemic therapy. The baseline characteristics of the two groups were equivalent except for Child–Pugh grade (P = 0.048) and AFP (P = 0.008), as shown in Table 1.

TABLE 1 Baseline characteristics of patients with pulmonary metastases from hepatocellular carcinoma.

	Thermal ablation (n = 63)	Radiotherapy (n = 43)	P-value
Age (years)			0.617
<60	38	28	
≥60	25	15	
Gender			1.000
Female	5	3	
Male	58	40	
Tumor number			0.161
≤3	25	23	
>3	38	20	
Distribution of pulmonary metastatic tumors			0.926
Unilateral	24	16	
Bilateral	39	27	
Maximum tumor diameter, mm (mean ± SD)	17.5 ± 10.1	21.2 ± 16.8	0.205
Treatment of primary liver cancer			0.277
Surgery	46	41	
Locoregional treatment	52	32	
Systemic therapy	13	15	
History of previous pulmonary surgery			0.170
No	62	39	
Yes	1	4	
Lung metastasis			0.899
Metachronous	60	42	
Synchronous	3	1	
Extrapulmonary metastasis			0.052
No	58	34	
Yes	5	9	
Child–Pugh grade			**0.048**
A	52	41	
B	11	2	
Performance status			0.962
0	54	37	
1	9	6	
AFP (ng/ml)			**0.008**
<400	34	34	
≥400	29	9	

AFP, α-fetoprotein.
The bold values are statistically significant with p <0.05.

Local tumor progression-free survival

The cumulative 1- and 3-year LTPFS rates were 50 and 19% in the thermal ablation group and 65 and 25% in the helical tomotherapy group. The median LTPFS values of the thermal ablation and helical tomotherapy groups were 12.1 months (95% CI: 6.8–17.4 months) *vs*. 18.8 months (95%CI: 10.5–27.1 months) (P = 0.25), respectively (Figure 2). The multivariate analysis showed that serum AFP level (P = 0.003) was associated with LTPFS with statistical significance (Table 2).

Overall survival

The cumulative 1- and 3-year OS rates were 75 and 26% in the thermal ablation group and 77 and 37% in the helical tomotherapy group. The median OS of the thermal ablation and helical tomotherapy groups were 18.0 months (95%CI: 12.6–23.3 months) and 23.4 months (95%CI: 4.4–42.5 months) (P = 0.38) (Figure 3A).

The results of the univariate and multivariate analysis indicated that tumor number (P = 0.016) and AFP (P = 0.010) were correlated with OS with statistical significance (Table 3).

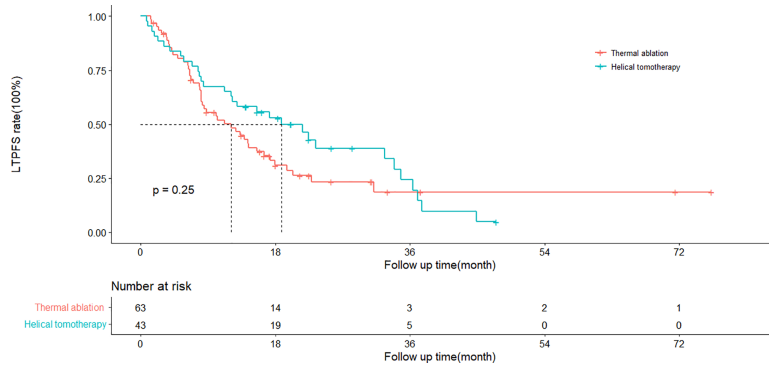

FIGURE 2
Kaplan–Meier curves of local tumor progression-free survival (LTPFS) in patients with pulmonary metastases from hepatocellular carcinoma who underwent thermal ablation or helical tomotherapy (thermal ablation group: n = 63, median LTPFS = 22.5 months; helical tomotherapy group: n = 43, median LTPFS = not reached; P = 0.13).

The subgroup analyses of OS in patients with different serum AFP levels showed that the median OS of patients with low AFP levels (<400 ng/ml) and high AFP levels (≥400 ng/ml) was 21.4 months (95%CI: 16.9–25.9 months) and 15.6 months (95%CI: 13.7–17.5 months), respectively, in the thermal ablation group but 33.9 months (95%CI: 12.4–55.4 months) and 9.3 months (95%CI: 6.6–12.1 months), respectively, in the helical tomotherapy group. The median OS of patients with low AFP levels or high AFP levels was not significantly different in the thermal ablation group compared with that in the helical tomotherapy group (P = 0.57 and P = 0.64, respectively) (Figures 3B, C).

Complications

There was no treatment-related death (grade 5 AE), grade 4 AE, and grade 3 AE in either the thermal ablation group or the helical tomotherapy group. Three patients in the thermal ablation group developed grade 2 AEs, including two patients (3.2%) with pneumothorax requiring thoracocentesis drainage and one patient (1.6%) with pleural effusion requiring thoracocentesis drainage. Grade 1 AEs, including mild pneumothorax (16 patients, 25.4%), mild pleural effusion (23 patients, 36.5%), and mild pneumonia (2 patients, 3.2%), were recorded in the thermal ablation group. Grade 2 radiation pneumonitis was recorded in two patients (4.7%) in the helical tomotherapy group. There was no grade 1 AE in the helical tomotherapy group (Table 4).

Discussion

The lung is one of the most frequent sites of extrapulmonary primary tumors' metastatic spread, and systemic therapy has historically been regarded as the standard of care for this (6). However, some patients are not candidates for or unwilling to receive systemic therapy. For these patients, locoregional treatments, such as metastasectomy, radiotherapy, and thermal ablation, can be their choices. Although metastasectomy has traditionally been the mainstay of locoregional therapy, stereotactic ablative radiotherapy and thermal ablation are getting more and more accepted for they are non-invasive or less invasive, repeatable, safe, and others (6, 10). Percutaneous thermal ablation, such as RFA and MWA, has been demonstrated as a technically feasible and relatively safe treatment with impressive outcomes for patients with pulmonary metastases, and the majority of existing data is in the area of metastases colorectal carcinoma (6, 18, 19). In China, expert consensus recommended thermal ablation as a curative or palliative treatment for pulmonary metastases (13). Helical tomotherapy can deliver IMRT at a conformal high dose to a target while minimizing the high-dose radiation volume for the lung, the mean lung dose, and surrounding OARs, resulting in better dose uniformity, dose gradients, and protection for the organs at risk (20, 21). Due to the theoretical advantages of this technique, helical tomotherapy and its application in multiple tumor diseases, such as hepatocellular carcinoma and lung carcinoma, are becoming more prevalent (22–27). Our previous clinical studies had demonstrated its favorable tolerance, feasibility, and promising outcome for pulmonary metastasis from hepatocellular carcinoma (22, 27).

In this study, the 1- and 3-year LTPFS rates were 50 and 19% for the thermal ablation group and 65 and 25% for the helical tomotherapy group. The Kaplan–Meier method showed that the LTPFS rate of the thermal ablation group was a little lower than the helical tomotherapy group, but there was no statistical difference between the two groups (P = 0.25). A previous study (28) analyzing outcomes of percutaneous thermal ablation for pulmonary metastases from HCC showed that the 1- and 3-year LTPFS rates were 60.7 and 34.2%, which were better than the results of our

TABLE 2 Univariate and multivariate analyses of prognostic factors for local tumor progression-free survival.

	Univariate model		Multivariate model	
	HR (95%CI)	*P*	HR (95%CI)	*P* [a]
Gender				
Female				
Male	0.767 (0.343–1.716)	0.518		
Age (years)				
<60				
≥60	1.055 (0.652–1.707)	0.828		
Treatment of pulmonary metastatic tumors				
Thermal ablation				
Radiotherapy	0.761 (0.478–1.212)	0.251		
Lung metastasis				
Metachronous				
Synchronous	0.901 (0.220–3.685)	0.884		
History of previous pulmonary surgery				
No				
Yes	1.653 (0.601–4.548)	0.330		
Maximum tumor diameter (mm)				
<10				
≥10	2.113 (1.126–3.966)	0.020	1.733 (0.904–3.322)	0.097
Tumor number				
≤3				
>3	2.041 (1.277–3.262)	0.003	1.363 (0.801–2.318)	0.253
Distribution of pulmonary metastatic tumors				
Unilateral				
Bilateral	1.694 (1.046–2.745)	0.032	1.632 (0.974–2.814)	0.078
Extrapulmonary metastasis				
No				
Yes	1.251 (0.653–2.395)	0.500		
Child–Pugh grade				
A				
B	1.055 (0.505–2.203)	0.887		
AFP (ng/ml)				
<400				
≥400	2.353 (1.477–3.749)	<0.001	2.126 (1.298–3.482)	**0.003**

AFP, α-fetoprotein. [a]Cox regression was used.
The bold value is statistically significant with $p < 0.05$.

study. This might be attributed to the patients in our study who owned a higher tumor burden, which meant more and larger pulmonary metastases. Another study showed that the 1- and 2-year progression-free survival (PFS) rates of RFA for pulmonary metastases from HCC were 59.7 and 28.2% (16). Jo et al. depicted that the 1-year PFS of helical tomotherapy for pulmonary oligometastases from hepatocellular carcinoma was 22.4%, and the median PFS was 4.9 months (17).

Hiraki et al. (29) retrospectively analyzed the results of percutaneous radiofrequency ablation for pulmonary metastases from hepatocellular carcinoma. They demonstrated that the 1- and 3-year overall survival rates were 87 and 57%, respectively, and the median survival time was 37.7 months. Another study using RFA for 26 patients with pulmonary metastases from HCC reported OS rates that were 88.5% at 1 year and 69.8% at 36 months (30). In this study, the 1- and 3-year OS rates were 75 and 26% for thermal ablation and 77 and 37% for helical tomotherapy. The OS rates of the previous research were higher than in our study. The possible explanations were that the present study included more patients, and the tumor diameters were larger than in the above-mentioned studies. A multicenter study examined the clinical outcomes of hypofractionated radiotherapy for pulmonary metastases from HCC and showed that the median OS was 16.3 months and the 1-year OS rate was 65.5% (17).

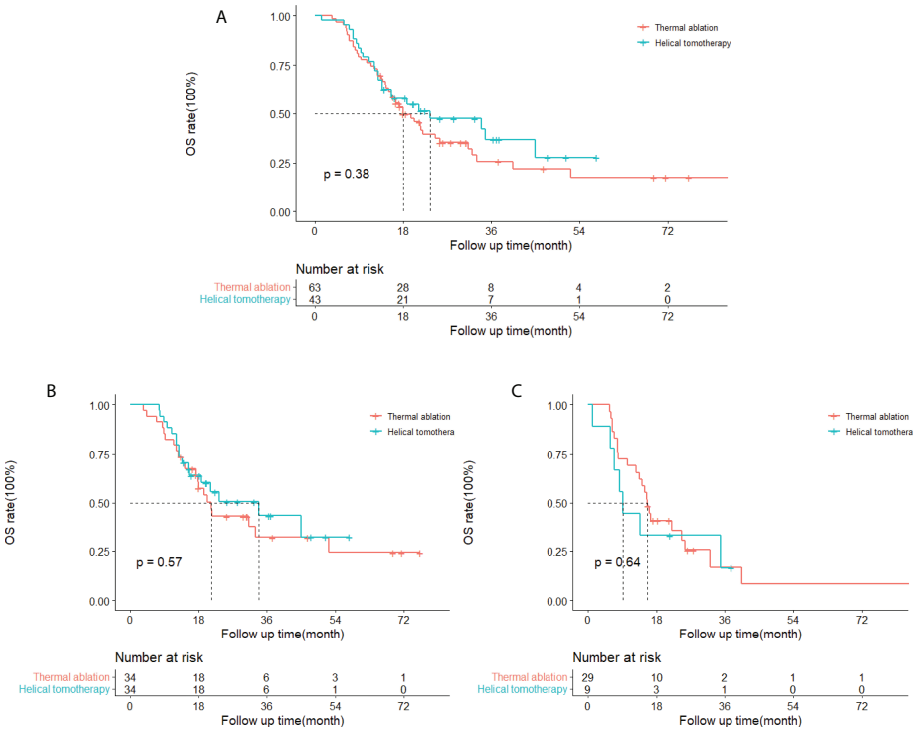

FIGURE 3
Kaplan–Meier curves of overall survival (OS) in patients with pulmonary metastases from hepatocellular carcinoma who underwent thermal ablation or helical tomotherapy. **(A)** Whole study population (thermal ablation group: *n* = 63, median OS = 18.0 months; helical tomotherapy group: *n* = 43, median OS = 23.4 months; *P* = 0.38). **(B)** Patients with low α-fetoprotein (AFP) level (AFP <400 ng/ml) (thermal ablation group: *n* = 34, median OS = 21.4 months; helical tomotherapy group: *n* = 34, median OS = 33.9 months; *P* = 0.57). **(C)** Patients with high AFP level (AFP≥400 ng/ml) (thermal ablation group: *n* = 29, median OS = 15.6 months; helical tomotherapy group: *n* = 9, median OS = 9.3 months; *P* = 0.64).

Natsuizaka et al. (31) investigated the prognostic factors for patients with extrahepatic metastases HCC and found that Child–Pugh class, metastasis to multiple extrahepatic organs, and serum AFP level were prognostic factors. Hiraki et al. (29) indicated that no viable intrahepatic recurrence, no liver cirrhosis, Child–Pugh A class, and serum AFP level lower than 10 ng/ml were associated with better survival for patients with pulmonary metastases from HCC undergoing percutaneous RFA. However, Kwon et al. (32) investigated patients with HCC accepting pulmonary metastasectomy and found that there were no independent prognostic factors. The present study found that survival after thermal ablation or helical tomotherapy of pulmonary metastases mainly relied on the tumor number and the serum AFP level. Patients with pulmonary metastases more than three (HR: 2.112, 95%CI: 1.153–3.868, *P* = 0.016) or a serum AFP level higher than 400 ng/ml (HR:1.933, 95%CI: 1.169–3.196, *P* = 0.010) correlated with poorer overall survival. Serum AFP level was also associated with LTPFS, with a higher AFP level (HR: 2.126, 95%CI: 1.298–3.482, *P* = 0.003) correlated with worse LTPFS. In addition, the subgroup analyses showed that thermal ablation and helical tomotherapy achieved similar OS in the low-AFP-level and the high-AFP-level groups, suggesting that these two treatments could acquire comparable outcomes.

The incidence of major complications was 0–25% (16, 28–30) in the thermal ablation group, most of which were pneumothorax requiring chest tube placement, and 0–12.1% (17, 33, 34) in the helical tomotherapy group. Ochiai et al. (34) compared the results of RFA and SBRT in solitary lung tumors and reported similar major complication rates for both groups (*P* > 0.999). The present study results were consistent with previous studies.

There are some limitations of this study. First, its retrospective nature was an important limitation. Some patients in this study lacked pathological confirmation and were diagnosed with clinical evidence, including radiological performance and serum AFP level, which the second limitation. Third, the sample size of this study was small, restricting the statistical power of the present study.

In conclusion, thermal ablation and helical tomotherapy provided similar local tumor progression-free survival and overall survival for pulmonary metastases from hepatocellular carcinoma with equal safety.

TABLE 3 Univariate and multivariate analyses of prognostic factors for overall survival.

	Univariate model		Multivariate model	
	HR (95%CI)	*P*	HR (95%CI)	*P*[a]
Gender				
Female				
Male	1.124 (0.449–2.816)	0.803		
Age (years)				
<60				
≥60	1.281 (0.781–2.103)	0.327		
Treatment of pulmonary metastatic tumors				
Thermal ablation				
Radiotherapy	0.800 (0.485–1.320)	0.382		
Lung metastasis				
Metachronous				
Synchronous	0.343 (0.047–2.484)	0.290		
History of previous pulmonary surgery				
No				
Yes	2.139 (0.768–5.955)	0.145		
Maximum tumor diameter (mm)				
<10				
≥10	1.321 (0.707–2.470)	0.383		
Tumor number				
≤3				
>3	2.602 (1.555–4.354)	<0.001	2.112 (1.153–3.868)	**0.016**
Distribution of pulmonary metastatic tumors				
Unilateral				
Bilateral	2.031 (1.190–3.467)	0.009	1.475 (0.779–2.795)	0.233
Extrapulmonary metastasis				
No				
Yes	1.775 (0.923–3.412)	0.085	1.828 (0.942–3.549)	0.074
Child–Pugh grade				
A				
B	1.400 (0.714–2.746)	0.327		
AFP (ng/ml)				
<400				
≥400	1.845 (1.135–3.000)	0.014	1.933 (1.169–3.196)	**0.010**

AFP, α-fetoprotein. [a]Cox regression was used.
The bold value is statistically significant with $p < 0.05$.

TABLE 4 Adverse events for two groups.

	Grade 2 AE	Grade 1 AE
Thermal ablation		
Pneumothorax	2	16
Pleural effusion	1	23
Pneumonitis	0	2
Total	3	41
Radiotherapy		
Radiation pneumonitis	2	0
Total	2	0

AE, adverse event.

Data availability statement

The original contributions presented in the study are included in the article/supplementary material. Further inquiries can be directed to the corresponding authors.

Ethics statement

The studies involving human participants were reviewed and approved by the Institutional Review Boards of the Zhongshan Hospital, Fudan University. Written informed consent for

participation was not required for this study in accordance with the national legislation and the institutional requirements.

Author contributions

LL and JH conceived and designed the project. ZY and ZZ provided administrative support. FW, SF, QS, and DZ collected the data. FW, SF, QS, and HyS analyzed and interpreted the data. All authors contributed to the article and approved the submitted version.

Funding

This study has received funding from the Shanghai Municipal Health Commission (no. 201940409).

Conflict of interest

The authors declare that the research was conducted in the absence of any commercial or financial relationships that could be construed as a potential conflict of interest.

Publisher's note

References

1. An X, Li F, Mou C, Li D. A systematic review and meta-analysis on prognosis and survival of hepatocellular carcinoma with lung metastasis after hepatectomy. *Ann Palliat Med* (2021) 10(8):9039–48. doi: 10.21037/apm-21-1784

2. Reig M, Forner A, Rimola J, Ferrer-Fàbrega J, Burrel M, Garcia-Criado Á, et al. BCLC strategy for prognosis prediction and treatment recommendation: The 2022 update. *J Hepatol* (2022) 76(3):681–93. doi: 10.1016/j.jhep.2021.11.018

3. Sohn W, Paik YH, Cho JY, Lim HY, Ahn JM, Sinn DH, et al. Sorafenib therapy for hepatocellular carcinoma with extrahepatic spread: Treatment outcome and prognostic factors. *J Hepatol* (2015) 62(5):1112–21. doi: 10.1016/j.jhep.2014.12.009

4. Chen J, Lu S, Zhang Y, Xu L, Chen J, Wang J, et al. Sorafenib monotherapy versus sorafenib combined with regional therapies for hepatocellular carcinoma patients with pulmonary oligometastases: A propensity score-matched analysis. *J Cancer* (2018) 9(10):1745–53. doi: 10.7150/jca.24568

5. Yau T, Chan P, Ng KK, Chok SH, Cheung TT, Fan ST, et al. Phase 2 open-label study of single-agent sorafenib in treating advanced hepatocellular carcinoma in a hepatitis b-endemic Asian population: Presence of lung metastasis predicts poor response. *Cancer* (2009) 115(2):428–36. doi: 10.1002/cncr.24029

6. Antonoff MB. The roles of surgery, stereotactic radiation, and ablation for treatment of pulmonary metastases. *J Thorac Cardiovasc Surg* (2022) 163(2):495–502. doi: 10.1016/j.jtcvs.2021.01.143

7. Zabaleta J, Iida T, Falcoz PE, Salah S, Jarabo JR, Correa AM, et al. Individual data meta-analysis for the study of survival after pulmonary metastasectomy in colorectal cancer patients: A history of resected liver metastases worsens the prognosis. *Eur J Surg Oncol* (2018) 44(7):1006–12. doi: 10.1016/j.ejso.2018.03.011

8. Han KN, Kim YT, Yoon JH, Suh KS, Song JY, Kang CH, et al. Role of surgical resection for pulmonary metastasis of hepatocellular carcinoma. *Lung Cancer* (2010) 70(3):295–300. doi: 10.1016/j.lungcan.2010.02.014

9. Yano T, Shoji F, Maehara Y. Current status of pulmonary metastasectomy from primary epithelial tumors. *Surg Today* (2009) 39(2):91–7. doi: 10.1007/s00595-008-3820-9

10. Boyer MJ, Ricardi U, Ball D, Salama JK. Ablative approaches for pulmonary metastases. *Thorac Surg Clin* (2016) 26(1):19–34. doi: 10.1016/j.thorsurg.2015.09.004

11. Xiang ZW. Progress in the treatment of pulmonary metastases after liver transplantation for hepatocellular carcinoma. *World J Hepatol* (2015) 7(20):2309. doi: 10.4254/wjh.v7.i20.2309

12. Liu BD, Ye X, Fan WJ, Li XG, Feng WJ, Lu Q, et al. Expert consensus on image-guided radiofrequency ablation of pulmonary tumors: 2018 edition: Expert consensus on RFA. *Thorac Cancer* (2018) 9(9):1194–208. doi: 10.1111/1759-7714.12817

13. Ye X, Fan W, Wang H, Wang J, Wang Z, Gu S, et al. Expert consensus workshop report: Guidelines for thermal ablation of primary and metastatic lung tumors (2018 edition). *J Cancer Res Ther* (2018) 14(4):730. doi: 10.4103/jcrt.JCRT_221_18

14. Zhou J, Sun H, Wang Z, Cong W, Wang J, Zeng M, et al. Guidelines for the diagnosis and treatment of hepatocellular carcinoma (2019 edition). *Liver Cancer* (2020) 9(6):682–720. doi: 10.1159/000509424

15. Uhlig J, Mehta S, Case MD, Dhanasopon A, Blasberg J, Homer RJ, et al. Effectiveness of thermal ablation and stereotactic radiotherapy based on stage I lung cancer histology. *J Vasc Interv Radiol* (2021) 32(7):1022–28.e4. doi: 10.1016/j.jvir.2021.02.025

16. Li X, Wang J, Li W, Huang Z, Fan W, Chen Y, et al. Percutaneous CT-guided radiofrequency ablation for unresectable hepatocellular carcinoma pulmonary metastases. *Int J Hyperthermia* (2012) 28(8):721–8. doi: 10.3109/02656736.2012.736669

17. Jo IY, Park HC, Kim ES, Yeo SG, Kim M, Seong J, et al. Stereotactic ablative radiotherapy for pulmonary oligometastases from primary hepatocellular carcinoma: a multicenter and retrospective analysis (KROG 17-08). *Jpn J Clin Oncol* (2022) 52(6):616–22. doi: 10.1093/jjco/hyac028

18. de Baère T, Aupérin A, Deschamps F, Chevallier P, Gaubert Y, Boige V, et al. Radiofrequency ablation is a valid treatment option for lung metastases: experience in 566 patients with 1037 metastases. *Ann Oncol* (2015) 26(5):987–91. doi: 10.1093/annonc/mdv037

19. Vogl TJ, Naguib NNN, Gruber-Rouh T, Koitka K, Lehnert T, Nour-Eldin NEA. Microwave ablation therapy: Clinical utility in treatment of pulmonary metastases. *Radiology* (2011) 261(2):643–51. doi: 10.1148/radiol.11101643

20. Welsh JS, Patel RR, Ritter MA, Harari PM, Mackie TR, Mehta MP. Helical tomotherapy: An innovative technology and approach to radiation therapy. *Technol Cancer Res Treat* (2002) 1(4):311–6. doi: 10.1177/153303460200100413

21. Ling-ling M, Lin-chun F, Yun-lai W, Xiang-kun D, Chuan-bin X. Dosimetric comparison between helical tomotherapy and intensity-modulated radiation therapy plans for non-small cell lung cancer. *Chin Med J (Engl)* (2011) 124(11):1667–71. doi: 10.3760/cma.j.issn.0366-6999.2011.11.012

22. Lin G, Xiao H, Zeng Z, Xu Z, He J, Sun T, et al. Constraints for symptomatic radiation pneumonitis of helical tomotherapy hypofractionated simultaneous multitarget radiotherapy for pulmonary metastasis from hepatocellular carcinoma. *Radiother Oncol* (2017) 123(2):246–50. doi: 10.1016/j.radonc.2017.02.015

23. He J, Huang Y, Chen Y, Shi S, Ye L, Hu Y, et al. Feasibility and efficacy of helical intensity-modulated radiotherapy for stage III non-small cell lung cancer in comparison with conventionally fractionated 3D-CRT. *J Thorac Dis* (2016) 8(5):862–71. doi: 10.21037/jtd.2016.03.46

24. Chi A, Jang SY, Welsh JS, Nguyen NP, Ong E, Gobar L, et al. Feasibility of helical tomotherapy in stereotactic body radiation therapy for centrally located early stage Non–Small-cell lung cancer or lung metastases. *Int J Radiat Oncol* (2011) 81(3):856–62. doi: 10.1016/j.ijrobp.2010.11.051

25. Shi S, Zeng Z, Ye L, Huang Y, He J. Risk factors associated with symptomatic radiation pneumonitis after stereotactic body radiation therapy for stage I non–small cell lung cancer. *Technol Cancer Res Treat* (2017) 16(3):316–20. doi: 10.1177/1533034616661665

26. Nagai A, Shibamoto Y, Yoshida M, Inoda K, Kikuchi Y. Safety and efficacy of intensity-modulated stereotactic body radiotherapy using helical tomotherapy for lung cancer and lung metastasis. *BioMed Res Int* (2014) 2014:1–8. doi: 10.1155/2014/473173

27. Sun T, He J, Zhang S, Sun J, Zeng M, Zeng Z. Simultaneous multitarget radiotherapy using helical tomotherapy and its combination with sorafenib for pulmonary metastases from hepatocellular carcinoma. *Oncotarget* (2016) 7 (30):48586–99. doi: 10.18632/oncotarget.9374

28. Zhuhui Y, Liu B, Hu C, Li Z, Zheng J, Li W. Clinical outcomes of percutaneous thermal ablation for pulmonary metastases from hepatocellular carcinoma: a retrospective study. *Int J Hyperthermia* (2020) 37(1):651–9. doi: 10.1080/02656736.2020.1775899

29. Hiraki T, Yamakado K, Ikeda O, Matsuoka T, Kaminou T, Yamagami T, et al. Percutaneous radiofrequency ablation for pulmonary metastases from hepatocellular carcinoma: Results of a multicenter study in Japan. *J Vasc Interv Radiol* (2011) 22(6):741–8. doi: 10.1016/j.jvir.2011.02.030

30. Lassandro G, Picchi SG, Bianco A, Di Costanzo G, Coppola A, Ierardi AM, et al. Effectiveness and safety in radiofrequency ablation of pulmonary metastases from HCC: a five years study. *Med Oncol* (2020) 37(4):25. doi: 10.1007/s12032-020-01352-2

31. Natsuizaka M, Omura T, Akaike T, Kuwata Y, Yamazaki K, Sato T, et al. Clinical features of hepatocellular carcinoma with extrahepatic metastases. *J Gastroenterol Hepatol* (2005) 20(11):1781–7. doi: 10.1111/j.1440-1746.2005.03919.x

32. Kwon JB, Park K, Kim YD, Seo JH, Moon SW, Cho DG, et al. Clinical outcome after pulmonary metastasectomy from primary hepatocellular carcinoma: Analysis of prognostic factors. *World J Gastroenterol* (2008) 14(37):5717. doi: 10.3748/wjg.14.5717

33. He J, Huang Y, Shi S, Hu Y, Zeng Z. Comparison of effects between central and peripheral stage I lung cancer using image-guided stereotactic body radiotherapy *via* helical tomotherapy. *Technol Cancer Res Treat* (2015) 14 (6):701–7. doi: 10.1177/1533034615583206

34. Ochiai S, Yamakado K, Kodama H, Nomoto Y, Ii N, Takaki H, et al. Comparison of therapeutic results from radiofrequency ablation and stereotactic body radiotherapy in solitary lung tumors measuring 5 cm or smaller. *Int J Clin Oncol* (2015) 20(3):499–507. doi: 10.1007/s10147-014-0741-z

frontiers | Frontiers in Oncology

TYPE Original Research
PUBLISHED 22 August 2022
DOI 10.3389/fonc.2022.976777

OPEN ACCESS

EDITED BY
Xin Ye,
Qianfoshan Hospital, Shandong University, China

REVIEWED BY
Nan Wang,
Qianfoshan Hospital, Shandong University, China
Zhengyu Lin,
First Affiliated Hospital of Fujian Medical University, China

*CORRESPONDENCE
Hai-Liang Li
lihailianggy@163.com

†These authors have contributed equally to this work and share first authorship

SPECIALTY SECTION
This article was submitted to Thoracic Oncology, a section of the journal Frontiers in Oncology

RECEIVED 23 June 2022
ACCEPTED 11 July 2022
PUBLISHED 22 August 2022

CITATION
Hu H-T, Zhao X-H, Guo C-Y, Yao Q-J, Geng X, Zhu W-B, Li H-L, Fan W-J and Li H-L (2022) Local ablation of pulmonary malignancies abutting pleura: Evaluation of midterm local efficacy and safety.
Front. Oncol. 12:976777.
doi: 10.3389/fonc.2022.976777

Local ablation of pulmonary malignancies abutting pleura: Evaluation of midterm local efficacy and safety

Hong-Tao Hu[1†], Xiao-Hui Zhao[1†], Chen-Yang Guo[1], Quan-Jun Yao[1], Xiang Geng[1], Wen-Bo Zhu[1], Hong-Le Li[2], Wei-Jun Fan[3] and Hai-Liang Li[1*]

[1]Department of Minimal-Invasive Intervention, the Affiliated Cancer Hospital of Zhengzhou University & Henan Cancer Hospital, Zhengzhou, China, [2]The Affiliated Cancer Hospital of Zhengzhou University & Henan Cancer Hospital, Zhengzhou, China, [3]Department of Minimally Invasive Interventional Therapy, Sun Yat-Sen University Cancer Center, Guangzhou, China

Objective: To retrospectively evaluate the efficacy and safety of local ablation treatment for adjacent pleural lung tumors.

Materials and methods: Sixty-two patients who underwent pulmonary nodule ablation at the Affiliated Cancer Hospital of Zhengzhou University were enrolled between January 2016 and December 2020. All patients were followed up with enhanced computed tomography or magnetic resonance imaging within 48 h after treatment and 2, 4, 6, 9, and 12 months after treatment. All patients were followed for at least 12 months.

Results: A total of 84 targeted tumors (62 patients) underwent 94 ablations. In the 12-month follow-up images, 69 of the 84 targeted tumors were completely ablated, 15 had incomplete ablation, and the 12-month incomplete ablation rate was 17.8% (15/84). Of the 15 incompletely ablated tumors, six had partial responses, five had stable disease, and four had progressive disease. The most common adverse event was pneumothorax, with an incidence of 54.8% (34/62). The second most common complication was pleural effusion, with an incidence rate of 41.9% (26/62). The incidence of needle-tract bleeding was 21% (13/62) and all patients were cured using hemostatic drugs. Serious complications were bronchopleural fistula in four patients (6.5%, 4/62) and needle tract metastasis in one patient. Four cases of bronchopleural fistula were found in the early stages and were cured after symptomatic treatment.

Conclusion: Local ablation is effective for the treatment of adjacent pleural lung tumors, and its operation is safe and controllable.

KEYWORDS

lung malignancies, microwave ablation, radiofrequency ablation, pleura, cryoablation

Introduction

According to statistics from the American Cancer Society, lung cancer is the leading cause of cancer death in the United States, with approximately 350 people dying of lung cancer every day (1). With societal development and the aggravation of air pollution in developing countries, the incidence of lung malignancies is on the rise (2). Surgical resection has always been the main treatment for patients with early non-small cell lung cancer and some patients with pulmonary metastatic diseases (3, 4). However, more than 20% of patients with early non-small cell lung cancer are not suitable for surgery because of various factors (such as old age, severe lung function impairment, or other complications) (3). The standard local treatment option for these inoperable patients is stereotactic body radiotherapy (SBRT), which has a local control rate of 90% for early lung cancer and has achieved an effect similar to that of surgery (5, 6).

In recent years, image-guided local ablation has been rapidly developed as an alternative to radiotherapy, including radiofrequency ablation (RFA), microwave ablation (MWA), and cryoablation. Compared with SBRT, local ablation also has a good local control rate for inoperable early lung cancer (7–9). Many studies have reported the use of ablation in the treatment of early non-small cell lung cancer and oligometastatic lung cancer (10–12), but there are few reports on the ablation of adjacent pleural lung cancer or pulmonary metastases. The development of its efficacy and complications have not been discussed in depth. The purpose of this study was to retrospectively evaluate the local efficacy and safety of local ablation in the treatment of adjacent pleural lung tumors.

Materials and methods

Patients and admission criteria

Before conducting this retrospective study, we obtained approval from the ethics committee of the Affiliated Cancer Hospital of Zhengzhou University. All patients in the study received ablation treatment for lung tumors in our hospital and signed a written informed consent form for ablation treatment prior to the treatment. From January 2016 to December 2020, 522 patients with concurrent local ablation of pulmonary malignancies were admitted to our department, including 306 patients who underwent local radical ablation and 62 patients who met the criteria of this study. The inclusion criteria for this study were as follows: (A) the patient's lung lesion was histologically diagnosed as a malignant tumor; (B) if the lung lesion was a primary tumor, it must be non-small-cell lung cancer; (C) because of personal reasons, the patient was unsuitable for surgical treatment (such as insufficient cardiopulmonary function reserve) or unwilling to undergo surgical resection; (D) the number of lesions in patients was ≤3 and confined to one side of the lung, and the maximum diameter of a single tumor was ≤30 mm; (E) the patient had at least one lesion located ≤5 mm away from the pleura; and (F) if the intrapulmonary lesion was a metastatic tumor, it should be stable for at least 3 months after systemic treatment, with no new metastatic lesion in the lung. The exclusion criteria were as follows: (A) the primary malignant tumor was not effectively controlled; (B) primary lung cancer was accompanied by extrapulmonary metastasis or spread; (C) there were multiple lesions on both sides of the lung; (D) the maximum diameter of a single tumor was >30 mm; (E) imaging indicated mediastinal lymph node metastasis or had invaded the chest wall or mediastinum; and (F) severe coagulation dysfunction, systemic infection, thrombocytopenia, or other conditions unsuitable for lung tumor ablation.

Pre-treatment examination and planning

All patients underwent comprehensive imaging and laboratory examinations prior to local ablation. This included chest enhanced computed tomography (CT) or magnetic resonance imaging (MRI), as well as complete blood count and coagulation indices in laboratory examinations, including bleeding time, partial thromboplastin time, and international normalized ratio. The patients stopped using anticoagulants or antiplatelet drugs within 3 days to 1 week before surgery, and the coagulation function was rechecked the day before surgery to ensure that it was within the normal range. Before the surgery, two associate professors jointly planned the patient's position and puncture path according to the location and number of tumors. Prophylactic antibiotics were not routinely administered.

Ablation procedure

Local ablation was performed by three interventional physicians under sterile conditions in the CT room (HL.L, CY.G, and HT.H, with 20, 20, and 15 years of experience in lung tumor ablation, respectively). Twenty patients were treated under general anesthesia and 42 patients were treated with local anesthesia combined with analgesia. A GE large-hole CT machine was used (the scanning parameters were 30 mAs, 120 kV, and 5 mm thickness), and electrocardiogram (ECG) monitoring was used during the entire process. According to the preoperative planned body position and needle insertion path, the patients were asked to lie on their back, prone, or side on the CT workbench. After scanning and positioning, the needle insertion path was confirmed (Figure 1A). After disinfection, a predetermined ablation equipment electrode was used to insert the lesion location according to the

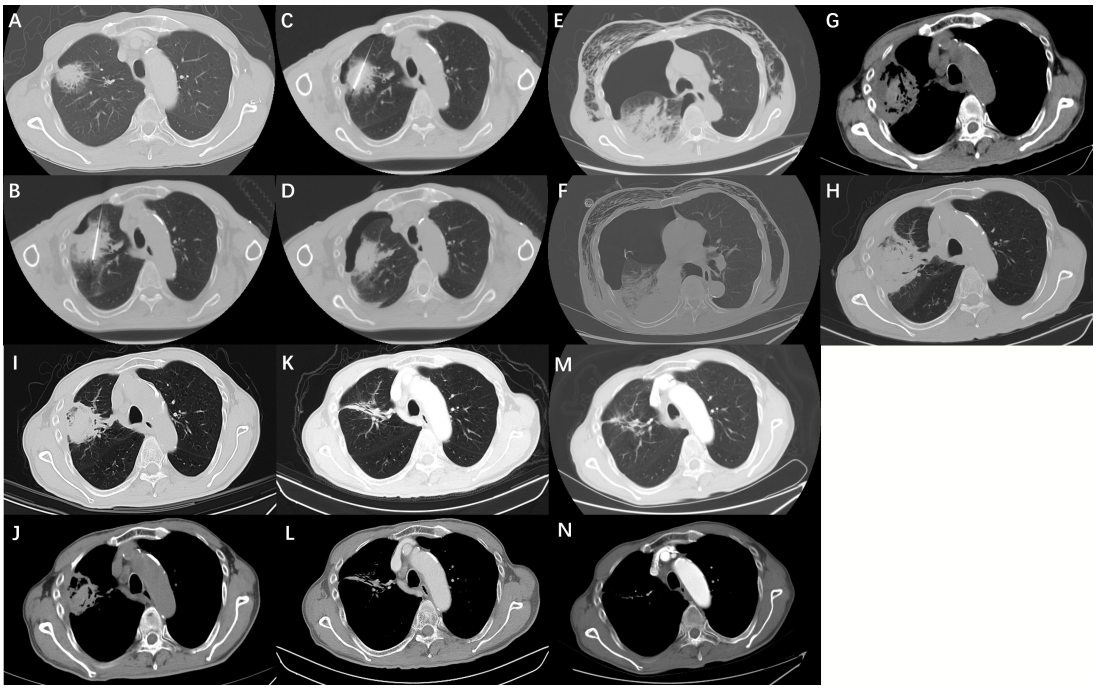

FIGURE 1
(A) A 69-year-old male presented with a tumor in the right upper lobe of his lung. **(B, C)** The biopsy specimen was diagnosed as lung adenocarcinoma. Lung function is poor owing to emphysema and cannot be surgically removed. Radiofrequency ablation was performed at our department. **(D)** After ablation was completed, the computed tomography scan showed a small amount of pneumothorax in the right upper lung. The patient had no symptoms of chest tightness or discomfort and no related treatment was performed. **(E)** The day after the ablation of the lung cancer, the patient complained of fever, chest tightness, and subcutaneous emphysema, and a computed tomography (CT) scan showed increased pneumothorax with subcutaneous emphysema and pleural effusion. **(F)** Considering that the patient had a bronchopleural fistula, a pleural drainage was performed using a 10F pigtail catheter, and anti-infective therapy was given. Ten days after continuous chest drainage combined with anti-infective therapy, the patient's chest tightness and fever disappeared completely. **(G, H)** A repeat CT scan showed that the pneumothorax and pleural effusion had completely disappeared, and the original lung tumor showed extensive necrosis. The patient recovered and was discharged from the hospital. **(I, J)** The CT scan of the patient 2 months after discharge showed that the extent of tumor ablation was smaller than before, and the contrast-enhanced CT examination 1 year after ablation showed that the necrotic tumor was absorbed, showing a cord shadow **(K, L)**. **(M, N)** Contrast-enhanced CT 2 years after ablation showed that the original residual cable shadow was further absorbed and reduced.

designed best path (Figures 1B, C). Argon-helium knife ablation was started with all the focal electrodes in place (if there were multiple or large lesions), MWA and RFA was performed successively using a single lesion (if there were multiple lesions), and all tumors on one side of the lung were ablated at one time without serious complications. All ablation procedures were performed in accordance with the recommendations of the equipment manufacturer, and the ablation range was beyond 5 mm on both sides of the tumor to ensure an adequate range of ablation safety. CT scans were used during ablation to assess the adequacy of the ablation range and monitor related complications. If ablation complications occurred, treatment termination was decided according to the severity of the event and the degree of intervention required. Because all tumors in this study were adjacent to the pleura, after treatment, the electrode was removed without any coagulation of the needle track. A CT scan was performed immediately to confirm the ablation range and presence of complications (Figure 1D). If any complications occurred, corresponding measures were performed. If there were no complications or treatments, the puncture point was disinfected again and covered with an application. The patients underwent continuous ECG monitoring for 12 h after returning to the ward.

Follow-up after ablation

A chest CT scan was performed within 48 h after treatment to determine if there were delayed complications, such as delayed pneumothorax (Figures 1E, F) and bleeding. CT or MRI follow-up studies were performed at 2, 4, 6, 9, 12, and 18 months after discharge to evaluate efficacy and complications (Figures 1G–N). The follow-up CT or MRI scan scheme was plain scanning plus multiphase enhancement. The postoperative CT images were evaluated by two senior doctors (JC.X and QJ.Y, with 20 and 15 years of experience, respectively) who were not

involved in the ablation surgery. The shortest follow-up period for patients in this study was 12 months. Complete ablation of the tumor was confirmed by enhancing the enhanced signs of CT or MRI. Irregular focal soft tissue enhancement was considered to be a sign of residue or recurrence. An annular thin-wall symmetric reinforcement of <5 mm was observed 6 months after ablation, which was considered a sign of enhancement of peripheral normal tissue after complete ablation of the tumor (13, 14). A review revealed residual or enlarged focal soft tissue enhancement lesions that were considered as lesions with incomplete primary ablation from 1 to 12 months after the initial ablation (14). The lesions were ablated again, after excluding tumor diffusion or metastasis. The method and process of ablation were the same as those described above.

Study end point

The main endpoints of this study were single complete ablation rate and complications. The single complete ablation rate was defined as the absence of tumor recurrence within 12 months after the first local ablation. Adverse reactions were evaluated according to the expert consensus for image-guided RFA of pulmonary tumors (2015 version) (14).

Statistical methods

The Shapiro-Wilk test was used to determine the normality of the quantitative data. Continuous numerical variables of normal distribution are expressed as mean ± standard deviation, and continuous numerical variables that do not conform to normal distribution are described by the median and interquartile range. Count data are expressed as percentages. All statistical analyses were performed using SPSS software (version 23.0; SPSS, Chicago, IL, USA).

Results

Patients and tumors

By December 2020, 62 patients were enrolled, including 41 males and 21 females, with a mean age of 59.76 ± 13.94 years. Among the 62 patients with lung tumors, 28 had lung cancer (seven cases of squamous cell carcinoma and 21 cases of adenocarcinoma). There were 34 cases of lung metastasis, including 24 cases of rectal cancer, five cases of liver cancer, and five cases of mammary cancer (Table 1). There were 84 lesions were near the pleura (31 subpleural tumors of lung cancer and 53 subpleural tumors of lung metastases). There were 81 lesions in the costopleura and 13 in the diaphragmatic pleura. Among them, 12 lesions were ablated with argon-helium knife (eight patients), 14 lesions with MWA (10 patients), and 58 lesions with RFA (44 patients).

TABLE 1 Baseline characteristics of the study patients.

Characteristics	Number of cases N = 62	Number of lesions N = 84
Gender, No. (%)		
Male	41 (66.13%)	–
Female	21 (33.87%)	–
Age (years), mean ± SD	59.76 ± 13.94	–
Tumor size(mm)*, median (IQR)	19.00(16.00-25.00)	
Primary tumor site, No. (%)		
Lung		
Squamous	7 (11.29%)	8 (9.52%)
Adenocarcinoma	21 (33.87)%	23 (38.10%)
Colorectal	24 (38.71%)	36 (42.86%)
Breast	5 (8.06%)	8 (9.52%)
Live	5 (8.06%)	9 (10.71%)
Treatment		
RFA	44 (70.97%)	58 (69.05%)
MWA	10 (16.13%)	14 (16.67%)
Argon-helium knife	8 (12.90%)	12 (14.29%)

*Multiple lesions in the lung were treated by ablation one by one, and the largest diameter of each lesion was counted here.RFA, radiofrequency ablation; MWA, microwave ablation.

Treatment and follow-up

The 84 lung lesions that were observed in the 62 patients with malignant lung tumors were successfully ablated. Intraoperative CT showed that all tumors were covered by the ablation range, and the technical success rate was 100%. As of December 31, 2021, all patients were followed up using enhanced CT or MRI after local ablation and completed at least 12 months of follow-up. For patients with suspected tumor edge activity on CT images, enhanced MRI were added to further evaluate tumor activity. During the follow-up period, 54 of 62 patients achieved complete ablation (two patients underwent ablation twice), and 69 of 84 targeted tumors were ablated completely. Even after two ablations (eight patients), 15 target lesions showed tumor residue, recurrence, or progression during the follow-up period. The 12-month follow-up showed that the complete ablation rate of all lesions was 82.1% (69/84) and the 12-month complete response (CR) rate of 62 patients was 87.0% (54/62). Of the eight patients with lung tumor progression after local ablation, six received systemic chemotherapy combined with radiotherapy, and two received systemic chemotherapy. As of the last follow-up, among the 54 patients who achieved complete ablation within 12 months, four

10.3389/fonc.2022.976777

TABLE 2 12-month complete ablation rates and follow-up.

Follow-up	Complete ablation		Incomplete ablation	
	Number of cases	Number of lesions	Number of cases	Number of lesions
12-month ablation rate	87.10%	82.1%	12.90%	17.86%
Treatment				
RFA	38/44	49/58	6/44	9/58
MWA	9/10	11/14	1/10	3/14
Argon-helium knife	7/8	9/12	1/8	3/12
Treatment after progression				
Systemic chemotherapy	*		2	
Systemic chemotherapy + radiotherapy	*		6	
Condition assessment				
Stable condition	47		2	
Disease progression	7		4	
Death	0		2	

*Since complete ablation was achieved, no other treatments were performed during the follow-up period.

patients had new intrapulmonary tumors and three had distant metastasis. Among the eight patients with incomplete ablation, four patients had tumor progression, two were stable, and two died due to multiple organ failure (Table 2). Due to the large number of pulmonary metastases cases (54.8%, 34/62) in this study, these patients received other anticancer therapies after disease progression, so the overall survival was not analyzed in this study.

Complications

No ablation-related deaths occurred during ablation or within 30 days of treatment. The most common complication was pneumothorax, with an incidence of 54.8% (34/62), but only eight patients required fine tube drainage, and no patients needed surgical incision and drainage. Another common complication was pleural effusion formation, with an incidence of 41.9% (26/62), and 16 patients required catheter drainage of pleural effusion. The complications of local ablation included pain, postoperative syndrome, bleeding, coughing, and pleural reactions (Table 3). Of the 62 patients treated with local ablation, 20 (31.8%, 20/62) experienced intraoperative or postoperative pain, including 17 cases of mild pain without intervention and three cases of moderate and severe pain requiring drug treatment. However, all symptoms were relieved within 3-5 days after treatment. Postoperative syndromes, including low fever (<38.5°C), nausea, vomiting, and general malaise, occurred in 12 cases (22.7%, 12/62). Coughing was also a common complication in nine cases (19.7%, 9/62), including six mild and three severe cases of coughing. The incidence of needle bleeding was 21% (13/62), and all patients were cured by hemostatic drug infusions. The most serious complications were bronchopleural fistula in four patients (6.5%, 4/62) and needle track implantation in one patient. There were no other serious complications such as thoracic hemorrhage, phrenic

TABLE 3 Incidences of complications and associated factors.

Characteristics	Postoperative syndrome	Pain (Mid/moderate to severe)	Cough (Mild to moderate/severe)	Pneumothorax	Pleural effusion	Bleeding	Bronchopleural fistula
Total	12 (19.35%)	20 (17/3)	9 (6/3)	34 (54.8%)	26 (41.9%)	13 (21.0%)	3 (4.8%)
Treatment							
RFA	10	19(16/3)	8 (6/2)	31	25	10	2
MWA	1	0	1 (0/1)	2	0	2	1
Argon-helium knife	1	1 (1/0)	0	1	1	1	0
Primary tumor site							
Lung	4	10 (8/2)	5 (3/2)	16	12	6	1
Colorectal	6	9 (8/1)	4 (3/1)	14	13	5	2
Live	1	1 (1/0)	0	2	1	1	0
Breast	1	0	0	2	0	1	0

nerve injury, or air embolism. Four cases of bronchopleural fistula were found early, and they were cured after intrathoracic intubation and anti-infective treatment (Figures 1E–H). One patient was found to have needle tract implantation during the 3-month follow-up and was cured by the second ablation. Two patients had a cavity in the target tumor area on CT 2 months later. During the follow-up period, the cavity was gradually reduced and absorbed in one case, and there was no change in the other case. There were no signs of residual tumor activity or recurrence in these two patients.

Discussion

Some patients with early lung cancer or oligometastatic lung cancer cannot tolerate surgical resection because of their old age and/or poor cardiopulmonary function. In addition, some patients had previously undergone surgery at other sites and were unwilling to undergo surgical resection again. Therefore, image-guided percutaneous puncture and ablation, such as RFA, MWA, and cryoablation, is an alternative to surgery with the advantages of fewer complications, less trauma, good tolerance, high repeatability, and rapid recovery (15–17).

Although lung tumor ablation has been considered an alternative therapy for unresectable early lung cancer, ablation is still considered high-risk and prone to recurrence for early lung cancer adjacent to the pleura and oligometastatic lung cancer (18). The main reason is that an insufficient safe ablation range can lead to recurrence, and severe pleural injury may lead to bronchopleural fistula (18–19). Second, the ablation treatment for lung tumors is different from that for liver tumors. The lung parenchyma differs from the liver in terms of energy deposition, electrical conductivity, thermal diffusion, and thermal convection (20). The energy required for the treatment of lung tumors is usually lower than that required for the treatment of liver tumors of the same size. Proper control of the ablation range requires further exploration.

Our study showed that the complete ablation rate of tumors at 12 months was 82.1% (69/84), which is lower than the previously reported complete ablation rate of 93% at 18 months (21), and also lower than the 1-year progression-free survival rate of 94.0% reported by Huang et al. (22). The ablation effect may be affected by several factors: a) the tumor is close to the pleura, which limits the operator's ability to expand the scope of ablation; b) the pain caused by ablation of the adjacent pleural tumor under local anesthesia leads to a lack of sufficient ablation time or course of treatment, and may eventually form a residual tumor. Of the eight patients with incomplete ablation in our study, six were ablated under local anesthesia; and c) there are few choices for the puncture needle path near the pleural tumor, and the puncture technique is difficult, which often requires repeated needle adjustment and is prone to pneumothorax. Once pneumothorax occurs, the distance between the tumor and visceral pleura is further reduced, and the pleura is more likely to be damaged during ablation.

Our results showed that the 12-month CR rate in this group was 87%, which is similar to the previously reported 18-month CR rate of 88% (21). This may be due to the high proportion of primary lung cancer in our study (45.2%, 28/62) and only 15% of primary lung cancers, as reported by de Baere et al. (9/60) (22). Thomas et al. (23) reported a complete ablation rate of 73.1% for lung metastatic cancer ablation. The ablation success rate of patients with diameter ≤3 cm was higher than that of patients with diameter >3 cm. In addition, their study indicated that there was no significant interdependency between the histopathological types of metastatic tumors and the ablation effect. Our study also showed that the complete ablation rate of tumors was unrelated to the histopathological type of metastatic tumors. The complete ablation rate of metastatic lung cancer in our study was higher than that previously reported, which may be related to the fact that all tumors in our study were <30 mm, and the number of cases was lower.

Previous studies have shown that the duration of surgery and ablation of the free edge of the tumor are significantly related to the size of the tumor, and the ablation edge beyond the edge of the tumor by at least 5 mm is a key factor in ensuring complete ablation (24, 25). Our study demonstrated that for lung tumors adjacent to the pleura, complete ablation was achieved in most tumors, even if the margin of the tumor was <5 mm away from the pleura. We admit that this is a high rate of complete ablation combined with a high incidence of complications. The high success rate may be due to the following reasons: a) advances in equipment and technology have made the scope of ablation more accurate, ensuring the scope of ablation while minimizing damage to the surrounding tissue; b) multiple intermittent ablations were performed with low power and long time mode, and CT scanning was performed at each ablation interval to determine the ablation range in time to achieve accurate control of the ablation range; and c) for lesions <10 mm, pleural damage can be minimized by puncturing the needle parallel to the pleura adjacent to the tumor and close to the medial edge of the tumor. According to our experience, avoiding vertical pleural puncture of the tumor for ablation can reduce pleural damage. Nevertheless, there were four cases of bronchopleural fistula in this study, with an incidence rate of 6.5%, which was much higher than the 0.2%-0.6% reported in literature (26, 27). This is directly related to the fact that the distance from the lung tumor to the pleura was ≤5 mm in all patients in this study. Although the above methods have been adopted for treatment, the occurrence of bronchopleural fistula cannot be avoided, which shows that the degree of pleural injury caused by ablation is the most important factor affecting this complication.

Although the incidence of bronchopleural fistula is very low, it is difficult to manage, and its long-term presence may lead to more serious complications, such as infection and intractable

pneumothorax. This can be life-threatening, and its treatment is challenging (28). Needle ablation has been reported to be prone to bronchopleural fistula (29); however, needle ablation was not performed in our study. Therefore, pleural injury caused by the ablation procedure is the main cause of bronchopleural fistula formation. Rapid cure of bronchopleural fistula was achieved in four cases in our study. Our team benefited from early diagnosis, early treatment, and localized bronchiolar injury. It has been reported that the presence of bronchopleural fistula should be highly suspected for the persistence of delayed or recurrent pneumothorax because even a large number of pneumothorax cases will disappear quickly after drainage (26, 29–30). In our study, four patients showed no significant improvement after continuous postoperative drainage of pneumothorax and developed pleural effusion. We immediately administered anti-infective treatment and 8F-10F drainage tube placement to strengthen drainage. After 2 weeks, the pneumothorax and pleural effusion disappeared, and the patient was cured. The treatment of tracheopleural fistula in previous reports is very difficult, most of which require multiple surgical methods to perform the intervention (31). The rapid recovery of these four patients by minimally invasive surgery may be related to minor pleural damage because of the small subpleural nodules, which are terminal bronchioles. All these factors promote tracheopleural fistula closure after adequate anti-infective treatment and drainage. However, bronchopleural fistula after ablation of the central tumor may not be closed easily by drainage and anti-infective treatment alone, which requires early surgical intervention. On the other hand, previous studies have shown no significant difference in technical success, technical efficacy, local tumor control, and complications with artificial pneumothorax compared with no artificial pneumothorax (32). Although studies have shown that artificial air/hydrothorax can reduce pain in patients (33), it does not reduce the occurrence of bronchopleural fistula. Therefore, early detection, diagnosis, and treatment are effective treatments for this serious complication.

In this study, three ablation methods were used, mainly RFA, but there was no significant difference between the complete ablation rate, serious complications, and ablation equipment, indicating that as long as the ablation equipment is used correctly, RFA, MWA, or cryoablation can safely complete the ablation of lung tumors near the pleura. In this study, there was a case of needle track implantation caused by poor respiratory coordination under local anesthesia and repeated adjustment of the needle path. For this situation, we believe that there are two ways to reduce needle track implantation. (A) General anesthesia and apnea techniques can be used to improve puncture accuracy, and (B) needle track implantation metastasis could be avoided by sending it into the ablation electrode through the coaxial needle external sheath after coaxial needle puncture to the tumor edge. Further studies are needed to confirm the feasibility of this method.

This study had some limitations. First, the retrospective nature of this study may lead to data bias. Second, the small sample size cannot fully demonstrate the effectiveness of treatment and the incidence of complications. Third, this study used a variety of ablation methods, and the choice of different ablation methods is mainly related to doctors' treatment preferences, patients' choices, and medical insurance policies, which may also lead to biased results. These deficiencies are expected to be addressed through larger sample sizes and multicenter prospective studies in the future.

In short, good results can be achieved by using appropriate ablation methods and techniques for lung tumors near the subpleura, which are not suitable for surgical treatment. Although combined with high complication of tracheopleural fistula, if diagnosed early and if correct treatment is provided, this serious complication can be treated effectively in a short time and related death can be avoided. In the future, the rate of serious complications could decrease owing to the development of technology and equipment.

Data availability statement

The raw data supporting the conclusions of this article will be made available by the authors, without undue reservation.

Ethics statement

The studies involving human participants were reviewed and approved by Ethics Committee of the Affiliated Cancer Hospital of Zhengzhou University. The patients/participants provided their written informed consent to participate in this study. Written informed consent was obtained from the individual(s) for the publication of any potentially identifiable images or data included in this article.

Author contributions

Conception and design: Hai-LL. Patient selection and treatment: H-TH, X-HZ, C-YG, Q-JY, XG, W-BZ. Data collection, analysis and interpretation: H-TH, X-HZ, C-YG, Q-JY, XG. Data interpretation: Hai-LL, H-TH, C-YG, Q-JY. Undertook steering committee activities and critical statistical processing: H-TH, X-HZ. Manuscript writing: Hai-LL, H-TH, X-HZ. Manuscript reviewing: Hai-LL, H-TH,W-JF, Hong-LL. All authors contributed to the article and approved the submitted version.

Funding

Technology Major Project of the Ministry of Science and Technology of China (2018ZX10303502). Henan Province Medical Science and Technology Research Project (201701032). Medical Education Research Project of Henan Province (Wjlx2021334). Henan Province Natural Science Foundation (212300410403). Henan Province Natural Science Foundation (222300420574).

Acknowledgments

We thank all our authors listed in this manuscript, and also thank all the patients participated in the study.

Conflict of interest

The authors declare that the research was conducted in the absence of any commercial or financial relationships that could be construed as a potential conflict of interest.

Publisher's note

All claims expressed in this article are solely those of the authors and do not necessarily represent those of their affiliated organizations, or those of the publisher, the editors and the reviewers. Any product that may be evaluated in this article, or claim that may be made by its manufacturer, is not guaranteed or endorsed by the publisher.

References

1. Siegel RL, Miller KD, Fuchs HE, Jemal A. Cancer statistics, 2022. *CA Cancer J Clin* (2022) 72(1):7–33. doi: 10.3322/caac.21708

2. Zhang SZ, Zhang L, Xie L. Cancer burden in China during 1990-2019: Analysis of the global burden of disease. *BioMed Res Int* (2022) 2022:3918045. doi: 10.1155/2022/3918045

3. El-Sherif A, Gooding WE, Santos R, Pettiford B, Ferson PF, Fernando HC, et al. Outcomes of sublobar resection versus lobectomy for stage I non-small cell lung cancer: A 13-year analysis. *Ann Thorac surgery* (2006) 82(2):408–15. doi: 10.1016/j.athoracsur.2006.02.029

4. Menoux I, Antoni D, Truntzer P, Keller A, Massard G, Noël G. Stereotactic body radiation therapy for stage I non-small cell lung carcinomas: Moderate hypofractionation optimizes outcome. *Lung Cancer* (2018) 126:201–7. doi: 10.1016/j.lungcan.2018.11.013

5. Teke ME, Sarvestani AL, Hernandez JM, Fernando HC, Timmerman RD, Randomized A. Phase III study of sublobar resection (SR. versus stereotactic ablative radiotherapy (SAbR. @ in high-risk patients with stage I non-small cell lung cancer (NSCLC). *Ann Surg Oncol* (2022) 29(8):4686–7. doi: 10.1245/s10434-022-11584-3

6. Fakiris AJ, McGarry RC, Yiannoutsos CT, Papiez L, Williams M, Henderson MA, et al. Stereotactic body radiation therapy for earlystage non-small-cell lung carcinoma: four-year results of a prospective phase II study. *Int J Radiat Oncol Biol Phys* (2009) 75(3):677 –682. doi: 10.1016/j.ijrobp.2008.11.042

7. Vogl TJ, Naguib NN, Gruber-Rouh T, Koitka K, Lehnert T, Nour-Eldin NE, et al. Microwave ablation therapy: Clinical utility in treatment of pulmonary metastases. *Radiology* (2011) 261(2):643–451. doi: 10.1148/radiol.11101643

8. Li M, Qin Y, Mei A, Wang C, Fan L. Effectiveness of radiofrequency ablation therapy for patients with unresected stage IA non-small cell lung cancer. *J Cancer Res Ther* (2020) 16(5):1007–13. doi: 10.4103/jcrt.JCRT_1040_19

9. Gemmete JJ. Percutaneous radiofrequency ablation is ready for prime time in the treatment of colorectal pulmonary metastases. *Radiology* (2020) 294(3):696–7. doi: 10.1148/radiol.2020192558

10. Vogl TJ, Nour-Eldin NA, Albrecht MH, Kaltenbach B, Hohenforst-Schmidt W, Lin H, et al. Thermal ablation of lung tumors: Focus on microwave ablation. *Rofo* (2017) 189(9):828–43. doi: 10.1055/s-0043-109010

11. Li HW, Long YJ, Yan GW, Bhetuwal A, Zhuo LH, Yao HC, et al. Microwave ablation vs. cryoablation for treatment of primary and metastatic pulmonary malignant tumors. *Mol Clin Oncol* (2022) 16(3):62. doi: 10.3892/mco.2022.2495

12. Alzubaidi SJ, Liou H, Saini G, Segaran N, Scott Kriegshauser J, Naidu SG, et al. Percutaneous image-guided ablation of lung tumors. *J Clin Med* (2021) 10 (24):5783. doi: 10.3390/jcm10245783

13. Reisenauer JS, Eiken PW, Callstrom MR, Johnson GB, Pierson K, Lechtenberg B, et al. A prospective trial of CT-guided percutaneous microwave ablation for lung tumors. *J Thorac Dis* (2022) 14(4):939–51. doi: 10.21037/jtd-21-1636

14. Liu BD, Zhi XY. Chinese Society of thoracic and cardiovascular surgery lung cancer study group. expert consensus on image-guided radiofrequency ablation of pulmonary tumors–2015 edition. *Chin Clin Oncol* (2015) 4(2):27. doi: 10.3978/j.issn.2304-3865.2015.05.06

15. Fanucchi O, Ambrogi MC, Aprile V, Cioni R, Cappelli C, Melfi F, et al. Long-term results of percutaneous radiofrequency ablation of pulmonary metastases: A single institution experience. *Interact Cardiovasc Thorac Surg* (2016) 23(1):57–64. doi: 10.1093/icvts/ivw089

16. Ni Y, Xu H, Ye X. Image-guided percutaneous microwave ablation of early-stage non-small cell lung cancer. *Asia Pac J Clin Oncol* (2020) 16(6):320–5. doi: 10.1111/ajco.13419

17. Colak E, Tatlı S, Shyn PB, Tuncalı K, Silverman SG. CT-guided percutaneous cryoablation of central lung tumors. *Diagn Interv Radiol* (2014) 20 (4):316–22. doi: 10.5152/dir.2014.13440

18. Kim MS, Hong HP, Ham SY, Koo DH, Kang DY, Oh TY. Complications after 100 sessions of cone-beam computed tomography-guided lung radiofrequency ablation: A single-center, retrospective experience. *Int J Hyperthermia* (2020) 37(1):763–71. doi: 10.1080/02656736.2020.1784472

19. Tongdee T, Tantigate P, Tongdee R. Radiofrequency ablation of lung metastasis not suitable for surgery: Experience in siriraj hospital. *J Med Assoc Thai* (2015) 98(10):1019–27.

20. Ahmed M, Liu Z, Afzal KS, Weeks D, Lobo SM, Kruskal JB, et al. Radiofrequency ablation: effect of surrounding tissue composition on coagulation necrosis in a canine tumor model. *Radiology* (2004) 230:761–7. doi: 10.1148/radiol.2303021801

21. de Baère T, Palussière J, Aupérin A, Hakime A, Abdel-Rehim M, Kind M, et al. Midterm local efficacy and survival after radiofrequency ablation of lung tumors with minimum follow-up of 1 year: prospective evaluation. *Radiology* (2006) 240(2):587–96. doi: 10.1148/radiol.2402050807

22. Huang BY, Li XM, Song XY, Zhou JJ, Shao Z, Yu ZQ, et al. Long-term results of CT-guided percutaneous radiofrequency ablation of inoperable patients with stage ia non-small cell lung cancer: A retrospective cohort study. *Int J Surg* (2018) 53:143–50. doi: 10.1016/j.ijsu.2018.03.034

23. Vogl TJ, Naguib NN, Gruber-Rouh T, Koitka K, Lehnert T, Nour-Eldin NE, et al. Microwave ablation therapy: Clinical utility in treatment of pulmonary metastases. *Radiology* (2011) 261(2):643–451. doi: 10.1148/radiol.11101643

24. Bourgouin PP, Wrobel MM, Mercaldo ND, Murphy MC, Leppelmann KS, Levesque VM, et al. Comparison of percutaneous image-guided microwave ablation and cryoablation for sarcoma lung metastases: A 10-year experience. *AJR Am J Roentgenol* (2022) 218(3):494–504. doi: 10.2214/AJR.21.26551

25. Sahay A, Sahay N, Kapoor A, Kapoor J, Chatterjee A. Percutaneous image-guided radiofrequency ablation of tumors in inoperable patients - immediate complications and overall safety. *Indian J Palliat Care* (2016) 22(1):67–73. doi: 10.4103/0973-1075.173951

26. Sakurai J, Hiraki T, Mukai T, Mimura H, Yasui K, Gobara H, et al. Intractable pneumothorax due to bronchopleural fistula after radiofrequency

ablation of lung tumors. *J Vasc Interv Radiol* (2007) 18(1 Pt 1):141–5. doi: 10.1016/j.jvir.2006.10.011

27. Kodama H, Yamakado K, Murashima S, Takaki H, Uraki J, Nakatsuka A, et al. Intractable bronchopleural fistula caused by radiofrequency ablation: Endoscopic bronchial occlusion with silicone embolic material. *Br J Radiol* (2009) 82(983):e225–227. doi: 10.1259/bjr/23975691

28. Lois M, Noppen M. Bronchopleural fistulas: an overview of the problem with special focus on endoscopic management. *Chest* (2005) 128(6):3955–65. doi: 10.1378/chest.128.6.3955

29. Clasen S, Kettenbach J, Kosan B, et al. Delayed development of pneumothorax after pulmonary radiofrequency ablation. *Cardiovasc Interv Radiol* (2009) 32(3):484–90. doi: 10.1007/s00270-008-9489-z

30. Jin GY, Han YM, Lee YS, Lee YC. Radiofrequency ablation using a monopolar wet electrode for the treatment of inoperable non-small cell lung cancer: a preliminary report. *Korean J Radiol* (2008) 9(2):140–7. doi: 10.3348/kjr.2008.9.2.140

31. Baumann MH, Strange C, Heffner JE, Light R, Kirby TJ, Klein J, et al. AACP pneumothorax consensus group. management of spontaneous pneumothorax: An American college of chest physicians Delphi consensus statement. *Chest* (2001) 119 (2):590–602. doi: 10.1378/chest.119.2.590

32. Jia H, Tian J, Liu B, Meng H, Pan F, Li C. Efficacy and safety of artificial pneumothorax with position adjustment for CT-guided percutaneous transthoracic microwave ablation of small subpleural lung tumors. *Thorac Cancer* (2019) 10(8):1710–6. doi: 10.1111/1759-7714.13137

33. Hou X, Zhuang X, Zhang H, Wang K, Zhang Y. Artificial pneumothorax: a safe and simple method to relieve pain during microwave ablation of subpleural lung malignancy. *Minim Invasive Ther Allied Technol* (2017) 26(4):220–6. doi: 10.1080/13645706.2017.1287089

frontiers | Frontiers in Oncology

TYPE Original Research
PUBLISHED 23 August 2022
DOI 10.3389/fonc.2022.984932

OPEN ACCESS

EDITED BY
Xin Ye,
Qianfoshan Hospital, Shandong University, China

REVIEWED BY
Zhonglun Mai,
Southern Medical University Cancer Center, China
Yueyong Xiao,
Chinese People's Liberation Army General Hospital, China
Xiaoguang Li,
Beijing Hospital, Peking University, China
Zhengyu Lin,
First Affiliated Hospital of Fujian Medical University, China
Weijun Fan,
Sun Yat-sen University Cancer Center (SYSUCC), China

*CORRESPONDENCE
Fenglei Yu
yufenglei@csu.edu.cn

SPECIALTY SECTION
This article was submitted to Thoracic Oncology, a section of the journal Frontiers in Oncology

RECEIVED 02 July 2022
ACCEPTED 03 August 2022
PUBLISHED 23 August 2022

CITATION
Yang WY, He Y, Hu Q, Peng M, Zhang Z, Xie S and Yu F (2022) Survival benefit of thermal ablation therapy for patients with stage II-III non-small cell lung cancer: A propensity-matched analysis. *Front. Oncol.* 12:984932. doi: 10.3389/fonc.2022.984932

Survival benefit of thermal ablation therapy for patients with stage II-III non-small cell lung cancer: A propensity-matched analysis

Wei-Yu Yang[1,2], Yu He[1,2], Qikang Hu[1,2], Muyun Peng[1,2], Zhe Zhang[1,2], Shouzhi Xie[1,2] and Fenglei Yu[1,2]*

[1]Department of Thoracic Surgery, The Second Xiangya Hospital of Central South University, Changsha, China, [2]Hunan Key Laboratory of Early Diagnosis and Precise Treatment of Lung Cancer, The Second Xiangya Hospital of Central South University, Changsha, China

Background: Thermal ablation (TA) is considered a safe alternative to surgical resection for the treatment of non-small cell lung cancer (NSCLC). While previous studies have shown that TA is beneficial for stage I NSCLC patients, however, few have reported on TA efficacy in patients with stage II-III NSCLC. The current study investigated the impact of TA on the overall survival (OS) and cancer-specific survival (CSS) of patients with stage II-III NSCLC.

Methods: Data on patients with stage II-III NSCLC who did not undergo surgical resection between 2004 and 2015 were extracted from the Surveillance, Epidemiology, and End Results (SEER) database. Propensity score matching (PSM), Kaplan-Meier survival curves, and Cox regression were used for statistical analyses.

Results: A total of 57,959 stage II-III NSCLC patients who did not undergo surgical resection were included in this study, 261 of whom received TA. Overall, TA was associated with a longer OS ($p = 0.035$) and CSS ($p = 0.005$) than non-ablation. After 1:3 PSM, 252 patients receiving TA and 732 patients not receiving ablation were enrolled in the matched cohort. The OS ($p = 0.047$) and CSS ($p = 0.029$) remained higher in the TA group than in the non-ablation group after PSM. Cox regression analysis showed that age, sex, primary tumor site, pathological type, tumor size, radiotherapy, chemotherapy, and thermal

ablation were independently associated with OS and CSS (p <0.05). Subgroup analysis found that the advantages of TA were more pronounced among individuals ≥70 years of age, with tumor size ≤3.0 cm, or who did not receive radiotherapy.

Conclusion: TA could be an effective alternative treatment for stage II-III NSCLC patients unsuitable for surgical resection, particularly those ≥70 years of age, with tumor size ≤3.0 cm, or who have not received radiotherapy.

KEYWORDS

non-small cell lung carcinoma, thermal ablation, survival, stage II-III, SEER

Introduction

Lung cancer, one of the most prevalent and lethal malignancies worldwide, is a significant public health concern (1). In the United States, it is estimated that 235,760 new cases of lung cancer will be diagnosed in 2021, and 131,800 patients will die from the disease (2). Surgical resection is the preferred treatment for early-stage non-small cell lung cancer (NSCLC) (3, 4). However, a proportion of NSCLC patients are unsuitable for surgical resection for several reasons including advanced age, severe underlying disease, and refusal to undergo surgical intervention (5, 6). Thus, non-surgical treatment for NSCLC, including thermal ablation (TA) and stereotactic body radiotherapy (SBRT), has attracted increasing attention (7–11).

TA includes radiofrequency ablation (RFA), microwave ablation (MWA), and ultrasound ablation using various energy sources (12, 13). As a minimally invasive treatment technique, TA utilizes thermal energy to cause injuries to the targeted tissue (14). Of the ablation technologies in clinical use, RFA is the most widely used for the treatment of multiple conditions, including cardiac arrhythmias and liver, lung, kidney, and other tumors (12). MWA devices use higher frequency electromagnetic waves than RFA, allowing larger tissue volumes to be heated (13). Thermal injuries caused by TA may result in protein denaturation, enzyme inactivation, vascular injury, and ischemia-reperfusion, leading to irreversible cellular damage (15, 16). Previous studies indicate that TA is beneficial for stage I NSCLC patients (7, 17–19). Current guidelines from multiple societies specify that the best candidates for TA are stage I NSCLC patients who are not eligible for or amenable to surgical resection and SBRT (20, 21). However, few studies have reported on TA efficacy in patients with stage II-III NSCLC. Thus, it remains unknown whether inoperable stage II-III NSCLC patients may benefit from this technique.

According to the American Society of Clinical Oncology and Chinese Medical Association guidelines, inoperable stage III NSCLC patients should be offered concurrent chemoradiotherapy as a standard treatment (22, 23). Those who are not candidates for concurrent chemoradiation but are candidates for chemotherapy should be offered both sequential chemotherapy and radiation therapy. For inoperable stage II-III NSCLC patients who are unsuitable for chemoradiation, radiotherapy alone is the standard treatment with a survival benefit (23–25). The survival benefit of TA is comparable to SBRT in stage I NSCLC patients (26, 27). The current study performed a retrospective analysis to investigate whether inoperable stage II-III NSCLC patients can benefit from TA using patient data from the Surveillance, Epidemiology, and End Results (SEER) database.

Methods

Data source

Data were retrieved from the SEER 18 Registries Database (2000–2018). SEER is a national population-based registry program that collects the tumor-related clinical data and basic demographics of cancer patients (28). Since this database is publicly available and all records are de-identified, no ethics committee approval or informed consent is required.

Study population

Data from patients diagnosed with NSCLC during 2004–2015 were extracted from SEER. The third edition of the International Classification of Diseases for Oncology (ICD-O-3) was used to identify NSCLC. Patients were included in the study if they had a pathological diagnosis of NSCLC and their age at diagnosis was >18

years. Patients were excluded if (1) they received other surgical procedures beyond thermal ablation, or surgery information was unknown (2), their tumors were identified as TNM stage I or IV (3), they were identified in autopsy or death certificates (4), their survival data was unknown, or (5) information regarding age, sex, race, pathological type, primary tumor site, laterality, lymph node staging, marital status, or tumor size was missing.

The following information was extracted: year of diagnosis, age at diagnosis, sex, race, histological grade, pathological type, primary tumor site, laterality, lymph node staging, tumor size, radiotherapy, chemotherapy, surgery, marital status, cancer-specific survival (CSS), overall survival (OS), and survival months. TNM staging was reclassified according to the eighth edition of the American Joint Committee on Cancer (AJCC) staging manual. Patients were divided into TA and non-ablation groups based on the treatment they received. The primary endpoints in this study were OS and CSS. CSS was defined as the time from diagnosis to death attributed to NSCLC.

Propensity score matching

In retrospective cohort studies, treatment-related selection bias resulting from an imbalance in the baseline characteristics is inevitable (29). Propensity score matching (PSM) can reduce the selection bias, offset differing clinical features among groups, and bolster the evidence of a retrospective cohort study (30). The current study created a logistic regression model with propensity scores to balance the baseline characteristics between the TA and non-ablation groups. TA was defined as the dependent variable, while other baseline characteristics were included as the covariables. The PSM was performed in a 1:3 ratio using nearest neighbor matching with a caliper of 0.001. Chi-square or Fisher's exact tests were used to compare baseline characteristics between groups.

Statistical analysis

Analyses were performed using R version 4.0.0 and SPSS version 26.0. Kaplan-Meier methods and log-rank tests were used for survival analysis. Univariate and multivariable analyses were performed using Cox proportional hazards regression. Variables with p <0.10 from the univariable analysis were considered for multivariable analysis. Differences with p <0.05 were considered significant.

Results

Baseline characteristics

Data on 57,959 non-surgical patients who were diagnosed with stage II-III NSCLC during 2004–2015 were extracted from the SEER database. A total of 261 patients (0.45%) received TA and 57,698 patients (99.55%) did not. The baseline characteristics of the patients are shown in Table 1. There were significant differences in age (p = 0.003), race (p = 0.013), tumor site (p <0.001), pathological type (p <0.001), tumor size (p = 0.002), lymph node staging (p = 0.022) and chemotherapy (p = 0.003) between the TA and non-ablation groups in the unmatched cohort. After 1:3 PSM, 252 patients receiving TA and 732 patients without ablation were enrolled in the matched cohort. The baseline characteristics were well-balanced between the TA and non-ablation groups in the matched cohorts.

Survival analysis

Kaplan-Meier analysis revealed a significant difference in the OS of patients receiving TA and those who did not (p = 0.035) (Figure 1A). The median OS was 15 months (95% confidence interval (CI): 11.275–18.775) and 12 months (95% CI: 11.847–12.153) for the TA and non-ablation groups, respectively. The 3- and 5-year OS of the TA and non-ablation groups was 24.14% versus 18.82% and 14.39% versus 10.84%, respectively. Patients who received TA also had longer CSS than non-ablation patients (p = 0.005) (Figure 1B). After 1:3 matching, patients who received TA also had longer OS than non-ablation patients (p = 0.047) (Figure 1C). The median OS was 15 months (95% CI: 11.111–18.889) and 11 months (95% CI: 9.811–12.189) for the TA and non-ablation groups, respectively. The 3- and 5-year OS of the TA and non-ablation groups was 24.21% versus 19.51% and 14.98% versus 10.71%, respectively. CSS was also longer for patients in the TA group than in the non-ablation group (p = 0.029) (Figure 1D).

Univariate and multivariate COX regression analysis after PSM

Univariate survival analysis showed that age, sex, race, primary tumor site, histological grade, pathological type, tumor size, radiotherapy, and chemotherapy were significantly associated with OS (p < 0.05) (Table 2). Variables with p <0.10 from the univariable analysis were considered for multivariable analysis. The multivariable analysis showed that age, sex, primary tumor site, pathological type, tumor size, radiotherapy, chemotherapy, and thermal ablation were independently associated with OS (p <0.05). Regarding the pathological type, squamous cell carcinoma served as a reference, and adenocarcinoma (hazard ratio (HR) = 0.81, 95% CI: 0.69–0.95, p = 0.009) was shown to be a favorable prognostic factor for OS. However, large cell lung cancer (HR = 1.10, 95% CI: 0.68–1.77, p = 0.703) and the other pathological types (HR = 1.00, 95% CI: 0.64–1.56, p = 0.997) were not statistically related to OS. Compared with tumor size ≤3.0 cm, tumor sizes of 5.1–

TABLE 1 Characteristics of stage II-III NSCLC patients before and after PSM, n (%).

Characteristics	Before PSM				After PSM		
	Total	Non-ablation (*N* = 57,698)	Thermal ablation (*N* = 261)	*p* Value	Non-ablation (*N* = 732)	Thermal ablation (*N* = 252)	*p* Value
Age (years)				0.003			0.582
<70	25,216 (43.51)	25,079 (43.47)	137 (52.49)		360 (49.18)	129 (51.19)	
≥70	32,743 (56.49)	32,619 (56.53)	124 (47.51)		372 (50.82)	123 (48.81)	
Sex				0.072			0.621
Male	33,008 (56.95)	32,845 (56.93)	163 (62.45)		463 (63.25)	155 (61.51)	
Female	24,951 (43.05)	24,853 (43.07)	98 (37.55)		269 (36.75)	97 (38.49)	
Race				0.013			0.704
White	46,533 (80.29)	46,306 (80.26)	227 (86.97)		629 (85.93)	219 (86.90)	
Black	7,805 (13.47)	7,778 (13.48)	27 (10.34)		87 (11.89)	26 (10.32)	
Others	3,621 (6.25)	3,614 (6.26)	7 (2.68)		16 (2.19)	7 (2.78)	
Laterality				0.544			0.709
Left	23,719 (40.92)	23,617 (40.93)	102 (39.08)		275 (37.57)	98 (38.89)	
Right	34,240 (59.08)	34,081 (59.07)	159 (60.92)		457 (62.43)	154 (61.11)	
Tumor site				<0.001			0.030
Lung lobe	54,424 (93.90)	54,217 (93.97)	207 (79.31)		639 (87.30)	207 (82.14)	
Main bronchus	3,022 (5.21)	2,970 (5.15)	52 (19.92)		88 (12.02)	45 (17.86)	
Overlapping lesion of lung	513 (0.89)	511 (0.89)	2 (0.77)		5 (0.68)	0 (0.00)	
Histological grade				0.166			0.892
I/II	12,809 (22.10)	12,740 (22.08)	69 (26.44)		196 (26.78)	66 (26.19)	
III/IV	17,887 (30.86)	17,805 (30.86)	82 (31.42)		212 (28.96)	77 (30.56)	
Unknown	27,263 (47.04)	27,153 (47.06)	110 (42.15)		324 (44.26)	109 (43.25)	
Pathological type				<0.001			0.390
Squamous cell carcinoma	27,742 (47.86)	27,568 (47.78)	174 (66.67)		480 (65.57)	165 (65.48)	
Adenocarcinoma	26,197 (45.20)	26,125 (45.28)	72 (27.59)		226 (30.87)	72 (28.57)	
Large cell lung cancer	1,812 (3.13)	1,805 (3.13)	7 (2.68)		11 (1.50)	7 (2.78)	
Others	2,208 (3.81)	2,200 (3.81)	8 (3.07)		15 (2.05)	8 (3.17)	
Tumor size				0.002			0.984
≤3.0 cm	14,297 (24.67)	14,206 (24.62)	91 (34.87)		259 (35.38)	90 (35.71)	
3.1–5.0 cm	18,950 (32.70)	18,871 (32.71)	79 (30.27)		218 (29.78)	74 (29.37)	

(Continued)

TABLE 1 Continued

Characteristics	Before PSM				After PSM		
	Total	Non-ablation (*N* = 57,698)	Thermal ablation (*N* = 261)	*p* Value	Non-ablation (*N* = 732)	Thermal ablation (*N* = 252)	*p* Value
5.1–7.0 cm	13,797 (23.80)	13,746 (23.82)	51 (19.54)		145 (19.81)	48 (19.05)	
>7.0 cm	10,915 (18.83)	10,875 (18.85)	40 (15.33)		110 (15.03)	40 (15.87)	
Lymph node staging				0.022			0.992
N0	16,012 (27.63)	15,920 (27.59)	92 (35.25)		257 (35.11)	89 (35.32)	
N1	5,778 (9.97)	5,750 (9.97)	28 (10.73)		77 (10.52)	25 (9.92)	
N2	28,429 (49.05)	28,313 (49.07)	116 (44.44)		331 (45.22)	114 (45.24)	
N3	7,740 (13.35)	7,715 (13.37)	25 (9.58)		67 (9.15)	24 (9.52)	
Radiotherapy				0.883			0.741
Yes	34,901 (60.22)	34,745 (60.22)	156 (59.77)		427 (58.33)	150 (59.52)	
No	23,058 (39.78)	22,953 (39.78)	105 (40.23)		305 (41.67)	102 (40.48)	
Chemotherapy				0.003			0.752
Yes	33,541 (57.87)	33,414 (57.91)	127 (48.66)		357 (48.77)	120 (47.62)	
No	24,418 (42.13)	24,284 (42.09)	134 (51.34)		375 (51.23)	132 (52.38)	
Marital status				0.918			0.802
Married	29,572 (51.02)	29,438 (51.02)	134 (51.34)		368 (50.27)	129 (51.19)	
Not married	28,387 (48.98)	28,260 (48.98)	127 (48.66)		364 (49.73)	123 (48.81)	

NSCLC, non-small cell lung cancer; PSM, propensity score matching.

7.0 cm (HR = 1.31, 95% CI: 1.07–1.60, p = 0.009) and >7.0 cm (HR = 1.91, 95% CI: 1.52–2.40, p <0.001) were adverse prognostic factors for OS, and tumor sizes of 3.1–5.0 cm (HR = 1.12, 95% CI: 0.94–1.33, p = 0.203) did not significantly impact OS. The multivariable analysis of CSS showed that age, sex, primary tumor site, pathological type, tumor size, lymph node staging, radiotherapy, chemotherapy, and TA were independently associated with CSS (p <0.05) (Table 3). Overall, TA was associated with longer OS (p = 0.005) and CSS (p = 0.020).

Subgroup analysis after PSM

Kaplan-Meier was used to conduct subgroup analyses stratified by age and tumor size. When age was <70 years, there was no significant difference in the OS and CSS of the TA and non-ablation groups. The 3- and 5-year OS of the TA and non-ablation groups was 22.48% versus 25.95% and 17.40% versus 16.09%, respectively (p = 0.718, Figure 2A). The 3- and 5-year CSS of the TA and non-ablation groups was 29.07% versus 32.10% and 22.60% versus 22.51%, respectively (p = 0.760, Figure 2B). When age was ≥70 years, the TA group had longer OS and CSS than the non-ablation group. The 3- and 5-year OS of the TA and non-ablation groups was 26.02% versus 13.30% and 12.29% versus 5.61%, respectively (p = 0.001, Figure 2C). The 3- and 5-year CSS of the TA and non-ablation groups was 34.59% versus 20.82% and 23.84% versus 10.79%, respectively (p <0.001, Figure 2D).

In patients with tumor size ≤3.0 cm, the 3- and 5-year OS of the TA and non-ablation groups was 34.44% versus 17.87% and 18.86% versus 8.89%, respectively (p = 0.001, Figure 3A). The 3- and 5-year CSS of the TA and non-ablation groups was 46.55% versus 29.85% and 32.35% versus 17.06%, respectively (p = 0.002, Figure 3B). However, no significant difference was observed in the OS and CSS of the TA and non-ablation groups for tumor sizes of 3.1–5.0 cm (3-year OS: 22.97% versus 24.77%, p = 0.803, Figure 3C; 3-year CSS: 29.57% versus 30.65%, p = 0.716, Figure 3D), 5.1–7.0 cm (3-year OS: 18.75% versus

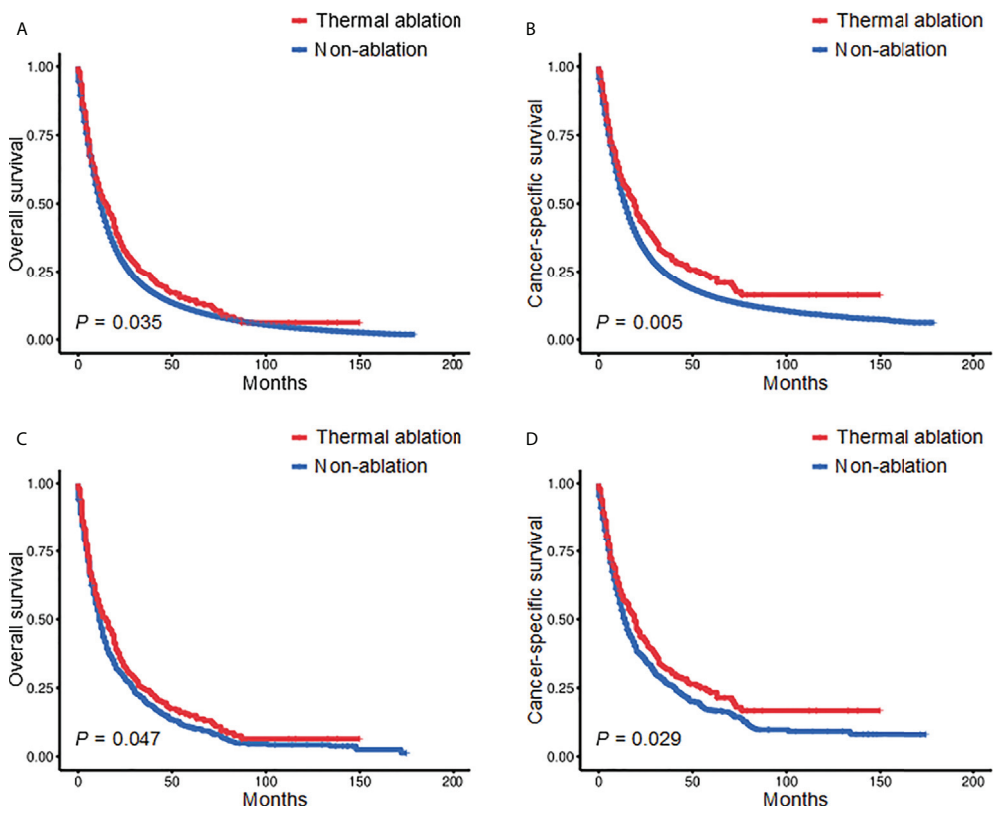

FIGURE 1
Kaplan-Meier survival curves of stage II-III NSCLC patients before **(A, B)** and after **(C, D)** PSM. NSCLC, non-small cell lung cancer; PSM, propensity score matching.

18.99%, $p = 0.672$, Figure 3E; 3-year CSS: 22.12% versus 23.76%, $p = 0.721$, Figure 3F), and >7.0 cm (3-year OS: 10.00% versus 13.64%, $p = 0.920$, Figure 3G; 3-year CSS: 15.12% versus 15.98%, $p = 0.884$, Figure 3H).

Cox proportional hazard analyses were performed to explore the survival benefit of TA for patients in different subgroups. TA improved the OS of patients who were ≥70 years of age (HR = 0.693, 95% CI: 0.560–0.857, $p < 0.001$) or white (HR = 0.841, 95% CI: 0.715–0.989, $p = 0.037$) and had right laterality (HR = 0.813, 95% CI: 0.670–0.987, $p = 0.037$), lung lobes (HR = 0.845, 95% CI: 0.716–0.998, $p = 0.047$), adenocarcinoma (HR = 0.743, 95% CI: 0.555–0.994, $p = 0.046$), tumor size ≤3.0 cm (HR = 0.647, 95% CI: 0.501–0.834, $p = 0.001$), N0 staging (HR = 0.708, 95% CI: 0.547–0.916, $p = 0.009$), non-radiotherapy (HR = 0.642, 95% CI: 0.508–0.812, $p < 0.001$) and non-chemotherapy (HR = 0.704, 95% CI: 0.573–0.864, $p = 0.001$) (Figure 4). For CSS, subgroup analysis stratified by age, sex, race, histological grade, tumor site, laterality, lymph node staging, tumor size, radiotherapy, chemotherapy, and marital status gave similar results (Figure 5). A statistically improved OS ($p = 0.046$) but not CSS ($p = 0.060$) was observed in patients with TA when the pathology type was adenocarcinoma.

Discussion

Data on 57,959 stage II-III NSCLC patients who were unsuitable for surgical resection were extracted from the SEER database. The findings revealed that TA improved the OS and CSS of stage II-III NSCLC patients who did not undergo surgical resection, particularly for those ≥70 years of age, with tumor size ≤3.0 cm, or who did not receive radiotherapy.

TA is considered a safe treatment for primary lung cancer (7, 20, 21). As an alternative therapy to surgical resection, TA causes irreversible damage to tumor cells using thermal energy (14, 31, 32). While previous studies have shown that TA is beneficial for stage I NSCLC patients (7, 18, 33), however, there is minimal data on the use of TA in stage II-III NSCLC patients. The current study found that TA could significantly improve the OS and CSS of stage II-III NSCLC patients without surgical resection. However, the effect of differences in clinicopathological features, such as age, race, tumor site, pathological type, tumor size, lymph node staging, and chemotherapy, cannot be overlooked. After PSM, baseline characteristics were similar between the TA and non-ablation groups in the adjusted cohorts and patients with TA still had

10.3389/fonc.2022.984932

TABLE 2 Univariate and multivariate analyses of OS after PSM.

Characteristics	Univariable		Multivariable	
	HR (95% CI)	*p* Value	HR (95% CI)	*p* Value
Age (years)				
<70	1.00		1.00	
≥70	1.43 (1.26-1.63)	<0.001	1.21 (1.04-1.41)	0.014
Sex				
Male	1.00		1.00	
Female	0.73 (0.63-0.83)	<0.001	0.77 (0.67-0.89)	<0.001
Race				
White	1.00		1.00	
Black	0.91 (0.74-1.11)	0.346	0.89 (0.72-1.10)	0.285
Others	0.63 (0.39-1.00)	0.049	0.68 (0.43-1.09)	0.112
Laterality				
Left	1.00			
Right	1.02 (0.89-1.17)	0.779		
Tumor site				
Lung lobe	1.00		1.00	
Main bronchus	0.96 (0.79-1.16)	0.664	1.16 (0.95-1.43)	0.150
Overlapping lesion of lung	5.45 (2.25-13.22)	<0.001	2.91 (1.18-7.16)	0.020
Histological grade				
I/II	1.00			
III/IV	0.82 (0.69-0.98)	0.030	0.97 (0.81-1.17)	0.761
Unknown	0.96 (0.82-1.12)	0.606	0.96 (0.81-1.13)	0.603
Pathological type				
Squamous cell carcinoma	1.00			
Adenocarcinoma	0.81 (0.70-0.93)	0.004	0.81 (0.69-0.95)	0.009
Large cell lung cancer	0.82 (0.52-1.32)	0.419	1.10 (0.68-1.77)	0.703
Others	1.01 (0.65-1.56)	0.956	1.00 (0.64-1.56)	0.997
Tumor size				
≤3.0 cm	1.00			
3.1–5.0 cm	0.90 (0.75-1.06)	0.202	1.12 (0.94-1.33)	0.203
5.1–7.0 cm	1.02 (0.85-1.23)	0.796	1.31 (1.07-1.60)	0.009
>7.0 cm	1.29 (1.06-1.57)	0.012	1.91 (1.52-2.40)	<0.001
Lymph node staging				
N0	1.00			
N1	1.04 (0.83-1.31)	0.743		
N2	1.02 (0.88-1.19)	0.754		
N3	1.15 (0.90-1.46)	0.257		
Radiotherapy				
Yes	1.00			
No	1.61 (1.41-1.84)	<0.001	1.49 (1.26-1.78)	<0.001
Chemotherapy				
Yes	1.00			
No	1.71 (1.50-1.95)	<0.001	1.57 (1.31-1.89)	<0.001
Marital status				
Married				
Not married	0.92 (0.80-1.04)	0.187		
Thermal ablation				
Yes	1.00			
No	1.16 (1.00-1.35)	0.052	1.25 (1.07-1.46)	0.005

OS, overall survival; PSM, propensity score matching; HR, hazard ratio; CI, confidence interval.

10.3389/fonc.2022.984932

TABLE 3 Univariate and multivariate analyses of CSS after PSM.

Characteristics	Univariable		Multivariable	
	HR (95% CI)	*p* Value	HR (95% CI)	*p* Value
Age (years)				
<70	1.00		1.00	
≥70	1.30 (1.12-1.51)	<0.001	1.24 (1.05-1.46)	0.013
Sex				
Male	1.00		1.00	
Female	0.71 (0.61-0.83)	<0.001	0.78 (0.66-0.92)	0.002
Race				
White	1.00			
Black	0.92 (0.73-1.16)	0.473		
Others	0.69 (0.42-1.14)	0.145		
Laterality				
Left	1.00			
Right	1.01 (0.87-1.17)	0.902		
Tumor site				
Lung lobe	1.00		1.00	
Main bronchus	1.06 (0.87-1.31)	0.555	1.15 (0.92-1.44)	0.216
Overlapping lesion of lung	6.76 (2.78-16.41)	<0.001	3.08 (1.25-7.63)	0.015
Histological grade				
I/II	1.00			
III/IV	0.92 (0.75-1.12)	0.409		
Unknown	1.02 (0.86-1.23)	0.793		
Pathological type				
Squamous cell carcinoma	1.00		1.00	
Adenocarcinoma	0.75 (0.64-0.89)	0.001	0.78 (0.66-0.93)	0.006
Large cell lung cancer	0.73 (0.42-1.26)	0.260	1.03 (0.59-1.79)	0.924
Others	0.88 (0.53-1.47)	0.626	1.00 (0.59-1.70)	0.985
Tumor size				
≤3.0 cm	1.00		1.00	
3.1–5.0 cm	1.07 (0.89-1.29)	0.473	1.34 (1.10-1.63)	0.004
5.1–7.0 cm	1.27 (1.03-1.56)	0.023	1.61 (1.29-2.01)	<0.001
>7.0 cm	1.63 (1.31-2.02)	<0.001	2.22 (1.73-2.84)	<0.001
Lymph node staging				
N0	1.00		1.00	
N1	1.06 (0.81-1.37)	0.692	1.24 (0.95-1.63)	0.111
N2	1.18 (1.00-1.40)	0.046	1.54 (1.28-1.86)	<0.001
N3	1.32 (1.01-1.71)	0.041	1.69 (1.28-2.22)	<0.001
Radiotherapy				
Yes	1.00		1.00	
No	1.46 (1.26-1.70)	<0.001	1.62 (1.33-1.96)	<0.001
Chemotherapy				
Yes	1.00		1.00	
No	1.47 (1.27-1.70)	<0.001	1.60 (1.30-1.97)	<0.001
Marital status				
Married	1.00			
Not married	0.95 (0.82-1.10)	0.487		
Thermal ablation				
Yes	1.00		1.00	
No	1.21 (1.02-1.43)	0.003	1.23 (1.03-1.46)	0.020

CSS, cancer-specific survival; PSM, propensity score matching; HR, hazard ratio; CI, confidence interval.

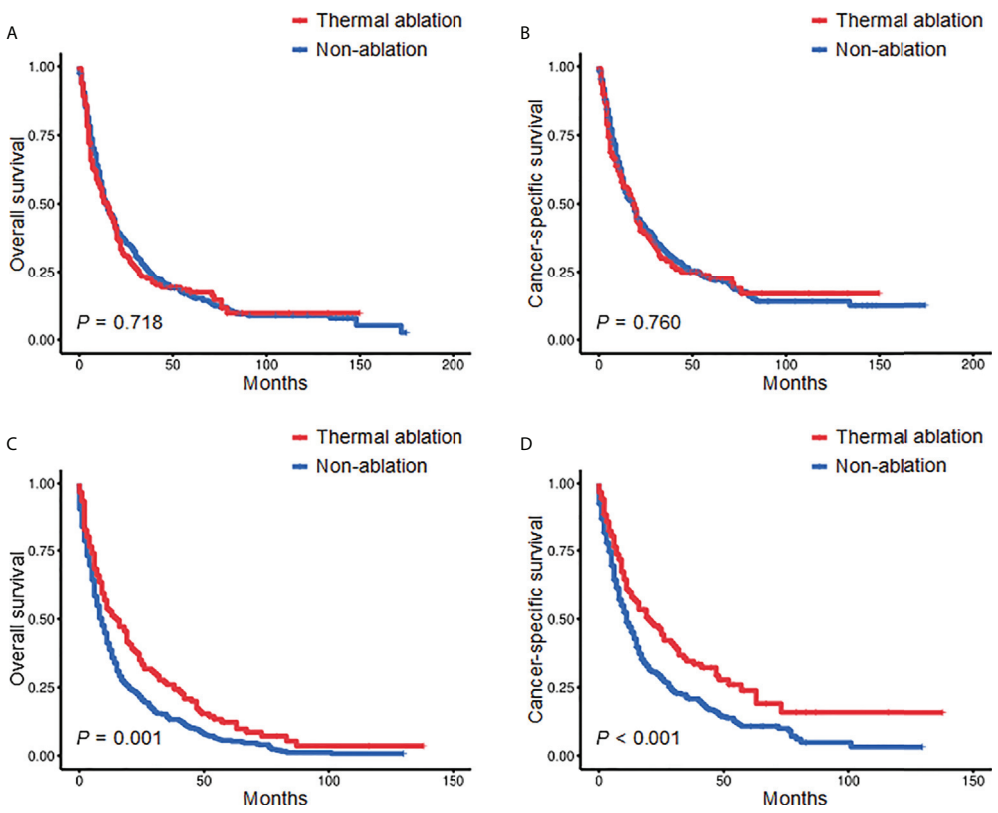

FIGURE 2
Kaplan-Meier survival curves comparing the TA and non-ablation groups when age was <70 years **(A, B)** or ≥70 years **(C, D)** after PSM. TA, thermal ablation; PSM, propensity score matching.

longer OS and CSS than those without. This finding is consistent with results from a study by Heon et al. (34) which retrospectively evaluated the efficacy of CT-guided RFA in 77 NSCLC patients. Among stage I-II NSCLC patients, the median OS for those receiving RFA alone was 28.2 months, which was similar to patients receiving surgery alone (p >0.05). For stage III-IV NSCLC patients who received chemotherapy, the median OS of those receiving RFA was longer than the OS of those with no ablation (42 months versus 29 months, p = 0.03).

Multivariate Cox regression analysis showed that age, sex, tumor site, pathological type, tumor size, radiotherapy, chemotherapy, and thermal ablation were independently associated with the OS and CSS of stage II-III NSCLC patients without surgical resection. Subgroup analysis stratified by age showed that TA improved the OS and CSS of individuals ≥70 years of age with stage II-III NSCLC. When age was <70 years, no significant difference in OS or CSS was observed between the TA and non-ablation groups. These results were similar to a study on stage I NSCLC patients (35). Zeng et al. compared the efficacy of TA and wedge resection and found that the OS and CSS of stage I NSCLC patients who received TA and wedge resection were comparable for individuals >75 years of age (p >0.05). However, the OS and CSS were significantly shorter for patients who received TA than those who received wedge resection among individuals ≤75 years of age (p <0.05). This may be because older patients have more medical comorbidities and poorer performance status. As a minimally invasive treatment technique, TA benefits elderly patients by significantly decreasing the likelihood of complications (36, 37).

There was a statistically significant difference in the OS and CSS of patients receiving TA and those without when tumor size was ≤3.0 cm. However, when tumor size was >3.0 cm, no significant differences in OS and CSS were observed between the groups. Xu et al. retrospectively evaluated the efficacy of MWA in 234 NSCLC patients (38). The median OS was 35 months for patients with tumor size <3.0 cm and only 16 months for patients with tumor size ≥3.0 cm (p <0.001). This may be because of the limited amount of tumor necrosis caused by TA. The occurrence of incomplete ablation for patients with large tumors may increase the risk of leaving tumor remnants and disease recurrence.

Cox proportional hazard analyses were performed to distinguish between several groups that benefitted more from TA. TA improved the OS and CSS of patients who were white or

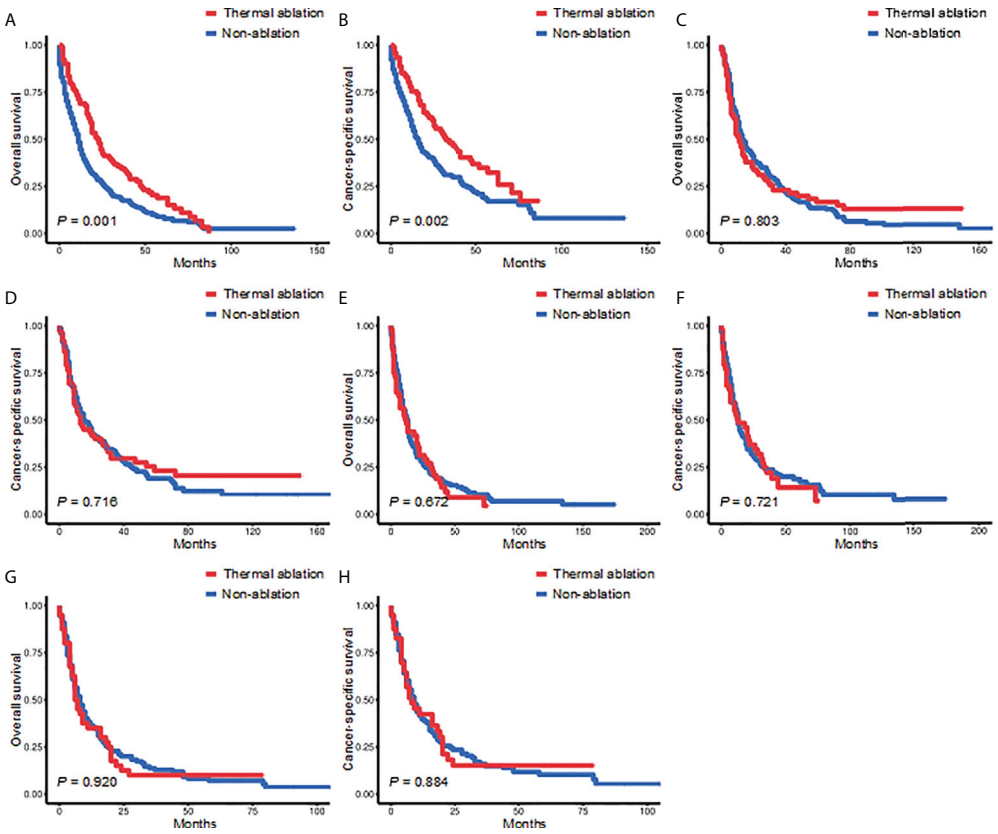

FIGURE 3
Kaplan-Meier survival curves for the TA and non-ablation groups when tumor size was ≤3.0 cm **(A, B)**, 3.1-5.0 cm **(C, D)**, 5.1-7.0 cm **(E, F)**, or >7.0 cm **(G, H)** after PSM. TA, thermal ablation; PSM, propensity score matching.

had right laterality, lung lobes, N0 staging, non-radiotherapy, and non-chemotherapy (p <0.05). Steber et al. reported the long-term outcomes from a prospective single-arm, phase 2 study of 13 inoperable NSCLC patients receiving combined RFA and external beam radiotherapy (EBRT) (39). The median progression-free survival of patients with combined RFA and EBRT was 37.8 months, similar to the survival of patients who received EBRT alone. Thus, RFA combined with EBRT was not recommended for patients with NSCLC.

No statistically significant differences were observed in the OS and CSS of patients receiving TA or no ablation among those receiving chemotherapy. The advantage of TA was more pronounced in patients without chemotherapy (p <0.05). Wei et al. (40) reported that the median OS of Stage III-IV lung adenocarcinoma patients was not significantly different between groups receiving MWA combined with chemotherapy or chemotherapy alone (23.9 months versus 17.3 months, p = 0.140). A study of 49 NSCLC patients by Li et al. (41) also showed no statistical difference in 3-year OS between those receiving MWA and chemotherapy or chemotherapy alone (21.057 months versus 17.843 months, p >0.05). In contrast, a study of 256 NSCLC patients by Xu et al. showed that the median OS was longer for patients with CT-guided RFA in combination with systemic chemotherapy than for those receiving chemotherapy alone (17.5 months versus 13.4 months, p <0.05) (42). Another retrospective study of 66 NSCLC patients reported by Feng et al. showed that patients who received MWA in combination with systemic chemotherapy had a longer median OS than those who received systemic chemotherapy alone (289.0 days versus 190.0 days, p = 0.018) (43). Overall, the effects of TA in combination with chemotherapy on OS and CSS remain unclear. Additional prospective multicenter randomized controlled trials are needed to explore the efficacy of TA in combination with chemotherapy in NSCLC patients.

Several factors may contribute to the survival benefits of TA among stage II-III NSCLC patients. First, TA can cause direct thermal injuries to targeted tissues. Temperatures exceeding 60°

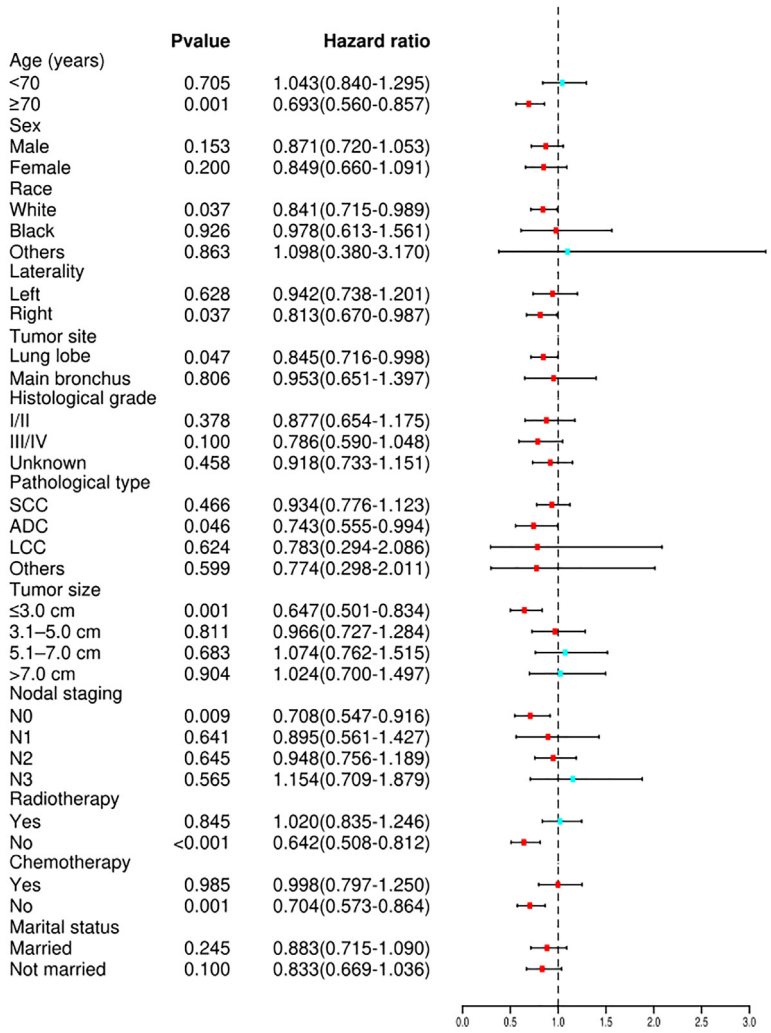

FIGURE 4
Forest plot depicting subgroup analysis of the OS between the TA and non-ablation groups after PSM. SCC, squamous cell carcinoma; ADC, adenocarcinoma; LCC, large cell carcinoma; OS, overall survival; TA, thermal ablation; PSM, propensity score matching.

C can cause cellular membrane lysis, protein denaturation, and enzyme inactivation, which lead to rapid coagulative necrosis (15, 44). Second, in the tumor periphery beyond the border of immediate tissue coagulation, TA can cause indirect thermal injuries, including vascular injury, ischemia-reperfusion, release of lysosomal contents (16, 45, 46). Finally, TA may result in the release of abundant immunogenic intracellular substrates, which can initiate and upregulate steps in the cancer immunity cycle required to elicit an anti-cancer immune response (47, 48).

The current study has several limitations. First, there was a lack of detail in the SEER database on targeted therapy, immunotherapy, and the results of genetic testing. Targeted therapies can inhibit the protein products of aberrant genes. Currently, oncogenic aberrations in eight genes (EGFR, ALK, ROS1, BRAF, KRAS, NTRK, MET, and RET) are approved therapies for NSCLC (49). Immunotherapies have also proven efficacious in NSCLC patients (50). However, the status of targeted therapy or immunotherapy and the results of genetic testing were not evaluated as variables in this study so the effects of these factors on prognosis could not be explored. Second, the type of TA modality may impact the prognosis. However, the SEER database was unable to differentiate between TA modalities (e.g., RFA, MWA, and ultrasound ablation), so this information could not be included. Third, a large proportion of cases in the SEER database had no detailed information on tumor extension, such as the description of various organ

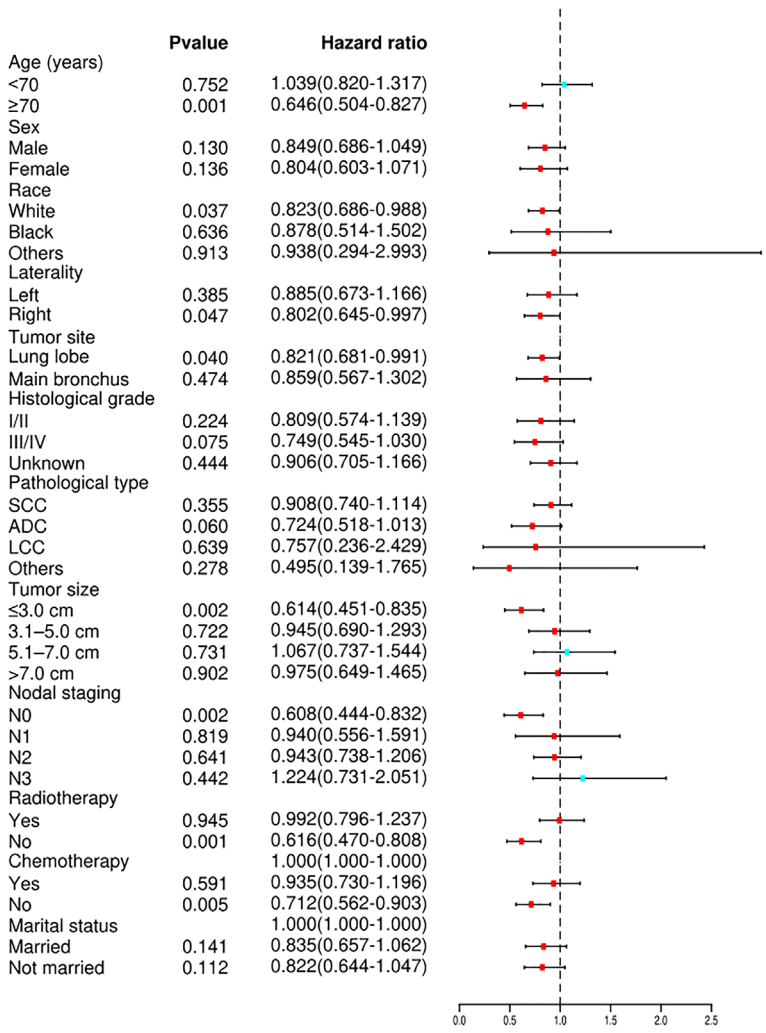

FIGURE 5
Forest plot depicting subgroup analysis of the CSS between the TA and non-ablation groups after PSM. SCC, squamous cell carcinoma; ADC, adenocarcinoma; LCC, large cell carcinoma; CSS, cancer-specific survival; TA, thermal ablation; PSM, propensity score matching.

invasions, so factors regarding the sith TNM stage could not be accurately transformed into the eighth TNM stage (subgroup, IIa, IIb, IIIa, IIIb, and IIIc) in stage II-III patients. Thus, stage II-III patients were not further stratified by stage, which may further bias the results. Finally, this study was retrospective so the strength of the results is weaker than it is for randomized controlled trials or prospective studies. Selection bias may be present because only patients with complete information were included.

Conclusion

In summary, TA could be an effective alternative treatment for stage II-III NSCLC patients unsuitable for surgical resection, particularly those ≥70 years of age, with tumor size ≤3.0 cm, or who did not receive radiotherapy.

Data availability statement

Publicly available data were analyzed in this study. The data can be found here: https://seer.cancer.gov/.

Ethics statement

Ethical review and approval was not required for the study on human participants in accordance with the local legislation and institutional requirements. Written informed consent for

participation was not required for this study in accordance with the national legislation and the institutional requirements.

Author contributions

W-YY and FY designed the study. W-YY and YH collected the data. W-YY, QH, and MP analyzed and interpreted the data. W-YY, ZZ, and SX drafted the manuscript. MP and FY proofread the manuscript for important intellectual content. All authors contributed to the article and approved the submitted version.

Funding

This work was supported by the National Natural Science Foundation of China (grant number 81972195), the Scientific Research Program of Hunan Provincial Health Commission (grant number 20201047), the Clinical Medical Technology Innovation Guide Project of Hunan Province (grant number 2020SK53408), and the National Clinical Key Specialty Construction Project.

Acknowledgments

The authors thank all the staff and participants of the SEER program.

Conflict of interest

The authors declare that the research was conducted in the absence of any commercial or financial relationships that could be construed as a potential conflict of interest.

Publisher's note

References

1. Sung H, Ferlay J, Siegel R, Laversanne M, Soerjomataram I, Jemal A, et al. Global cancer statistics 2020: Globocan estimates of incidence and mortality worldwide for 36 cancers in 185 countries. *CA: Cancer J Clin* (2021) 71(3):209–49. doi: 10.3322/caac.21660

2. Siegel RL, Miller KD, Fuchs HE, Jemal A. Cancer statistics, 2021. *CA Cancer J Clin* (2021) 71(1):7–33. doi: 10.3322/caac.21654

3. Dai C, Shen J, Ren Y, Zhong S, Zheng H, He J, et al. Choice of surgical procedure for patients with non-Small-Cell lung cancer ≤ 1 Cm or > 1 to 2 Cm among lobectomy, segmentectomy, and wedge resection: A population-based study. *J Clin Oncol* (2016) 34(26):3175–82. doi: 10.1200/jco.2015.64.6729

4. Saji H, Okada M, Tsuboi M, Nakajima R, Suzuki K, Aokage K, et al. Segmentectomy versus lobectomy in small-sized peripheral non-Small-Cell lung cancer (Jcog0802/Wjog4607l): A multicentre, open-label, phase 3, randomised, controlled, non-inferiority trial. *Lancet (London England)* (2022) 399 (10335):1607–17. doi: 10.1016/s0140-6736(21)02333-3

5. Okami J, Higashiyama M, Asamura H, Goya T, Koshiishi Y, Sohara Y, et al. Pulmonary resection in patients aged 80 years or over with clinical stage I non-small cell lung cancer: Prognostic factors for overall survival and risk factors for postoperative complications. *J Thorac Oncol* (2009) 4(10):1247–53. doi: 10.1097/JTO.0b013e3181ae285d

6. Qiang G, Liang C, Guo Y, Shi B, Tian Y, Song Z, et al. Video-assisted thoracoscopic lobectomy for elderly nonsmall cell lung cancer: Short-term and long-term outcomes. *J Cancer Res Ther* (2015) 11(4):793–7. doi: 10.4103/0973-1482.140930

7. Uhlig J, Ludwig JM, Goldberg SB, Chiang A, Blasberg JD, Kim HS. Survival rates after thermal ablation versus stereotactic radiation therapy for stage 1 non-small cell lung cancer: A national cancer database study. *Radiology* (2018) 289 (3):862–70. doi: 10.1148/radiol.2018180979

8. Ni Y, Huang G, Yang X, Ye X, Li X, Feng Q, et al. Microwave ablation treatment for medically inoperable stage I non-small cell lung cancers: Long-term results. *Eur Radiol* (2022) 32(8):5616–22. doi: 10.1007/s00330-022-08615-8

9. Iezzi R, Cioni R, Basile D, Tosoratti N, Posa A, Busso M, et al. Standardizing percutaneous microwave ablation in the treatment of lung tumors: A prospective multicenter trial (Malt study). *Eur Radiol* (2021) 31(4):2173–82. doi: 10.1007/s00330-020-07299-2

10. Lindberg K, Grozman V, Karlsson K, Lindberg S, Lax I, Wersäll P, et al. The hilus-trial-a prospective Nordic multicenter phase 2 study of ultracentral lung tumors treated with stereotactic body radiotherapy. *J Thorac Oncol* (2021) 16 (7):1200–10. doi: 10.1016/j.jtho.2021.03.019

11. Detillon D, Driessen EJM, Aarts MJ, Janssen-Heijnen MLG, van Eijck CHJ, Veen EJ. Changes in treatment patterns and survival in elderly patients with stage I non-Small-Cell lung cancer with the introduction of stereotactic body radiotherapy and video-assisted thoracic surgery. *Eur J Cancer (Oxford Engl 1990)* (2018) 101:30–7. doi: 10.1016/j.ejca.2018.06.016

12. Olive G, Yung R, Marshall H, Fong KM. Alternative methods for local ablation-interventional pulmonology: A narrative review. *Trans Lung Cancer Res* (2021) 10(7):3432–45. doi: 10.21037/tlcr-20-1185

13. Fallahi H, Prakash P. Antenna designs for microwave tissue ablation. *Crit Rev Biomed Eng* (2018) 46(6):495–521. doi: 10.1615/CritRevBiomedEng.2018028554

14. Maxwell AWP, Park WKC, Baird GL, Martin DW, Lombardo KA, Dupuy DE. Effects of a thermal accelerant gel on microwave ablation zone volumes in lung: A porcine study. *Radiology* (2019) 291(2):504–10. doi: 10.1148/radiol.2019181652

15. Huang L, Yang S, Bai M, Lin Y, Chen X, Li G, et al. Thermal shielding performance of self-healing hydrogel in tumor thermal ablation. *Colloids surfaces B Biointerfaces* (2022) 213:112382. doi: 10.1016/j.colsurfb.2022.112382

16. Bianchi L, Cavarzan F, Ciampitti L, Cremonesi M, Grilli F, Saccomandi P. Thermophysical and mechanical properties of biological tissues as a function of temperature: A systematic literature review. *Int J hyperthermia* (2022) 39(1):297–340. doi: 10.1080/02656736.2022.2028908

17. Chan MV, Huo YR, Cao C, Ridley L. Survival outcomes for surgical resection versus ct-guided percutaneous ablation for stage I non-small cell lung cancer (Nsclc): A systematic review and meta-analysis. *Eur Radiol* (2021) 31 (7):5421–33. doi: 10.1007/s00330-020-07634-7

18. Ambrogi MC, Fanucchi O, Dini P, Melfi F, Davini F, Lucchi M, et al. Wedge resection and radiofrequency ablation for stage I nonsmall cell lung cancer. *Eur Respir J* (2015) 45(4):1089–97. doi: 10.1183/09031936.00188014

19. Hiraki T, Gobara H, Mimura H, Matsui Y, Toyooka S, Kanazawa S. Percutaneous radiofrequency ablation of clinical stage I non-small cell lung cancer. *J Thorac Cardiovasc Surg* (2011) 142(1):24–30. doi: 10.1016/j.jtcvs.2011.02.036

20. Venturini M, Cariati M, Marra P, Masala S, Pereira PL, Carrafiello G. Cirse standards of practice on thermal ablation of primary and secondary lung tumours. *Cardiovasc interventional Radiol* (2020) 43(5):667–83. doi: 10.1007/s00270-020-02432-6

21. Postmus PE, Kerr KM, Oudkerk M, Senan S, Waller DA, Vansteenkiste J, et al. Early and locally advanced non-Small-Cell lung cancer (Nsclc): Esmo clinical practice guidelines for diagnosis, treatment and follow-up. *Ann Oncol* (2017) 28 (suppl_4):iv1–iv21. doi: 10.1093/annonc/mdx222

22. Daly ME, Singh N, Ismaila N, Antonoff MB, Arenberg DA, Bradley J, et al. Management of stage iii non-Small-Cell lung cancer: Asco guideline. *J Clin Oncol* (2022) 40(12):1356–84. doi: 10.1200/jco.21.02528

23. Oncology Society of Chinese Medical Association and Chinese Medical Association Publishing House (2022). Chinese medical association guideline for clinical diagnosis and treatment of lung cancer (2022 Eds). *Zhonghua Zhong Liu Za Zhi [Chinese J Oncol]* 44(6):457–90. doi: 10.3760/cma.j.cn112152-20220413-00255

24. Dawe DE, Christiansen D, Swaminath A, Ellis PM, Rothney J, Rabbani R, et al. Chemoradiotherapy versus radiotherapy alone in elderly patients with stage iii non-small cell lung cancer: A systematic review and meta-analysis. *Lung Cancer (Amsterdam Netherlands)* (2016) 99:180–5. doi: 10.1016/j.lungcan.2016.07.016

25. Sigel K, Lurslurchachai L, Bonomi M, Mhango G, Bergamo C, Kale M, et al. Effectiveness of radiation therapy alone for elderly patients with unresected stage iii non-small cell lung cancer. *Lung Cancer (Amsterdam Netherlands)* (2013) 82 (2):266–70. doi: 10.1016/j.lungcan.2013.06.011

26. Li M, Xu X, Qin Y, Zhang P, Shen C, Xia Q, et al. Radiofrequency ablation vs. stereotactic body radiotherapy for stage ia non-small cell lung cancer in nonsurgical patients. *J Cancer* (2021) 12(10):3057–66. doi: 10.7150/jca.51413

27. Uhlig J, Mehta S, Case MD, Dhanasopon A, Blasberg J, Homer RJ, et al. Effectiveness of thermal ablation and stereotactic radiotherapy based on stage I lung cancer histology. *J Vasc interventional Radiol* (2021) 32(7):1022–8.e4. doi: 10.1016/j.jvir.2021.02.025

28. Miller KD, Ostrom QT, Kruchko C, Patil N, Tihan T, Cioffi G, et al. Brain and other central nervous system tumor statistics, 2021. *CA Cancer J Clin* (2021) 71 (5):381–406. doi: 10.3322/caac.21693

29. Lim YJ, Kim Y, Kong M. Comparative survival analysis of preoperative and postoperative radiotherapy in stage ii-iii rectal cancer on the basis of long-term population data. *Sci Rep* (2018) 8(1):17153. doi: 10.1038/s41598-018-35493-2

30. Li X, An B, Ma J, He B, Qi J, Wang W, et al. Prognostic value of the tumor size in resectable colorectal cancer with different primary locations: A retrospective study with the propensity score matching. *J Cancer* (2019) 10(2):313–22. doi: 10.7150/jca.26882

31. Kyrylenko S, Gogotsi O, Baginskiy I, Balitskyi V, Zahorodna V, Husak Y, et al. Mxene-assisted ablation of cells with a pulsed near-infrared laser. *ACS Appl Materials Interfaces* (2022) 14(25):28683–96. doi: 10.1021/acsami.2c08678

32. Chen Y, Huang H, Li Y, Xiao W, Liu Y, Chen R, et al. Tigit blockade exerts synergistic effects on microwave ablation against cancer. *Front Immunol* (2022) 13:832230. doi: 10.3389/fimmu.2022.832230

33. Ambrogi MC, Fanucchi O, Cioni R, Dini P, De Liperi A, Cappelli C, et al. Long-term results of radiofrequency ablation treatment of stage I non-small cell lung cancer: A prospective intention-to-Treat study. *J Thorac Oncol* (2011) 6 (12):2044–51. doi: 10.1097/JTO.0b013e31822d538d

34. Lee H, Jin GY, Han YM, Chung GH, Lee YC, Kwon KS, et al. Comparison of survival rate in primary non-Small-Cell lung cancer among elderly patients treated with radiofrequency ablation, surgery, or chemotherapy. *Cardiovasc interventional Radiol* (2012) 35(2):343–50. doi: 10.1007/s00270-011-0194-y

35. Zeng C, Lu J, Tian Y, Fu X. Thermal ablation versus wedge resection for stage I non-small cell lung cancer based on the eighth edition of the tnm classification: A population study of the us seer database. *Front Oncol* (2020) 10:571684. doi: 10.3389/fonc.2020.571684

36. Gironés R, Torregrosa D, Gómez-Codina J, Maestu I, Tenias JM, Rosell R. Prognostic impact of comorbidity in elderly lung cancer patients: Use and comparison of two scores. *Lung Cancer (Amsterdam Netherlands)* (2011) 72 (1):108–13. doi: 10.1016/j.lungcan.2010.07.001

37. Yang H, Li M, Mei T. Survival benefit of thermal ablation combined with chemotherapy for the treatment of stage iv nonsmall cell lung cancer: A propensity-matched analysis. *Int J hyperthermia* (2022) 39(1):348–57. doi: 10.1080/02656736.2022.2038281

38. Xu S, Qi J, Li B, Li XG. Survival prediction for non-small cell lung cancer patients treated with ct-guided microwave ablation: Development of a prognostic nomogram. *Int J hyperthermia* (2021) 38(1):640–9. doi: 10.1080/02656736.2021.1914353

39. Steber CR, Hughes RT, Urbanic J, Clark H, Petty WJ, Blackstock AW, et al. Long-term outcomes from a phase 2 trial of radiofrequency ablation combined with external beam radiation therapy for patients with inoperable non-small cell lung cancer. *Int J Radiat oncology biology Phys* (2021) 111(1):152–6. doi: 10.1016/j.ijrobp.2021.04.020

40. Wei Z, Ye X, Yang X, Huang G, Li W, Wang J, et al. Microwave ablation plus chemotherapy improved progression-free survival of advanced non-small cell lung cancer compared to chemotherapy alone. *Med Oncol (Northwood London England)* (2015) 32(2):464. doi: 10.1007/s12032-014-0464-z

41. Li C, Wang J, Shao JB, Zhu LM, Sun ZG, Zhang N. Microwave ablation combined with chemotherapy improved progression free survival of iv stage lung adenocarcinoma patients compared with chemotherapy alone. *Thorac Cancer* (2019) 10(7):1628–35. doi: 10.1111/1759-7714.13129

42. Xu F, Cai Z, Xu B, Song J, Liu H, Li X, et al. Clinical research on the combined use of systemic chemotherapy and ct-guided radiofrequency ablation in treatment of lung cancer. *Lasers Med Sci* (2022) 37(1):233–9. doi: 10.1007/s10103-020-03222-9

43. Feng K, Lu Y. Clinical analysis of systemic chemotherapy combined with microwave ablation in the treatment of lung cancer. *Asian J Surg* (2022) 45 (5):1107–12. doi: 10.1016/j.asjsur.2021.08.013

44. Geoghegan R, Ter Haar G, Nightingale K, Marks L, Natarajan S. Methods of monitoring thermal ablation of soft tissue tumors - a comprehensive review. *Med Phys* (2022) 49(2):769–91. doi: 10.1002/mp.15439

45. Huang XW, Nie F, Wa ZC, Hu HT, Huang QX, Guo HL, et al. Thermal field distributions of ablative experiments using cyst-mimicking phantoms: Comparison of microwave and radiofrequency ablation. *Acad Radiol* (2018) 25(5):636–42. doi: 10.1016/j.acra.2017.11.010

46. Kok HP, Cressman ENK, Ceelen W, Brace CL, Ivkov R, Grüll H, et al. Heating technology for malignant tumors: A review. *Int J hyperthermia* (2020) 37 (1):711–41. doi: 10.1080/02656736.2020.1779357

47. Rangamuwa K, Leong T, Weeden C, Asselin-Labat ML, Bozinovski S, Christie M, et al. Thermal ablation in non-small cell lung cancer: A review of treatment modalities and the evidence for combination with immune checkpoint inhibitors. *Trans Lung Cancer Res* (2021) 10(6):2842–57. doi: 10.21037/tlcr-20-1075

48. Dromi SA, Walsh MP, Herby S, Traughber B, Xie J, Sharma KV, et al. Radiofrequency ablation induces antigen-presenting cell infiltration and amplification of weak tumor-induced immunity. *Radiology* (2009) 251(1):58–66. doi: 10.1148/radiol.2511072175

49. Rivera-Concepcion J, Uprety D, Adjei AA. Challenges in the use of targeted therapies in non-small cell lung cancer. *Cancer Res Treat* (2022) 54(2):315–29. doi: 10.4143/crt.2022.078

50. Cascone T, Fradette J, Pradhan M, Gibbons DL. Tumor immunology and immunotherapy of non-Small-Cell lung cancer. *Cold Spring Harbor Perspect Med* (2022) 12(5):22. doi: 10.1101/cshperspect.a037895

frontiers | Frontiers in Oncology

TYPE Original Research
PUBLISHED 23 August 2022
DOI 10.3389/fonc.2022.981789

OPEN ACCESS

EDITED BY
Yuliang Li,
The Second Hospital of Shandong University, China

REVIEWED BY
Paul Zarogoulidis,
G. Papanikolaou General Hospital, Greece
Weijun Fan,
Sun Yat-sen University Cancer Center (SYSUCC), China

*CORRESPONDENCE
Zhengyu Lin
linsinlan@aliyun.com

†These authors have contributed equally to this work and share first authorship

SPECIALTY SECTION
This article was submitted to Thoracic Oncology, a section of the journal Frontiers in Oncology

RECEIVED 29 June 2022
ACCEPTED 15 July 2022
PUBLISHED 23 August 2022

CITATION
Chen J, Qi L, Chen J, Lin QF, Yan Y, Chen j and Lin Z (2022) Microwave ablation therapy assisted by artificial pneumothorax and artificial hydrothorax for lung cancer adjacent to the vital organs.
Front. Oncol. 12:981789.
doi: 10.3389/fonc.2022.981789

Microwave ablation therapy assisted by artificial pneumothorax and artificial hydrothorax for lung cancer adjacent to the vital organs

Jian Chen[1†], Liqin Qi[2†], Jin Chen[1], Qingfeng Lin[1], Yuan Yan[1], Jie Chen[3] and Zhengyu Lin[1,4*]

[1]Department of Interventional Radiology, First Affiliated Hospital of Fujian Medical University, Fuzhou, China, [2]Department of Endocrinology, Fujian Institute of Endocrinology, Fujian Medical University Union Hospital, Fuzhou, China, [3]Department of Interventional Radiology, Sanming Second Hospital, Sanming, China, [4]Fujian Provincial Key Laboratory of Precision Medicine for Cancer, First Affiliated Hospital of Fujian Medical University, Fuzhou, China

Objectives: This study aimed to investigate the technical methods and safety of artificial pneumothorax and artificial hydrothorax in the treatment of lung cancer adjacent to vital organs by CT-guided microwave ablation.

Subjects and Methods: Three of the six patients were men and three were women, with a mean age of 66.0 years (range 47–78 years). There patients had primary pulmonary adenocarcinoma, one had lung metastasis from liver cancer, one had lung metastasis from colon cancer, and one had lung metastasis from bladder cancer. There were four patients with a single lesion, one with two lesions, and one with three lesions. The nine lesions had a mean diameter of 1.1 cm (range 0.4–1.9). In three patients, the lung cancer was adjacent to the heart, and in the remaining three, it was close to the superior mediastinum. Six patients were diagnosed with lung cancers or lung metastases and received radical treatment with microwave ablation (MWA) assisted by artificial pneumothorax and artificial hydrothorax in our hospital. Postoperative complications were observed and recorded; follow-up was followed to evaluate the therapeutic effect.

Results: The artificial pneumothorax and artificial hydrothorax were successfully created in all six patients. A suitable path for ablation needle insertion was also successfully established, and microwave ablation therapy was carried out. 2 patients developed pneumothorax after operation; no serious complications such as operation-related death, hemothorax, air embolism and infection occurred.Moreover, 4–6 weeks later, an enhanced CT re-examination revealed no local recurrence or metastasis, and the rate of complete ablation was 100%.

Conclusions: Microwave ablation, assisted by artificial pneumothorax, artificial hydrothorax, is a safe and effective minimally invasive method for treating lung

cancer adjacent to the vital organs, and optimizing the path of the ablation needle and broadening the indications of the ablation therapy

KEYWORDS

lung cancer, artificial pneumothorax, artificial hydrothorax, microwave ablation, x-ray computed tomography

Introduction

Lung cancer was the most common cancer in men, accounting for about 24.6% (549,800) of all new cancers in China;and was the second common cancer in women. And lung cancer was the most common cause of cancer death both for both sexes in China (1).Surgical resection remains the reference standard for the treatment of localized non-small cell lung cancer. However, only 20% of all diagnosed lung cancers are surgically resectable (2). Microwave ablation (MWA) has been proved to be safe and effective in the treatment of primary and metastatic lung tumor (3–5). MWA can be an alternative treatment

modality for early-stage NSCLC patients who are ineligible for surgery (6–10). When the lung lesions were adjacent to the vital organs (including the esophagus, trachea, heart, great vessels, diaphragm, and mediastinum), it was difficult to clearly show the effective puncture path and perform the ablation using a conventional CT scan. Alternatively, due to an insufficient safety margin, conventional percutaneous ablation is likely to cause thermal damage to the vital organs, resulting in serious complications. To address this technical issue, microwave ablation therapy with artificial pneumothorax, artificial hydrothorax, and body position adjustment was used for lung cancer adjacent to the vital organs, with satisfactory effects. The report is as follows.

Materials and methods

Clinical data

From November 2020 to March 2022, six patients were diagnosed with lung cancer adjacent to the vital organs (including the esophagus, trachea, heart, great vessels, diaphragm, and mediastinum) and received radical treatment with microwave ablation (MWA) assisted by artificial pneumothorax and artificial hydrothorax in our hospital. Three of the six patients were men and three were women, with a mean age of 66.0 years (range 47–78 years). There patients had primary pulmonary adenocarcinoma, one had lung metastasis from liver cancer, one had lung metastasis from colon cancer, and one had lung metastasis from bladder cancer. There were four patients with a single lesion, one with two lesions, and one with three lesions. The nine lesions had a mean diameter of 1.1 cm (range 0.4–1.9). In three patients, the lung cancer was adjacent to the heart, and in the remaining three, it was close to the superior mediastinum. Inclusion criteria were as follows: ① patients with primary or metastatic lung cancer confirmed by puncture histological biopsy or imaging examination; ② patients who could not tolerate surgical resection due to poor cardiopulmonary function or old age; ③ patients who refused surgical resection; ④ patients who had a new or residual lesion after surgical resection and were unable to tolerate or refused re-surgery; ⑤ patients with multiple ground-glass nodules (GGNs) (ablation of the primary lesion first before considering the ablation of the other lesions according to the progression); ⑥ patients with lesions adjacent to the vital organs, with a distance ≤ 0.5 cm, and were more likely to suffer thermal damage to the vital organs; and ⑦ patients with a total number of unilateral lung metastases ≤3, total number of bilateral lung metastases ≤5, and maximum tumor diameter ≤3 cm. Exclusion criteria were as follows: ① patients suffering from severe cardiac, hepatic, pulmonary, or renal failure, ② patients with platelet count $<50\times10^9$/L, ③ patients with severe bleeding proclivity and coagulation dysfunction that could not be corrected in a timely manner, and ④ patients with severe pulmonary fibrosis and pulmonary hypertension. Table 1 shows the general conditions of the patients.

Instruments and equipment

①64 fit multi-slice spiral computed tomography (CT) scanner (Siemens SOMATOM definition AS, Germany). ②MTC-3C MWA system (Vision-China Medical Devices R&D Center/KY-2450B MWA system (Nanjing Great Wall Institute for Application of Microwave Energy), the microwave emission frequency is (2450 ± 50) MHz, and the output power is 0–100 W. ③Water-cooled MWA antenna (effective length is 100–180 mm, outer diameter is 15–18 G, and emission length of the end microwave is 15 mm). ④Catheter (8F-20cm, Guangdong Baihe Medical Technology Co.,Ltd)

TABLE 1 Clinical data of 6 patients with lung cancer and the results of microwave ablation therapy assisted by artificial pneumothorax and artificial hydrothorax.

Number	Gender	Age (year)	Primary tumor and pathological classification	tumor stage	Number of tumors (pcs)	maximum tumor diameter (cm)	Artificial pneumothorax volume (ml	Artificial pleural effusion volume (ml)	complication
1	woman	72	pulmonary adenocarcinoma	I	2	1.7	200	400	none
2	man	55	colon cancer	IV	1	1.0	200	200	pneumothorax
3	woman	68	bladder cancer	IV	1	1.3	200	400	none
4	woman	76	pulmonary adenocarcinoma	I	1	1.9	200	300	none
5	man	47	liver cancer	IIIb	3	1.0	300	500	pneumothorax
6	man	78	pulmonary adenocarcinoma	I	1	1.5	100	500	none

Preoperative preparation

The size, location, and adjacent important organs and blood vessels of the lesions were detected by conventional CT plain scans and enhanced examinations within 2 weeks before the operation (Figure 1). Blood routine examinations and coagulation time were evaluated to exclude hemorrhagic diseases. The patients fasted for 4 h before the operation, and the venous channels were opened.The patients underwent breath–holding training according to the preoperative imaging data.

Operating procedures

Artificial pneumothorax

The patient was positioned supine, the examination couch was adjusted to the level of the diaphragm dome on the puncture side, and a positioning fence was taped to the body surface where the needle was to be inserted. The laser positioning light was activated, and the needle insertion site was determined while keeping the heart in mind. Before the puncture, routine disinfection and placement of surgical drape were performed, as well as layer-by-layer infiltration anesthesia with 2% lidocaine. When the bevel tip of the 5-ml syringe needle reached the pleura, the syringe would be removed, a transparent rubber tube would be connected, and a little sterile saline would be injected into the tube to form a water column (Figure 2); when the needle tip broke through the parietal pleura and the water column was drawn into the pleural cavity containing certain negative pressure, the rubber tube would be removed, a three-way tube and a 50-ml syringe would be connected, and an appropriate amount of air (100–300 ml) would be injected into the pleural cavity (Figure 3). Following that, the patient was evaluated for chest tightness, shortness of breath, and other uncomfortable symptoms. The three-way tube was closed after the artificial pneumothorax was created.

FIGURE 1
Preoperative scan: Preoperative CT showed a nodule in the right upper lobe. Invasive adenocarcinoma of the right upper lobe of a 78-year-old man.

FIGURE 2
The artificial pneumothorax was created: Intraoperative scan was acquired with the patient in the supine position. the examination couch was adjusted to the level of the diaphragm dome on the puncture side. When the bevel tip of the 5-ml syringe needle reached the pleura, the syringe would be removed, a transparent rubber tube would be connected, and a little sterile saline would be injected into the tube to form a water column.

Artificial hydrothorax

Following the establishment of the artificial pneumothorax, a positioning fence is attached to the proposed tube placement site on the body surface, and the laser positioning light is activated to determine the needle entry point. Before the puncture, routine disinfection and placement of surgical drape were performed, as well as layer-by-layer infiltration anesthesia with 2% lidocaine. The guide wire was inserted after the puncture needle gradually reached the pleural cavity containing the artificial pneumothorax, and an 8F central venous catheter was indwelled along the guide wire (Figure 4). To isolate the lesion and the adjacent vital organs, an appropriate amount of normal saline (200–500 ml) was injected into the catheter to form an isolation belt (Figure 5). The injection process should be done slowly in order to see if the patient develops chest tightness, shortness of breath and other symptoms. It was decided to make an artificial hydrothorax.

Microwave ablation therapy

Following the establishment of the artificial pneumothorax and artificial hydrothorax, the size, location, blood flow, and other characteristics of the tumor were reconfirmed using the preoperative CT of the patient, and the patient's body position was adjusted to the optimal puncture position (Figure 6). Next, guided by CT, the needle was gradually inserted through the microwave antenna to the bottom of the lesion for ablation (Figures 7–9). The appropriate microwave output power and ablation time were chosen based on the tumor size and shape. The preset microwave ablation power was set to 50–80 W, and the ablation time was limited to 20 min (Figure 10).

Immediate efficacy evaluation and follow-up

Evaluation of immediate efficacy (11) was as follows: ① preliminary evaluation of the success of the operating technique and ② observation of the ablation boundary. Recommendation: For complete ablation, the post-ablation ground-glass opacity around the post-ablation target zone should be at least 5 mm greater than the boundary of the gross tumor region (GTR); ③ Complications should be observed.

Local therapeutic efficacy evaluation (12, 13): The lesion on the enhanced chest CT re-examination 4–6 weeks after surgery served as the baseline for judging efficacy. ① Complete ablation

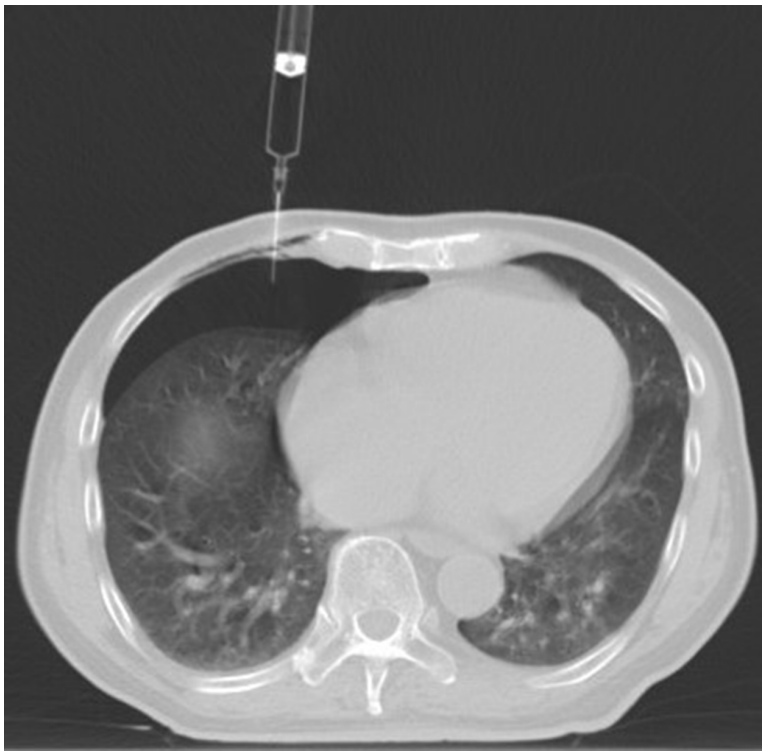

FIGURE 3
When the needle tip broke through the parietal pleura and the water column was drawn into the pleural cavity containing certain negative pressure, and an appropriate amount of air (100 ml) would be injected into the pleural cavity.

FIGURE 4
The artificial hydrothorax was created: Following the establishment of the artificial pneumothorax, the guide wire was inserted after the puncture needle gradually reached the pleural cavity containing the artificial pneumothorax, and an 8F central venous catheter was indwelled along the guide wire.

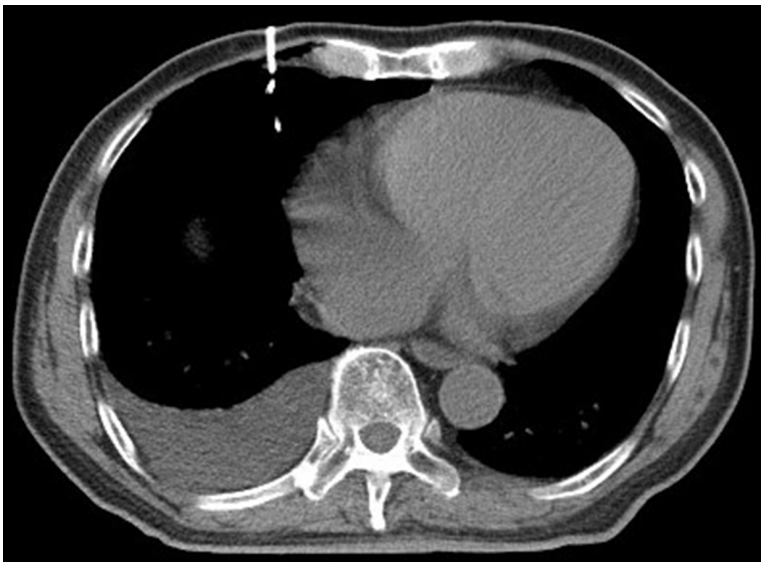

FIGURE 5
To isolate the lesion and the adjacent vital organs, an appropriate amount of normal saline (500 ml) was injected into the catheter to form an isolation belt.

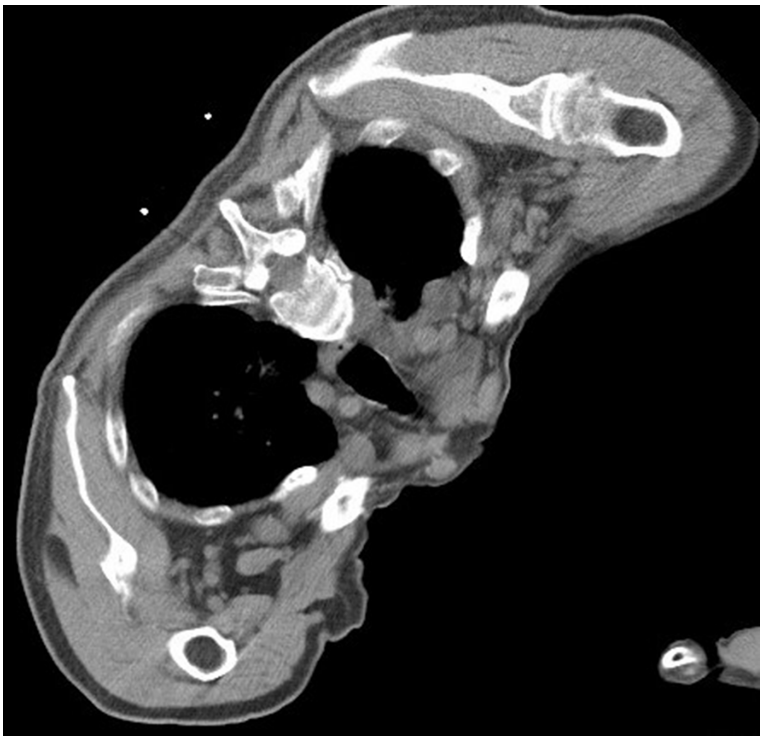

FIGURE 6
Intraoperative scan: the patient's body position was adjusted to isolate the lesion and the adjacent vital organs, and the appropriate amount of normal saline was to form an isolation belt.

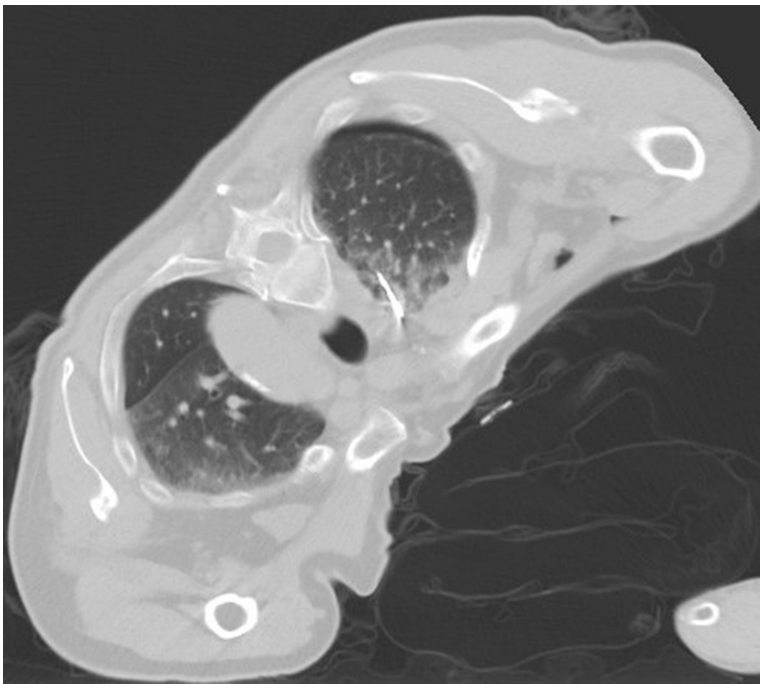

FIGURE 7
Guided by CT, the needle was gradually inserted through the microwave antenna to the bottom of the lesion for ablation.

(presence of any of the following manifestations): disappearance of the lesion, complete formation of the cavity, fibrosis of the lesion (scar), reduction, no change or enlargement of the solid nodule (no signs of abnormal enhancement of the contrast agent on the CT scan), atelectasis (absence of any signs of abnormal enhancement of the contrast agent on the CT scan of the lesion in the atelectasis) (Figures 11, 12). ② Incomplete ablation (presence of any of the following manifestations): (a) On the cavity formation and fibrosis edges of the lesion, there were still typical imaging manifestations of GGN; (b) there was fibrosis in part of the lesion, but there were still some solid components, and the solid part showed enhancement on the CT scan and/or the tumor showed metabolic activity on the positron emission tomography-computed tomography (PET-CT) scan; (c) the solid nodule did not change in size or enlargement, but it did show signs of abnormal contrast enhancement on CT scan and/or abnormal metabolic activity on PET-CT scan.

Statistical methods

Data were analyzed using IBM SPSS Statistics for Windows, version 22.0 (IBM Corp., New York). Measurement data were expressed as means ± standard deviation, whereas counting data were expressed as percentages and were compared by Chi-square tests. P <0.05 was considered a statistically significant difference.

Results

Ablation results

After injections with a mean amount of gas of 200.0 ml (range 100–300) and a mean amount of normal saline of 383.3 ml (range 200–500), the artificial pneumothorax and artificial hydrothorax were successfully created in all six patients. A suitable path for ablation needle insertion was also successfully established, and microwave ablation therapy was carried out. For the creation of the artificial pneumothorax and artificial hydrothorax, the surgery time increased by an average of 21.5min (range 16.5–39.6), and the number of local scans increased by an average of 8 times (range 5–12). The conventional CT scan performed 3 days after ablation confirmed that all lesions had been completely abated. Moreover, 4–6 weeks later, an enhanced CT re-examination revealed no local recurrence or metastasis, and the rate of complete ablation was 100%.

Complication

All patients tolerated the surgery. two patients developed pneumothorax after operation, which improved after intubation and drainage; no serious complications such as

FIGURE 8
Intraoperative scan: the Reconstructed CT image.

operation-related death, hemothorax, air embolism and infection occurred.

Discussion

As a precise and minimally invasive technique, local microwave ablation has grown in popularity in recent years. It has been used to treat lung cancer, especially early-stage lung cancer, with remarkable therapeutic results (3–10, 14). MWA operates under the action of a microwave electromagnetic field: the polar molecules in the tumor tissue, such as water molecules and protein molecules, vibrate at an extremely high speed, causing the collision and friction between molecules, producing a high temperature of up to 60°C–150°C in a short period of time, and resulting in coagulative necrosis of cells. Concentrated in a certain range by the radiator, the microwave energy can be effectively radiated to the desired target zone. Thermal microwave radiation causes more convection and less thermal precipitation in the lung (12, 13, 15). Therefore, this technique has a minimal invasion,

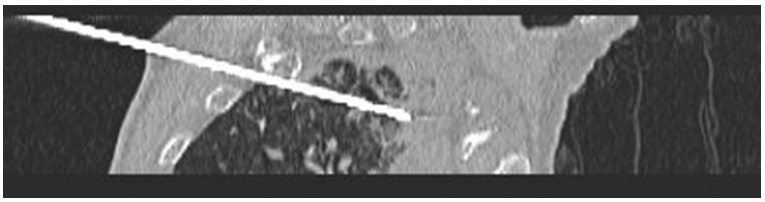

FIGURE 9
Intraoperative scan: the Reconstructed CT image.

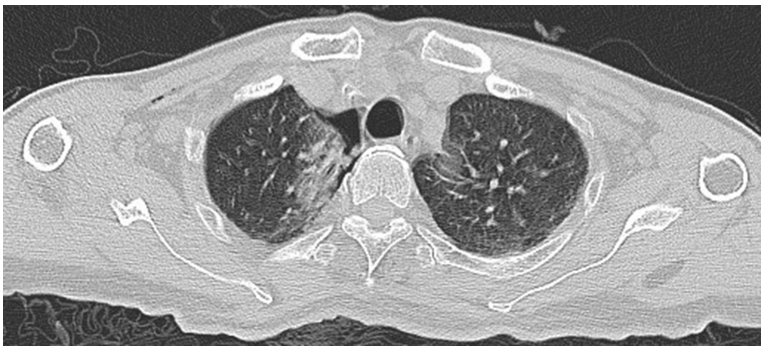

FIGURE 10
Post-ablation scan: The lesion was achieved complete ablationthe: post-ablation ground-glass opacity around the post-ablation target zone should be at least 5 mm greater than the boundary of the gross tumor region.

definite curative effect, high safety, strong repeatability, and suitability for a wide range of people.

The artificial pneumothorax or artificial hydrothorax is a useful adjunct in the clinical treatment of various diseases. Professor Lin Zhengyu and his team successfully performed puncture biopsy in 11 patients with mediastinal lesions, using artificial pneumothorax and body position adjustment, with no pneumothorax or bleeding complications (16). Moreover, artificial pneumothorax is a safe and effective method for pain relief during MWA of subpleural lung tumors (17, 18). In addition, artificial pneumothorax or hydrothorax has been used with significant success in thermal ablation of tumors adjacent to lung tissue in the lower lobe or near the diaphragm dome (19–21). In this study, because the lung lesions were adjacent to the vital organs, it was difficult to clearly show the effective puncture path and perform the ablation using a conventional CT scan. Alternatively, due to an insufficient safety margin, conventional percutaneous ablation is likely to cause thermal damage to the vital organs, resulting in serious complications. The introduction of artificial pneumothorax and artificial hydrothorax not only solves this problem but also broadens the scope of microwave ablation therapy. It is easy to create an artificial pneumothorax, and it is also simple to separate lesions from adjacent structures using an artificial pneumothorax and body position adjustment. However, after the artificial pneumothorax was established, the isolated local visceral pleura becomes significantly more elastic, and the local pulmonary motion increases, making the pulmonary nodules more likely to displace during the puncture with ablation needle. And because such displacement makes puncturing the pulmonary nodules more difficult, it is often difficult to puncture into the center of the lesion for ablation. When compared to artificial pneumothorax, isolation with artificial hydrothorax has less impact on the elasticity of the local visceral pleura and local pulmonary motion, making it easier to puncture the pulmonary nodules, allowing for puncture into the center of the lesion for ablation and improving the efficacy of ablation. Because creating

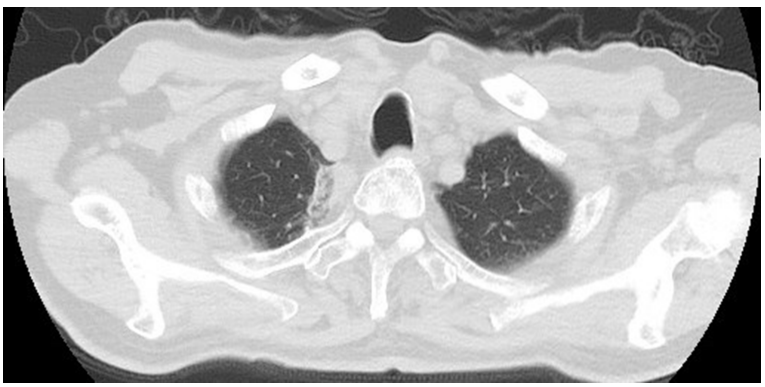

FIGURE 11
Cross-sectional image:Follow-up after 1 month found that the lesions were completely ablated, and no tumor lesions remained or recurred.

FIGURE 12
Coronal image:Follow-up after 1 month found that the lesions were completely ablated, and no tumor lesions remained or recurred.

artificial hydrothorax under CT guidance is relatively difficult, artificial pneumothorax is often created before artificial hydrothorax; if complicated with pleural hemorrhage, artificial hydrothorax may affect judgment of hemothorax. Therefore, artificial pneumothorax was used in combination with artificial hydrothorax in this study to successfully assist in the microwave ablation of lung cancer in six patients. This combination therapy not only provided a good puncture path for ablation, but it also protected the adjacent vital organs from thermal damage during thermal ablation, resulting in remarkable results. Excessive gas or liquid in the pleural cavity will impair respiratory functions and may cause chest tightness, shortness of breath, dyspnea, and chest pain, especially in patients with poor lung function. In this study, the amount of injected gas and liquid was reduced by adjusting the body position of patients. There was no death or other special disease associated with surgery following ablation therapy, and there was no serious cardiopulmonary disease caused by the large amount of gas and liquid injected. These findings are sufficient to demonstrate the high safety of ablation therapy, which is assisted by artificial pneumothorax, artificial hydrothorax, and body position adjustment.

In this study, the rate of complete ablation was 100%, only two patients developed pneumothorax, and there were no serious complications such as ablation-related bleeding or infection after surgery, confirming that artificial pneumothorax combined with artificial hydrothorax and body position adjustment is extremely safe and effective. Artificial pneumothorax combined with MWA has the limitation that patients with pleural adhesions occurring after pulmonary surgery or lung cancer radiotherapy are not suitable for this therapy (18).Pleural adhesions can prevent sufficient lung tissue from being compressed and can also cause pleural tearing and bleeding. However, because the preoperative plain scan cannot always detect pleural adhesions, the degree and location of adhesions can only be determined after a certain amount of gas is injected and the lung tissue retracts.

Limitations

First, this is a single-center retrospective study with a small sample size and no statistical significance; the long-term efficacy and corresponding influencing factors should be investigated further in a controlled study with a large sample size. Second, in this study, the use of artificial pneumothorax and artificial hydrothorax increased surgery time and the number of local scans, which was time–consuming and increased the ionizing radiation received by patients. In addition, the follow–up of some patients was not regular

Conclusion

To summarize, microwave ablation, assisted by artificial pneumothorax, artificial hydrothorax, and body position adjustment, is a safe and effective minimally invasive method for treating lung cancer adjacent to the vital organs.

Data availability statement

The original contributions presented in the study are included in the article/supplementary materials. Further inquiries can be directed to the corresponding author.

Ethics statement

The studies involving human participants were reviewed and approved by the ethics committee of First Affiliated Hospital of Fujian Medical University. The patients/participants provided their written informed consent to participate in this study.

Author contributions

ZL conceptualized the study, prepared figures and tables. JianC wrote the article and prepared figures and tables. LQ collected the data, carried out the analysis, and prepared the figures and tables. JinC and QL participated in drafting and editing the article and assisted in the preparation of figures and tables. YY and JieC participated in figure preparation and drafting and editing the article. All authors contributed to the article and approved the submitted version.

Funding

This work was supported by the Start-up Fund for Scientific Research, Fujian Medical University (Grant number: 2017XQ1094).

Conflict of interest

The authors declare that the research was conducted in the absence of any commercial or financial relationships that could be construed as a potential conflict of interest.

Publisher's note

References

1. Zheng R, Zhang S, Zeng H, Wang S, Sun K, Chen R, et al. Cancer incidence and mortality in China, 2016. *J Natl Cancer Center* (2022) 5:38. doi: 10.1016/j.jncc.2022.02.002

2. Howington JA, Blum MG, Chang AC, Balekian AA, Murthy SC. Treatment of stage I and II non-small cell lung cancer: Diagnosis and management of lung cancer, 3rd ed: American college of chest physicians evidence-based clinical practice guidelines. *Chest* (2013) 143(5 Suppl):e278S–313S. doi: 10.1378/chest.12-2359

3. Wei Z, Ye X, Yang X, Zheng A, Huang G, Li W, et al. Microwave ablation in combination with chemotherapy for the treatment of advanced non-small cell lung cancer. *Cardiovasc Intervent Radiol* (2015) 38:135–42. doi: 10.1007/s00270-014-0895-0

4. Ye X, Fan W, Chen JH, Feng WJ, Gu SZ, Han Y, et al. Chinese Expert consensus workshop report: Guidelines for thermal ablation of primary and metastatic lung tumors. *Thorac Cancer* (2015) 6:112–21. doi: 10.1111/1759-7714.12152

5. Li H, Lin Z, Chen J, Guo R. Evaluation of the MR and pathology characteristics immediately following percutaneous MR-guided microwave ablation in a rabbit kidney VX2 tumor implantation model. *Int J Hyperthermia* (2019) 36(1):1197–206. doi: 10.1080/02656736.2019.1687944

6. Wang Y, Liu B, Cao P, Wang W, Wang W, Chang H, et al. Comparison between computed tomography-guided percutaneous microwave ablation and thoracoscopic lobectomy for stage I non-small cell lung cancer. *Thorac Cancer* (2018) 9(11):1376–82. doi: 10.1111/1759-7714.12842

7. Narsule CK, Sridhar P, Nair D, Gupta A, Oommen RG, Ebright MI, et al. Percutaneous thermal ablation for stage IA non-small cell lung cancer: Long-term follow-up. *J Thorac Dis* (2017) 9(10):4039–45. doi: 10.21037/jtd.2017.08.142

8. Yang X, Ye X, Huang G, Han X, Wang J, Li W, et al. Repeated percutaneous microwave ablation for local recurrence of inoperable stage I nonsmall cell lung cancer. *J Can Res Ther* (2017) 13:683–8. doi: 10.4103/jcrt.JCRT_458_17

9. Han X, Yang X, Ye X, Liu Q, Huang G, Wang J, et al. Computed tomography guided percutaneous microwave ablation of patients 75 years of age and older with early-stage nonsmall cell lung cancer. *Indian J Cancer* (2015) 52(Suppl 2):e56–60. doi: 10.4103/0019-509X.172514

10. Yang X, Ye X, Lin Z, Jin Y, Zhang K, Dong Y, et al. Computed tomography-guided percutaneous microwave ablation for treatment of peripheral ground glass opacity-lung adenocarcinoma: a pilot study. *J Cancer Res Ther* (2018) 14(4):764–71. doi: 10.4103/jcrt.JCRT_269_18

11. Ye X, Fan W, Wang Z, Wang J, Wang H, Wang J, et al. Expert consensus on thermal ablation for pulmonary subsolid nodules (2021 edition). *Chin J Lung Cancer* (2021) 17(5):1141–56. doi: 10.4103/jcrt.jcrt_1485_21

12. Ye X, Fan W, Wang H, Wang J, Wang Z, Gu S, et al. Ex per t consensus work shop repor t: Guidelines for thermal ablation of primary and metastatic lung tumors (2018 edition). *J Cancer Res Ther* (2018) 14(4):730–44. doi: 10.4103/jcrt.JCRT_221_18

13. Chu KF, Dupuy DE. Thermal ablation of tumours: biological mechanisms and advances in therapy. *Nat Rev Cancer* (2014) 14(3):199–208. doi: 10.1038/nrc3672

14. Ni Y, Xu H, Ye X. Image-guided percutaneous microwave ablation of early-stage non-small cell lung cancer. *Asia-Pac J Clin Oncol* (2020) 16(6):320–5. doi: 10.1111/ajco.13419

15. Ahmed M, Solbiati L, Brace CL, Breen DJ, Callstrom MR, Charboneau JW, et al. Image-guided tumor ablation: standardization of terminolog y and reporting criteria¬¬-a 10 -year update. *Radiology* (2014) 273(1):241–60. doi: 10.1148/radiol.14132958

16. Lin Z-Y, Li Y-G. Artificial pneumothorax with position adjustment for computed tomography-guided percutaneous core biopsy of mediastinum lesions – ScienceDirect. *Ann Thorac Surg* (2009) 87(3):920–4. doi: 10.1016/j.athoracsur.2008.10.020

17. Yang X, Zhang K, Ye X, Zheng A, Huang G, Li W, et al. Artificial pneumothorax for pain relief during microwave ablation of subpleural lung tumors. *Indian J Cancer* (2015) 52(6):80. doi: 10.4103/0019-509X.172519

18. Hou X, Zhuang X, Zhang H, Wang K, Zhang Y. Artificial pneumothorax: a safe and simple method to relieve pain during microwave ablation of subpleural lung malignancy. *Minimally Invasive Ther Allied Technol Mitat* (2017) 26(4):220–6. doi: 10.1080/13645706.2017.1287089

19. Zuo T, Lin W, Liu F, Xu J. Artificial pneumothorax improves radiofrequency ablation of pulmonary metastases of hepatocellular carcinoma close to mediastinum. *BMC Cancer* (2021) 21(1):505. doi: 10.21203/rs.3.rs-53230/v2

20. Fujiwara H, Arai Y, Ishii H, Kanazawa S. Computed tomography-guided radiofrequency ablation for subdiaphragm hepatocellular carcinoma: Safety and efficacy of inducing an artificial pneumothorax. *Acta Med Okayama* (2016) 70 (3):189–95. doi: 10.18926/AMO/54418

21. Lan S, Zhang Y, Wen Y, Li X. Application value of artificial pleural ascites in microwave ablation for liver cancer. *Acad J Guangzhou Med University* (2021) 49 (1):51–3.

frontiers | Frontiers in Oncology

TYPE Original Research
PUBLISHED 26 August 2022
DOI 10.3389/fonc.2022.938827

OPEN ACCESS

EDITED BY
Ping Zhan,
Nanjing University School of Medicine, China

REVIEWED BY
Ran Wang,
First Affiliated Hospital of Anhui Medical University, China
Song Xu,
Tianjin Medical University General Hospital, China
Tian Yunhong,
Guangzhou Medical University, China
Bin Xiong,
Huazhong University of Science and Technology, China

*CORRESPONDENCE
Xia Yang
yangxiajinan@163.com
Zhigang Wei
weizhigang321321@163.com
Xin Ye
yexintaian2020@163.com

†These authors have contributed equally to this work

SPECIALTY SECTION
This article was submitted to Thoracic Oncology, a section of the journal Frontiers in Oncology

RECEIVED 08 May 2022
ACCEPTED 02 August 2022
PUBLISHED 26 August 2022

CITATION
Huang Y, Wang J, Hu Y, Cao P, Wang G, Cai H, Wang M, Yang X, Wei Z and Ye X (2022) Microwave ablation plus camrelizumab monotherapy or combination therapy in non-small cell lung cancer. *Front. Oncol.* 12:938827. doi: 10.3389/fonc.2022.938827

Microwave ablation plus camrelizumab monotherapy or combination therapy in non-small cell lung cancer

Yahan Huang[1,2†], Jiao Wang[3†], Yanting Hu[1†], Pikun Cao[1], Gang Wang[1], Hongchao Cai[1], Meixiang Wang[1], Xia Yang[3*], Zhigang Wei[1,4*] and Xin Ye[1*]

[1]Department of Oncology, The First Affiliated Hospital of Shandong First Medical University & Shandong Provincial Qianfoshan Hospital, Shandong Lung Cancer Institute, Shandong Key Laboratory of Rheumatic Disease and Translational Medicine, Jinan, China, [2]Shandong First Medical University & Shandong Academy of Medical Sciences, Jinan, China, [3]Department of Oncology, Shandong Provincial Hospital Affiliated to Shandong First Medical University, Jinan, China, [4]Cheeloo College of Medicine, Shandong University, Jinan, China

Purpose: Immunotherapy has become widely applied in non-small cell lung cancer (NSCLC) patients. However, the relatively low response rate of immunotherapy monotherapy restricts its application. Combination therapy improves the response rate and prolongs patient survival; however, adverse events (AEs) associated with immunotherapies increase with combination therapy. Therefore, exploring combination regimens with equal efficacy and fewer AEs is urgently required. The aim of this study was to evaluate the efficacy and safety of microwave ablation (MWA) plus camrelizumab monotherapy or combination therapy in NSCLC.

Materials and Methods: Patients with pathologically confirmed, epidermal growth factor receptor/anaplastic lymphoma kinase-wild-type NSCLC were retrospectively enrolled in this study. Patients underwent MWA to the pulmonary lesions first, followed by camrelizumab monotherapy or combination therapy 5–7 days later. Camrelizumab was administered with the dose of 200 mg every 2 to 3 weeks. Treatment was continued until disease progression or intolerable toxicities. The technical success and technique efficacy of ablation, objective response rate (ORR), progression-free survival (PFS), overall survival (OS), complications of ablation, and AEs were recorded.

Results: From January 1, 2019 to December 31, 2021, a total of 77 patients underwent MWA and camrelizumab monotherapy or combination therapy. Technical success was achieved in all patients (100%), and the technique efficacy was 97.4%. The ORR was 29.9%. The PFS and OS were 11.8 months (95% confidence interval, 9.5–14.1) and not reached, respectively. Smoking history and response to camrelizumab were correlated with PFS, and response to camrelizumab was correlated with OS in both the univariate and multivariate analyses. No periprocedural deaths due to ablation were observed. Complications were observed in 33 patients (42.9%). Major complications

included pneumothorax (18.2%), pleural effusion (11.7%), pneumonia (5.2%), bronchopleural fistula (2.6%), and hemoptysis (1.3%). Grade 3 or higher AEs of camrelizumab, including reactive capillary endothelial proliferation, fatigue, pneumonia, edema, and fever, were observed in 10.4%, 6.5%, 5.2%, 2.6%, and 2.6% of patients, respectively.

Conclusion: MWA combined with camrelizumab monotherapy or combination therapy is effective and safe for the treatment of NSCLC.

KEYWORDS

microwave ablation, camrelizumab, lung cancer, progression-free survival, overall survival, objective response rate

1 Introduction

Lung cancer is the leading cause of cancer-related mortality and morbidity in China and the second leading cause of cancer-related mortality worldwide (1, 2). Approximately 85% of lung cancers are non-small cell lung cancers (NSCLCs), of which adenocarcinoma and squamous cell carcinoma are the most common histological types (3). Most patients with lung cancer are diagnosed at an advanced stage, thus losing the opportunity for curative surgery. For these patients, the prognosis is quite poor, with a 5-year survival rate of only 0–10% (4).

The treatments for advanced NSCLC range from routine chemotherapy to novel targeted therapy and immunotherapy (5, 6). Compared with targeted therapy, which requires specific sensitive genetic mutations, immunotherapy targeting programmed death-1 (PD-1) or programmed death ligand-1(PD-L1) is more widely applied in NSCLC patients (7–9). However, the relatively low response rate of PD-1/PD-L1 antibody monotherapy restricts its application (7–9). The combination of PD-1/PD-L1 antibodies with other treatments including chemotherapy; anti-vascular endothelial growth factor receptor therapy plus chemotherapy; or another immunotherapy, mainly anti-cytotoxic lymphocyte antigen-4 antibody alone or in combination with chemotherapy, improves the response rate and prolongs survival (10–14). However, the adverse events (AEs) associated with immunotherapies increase with combination therapy (10–14). Therefore, exploring combination regimens with equal efficacy and fewer AEs is urgently required.

Accumulating evidence shows that microwave ablation (MWA) is an alternative treatment method for early-stage NSCLC patients with contraindications to surgery, such as cardiopulmonary insufficiency (15–17). Moreover, previous studies have verified that MWA plus chemotherapy or targeted therapy has a survival advantage over chemotherapy or targeted therapy alone (18–20). Our previous study showed that, for advanced NSCLC patients, the combination of MWA and camrelizumab (a PD-1 antibody designed by Hengrui Pharm, Jiangsu Province, China) improved the objective response rate (ORR) to 33.3%, which was higher than in previous reports where the ORR was around 20%. However, only 21 patients were included in the study, which limits the credibility of the results (21). Therefore, we conducted this retrospective study with a larger sample size to verify the efficacy and safety of MWA and camrelizumab monotherapy or combination therapy in advanced NSCLC.

Abbreviations: NSCLC, non-small cell lung cancer; PD-1, programmed death-1; PD-L1, programmed death ligand-1; AE, adverse event; MWA, microwave ablation; ORR, overall response rate; CT, computed tomography; CR, complete response; PR, partial response; PD, progressive disease; PFS, progression-free survival; OS, overall survival.

2 Materials and methods

2.1 Patients

Patients meeting the following criteria were retrospectively enrolled: 1) pathologically or cytologically confirmed NSCLC; 2) advanced tumor stage, including stages III (unfit for radical surgery or irradiation) and IV, or recurrence post-local radical therapy (e.g., surgery, irradiation, or thermal ablation); 3) Eastern Cooperative Oncology Group performance status of 0 to 2; 4) one or more measurable lesions other than those for which MWA was performed; 5) tumors located in the peripheral lung; 6) wild-type epidermal growth factor receptor and anaplastic lymphoma kinase based on genetic test results; and 7) sufficient hepatic, renal, and cardiac function for MWA and anti-PD-1 treatment.

The exclusion criteria were as follows: 1) small cell lung cancer or neuroendocrine tumor in combination with NSCLC; 2) other malignant tumors during the previous 5 years; 3) active

autoimmune disease requiring intervention; and 4) long-term administrations of hormones or anti-infective treatments within 2 weeks of MWA.

This study was conducted in accordance with the Declaration of Helsinki. The ethics committees of the First Affiliated Hospital of Shandong First Medical University and Shandong Provincial Hospital affiliated to Shandong First Medical University (SWYX: No.2019-004) approved this study. Written informed consent was obtained from all patients.

2.2 MWA procedure

All patients underwent preoperative analgesia. Local anesthesia was induced with 100 mg of lidocaine and 75 mg of bupivacaine. Sedation was induced with 10 mg of diazepam. The MWA procedure for lung tumors has been described in detail in our previous report (18). The operator briefly used computed tomography (CT) to locate the tumor before ablation, after which the antenna was inserted into the tumor step-by-step. CT was performed immediately after ablation to identify complications, such as pneumothorax and pleural effusion, and intervene if necessary. CT was also used to monitor the ablative response and range. The number of antennas was determined by the maximum transverse diameter of the tumor. When the tumor was 3 cm or larger, two antennas were used; otherwise, one antenna was used. The ablative zone was nearly 3.5 cm × 3 cm for MWA with the output was 60–80W/6–8 min. When the ground-glass opacity surpassed the tumor lesions by 5–10 mm, the ablation was terminated.

2.3 Camrelizumab administration

Anti-PD-1 treatment was administered 5–7 days after ablation. Camrelizumab was administered as a 30-minute intravenous infusion at a dose of 200 mg every 2 or 3 weeks until disease progression or unacceptable toxicity. For patients who received MWA plus camrelizumab as first-line treatment, camrelizumab was administered combined with chemotherapy, targeted therapy, or both. For those receiving this treatment as second- or later-line treatment, camrelizumab monotherapy was recommended. Chemotherapy regimens on a 21-day cycle, including pemetrexed (one dose of 500 mg/m^2), nab-paclitaxel (one dose of 260 mg/m^2), docetaxel (one dose of 75 mg/m^2), and nedaplatin (80 mg/m^2 over 2 days), were administered based on the physician's preference. For targeted therapy, apatinib (250 mg once daily) or anlotinib (12 mg once daily) for 2 weeks on a 21-day cycle was administered continuously. Bevacizumab (7.5–15 mg/m^2) was also administered once every 3 weeks to some patients.

2.4 Efficacy of MWA and camrelizumab

CT was conducted every 2 months during camrelizumab treatment and every 3 months thereafter.

Technical success and technique efficacy are commonly used to evaluate response to MWA. Technical success is a measure of whether the tumor was treated according to the protocol and covered completely by the ablation zone and was assessed during the procedure. Technique efficacy refers to a result of "complete ablation" of macroscopic tumors, as evidenced by follow-up imaging, at a prospectively defined time point (generally 1 month or later) (22).

The response to camrelizumab monotherapy or combination therapy was evaluated using the Response Evaluation Criteria in Solid Tumors version 1.1, which categorized responses as complete response (CR), partial response (PR), stable disease, or progressive disease (PD) (23). The ORR was defined as the proportion of patients who achieved CR and PR. The disease control rate was defined as the proportion of patients who did not show disease progression.

2.5 Safety of MWA and camrelizumab monotherapy or combination therapy

2.5.1 Complications of MWA

The complications of MWA were divided into major complications and minor complications according to the Society of Intervention Response criteria (24). Major complications were defined as events that led to substantial morbidity and disability, which increase the level of care or lengthen the hospital stay. A blood transfusion or interventional drainage procedure is generally required for these patients. All other complications were considered minor (22).

2.5.2 AEs of camrelizumab

The AEs of camrelizumab monotherapy or combination therapy were evaluated according to the Common Terminology Criteria of Adverse Events version 5.0 (25). Generally, when the severity of the AE reached or exceeded grade 3, camrelizumab treatment was paused, and intervention was conducted (22). Once the AEs were resolved, whether or not to resume camrelizumab treatment was decided on by the researchers. When disease progression occurred, patients could continue on camrelizumab until clinical symptom deterioration or PD confirmation in the imaging assessment.

2.6 Statistical analysis

SPSS software (version 17.0; SPSS Inc., Chicago, IL, USA) was used to perform the analyses. Numerical variables are

described as means and standard deviations or medians and interquartile ranges according to distribution. Categorical variables are described as percentages. Progression-free survival (PFS) was defined as the time from MWA to the first documentation of PD or death. Overall survival (OS) was defined as the time from MWA to death. PFS and OS curves were estimated using the Kaplan–Meier method. The associations between PFS and OS and clinical characteristics were analyzed using univariate Cox regression and log-rank tests. Factors with $P < 0.2$ in the univariate analysis were included in the multivariate Cox proportional hazard model, which was applied to estimate hazard ratios and corresponding 95% confidence intervals. All statistical tests were two-sided, and statistical significance was defined as $P < 0.05$.

3 Results

3.1 Baseline characteristics

3.1.1 Patients

From January 1, 2019 to December 31, 2021, A total of 132 patients underwent camrelizumab treatment were screened. Among them, 40 patients failed underwent MWA, 8 patients with stage IB to IIB and 4 patients with other cancers during the past 5 years. A total of 77 patients were retrospectively enrolled, with a mean age of 67.1 years (range, 48–82 years). Patient characteristics are shown in Table 1. Most patients were men (59, 76.6%), 65 years old or older (53, 68.8%), and smokers (53, 68.8%). Seventy-one patients had an Eastern Cooperative Oncology Group performance status of 1 (92.2%), and 60 had clinical stage IV disease (77.9%). Adenocarcinoma was the most common histological type (50, 64.9%). Most patients underwent MWA and camrelizumab monotherapy (45, 58.4%). For those who underwent camrelizumab combination therapy, a combination with chemotherapy (19 patients, 59.4%) was the most common, followed by targeted therapy (8 patients, 25.0%) and targeted therapy plus chemotherapy (5 patients, 15.6%). Two representative cases are shown in Figures 1, 2.

3.1.2 Pulmonary tumors

All 77 pulmonary tumors were treated with MWA. The mean maximal transverse diameter was 3.3 centimeters, and 39 tumors (50.6%) had a diameter of 3.0 cm or larger. The right lung (40, 51.9%) and upper lobe (42, 54.5%) were the most common tumor sites. The output power of the antenna was generally fixed at 40 W, with a mean ablative time of 14.6 minutes. More information on tumor size and ablation is shown in Table 2.

TABLE 1 Baseline characteristics of the enrolled patients.

	N=77	Percent (%)
Gender		
Male	59	76.6
Female	18	23.4
Age		
Mean±SD(years old)	67.1±7.6	
<65 years old	24	31.2
≥65 years old	53	68.8
Smoking history		
Smokers	53	68.8
Non-smokers	24	31.2
ECOG		
0	4	5.2
1	71	92.2
2	2	2.6
Pathology		
Adenocarcinoma	50	64.9
Non-adenocarcinoma	27	35.1
Pathology		
Squamous cell lung cancer	22	28.6
Non-Squamous cell lung cancer	55	71.4
Stage		
III	17	22.1
IV	60	77.9
Lymph nodes metastases		
No	23	29.9
Yes	54	70.1
Distant metastases		
No	19	24.7
Yes	58	75.3
EGFR mutations		
Positive	9	11.7
Negative	26	33.8
Unknown	42	54.5
ALK mutations		
Positive	0	0.0
Negative	35	45.5
Unknown	42	54.5
PD-L1 expression		
Positive	11	14.3
Negative	4	5.2
Unknown	62	80.5
PD-L1 positive (TPS)		
1%-49%	5	6.5
≥50%	6	7.8

ALK, anaplastic lymphoma kinase; ECOG, Eastern Cooperation of Oncology Group; EGFR, epidermal growth factor receptor; N, number; PD-L1, programmed death-ligand-1; SD, standard deviation; TPS, total proportion score.

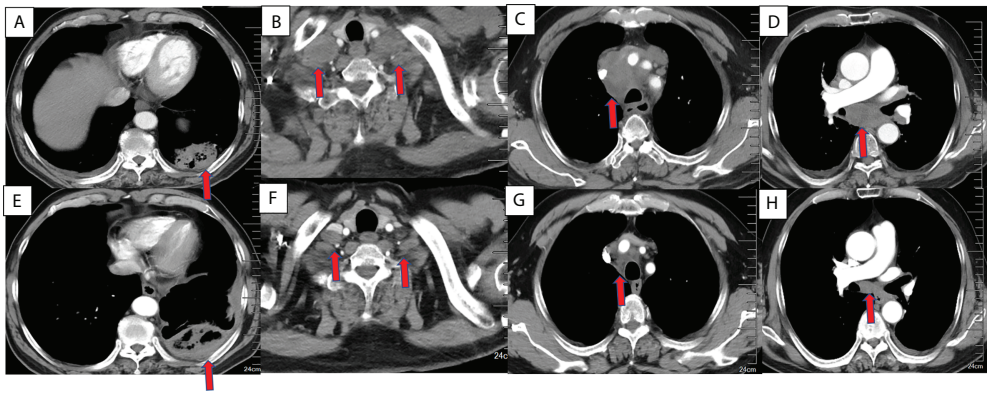

FIGURE 1
Chest CT findings of a 63-year-old male squamous cell lung cancer patient with a PD-L1 TPS of 1% who underwent MWA and camrelizumab monotherapy. **(A–D)** Baseline chest CT showing the primary tumor and lymph node metastases. **(A)** The primary tumor was located in the left lower lobe. **(B)** Bilateral supraclavicular lymph node metastases. **(C, D)** Mediastinal lymph node metastases in the 2R, 4R, 5, and 7 zones. **(E–H)** CT 2 months post-ablation and after four cycles of camrelizumab. **(E)**. Complete ablation was achieved in the primary tumor. **(F–H)**. Bilateral supraclavicular mediastinal lymph node metastases decreased dramatically. PD-L1, programmed death ligand-1; TPS, tumor proportion score; MWA, microwave ablation; CT, computed tomography.

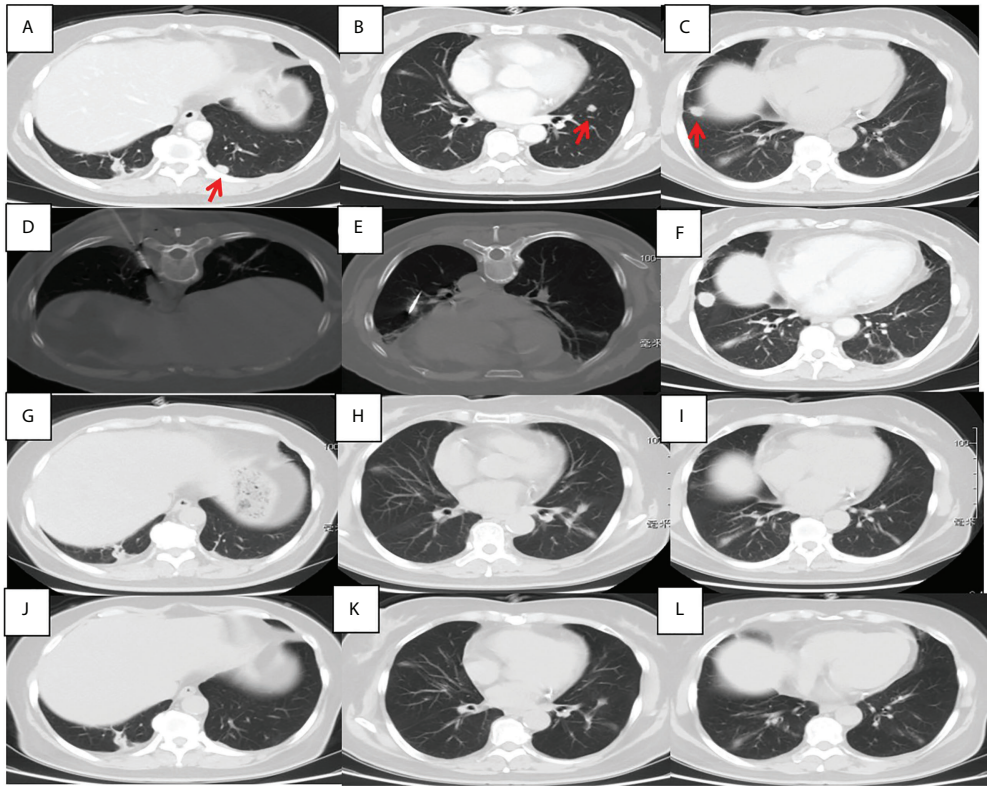

FIGURE 2
Chest CT findings of a 56-year-old female pulmonary adenocarcinoma patient with an unknown PD-L1 TPS who underwent MWA and camrelizumab monotherapy. **(A–C)** Baseline chest CT showing two metastases in the left lower lobe. **(D, E)** MWA was conducted for the tumor in the left lower lobe. **(F)** Two cycles of camrelizumab monotherapy were administered, after which the right metastasis enlarged. **(G–I)** Six months post-ablation, the left metastases achieved complete ablation and the right metastasis disappeared; complete response was achieved. **(J–L)** Nineteen months post-ablation, there was no indication of any pulmonary metastases. PD-L1, programmed death ligand-1; TPS, tumor proportion score; MWA, microwave ablation; CT, computed tomography.

3.2 Treatment efficacy

Although technical success was achieved in all patients (100%), the technique efficacy was 97.4% because two patients with tumors larger than 5 cm failed to achieve CR.

All patients underwent at least 1 cycle of camrelizumab treatment, and the median was 5 cycles (range, 1–53) (Table 3). Thirty-two patients (41.6%) received camrelizumab combination therapy. CR, PR, stable disease, and PD were achieved in 3, 20, 23, and 31 patients, respectively. The ORR and disease control rate were 29.9% and 59.7%, respectively.

3.3 Survival analysis

Patients were followed through April 4, 2022, with a median follow-up period of 13.7 (4.3–36.2) months. Forty-eight patients (62.3%) had PD, and 26 patients (33.8%) died. The median PFS was 11.8 months (95% confidence interval, 9.5–14.1). However, the median OS was not reached. Sex, smoking history, stage, and response to camrelizumab were correlated with PFS in the univariate analysis. Age, smoking history, tumor size, and response to camrelizumab were correlated with PFS in the multivariate analysis (Table 4, Figures 3A–D). Smoking history and response to camrelizumab correlated with PFS in both the univariate and multivariate analyses (Table 4). Patients with smoking history and with CR or PR to camrelizumab had superior PFS compared to those without a smoking history (13.8 months vs. 6.3 months, P = 0.002) and those who failed to achieve CR or PR (25.4 months vs. 9.3 months, P = 0.003), respectively (Figures 3E, F).

The response to camrelizumab was the only independent prognostic factor for OS in both the univariate and multivariate analyses. Patients who achieved an objective response had superior OS compared to those who had stable disease or PD (not reached vs. 19.4 months, P = 0.007). Although sex showed a tendency for significance in the univariate analysis, no

TABLE 2 Baseline characteristics of the tumors underwent MWA.

	N=77	Percent(%)
Tumor size (cm)		
Mean(±SD)	3.3±2.2	
<3	38	49.4
≥3	39	50.6
Location of tumors		
Left lung	37	48.1
Right lung	40	51.9
Location of tumors		
Upper lobe	42	54.5
Middle and lower lobe	35	45.5
Location of tumors		
Upper right lobe	19	24.6
Middle right lobe	9	11.7
Lower right lobe	11	14.3
Upper left lobe	23	29.9
Lower left lobe	15	19.5
Number of antennas		
1	31	40.3
2	43	55.8
3	3	3.9
Power		
30W	14	18.2
40W	30	39.0
50W	18	23.4
60W	15	19.5
Ablation Duration (minutes)		
Mean±SD	14.6±9.1	

SD, standard deviation; W, watt.

TABLE 3 Camrelizumab treatments.

	N=77	Percent (%)
Camrelizumab therapy		
Combination	32	41.6
Monotherapy	45	58.4
Treatment Regimen		
First line	29	37.7
Subsequent line	48	62.3
Combination regimens(N=32)		
Targeted therapy	8	25.0
Chemotherapy	19	59.4
Targeted and chemotherapy	5	15.6
Treatment interval		
Two weeks	45	58.4
Three weeks	32	41.6
Treatment interruption		
Yes	13	16.9
No	64	83.1
Response		
CR	3	3.9
PR	20	25.9
SD	23	29.9
PD	31	40.3
ORR		
CR+PR	23	29.9
SD+PD	54	70.1
DCR		
CR+PR+SD	46	59.7
PD	31	40.3
Disease progression		
Yes	48	62.3
No	29	37.7

CR, complete response; ORR, objective response rate; DCR, disease control rate; PD, progression disease; PR, partial response; SD, stable disease; MWA, microwave ablation.

TABLE 4 The univariate and multivariate analyses of progression free survival.

		Univariate analyses		Multivariate analyses				
	Median PFS (95% CI)	HR (95% CI)	*P* value	β	S.E.	Wald	df	HR (95% CI)	*P* value
Gender		2.220 (1.045-4.715)	0.008	-0.272	0.430	0.400	1	0.762 (0.328, 1.771)	0.527
Male	12.60 (8.784-16.41)								
Female	6.300 (0.000-12.56)								
Age		1.680 (0.927-3.044)	0.087	0.717	0.353	4.119	1	2.047 (1.025, 4.090)	0.042
<65	8.733 (1.032-16.43)								
≥65	13.63 (9.292-17.97)								
Smoking history		2.406 (1.227-4.718)	0.002	1.228	0.429	8.176	1	3.414 (1.471, 7.920)	0.004
Non-smokers	6.300 (0.323-12.27)								
Smokers	13.80 (5.362-22.30)								
Histology		1.276 (0.690-2.360)	0.437						
ADC	11.86 (7.937-15.80)								
Non-ADC	10.50 (8.280-12.72)								
Histology		1.081 (0.569-2.055)	0.811						
SCC	10.50 (8.369-12.63)								
Non-SCC	11.86 (7.919-15.82)								
Stage		0.447 (0.238-0.842)	0.040	0.331	0.473	0.491	1	1.393 (0.551, 3.519)	0.483
III	28.60 (13.68-25.70)								
IV	10.20 (6.899-13.43)								
Distant metastases		0.446 (0.242-0.823)	0.030						
No	28.60 (13.84-25.05)								
Yes	10.20 (6.975-13.36)								
Tumor size		1.644 (0.916, 2.950)	0.096	0.880	0.349	6.349	1	2.411 (1.216, 4.779)	0.012
<3 cm	14.67 (10.19-19.14)								
≥3 cm	9.133 (6.945-11.32)								
Camrelizumab treatment		1.007 (0.560, 1.812)	0.980						
Monotherapy	10.50 (6.930-14.10)								
Combination	11.87 (6.623-17.11)								
Treatment interval		1.291 (0.720, 2.315)	0.391						
3 weeks	10.43 (6.442-14.42)								
2 weeks	12.20 (9.084-15.32)								
Response to camrelizumab		0.355 (0.200-0.628)	0.002	1.318	0.418	9.960	1	3.735 (1.648, 8.465)	0.002
SD+PD	9.100 (4.903-12.56)								
CR+PR	25.40 (8.347-42.45)								
Response to camrelizumab		6.141 (3.079-12.25)	<0.0001						
CR+PR+SD PD	22.00 (19.95-14.13) 4.000 (1.227-6.839)								

ADC, Adenocarcimona; CR, complete response; ECOG, Eastern Cooperation of Oncology Group; Non-ADC, non-adenocarcinoma; Non-SCC, non-squamous lung cancer; PD, progression disease; PR, partial response; SCC, squamous cell lung cancer; SD, stable disease.

significant difference was observed in the multivariate analysis (Table 5; Figures 4).

3.4 Safety of MWA plus camrelizumab

No peri-procedural death from ablation was observed. Complications were observed in 33 patients (42.9%). Major complications included pneumothorax (14, 18.2%), pleural effusion (9, 11.7%), pneumonia (4, 5.2%), bronchopleural fistula (2, 2.6%), and hemoptysis (1, 1.3%), which were all treated by chest tube insertion, anti-infection therapy, blood transfusion, or symptomatic treatment. Minor complications of pneumothorax, pleural effusion, and hemorrhage were identified in 10, 9, and 1 patient(s), respectively (Table 6).

AEs were identified in 40 patients (51.9%), and serious AEs were observed in 12 patients (15.6%). Common AEs of camrelizumab included reactive capillary endothelial proliferation (22, 28.6%), fatigue (9, 11.7%), pneumonia (7, 9.1%), edema (5, 6.5%), and fever (5, 6.5%). Grade 3 or higher

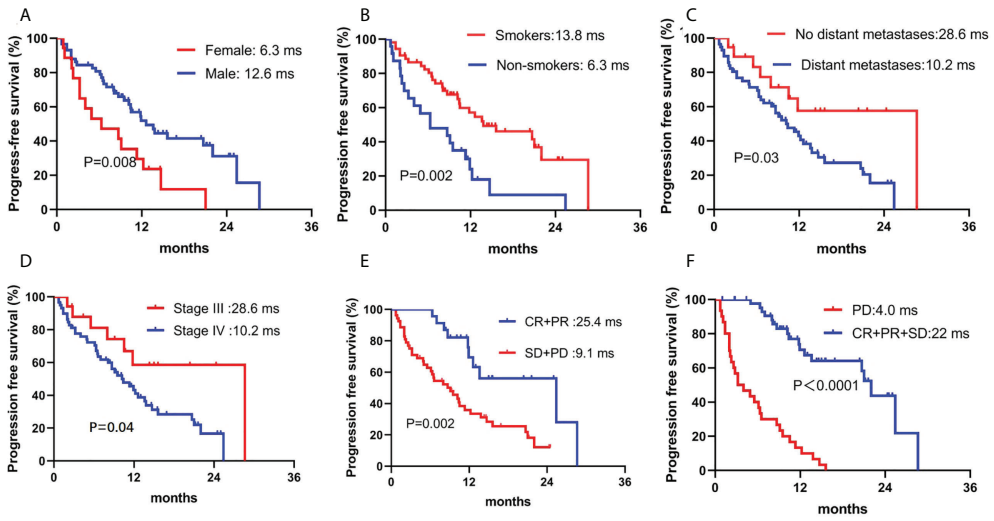

FIGURE 3
Correlation between PFS and **(A)** sex, **(B)** smoking history, **(C)** distant metastases, **(D)** stage, **(E)** ORR, and **(F)** DCR. PFS: progression-free survival; ORR, overall response rate; DCR, disease control rate.

AEs developed in a corresponding 10.4%, 6.5%, 5.2%, 2.6%, and 2.6% of patients, respectively. Two patients died of serious immune-associated pneumonia (Table 7).

4 Discussion

In this study, we explored the use of a combination of MWA and camrelizumab for NSCLC treatment. A total of 77 patients were enrolled. The technical success and technique efficacy were 100% and 97.4%, respectively. The ORR was 29.9%. The PFS and OS were 11.8 months and not reached, respectively. No ablation-associated deaths occurred. Complications were observed in 33 patients (42.9%), and grade 3 or higher AEs of camrelizumab were identified in 12 (15.6%) patients. MWA plus camrelizumab monotherapy or combination therapy in NSCLC is an effective and safe treatment regimen.

Camrelizumab was approved as the first-line treatment for advanced NSCLC based on the results of two multicenter, randomized phase III clinical trials (23, 24). CameL was the first phase III clinical trial of camrelizumab as a first-line regimen for advanced, non-squamous NSCLC. PFS was significantly prolonged with camrelizumab plus chemotherapy compared with chemotherapy alone (11.3 months vs. 8.3 months; hazard ratio 0.60; P = 0.0001) (26). The other phase III clinical trial, CameL-sq, compared the combination of camrelizumab and chemotherapy with placebo plus chemotherapy as first-line treatment for advanced squamous cell lung cancer. The camrelizumab plus chemotherapy arm achieved a PFS of 8.5 months, and the OS was not reached, whereas the PFS and OS of the placebo plus chemotherapy arm were 4.9 months and 14.5 months, respectively (27). Camrelizumab is usually combined with anti-vascular endothelial growth factor targeted therapy. In patients receiving camrelizumab in combination with apatinib as subsequent treatment, the median PFS is 5.7 months, and the OS is 15.5 months (28). Further, in patients receiving camrelizumab and anlotinib, the ORR is 28.4%, and the PFS and OS are 6.9 months and 14.5 months, respectively. These results verify that camrelizumab could be used for advanced NSCLC (29).

According to the National Comprehensive Cancer Network guidelines, thermal ablation, including MWA, could be an alternative treatment for patients with contraindications to radical surgery (30). Moreover, MWA could be a treatment option for NSCLC patients with oligometastases or oligoprogression (31, 32). Several studies have explored the application of MWA in advanced NSCLC and have verified that MWA can prolong survival and improve prognosis (18–20). Our previous study explored the combination of MWA plus camrelizumab in 21 patients; the ORR was 33.3%, and the median PFS was 5.1 months (21). In this large-sample, retrospective study, the ORR was similar to that in our previous report. The PFS was significantly prolonged by this treatment and was similar to that of combination camrelizumab and platinum-doublet chemotherapy, indicating that camrelizumab plus MWA may be an alternative combination regimen.

With regard to the efficacy of MWA, previous reports have shown a technique efficacy of nearly 100%; however, we achieved

TABLE 5 The univariate and multivariate analyses of overall survival.

		Univariate analyses		Multivariate analyses					
	Median OS (95% CI)	HR(95% CI)	*P* value	β	S.E.	Wald	df	HR(95% CI)	*P* value
Gender(Female *vs.* Male)		2.046(0.909, 4.604)	0.084	0.275	0.439	0.394	1	1.317(0.557, 3.112)	0.530
Male	*26.54(22.61-30.47)								
Female	14.67(7.628-21.70)								
Age		1.368(0.574, 3.260)	0.480						
<65	*26.34(20.43-32.24)								
≥65	* 24.11(19.73-28.48)								
Smoking history		1.312(0.582, 2.956)	0.512						
Non-smokers	21.00(13.91-28.01)								
Smokers	*24.88(20.96-28.80)								
Histology		1.307(0.567, 3.012)	0.530						
ADC	*24.01(19.57-28.45)								
Non-ADC	*25.94(20.76-31.13)								
Histology		1.186(0.497, 2.826)	0.701						
SCC	*25.49(19.76-31.21)								
Non-SCC	*24.44(20.21-28.68)								
Stage		1.736(0.596, 5.057)	0.312						
III	*23.30(18.82-27.79)								
IV	* 23.96(19.91-27.99)								
Distant metastases		2.037(0.700, 5.928)	0.192	0.392	0.576	0.465	1	1.481(0.479, 4.577)	0.495
Yes	* 23.56(19.44-27.68)								
No	* 23.77(19.62-27.91)								
Tumor size		1.054(0.487, 2.285)	0.893						
<3 cm	* 24.74(19.94-29.54)								
≥3 cm	* 25.07(19.94-30.19)								
Camrelizumab treatment		1.184(0.546, 2.565)	0.669						
Monotherapy	* 24.93(20.20-29.66)								
Combination	* 24.15(18.74-29.57)								
Treatment interval		1.096(0.502, 2.389)	0.818						
3 weeks	* 25.32(20.20-30.43)								
2 weeks	* 24.48(19.67-29.28)								
Response to camrelizumab		15.10(6.830, 33.38)	0.0003	2.651	1.026	6.674	1	14.17(1.896, 105.8)	0.010
CR+PR	*not reached								
SD+PD	*19.40(11.17-27.63)								
Response to camrelizumab		9.850(1.035, 93.78)	<0.0001						
CR+PR+SD	* not reached								
PD	*10.3(3.454-24.15)								

*Mean overall survival. ADC, Adenocarcimona; CR, complete response; ECOG:Eastern Cooperation of Oncology Group;Non-ADC, Non-adenocarcinoma; Non-SCC: Non-squamous lung cancer; PD, Progression disease; PR, Partial response; SCC: Squamous cell lung cancer; SD, Stable disease.

a technique efficacy of only 97.4%. This was because two patients with tumors ≥5 cm failed to achieve complete ablation. Several studies have shown that the rate of completed ablation decreases for tumors ≥3 cm (33, 34). According to previous reports, major complications of MWA include pneumothorax, pleural effusion, pneumonia, bronchopleural fistula, and hemoptysis, which is in accordance with our study results (35, 36). Pneumothorax and pleural effusion were the most common complications of MWA observed in this study. No ablation-associated deaths were observed, indicating that ablation is a safe treatment method.

Patients who underwent camrelizumab combination treatment also had AEs. The common AEs of combination camrelizumab and chemotherapy include decreased neutrophil count, decreased white blood cell count, anemia, and decreased platelet count (26, 27). For combination targeted therapy and camrelizumab, hypertension, palmar-plantar erythrodysesthesia syndrome, increased gamma-glutamyl transferase, transaminitis, and proteinuria are common AEs (28, 29). In this study, the most common AEs were reactive capillary endothelial proliferation, fatigue, pneumonia, edema, and

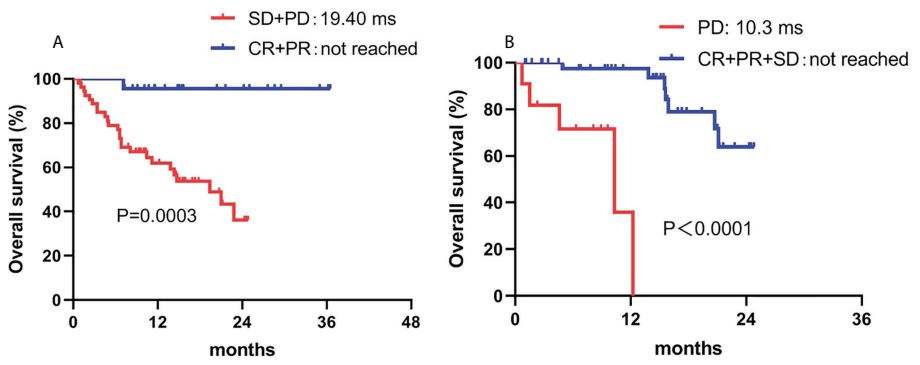

FIGURE 4
Correlation between OS and **(A)** ORR and **(B)** DCR. ORR, overall response rate; DCR, disease control rate.

TABLE 6 The complications of microwave ablation.

	N=77	Percent(%)
Complications	33	42.9
Major complications		
Pneumothorax	14	18.2
Pleural effusion	9	11.7
Pneumonia	4	5.2
Bronchopleural fistula	2	2.6
Hemorrhage	1	1.3
Minor complications		
Pneumothorax	10	13.0
Pleural effusion	9	11.7
Hemorrhage	1	1.3

TABLE 7 The adverse events of camrelizumab.

Adverse events	All (N)	Percent (%)	≥Grade 3 (N)	Percent (%)
Total	40	51.9	12	15.6
Reactive capillar hemangiomas	22	28.6	8	10.4
Fatigue	9	11.7	5	6.5
Pneumonia	7	9.1	4	5.2
Edema	5	6.5	2	2.6
Fever	5	6.5	2	2.6
Hemorrhagic tendency	3	3.9	0	0.0
Alanine transaminase elavation	2	2.6	2	2.6
Acute myocardial infarction	2	2.6	2	2.6
Autoallergic	2	2.6	1	1.3
Leukopenia	1	1.3	1	1.3
Neutropenia	1	1.3	1	1.3

fever. Moreover, grade 3 or higher AEs were observed in 15.6% of patients. These results proved that camrelizumab monotherapy or combination therapy is safe for advanced NSCLC.

The combination of MWA and immunotherapy had similar ORR with other combinations such as immunotherapy with chemotherapy and immunotherapy with targeted therapy. Meanwhile, we could identify that the ORR of MWA plus immunotherapy alone or combination therapy had a superior response compared to previous reports of immunotherapy alone. Several potential mechanisms may have led to this advantage, one was that MWA could have increased the probability of CD8+ tumor infiltrating lymphocytes (TIL) and Natural killer (NK) cells, and the other was that MWA could have increased the peripheral IL-2 and IFN-γ (37). Both CD8+ TIL and cell factors could have enhanced the immune effects, which may have exerted a synergic effect with immunotherapy. Moreover, PD-1 blockade boosts radiofrequency ablation-elicited adaptive immune responses by update PD-L1 expression in colorectal liver metastases (38). PD-L1 expression predicts the superior response to immunotherapy (38). Integrating locoregional therapies such as radiofrequency ablation into anti-PD-1/PD-L1 agent regimens may help release tumor-associated antigens and mediate T-cell immune enhancement and, in the long run, improve the ongoing efficacy of checkpoint inhibitors (39).

Compared with our previous study, the median PFS was prolonged in this study. Three major factors led to the differences. First, 41.6% of patients received immunotherapy combination treatment in this study, whereas all the patients underwent only immunotherapy in the previous study. Second, the median follow-up period reached 13.7 months in this study, but the median follow-up period then was just 6 months. Third, 77 patients were enrolled in this study, but only 21 patients were enrolled in the previous study.

This study had two major limitations. First, patients treated with either camrelizumab monotherapy or combination therapy were included in the study, and it is likely that combination therapy had an effect on the ORR or survival. Second, for patients who received camrelizumab combination therapy, the regimens included chemotherapy, targeted therapy, and chemotherapy plus targeted therapy.

In conclusion, MWA plus camrelizumab monotherapy or combination therapy is an effective and safe treatment regimen for advanced NSCLC. Further prospective, randomized, controlled studies are warranted.

Data availability statement

The raw data supporting the conclusions of this article will be made available by the authors, without undue reservation.

Ethics statement

The studies involving human participants were reviewed and approved by The ethics committees of the First Affiliated Hospital of Shandong First Medical University and Shandong Provincial Hospital affiliated to Shandong First Medical University approved this study. The patients/participants provided their written informed consent to participate in this study. Written informed consent was obtained from the individual(s) for the publication of any potentially identifiable images or data included in this article.

Author contributions

YHH, JW, YTH: Conceptualization, data curation, methodology, and writing—original draft. YTH, ZW, XYa, XYe: Data curation, methodology, resources, and writing—final draft. GW, HC, MW: Writing— review and editing. All authors contributed to the article and approved the submitted version.

Funding

The study was approved by the National Natural Science Foundation (No. 81901851 and No. 82072028).

Conflict of interest

The authors declare that the research was conducted in the absence of any commercial or financial relationships that could be construed as a potential conflict of interest.

Publisher's note

All claims expressed in this article are solely those of the authors and do not necessarily represent those of their affiliated organizations, or those of the publisher, the editors and the reviewers. Any product that may be evaluated in this article, or claim that may be made by its manufacturer, is not guaranteed or endorsed by the publisher.

References

1. Xia C, Dong X, Li H, Cao M, Sun D, He S, et al. Cancer statistics in China and united states, 2022: Profiles, trends, and determinants. *Chin Med J* (2022) 135 (5):584–90. doi: 10.1097/CM9.0000000000002108

2. Siegel RL, Miller KD, Fuchs HE, Jemal A. Cancer statistics, 2022. *CA: Cancer J Clin* (2022) 72(1):7–33. doi: 10.3322/caac.21708

3. Molina JR, Yang P, Cassivi SD, Schild SE, Adjei AA. Non-small cell lung cancer: Epidemiology, risk factors, treatment, and survivorship. *Mayo Clinic Proc* (2008) 83(5):584–94. doi: 10.4065/83.5.584

4. Goldstraw P, Chansky K, Crowley J, Rami-Porta R, Asamura H, Eberhardt WE, et al. The iaslc lung cancer staging project: Proposals for revision of the tnm stage groupings in the forthcoming (Eighth) edition of the tnm classification for lung cancer. *J Thorac Oncol Off Publ Int Assoc Study Lung Cancer* (2016) 11(1):39–51. doi: 10.1016/j.jtho.2015.09.009

5. Thai AA, Solomon BJ, Sequist LV, Gainor JF, Heist RS. Lung cancer. *Lancet (London England)* (2021) 398(10299):535–54. doi: 10.1016/s0140-6736(21)00312-3

6. Steuer CE, Ramalingam SS. Advances in immunotherapy and implications for current practice in non-Small-Cell lung cancer. *JCO Oncol Pract* (2021) 17 (11):662–8. doi: 10.1200/op.21.00305

7. Reck M, Rodríguez-Abreu D, Robinson AG, Hui R, Csőszi T, Fülöp A, et al. Pembrolizumab versus chemotherapy for pd-L1-Positive non-Small-Cell lung cancer. *New Engl J Med* (2016) 375(19):1823–33. doi: 10.1056/NEJMoa1606774

8. Mok TSK, Wu YL, Kudaba I, Kowalski DM, Cho BC, Turna HZ, et al. Pembrolizumab versus chemotherapy for previously untreated, pd-L1-Expressing, locally advanced or metastatic non-Small-Cell lung cancer (Keynote-042): A randomised, open-label, controlled, phase 3 trial. *Lancet (London England)* (2019) 393(10183):1819–30. doi: 10.1016/s0140-6736(18)32409-7

9. Herbst RS, Giaccone G, de Marinis F, Reinmuth N, Vergnenegre A, Barrios CH, et al. Atezolizumab for first-line treatment of pd-L1-Selected patients with nsclc. *New Engl J Med* (2020) 383(14):1328–39. doi: 10.1056/NEJMoa1917346

10. Gandhi L, Rodríguez-Abreu D, Gadgeel S, Esteban E, Felip E, De Angelis F, et al. Pembrolizumab plus chemotherapy in metastatic non-Small-Cell lung cancer. *New Engl J Med* (2018) 378(22):2078–92. doi: 10.1056/NEJMoa1801005

11. Paz-Ares L, Luft A, Vicente D, Tafreshi A, Gümüş M, Mazières J, et al. Pembrolizumab plus chemotherapy for squamous non-Small-Cell lung cancer. *New Engl J Med* (2018) 379(21):2040–51. doi: 10.1056/NEJMoa1810865

12. West H, McCleod M, Hussein M, Morabito A, Rittmeyer A, Conter HJ, et al. Atezolizumab in combination with carboplatin plus nab-paclitaxel chemotherapy compared with chemotherapy alone as first-line treatment for metastatic non-squamous non-Small-Cell lung cancer (Impower130): A multicentre, randomised, open-label, phase 3 trial. *Lancet Oncol* (2019) 20(7):924–37. doi: 10.1016/s1470-2045(19)30167-6

13. Hellmann MD, Ciuleanu TE, Pluzanski A, Lee JS, Otterson GA, Audigier-Valette C, et al. Nivolumab plus ipilimumab in lung cancer with a high tumor mutational burden. *New Engl J Med* (2018) 378(22):2093–104. doi: 10.1056/NEJMoa1801946

14. Paz-Ares L, Ciuleanu TE, Cobo M, Schenker M, Zurawski B, Menezes J, et al. First-line nivolumab plus ipilimumab combined with two cycles of chemotherapy in patients with non-Small-Cell lung cancer (Checkmate 9la): An international, randomised, open-label, phase 3 trial. *Lancet Oncol* (2021) 22 (2):198–211. doi: 10.1016/s1470-2045(20)30641-0

15. Ni Y, Huang G, Yang X, Ye X, Li X, Feng Q, et al. Microwave ablation treatment for medically inoperable stage I non-small cell lung cancers: Long-term results. *Eur Radiol* (2022) 32(8):5616–22. doi: 10.1007/s00330-022-08615-8

16. Nance M, Khazi Z, Kaifi J, Avella D, Alnijoumi M, Davis R, et al. Computerized tomography-guided microwave ablation of patients with stage I non-small cell lung cancers: A single-institution retrospective study. *J Clin Imaging Sci* (2021) 11:7. doi: 10.25259/jcis_224_2020

17. Narsule CK, Sridhar P, Nair D, Gupta A, Oommen RG, Ebright MI, et al. Percutaneous thermal ablation for stage ia non-small cell lung cancer: Long-term follow-up. *J Thorac Dis* (2017) 9(10):4039–45. doi: 10.21037/jtd.2017.08.142

18. Wei Z, Yang X, Ye X, Feng Q, Xu Y, Zhang L, et al. Microwave ablation plus chemotherapy versus chemotherapy in advanced non-small cell lung cancer: A multicenter, randomized, controlled, phase iii clinical trial. *Eur Radiol* (2020) 30 (5):2692–702. doi: 10.1007/s00330-019-06613-x

19. Ni Y, Ye X, Yang X, Huang G, Li W, Wang J, et al. Microwave ablation for non-small cell lung cancer with synchronous solitary extracranial metastasis. *J Cancer Res Clin Oncol* (2020) 146(5):1361–7. doi: 10.1007/s00432-020-03176-z

20. Xu X, Ye X, Liu G, Zhang T. Targeted percutaneous microwave ablation at the pulmonary lesion combined with mediastinal radiotherapy with or without concurrent chemotherapy in locally advanced non-small cell lung cancer evaluation in a randomized comparison study. *Med Oncol (Northwood London England)* (2015) 32(9):227. doi: 10.1007/s12032-015-0672-1

21. Wei Z, Yang X, Ye X, Huang G, Li W, Han X, et al. Camrelizumab combined with microwave ablation improves the objective response rate in advanced non-small cell lung cancer. *J Cancer Res Ther* (2019) 15(7):1629–34. doi: 10.4103/jcrt.JCRT_990_19

22. Ahmed M, Solbiati L, Brace CL, Breen DJ, Callstrom MR, Charboneau JW, et al. Image-guided tumor ablation: Standardization of terminology and reporting criteria–a 10-year update. *Radiology* (2014) 273(1):241–60. doi: 10.1148/radiol.14132958

23. Eisenhauer EA, Therasse P, Bogaerts J, Schwartz LH, Sargent D, Ford R, et al. New response evaluation criteria in solid tumours: Revised recist guideline (Version 1.1). *Eur J Cancer (Oxford Engl 1990)* (2009) 45(2):228–47. doi: 10.1016/j.ejca.2008.10.026

24. Cardella JF, Kundu S, Miller DL, Millward SF, Sacks D. Society of interventional radiology clinical practice guidelines. *J Vasc intervent Radiol JVIR* (2009) 20(7 Suppl):S189–91. doi: 10.1016/j.jvir.2009.04.035

25. Ciunci CA, Reibel JB, Evans TL, Mick R, Bauml JM, Aggarwal C, et al. Phase ii trial of combination nab-paclitaxel and gemcitabine in non-squamous non-small cell lung cancer after progression on platinum and pemetrexed. *Clin Lung Cancer* (2022) 23(4):e310-16. doi: 10.1016/j.cllc.2022.02.004

26. Zhou C, Chen G, Huang Y, Zhou J, Lin L, Feng J, et al. Camrelizumab plus carboplatin and pemetrexed versus chemotherapy alone in chemotherapy-naive patients with advanced non-squamous non-Small-Cell lung cancer (Camel): A randomised, open-label, multicentre, phase 3 trial. *Lancet Respir Med* (2021) 9 (3):305–14. doi: 10.1016/s2213-2600(20)30365-9

27. Ren S, Chen J, Xu X, Jiang T, Cheng Y, Chen G, et al. Camrelizumab plus carboplatin and paclitaxel as first-line treatment for advanced squamous nsclc (Camel-sq): A phase 3 trial. *J Thorac Oncol Off Publ Int Assoc Study Lung Cancer* (2022) 17(4):544–57. doi: 10.1016/j.jtho.2021.11.018

28. Zhou C, Wang Y, Zhao J, Chen G, Liu Z, Gu K, et al. Efficacy and biomarker analysis of camrelizumab in combination with apatinib in patients with advanced nonsquamous nsclc previously treated with chemotherapy. *Clin Cancer Res an Off J Am Assoc Cancer Res* (2021) 27(5):1296–304. doi: 10.1158/1078-0432.Ccr-20-3136

29. Wang P, Fang X, Yin T, Tian H, Yu J, Teng F. Efficacy and safety of anti-Pd-1 plus anlotinib in patients with advanced non-Small-Cell lung cancer after previous systemic treatment failure-a retrospective study. *Front Oncol* (2021) 11:628124. doi: 10.3389/fonc.2021.628124

30. Ettinger DS, Wood DE, Aisner DL, Akerley W, Bauman JR, Bharat A, et al. Nccn guidelines insights: Non-small cell lung cancer, version 2.2021. *J Natl Compr Cancer Network JNCCN* (2021) 19(3):254–66. doi: 10.6004/jnccn.2021.0013

31. Wei Z, Ye X, Yang X, Huang G, Li W, Han X, et al. Efficacy and safety of microwave ablation in the treatment of patients with oligometastatic non-Small-Cell lung cancer: A retrospective study. *Int J hyperthermia Off J Eur Soc Hyperthermic Oncol North Am Hyperthermia Group* (2019) 36(1):827–34. doi: 10.1080/02656736.2019.1642522

32. Ni Y, Peng J, Yang X, Wei Z, Zhai B, Chi J, et al. Multicentre study of microwave ablation for pulmonary oligorecurrence after radical resection of non-Small-Cell lung cancer. *Br J Cancer* (2021) 125(5):672–8. doi: 10.1038/s41416-021-01404-y

33. Wei Z, Ye X, Yang X, Huang G, Li W, Wang J, et al. Microwave ablation plus chemotherapy improved progression-free survival of advanced non-small cell lung cancer compared to chemotherapy alone. *Med Oncol (Northwood London England)* (2015) 32(2):464. doi: 10.1007/s12032-014-0464-z

34. Wei Z, Ye X, Yang X, Zheng A, Huang G, Li W, et al. Microwave ablation in combination with chemotherapy for the treatment of advanced non-small cell lung cancer. *Cardiovasc intervent Radiol* (2015) 38(1):135–42. doi: 10.1007/s00270-014-0895-0

35. Yang X, Ye X, Zheng A, Huang G, Ni X, Wang J, et al. Percutaneous microwave ablation of stage I medically inoperable non-small cell lung cancer: Clinical evaluation of 47 cases. *J Surg Oncol* (2014) 110(6):758–63. doi: 10.1002/jso.23701

36. Han X, Yang X, Huang G, Li C, Zhang L, Qiao Y, et al. Safety and clinical outcomes of computed tomography-guided percutaneous microwave ablation in patients aged 80 Years and older with early-stage non-small cell lung cancer: A multicenter retrospective study. *Thorac Cancer* (2019) 10(12):2236–42. doi: 10.1111/1759-7714.13209

37. Zhu J, Yu M, Chen L, Kong P, Li L, Ma G, et al. Enhanced antitumor efficacy through microwave ablation in combination with immune checkpoints blockade in breast cancer: A pre-clinical study in a murine model. *Diagn Interv Imaging* (2018) 99(3):135–42. doi: 10.1016/j.diii.2017.12.011

38. Shi L, Chen L, Wu C, Zhu Y, Xu B, Zheng X, et al. PD-1 blockade boosts radiofrequency ablation-elicited adaptive immune responses against tumor. *Clin Cancer Res* (2016) 22(5):1173–84. doi: 10.1158/1078-0432.CCR-15-1352

39. Yin J, Dong J, Gao W, Wang Y. A case report of remarkable response to association of radiofrequency ablation with subsequent atezolizumab in stage IV nonsmall cell lung cancer. *Med (Baltimore)* (2018) 97(44):e13112. doi: 10.1097/MD.0000000000013112

frontiers | Frontiers in Oncology

TYPE Original Research
PUBLISHED 05 October 2022
DOI 10.3389/fonc.2022.962630

OPEN ACCESS

EDITED BY
Manash K. Paul,
California State University,
United States

REVIEWED BY
Agasthian Thirugnanam,
Mount Elizabeth Novena
Hospital, Singapore
Rajesh Parmar,
University of California, Los Angeles,
United States

*CORRESPONDENCE
Xia Yang
yangxia_jinan@163.com
Xin Ye
yexintaian2020@163.com

†These authors have contributed equally to this work

SPECIALTY SECTION
This article was submitted to Thoracic Oncology, a section of the journal Frontiers in Oncology

RECEIVED 06 June 2022
ACCEPTED 12 September 2022
PUBLISHED 05 October 2022

CITATION
Han X, Wei Z, Zhao Z, Yang X and Ye X (2022) Cost and effectiveness of microwave ablation versus video-assisted thoracoscopic surgical resection for ground-glass nodule lung adenocarcinoma.
Front. Oncol. 12:962630.
doi: 10.3389/fonc.2022.962630

Cost and effectiveness of microwave ablation versus video-assisted thoracoscopic surgical resection for ground-glass nodule lung adenocarcinoma

Xiaoying Han[1†], Zhigang Wei[2,3†], Zhenxing Zhao[4], Xia Yang[1*] and Xin Ye[2*]

[1]Department of Oncology, Shandong Provincial Hospital Affiliated to Shandong First Medical University, Jinan, China, [2]Department of Oncology, The First Affiliated Hospital of Shandong First Medical University and Shandong Provincial Qianfoshan Hospital, Shandong Key Laboratory of Rheumatic Disease and Translational Medicine, Shandong Lung Cancer Institute, Jinan, China, [3]Cheeloo College of Medicine, Shandong University, Jinan, China, [4]Shandong First Medical University, Jinan, China

Purpose: To retrospectively evaluate the cost and effectiveness in consecutive patients with ground-glass nodules (GGNs) treated with video-assisted thoracoscopic surgery (VATS; i.e., wedge resection or segmentectomy) or microwave ablation (MWA).

Materials and methods: From May 2017 to April 2019, 204 patients who met our study inclusion criteria were treated with VATS (n = 103) and MWA (n = 101). We calculated the rate of 3-year overall survival (OS), local progression-free survival (LPFS), and cancer–specific survival (CSS), as well as the cost during hospitalization and the length of hospital stay.

Results: The rates of 3-year OS, LPFS, and CSS were 100%, 98.9%, and 100%, respectively, in the VATS group and 100%, 100% ($p = 0.423$), and 100%, respectively, in the MWA group. The median cost of VATS vs. MWA was RMB 54,314.36 vs. RMB 21,464.98 ($p < 0.001$). The length of hospital stay in the VATS vs. MWA group was 10.0 vs. 6.0 d ($p < 0.001$).

Conclusions: MWA had similar rates of 3-year OS, LPFS, and CSS for patients with GGNs and a dramatically lower cost and shorter hospital stay compared with VATS. Based on efficacy and cost, MWA provides an alternative treatment option for patients with GGNs.

KEYWORDS

lung adenocarcinoma, microwave ablation, video-assisted thoracoscopic surgery, ground-glass nodule, cost effectiveness

Introduction

Although the incidence of lung cancer is the second-highest of all cancers globally (1), it is the leading cause of cancer deaths in both China and the USA. By 2022, China and the USA are expected to have approximately 870,982 and 238,032 new lung cancer cases and 766,898 and 144,913 lung cancer deaths, respectively (2). Early detection, early diagnosis, and early treatment are critical for mortality reduction. In 2011, the National Lung Screening Trial was the first to report that lung cancer mortality in high-risk populations could be reduced by 20% by screening with low-dose computed tomography (LDCT) instead of standard chest X-ray (3). The widespread application of LDCT has increased the detection rate of asymptomatic pulmonary nodules, and it is estimated that pulmonary nodules are detected in 20%–80% of patients screened in China (4–7). A pulmonary nodule (ground-glass nodule, GGN) is often considered a predictor of a precancerous lesion or early-stage lung cancer. However, more than 97% of GGNs identified by LDCT are benign, with only 0.7%–2.3% of GGNs diagnosed as lung cancer (8–10). GGN lung adenocarcinoma is characterized by indolent development with few distant metastases and has a favorable prognosis, with a 5-year survival rate of 100% after surgery (11–16). Thus, GGN lung adenocarcinoma is deemed a special subtype of lung cancer that differs from traditional early-stage lung cancer.

The primary therapy for cases of GGN lung adenocarcinoma is surgical resection (video-assisted thoracoscopic surgery, VATS) with curative intent. However, there are several limitations to the application of VATS (10, 17). First, premature surgical intervention for GGNs, particularly precancerous lesions, leads to early and unnecessary organ damage and loss of lung function. Moreover, early surgery does significantly improve the overall survival (OS) of patients when compared with those who choose follow-up and elective surgery as interventions. Second, there are no clear selection criteria for surgical intervention of multiple pulmonary nodules and no principles for the follow-up management of residual nodules. Third, because the preoperative diagnosis of pulmonary nodules is based on imaging results and not pathological evidence, surgical resection of pulmonary nodules may be unnecessary and cause needless postoperative complications if the lesions are benign. Fourth, as the population ages, an increasing number of patients aged >75 years are being diagnosed with early-stage lung cancer, and surgery is almost impossible in these cases. Therefore, many novel local treatment approaches have been developed, including image-guided thermal ablation therapy. This precise and minimally invasive technique has been used to treat early-stage lung cancer and includes radiofrequency ablation, microwave ablation (MWA), cryoablation, and laser ablation. MWA was first applied to lung tumors in 2002 (18), and its use has increased over the years (19).

MWA has been proved one of the effective methods to treat GGN lung adenocarcinoma (20–24). Although cost-effectiveness analysis is a proven analytic technique to assess the relative benefit of a given treatment strategy, the cost-effectiveness analysis of MWA in GGN lung adenocarcinoma patients has remained unexplored. Therefore, we performed a cost-effectiveness analysis comparing VATS and MWA for patients with GGN lung adenocarcinoma and analyzed 3-year OS, local progression-free survival (LPFS), and cancer–specific survival (CSS), as well as the length of hospital stay and cost during hospitalization.

Materials and methods

Patient inclusion and exclusion criteria

This retrospective study was approved by the Ethics Committee of Shandong Provincial Hospital, affiliated with Shandong First Medical University. The study complied with the ethical principles of the World Medical Association's Declaration of Helsinki. Written informed consent was obtained from all participants.

From May 2017 to April 2019, 204 consecutive patients with GGNs confirmed by contrast-enhanced computed tomography (CT) and pathology were treated in our institute. Of them, 103 underwent VATS (VATS group) and 101 underwent CT-guided MWA (MWA group). The treatment decisions for each patient were made by a multidisciplinary tumor board that included medical oncologists, thoracic surgeons, respiratory physicians, radiologists, and pathologists who reviewed the medical history, physical examination results, and recent imaging studies. For those patients undergoing MWA, contrast-enhanced chest CT (within 2 weeks before MWA) was considered a key imaging assessment in revealing the tumor size, location, and the relationship with neighboring vital organs, blood vessels, the trachea, or bronchi.

The study inclusion criteria were as follows: (1) Eastern Cooperative Oncology Group performance status 0–2; (2) patients aged ≥18 years and nonpregnant females; (3) a solitary pure GGN or mixed ground-glass opacities (mGGOs; lesions with a ratio of consolidation diameter to tumor diameter of <0.25 at a slice thickness ≤ 1 mm) demonstrated by CT, with a diameter ≤30 mm and without lymph node involvement or distant metastasis; (4) histological diagnosis of adenocarcinoma in situ, minimally invasive adenocarcinoma or invasive adenocarcinoma (25) through percutaneous coaxial needle biopsy (26–28) or using a postoperative specimen; (5) an expected lifespan of ≥12 months; and (6) no chemotherapy or radiotherapy performed after the procedure. The exclusion criteria were as follows: (1) the presence of regional lymph node metastasis or distant metastasis verified by enhanced CT, positron emission tomography-CT, and enhanced magnetic

resonance imaging; (2) GGNs accompanied by other malignant tumors; and (3) untreatable coagulopathies and/or platelet count $< 50 \times 10^9$/L. The histological diagnoses were either confirmed by conventional paraffin sections in separate procedures or by frozen sections and postprocedural paraffin sections in the same procedure.

Instrument and MWA procedure

CT (GE Lightspeed 64 VCT, General Electric, or NeuViz 64, Neusoft Medical Systems) was used to guide MWA, which was performed with an MTC-3C MWA system (Vison-China Medical Devices R&D Center), ECO-100A1 MWA system (ECO Medical Instrument Co., Ltd.), or KY-2450B MWA system (CANYOU Medical Inc.) at a frequency of 2450 ± 50 MHz. The adjustable continuous wave output power ranged from 0 to 100 W. For the microwave antenna, the effective length was 100–180 mm, and the outside diameter was 14–19 G (19 G antenna has the advantages of high puncture accuracy and few complications), with a 1.5 cm radiating tip (tapered end). The surface temperature of the antennae was cooled with a water circulation cooling system.

We performed our standard MWA procedure as per our previous descriptions (29–31). A treatment plan was designed immediately following pre-procedural CT and was based on the tumor location and size, as well as adjacent structures. The appropriate body placement, puncture site on the body surface, optimal puncture trajectory, and antenna number were confirmed. All percutaneous MWA procedures were performed using a sterile technique under local anesthesia, with the patients under moderate sedation. After achieving satisfactory anesthesia, the procedure was performed by positioning the antenna into the initially planned site. After using CT to ascertain that the antennae were properly positioned, we performed MWA at the predetermined power and time. The range of the ablation zone was monitored in real-time on CT, and when it was 5–10 mm beyond the lesion boundary, the ablation procedure was terminated, the antennae were immediately withdrawn from the lesion, and the puncture wound was disinfected and bandaged. At the end of the procedure, a repeat whole-lung CT scan was performed to assess technical success and immediate complications. The procedure was defined as a technical success when the tumor was treated according to protocol and completely covered (i.e., the ablation zone completely overlapped or encompassed the target tumor plus an ablative margin). The patient's electrocardiographic tracing, heart rate, respiratory rate, oxygen saturation, and blood pressure were continuously monitored throughout the MWA session and for an additional 6 h after their safe return to the ward (Figure 1).

Equipment and VATS procedure

The VATS procedure was performed using an IMAGE1 HD video system (Karl Storz, Inc., Germany), a Harmonic ultrasonic scalpel (Ethicon Endo-Surgery, LLC, Puerto Rico, USA), and an Endo GIA Ultra Universal Stapler (Covetingly, MA, USA).

The VATS procedure was performed under general anesthesia with single-lung ventilation, which was accomplished with either dual-lumen endotracheal tubes or single-lumen tubes and bronchial blockers. The patient was placed in a left-sided lateral position with the right hemithorax

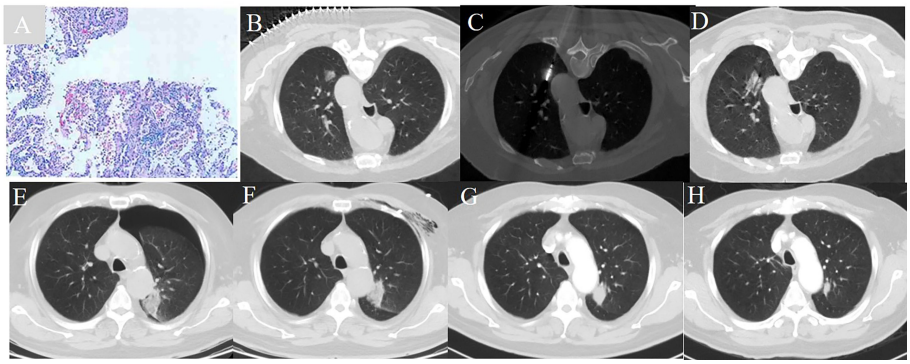

FIGURE 1
A 72 year-old man with a history of COPD and a FEV1 value of 51.2% underwent CT guided microwave ablation after pathological diagnosis of adenocarcinoma in situ. **(A)** Pathology verified adenocarcinoma in situ. **(B)** A ground glass nodule with a diameter of 1.7 cm located in the left upper lobe. **(C)** MWA was conducted with the power of 65 W for a total of 4.5 min. **(D)** The immediate CT scan showed the nodule was surpassed by the exudative change. **(E)** A CT scan showed moderate pneumothorax 24 hours post-ablation. **(F)** Pneumothorax was resolved 72 hours post-ablation. **(G)** The ablative zone shrank and increased in density one month post-ablation. **(H)** The CT ablative zone further reduced one year post-ablation.

slightly overextended so that the intercostal spaces could be expanded to facilitate the operation. A single incision approximately 4 cm long was made along the fifth intercostal space just anterior to the midaxillary line. Hilar dissection was performed through the anterior incision. Dissection of the pulmonary vessels and bronchi was performed in the same manner as in open surgery. Endoscopic linear staplers were used for individual vessel and bronchial ligation. Parenchymal resection margin ≥ 2 cm should be achieved. The lobe was placed in a specimen bag for retrieval after complete resection. Mediastinal lymph nodes were not dissected or only sampled. After the operation, a 28 F chest tube was placed at the apex of the thorax, and an 18 F soft tube was left in the part of the thorax most dependent on drainage. No extra incision was made for drainage. Both chest tubes were connected to a water seal drainage system without suction. The 28 F tube was removed 48 h after surgery when there was no air leak and the lung showed good expansion. The 18 F tube was kept until discharge, when the drainage was <150 mL/d (32–34) (Figure 2).

Follow-up and outcome assessment

Contrast-enhanced chest CT was performed monthly for the first 3 months post-MWA and -VATS and then every 3 months for the first year. Thereafter, the follow-up intervals were extended to 6 months. For those patients who underwent MWA, we assessed the local ablation effect by signs and dynamic changes in the lesion on a series of repeated contrast-enhanced CT scans and used the lesion at 4–6 weeks post-MWA as the baseline for comparisons. The local effect of the ablative response included complete ablation, incomplete ablation, and local progression (35, 36). For the patients who underwent VATS, we applied the Response Evaluation Criteria in Solid Tumors version 1.1 to assess responses (37). We used the follow −up results to assess the 3-year LPFS, CSS, and OS. LPFS was defined as the time interval from the initial MWA or VATS to the first radiologic evidence of local progression. CSS was defined as the time interval from the initial MWA or VATS to 3 years or cancer−related death. The OS was defined as the time interval from the initial MWA or VATS to death from any cause. We also recorded the length of the hospital stay. The during of hospital stay including both the periods before and after ablation

Cost

We identified the direct and indirect costs of MWA and VATS but only included the direct costs during hospitalization in this study. The direct costs included the cost of MWA or VATS treatment during hospitalization, mainly comprising the fees for medicine, laboratory tests, examination, anesthesia, ICU, operation, medical supplies, blood transfusion, etc. (38–41). The cost of hospitalization was determined by reviewing the billing details of hospitalization expenses.

Complication assessment

Complications were assessed based on the number of ablation procedures. The severity of injuries to patients was classified as major or minor according to the Cirse Quality

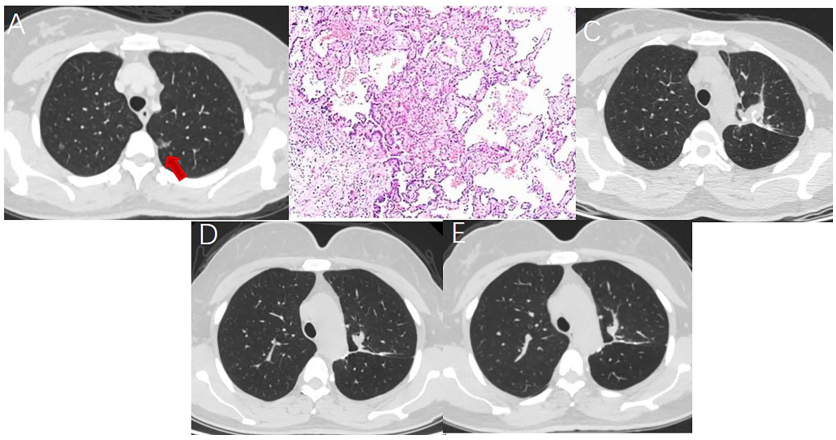

FIGURE 2
A 52 year-old woman with multiple GGNs underwent resection of apical posterior segment of left upper lobe and lymph node sampling. **(A)** A ground glass nodule with a diameter of 1.5cm located in the left upper lobe. **(B)** Postoperative pathology showed minimal invasive adenocarcinoma with no lymph node metastasis. **(C)** Soft tissue-density mass and linear stapler can be seen in the operation area on the CT image one month after surgery. **(D)** The soft tissue density mass in the operation area shrank 7 months after surgery. **(E)** The operation area formed fibrous scar 14 months after surgery.

Assurance Document and Standards for Classification of Complications: The Cirse Classification System (42, 43). Major complications were defined as events that led to substantial morbidity and disability (e.g., unexpected loss of an organ), an increased level of care, hospital admission, or a substantially prolonged hospital stay (classifications 3–5). This also included any case where a blood transfusion or an interventional drainage procedure were required. Any patient's death within 30 d after image-guided tumor ablation was addressed (classification 6). All other events were considered minor complications (classifications 1–2). VATS complications were classified according to surgical complications (44).

Statistical analysis

All statistical analyses were performed using SPSS 17.0 software (SPSS, Chicago, IL, USA). Categorical variables were presented as numbers and percentages. Continuous data were presented as means and standard deviations. We compared local and control rates using the chi-square test and length of hospital stay and cost using an independent *t*-test. Survival curves were constructed using the Kaplan–Meier method and compared by the log-rank test. A p value < 0.05 was considered statistically significant.

Results

As of April 1, 2022, no patients were lost follow–up, and the median follow-up time was 40.1 and 42.6 months in the VATS and MWA groups, respectively. All patients are under clinical observation and have not received any antitumor treatments, such as stereotactic radiation therapy, chemotherapy, targeted therapy, and immunotherapy.

Compared with the VATS group, those in the MWA group were older (66.40 vs. 56.70 years), predominantly male (54.5% vs. 40.8%), and had higher comorbidity of cardiovascular (28.7% vs. 9.7%) and pulmonary disease (33.7% vs. 12.6%). Other characteristics were comparable between the two groups (Table 1).

Survival

In the VATS group, 1 (1.0%) patient showed local tumor progression 36.4 months after VATS and was subsequently treated with radiation therapy. At the 3–year follow–up, 103 of 104 VATS tumors were controlled. The 3–year LPFS, CSS, and OS rates were 98.9%, 100%, and 100%, respectively. No mediastinal lymph node and distant metastases were observed in any patients in the VATS or MWA groups.

In the MWA group, 4 (4.0%) patients showed local tumor progression. These patients underwent a second MWA, and complete ablation was achieved. At the 3–year follow–up, all ablated tumors (105 sessions) were under control. The 3–year LPFS, CSS, and OS rates were all 100%. There was no significant difference in 3-year LPFS (p = 0.423), OS(p=1.000), and CSS (p=1.000) between the VATS and MWA groups.

Cost and length of hospital stay

The mean length of hospital stay for the MWA group was significantly lower compared with the VATS group 6.0 vs. 10.0 d (p<0.001). Furthermore, the median cost, medicine fee, and medical supplies fee for the MWA group was lower than the VATS group (RMB 21,464.98 vs. RMB 54,314.36, RMB 2,516.23 vs. RMB 8,970.04, and RMB 7,568.14 vs. RMB 27,167.25, respectively; p < 0.001 for all). However, the laboratory and examination fees were similar between the two groups (5,252.70 vs. 6,103.50, p = 0.191). Other fees, including the operation, anesthesia, ICU, and blood transfusion fees, were only observed in the VATS group (Table 2).

Complications

The MWA and VATS procedures were successfully performed in all patients. Perioperative complications are listed in Table 3. Infection occurred in two patients in the VATS group. No respiratory failure was observed in either group. There were 51 (50.5%) and 7 (6.8%) patients in the MWA and VATS groups, respectively, who suffered slight pneumothorax after the procedure (p < 0.001). Only 10 patients (19.6) underwent classification 3 pneumothorax and chest tube drainage was conducted in the MWA group. No one underwent respiratory failure was observed in both groups.

Forced expiratory volume in the first second and forced vital capacity was similar between pre-ablation and one-month post-ablation. There were no significant differences in the incidence of mortality, pleural effusion, coronary/cerebral vascular events, and bleeding requiring reoperation between the two groups.

Discussion

During the past 2 decades, VATS has been established as the gold-standard surgical approach for lobectomy in patients with early-stage non-small-cell lung carcinoma (including GGN lung adenocarcinoma). VATS shows various advantages over open surgery, such as decreased blood loss, less pain, shorter hospital stay, more rapid recovery, preserved postoperative pulmonary function, and decreased inflammatory response. Furthermore, the early and late outcomes of VATS are comparable to or even superior to those of open thoracotomy (45–50). At present, many clinical studies have reported the efficacy and safety of

TABLE 1 Baseline characteristics of enrolled patients.

Characteristics	MWA group (%) N = 101	VATS group (%) N = 103	*p*
Age (years, range)	66.40 ± 11.35 (27,88)	56.70 ± 9.01 (31,82)	<0.001
Sex			0.050
Male	55 (54.5)	42 (40.8)	
Female	46 (45.5)	61 (59.2)	
ECOG			NA
0–1	101 (100.0)	103 (100.0)	
2	0 (0.0)	0 (0.0)	
Comorbidity			
Cardiovascular diseases	29 (28.7)	10 (9.7)	0.001
Pulmonary diseases	34 (33.7)	14 (13.6)	0.001
Diabetes	16 (15.8)	13 (12.6)	0.510
Smoking			0.148
No	64 (63.4)	75 (72.8)	
Yes	37 (36.6)	28 (27.2)	
Location of GGN			0.068
Right upper lobe	32 (31.7)	32 (31.1)	
Right middle lobe	4 (4.0)	0 (0.0)	
Right lower lobe	18 (17.8)	25 (24.3)	
Left upper lobe	27 (26.7)	35 (34.0)	
Left lower lobe	20 (19.8)	11 (10.7)	
Size of GGN (mm)			<0.001
Mean ± SD (range)	16 (15.8)	28 (27.2)	
Size of GGN (mm)			NA
≤ 10	16 (15.8)	28 (27.2)	
> 10, ≤ 20	51 (50.5)	65 (63.1)	
> 20	34 (33.7)	10 (9.7)	
CT finding (GGN type)			0.061
pGGN	35 (34.7)	49 (47.6)	
mGGN	66 (65.3)	54 (52.4)	
Histology of GGN			<0.001
AIS	28 (27.7)	32 (31.1)	
MIA	13 (12.9)	44 (42.7)	
IA	60 (59.4)	27 (26.2)	
T stage at diagnosis			0.069
T1a	8 (13.3)	2 (7.4)	
T1b	31 (51.7)	21 (77.8)	
T1c	21 (35.0)	4 (14.8)	

AAH, atypical adenomatous hyperplasia; AIS, adenocarcinoma in situ; CT, computed tomography; GGN, ground glass nodule; IA, invasive adenocarcinomas; mGGO, mixed ground glass opacity; MIA, minimally invasive adenocarcinomas; MWA, microwave ablation; pGGN, pure ground glass nodule; SD, standard deviation; VATS, Video-Assisted Thoracoscopic Surgery. NA, not application.

percutaneous CT-guided MWA to treat GGN lesions (20–22, 51, 52). However, few studies have compared the differences in clinical outcomes, cost, and complications between MWA and VATS for GGN lung adenocarcinoma.

The follow–up results of this study showed a 3-year OS, LPFS, and CSS rate of 100% vs. 100%, 98.9% vs. 100%, and 100% vs. 100% in the VATS vs. MWA groups, respectively. No significant differences were observed in log-rank analysis between the groups (p = 0.171). Our findings suggest that MWA has similar efficacy to VATS in patients with GGN lung adenocarcinoma. Wang et al. reported a similar finding (52). For both MWA and VATS in the treatment of GGOs, the 3 year-OS and CSS were both 100%, local disease progression was only observed in 5 patients, which was significantly superior to those with solid tumors.

Our results demonstrate that MWA is less costly and results in a better quality of life (fewer complications) compared with VATS for patients with GGN lung adenocarcinoma (Table 3).

TABLE 2 The comparation of cost between the two groups.

	MWA group	VATS group	P
Hospital stay	6.00 (5.00,9.00)	11.00 (8.00,12.00)	<0.001
Medicine fee	2516.23 (1588.50,4293.94)	8970.04 (6776.80,11659.47)	<0.001
Laboratory and examination fee	5252.70 (4647.95,11499.00)	6103.50 (5095.40,7576.40)	0.191
Operation fee	–	5455.00 (4690.00,5455.00)	<0.001
Anesthesia fee	–	3383.05 (3200.05,3545.08)	–
ICU fee	–	0.00 (0.00,0.00)	–
Medical supplies fee	7568.14 (6571.54,11469.71)	27167.25 (21147.66,31708.96)	<0.001
Blood transfusion fee	–	790.00 (150.00,950.00)	–
All	21464.98 (17373.77, 26576.84)	54314.36 (47673.58,62733.88)	<0.001

ICU, intense care unit; MWA, microwave ablation; VATS, Video-Assisted Thoracoscopic Surgery.

The primary cost differences were associated with expenses related to the anesthesia, ICU, medical supplies, blood transfusion, and medicine fees. This suggests the superiority of the MWA approach compared with VATS and should consequently, from an economic standpoint, not discourage physicians or thoracic surgeons from implementing MWA in their practice. The length of hospital stay in the MWA group was shorter than in the VATS group because MWA for patients with GGN lung adenocarcinoma does not require general anesthesia or a stay in ICU. Additionally, there is less trauma and faster recovery. Furthermore, there are few serious complications post-MWA, which is one of the reasons for the shorter hospital stay.

For patients with multiple GGOs, ENB-guided microwave ablation combined with uniportal VATS is a treatment regimen. However, compared with CT guidance, the bronchoscopy guidance means the longer treatment interval and more cost. For those lesions located in the peripheral of the lung, CT guided MWA was superior to bronchoscopy guided MWA. However, for the GGOs located in the middle of the lung, the bronchoscopy guided MWA had the advantage (53). For patients with GGOs and contradiction to surgery, cryoablation was a treatment regimen. Compared with radical surgery, the cryoablation procedures are associated with less trauma, high efficacy rates, and fast recovery and is therefore applicable across a wide range of patient populations (54, 55).

Although compared with VATS, MWA had more pneumothorax, those with classification 3 pneumothorax was few. The pneumothorax did not affect the respiratory function and no respiratory failure was observed. So, the MWA in the treatment of GGN was safe.

There were some limitations to this study. First, it was a retrospective single-institution study. Second, there was a relatively small number of cases and a relatively short follow-up period. Third, we used the direct cost of medical treatment in a single hospital and did not calculate the indirect costs. Additionally, the cost of hospital readmission for serious complications related to MWA and VATS treatment after discharge and the cost of outpatient treatment during follow-up were not calculated. Fourth, due to the unbalanced development of MWA and VATS technology in different regions in China, the study population is not representative of the other regions of China. Therefore, a prospective, multicenter, randomized controlled study is necessary to evaluate cost and effectiveness in patients with early-stage GGN lung adenocarcinoma treated with MWA vs. VATS.

In conclusion, this study suggests MWA as an effective and safe option to treat early-stage GGN lung adenocarcinoma, with efficacy similar to VATS, a lower cost, and a shorter hospital stay. Despite being a newly incorporated technology, MWA provides an alternative treatment for this disease. In the future, a

TABLE 3 The complications of enrolled patients.

Characteristic	MWA group	VATS group	p
Mortality	0 (0.0)	0 (0.0)	NA
Pain (post procedure)	3 (3.0)	5 (4.9)	0.721
Pneumothorax	51 (50.5)	7 (6.8)	<0.001
Pleural effusion	55 (54.5)	48 (46.6)	0.262
Infection	3 (3.0)	2 (1.9)	0.681
All	73 (72.3)	52 (50.0)	0.001

MWA, microwave ablation; NA, not application; VATS, Video-Assisted Thoracoscopic Surgery.

prospective, multicenter, randomized controlled study is necessary to evaluate the cost and efficacy of MWA in the treatment of early-stage GGN lung adenocarcinoma.

Data availability statement

The original contributions presented in the study are included in the article/supplementary material. Further inquiries can be directed to the corresponding authors.

Ethics statement

The studies involving human participants were reviewed and approved by Shandong Provincial Hospital affiliated to Shandong First Medical University. Written informed consent to participate in this study was provided by the participants' legal guardian/next of kin.

Author contributions

XYa and XYe: Conceptualization, data curation, methodology, and writing—original draft. XH, ZW, ZZ, XYa, and XYe: Data curation, methodology, resources, and writing—final draft. All authors contributed to the article and approved the submitted version.

Funding

This study received funding from the National Natural Science Foundation of China (81502610 and 82072028) and the Shandong Provincial Natural Science Foundation, China (ZR2021MH143 and ZR2020MH294).

Conflict of interest

The authors declare that the research was conducted in the absence of any commercial or financial relationships that could be construed as a potential conflict of interest.

Publisher's note

References

1. International Agency for Research on Cancer, WHO. *Latest global cancer data: cancer burden rises to 19.3 million new cases and 10.0 million cancer deaths in (2020).* Available at: https://www.iarc.fr/faq/latest-global-cancer-data-2020-qa/ (Accessed 18 Apr 2021).

2. Xia C, Dong X, Li H, Cao M, Sun D, He S, et al. Cancer statistics in China and united states, 2022: Profiles, trends, and determinants. *Chin Med J (Engl)* (2022) 135(5):584–90. doi: 10.1097/CM9.0000000000002108

3. National Lung Screening Trial Research T, Aberle DR, Adams AM, Berg CD, Black WC, Clapp JD, et al. Reduced lung-cancer mortality with low-dose computed tomographic screening. *N Engl J Med* (2011) 365(5):395–409. doi: 10.1056/NEJMoa1102873

4. Fan L, Wang Y, Zhou Y, Li Q, Yang W, Wang S, et al. Lung cancer screening with low-dose ct: Baseline screening results in shanghai. *Acad Radiol* (2019) 26 (10):1283–91. doi: 10.1016/j.acra.2018.12.002

5. He YT, Zhang YC, Shi GF, Wang Q, Xu Q, Liang D, et al. Risk factors for pulmonary nodules in north China: A prospective cohort study. *Lung Cancer* (2018) 120:122–9. doi: 10.1016/j.lungcan.2018.03.021

6. Xu GH, Huang HX, Chen B, Lou Y, Wang DY, Wu JB, et al. A study on the first chest low-dose CT screening and susceptible factors of pulmonary nodules in 23,695 physical examinees in a medical examination center. *Fudan Xue Bao (Yi Xue Ban)* (2020) 47(5):654–9. doi:10.3969/j.issn.1672-8467.2020.05.003

7. Yang W, Qian F, Teng J, Wang H, Manegold C, Pilz LR, et al. Community-based lung cancer screening with low-dose ct in China: Results of the baseline screening. *Lung Cancer* (2018) 117:20–6. doi: 10.1016/j.lungcan.2018.01.003

8. Liu Y, Luo H, Qing H, Wang X, Ren J, Xu G, et al. Screening baseline characteristics of early lung cancer on low-dose computed tomography with computer-aided detection in a Chinese population. *Cancer Epidemiol* (2019) 62:101567. doi: 10.1016/j.canep.2019.101567

9. Poonia DR, Sehrawat A, Gupta MK. Lung cancer screening: An unending tale. *J Cancer Res Ther* (2021) 17(6):1289–93. doi: 10.4103/jcrt.JCRT_888_20

10. Ye X, Fan W, Wang Z, Wang J, Wang H, Wang J, et al. Expert consensus on thermal ablation therapy of pulmonary subsolid nodules (2021 edition). *J Cancer Res Ther* (2021) 17(5):1141–56. doi: 10.4103/jcrt.jcrt_1485_21

11. Kakinuma R, Noguchi M, Ashizawa K, Kuriyama K, Maeshima AM, Koizumi N, et al. Natural history of pulmonary subsolid nodules: A prospective multicenter study. *J Thorac Oncol* (2016) 11(7):1012–28. doi: 10.1016/j.jtho.2016.04.006

12. Lee HW, Jin KN, Lee JK, Kim DK, Chung HS, Heo EY, et al. Long-term follow-up of ground-glass nodules after 5 years of stability. *J Thorac Oncol* (2019) 14(8):1370–7. doi: 10.1016/j.jtho.2019.05.005

13. Shigefuku S, Shimada Y, Hagiwara M, Kakihana M, Kajiwara N, Ohira T, et al. Prognostic significance of ground-glass opacity components in 5-year survivors with resected lung adenocarcinoma. *Ann Surg Oncol* (2021) 28(1):148–56. doi: 10.1245/s10434-020-09125-x

14. Zhang Y, Chen H. Commentary: Is sublobar resection enough for ground-glass opacity-dominant lung adenocarcinoma? *J Thorac Cardiovasc Surg* (2022) 163(1):303–4. doi: 10.1016/j.jtcvs.2020.09.126

15. Zhang Y, Fu F, Chen H. Management of ground-glass opacities in the lung cancer spectrum. *Ann Thorac Surg* (2020) 110(6):1796–804. doi: 10.1016/j.athoracsur.2020.04.094

16. Zhang Y, Ma X, Shen X, Wang S, Li Y, Hu H, et al. Surgery for pre- and minimally invasive lung adenocarcinoma. *J Thorac Cardiovasc Surg* (2022) 163 (2):456–64. doi: 10.1016/j.jtcvs.2020.11.151

17. Altorki N, Vimolratana M. Commentary: Surgery for ground-glass nodules: Free lunch or slippery slope? *J Thorac Cardiovasc Surg* (2022) 163(2):465–6. doi: 10.1016/j.jtcvs.2020.12.073

18. Feng W, Liu W, Li C, Li Z, Li R, Liu F, et al. Percutaneous microwave coagulation therapy for lung cancer. *Zhonghua Zhong Liu Za Zhi* (2002) 24 (4):388–90.

19. Ni Y, Xu H, Ye X. Image-guided percutaneous microwave ablation of early-stage non-small cell lung cancer. *Asia Pac J Clin Oncol* (2020) 16(6):320–5. doi: 10.1111/ajco.13419

20. Chi J, Wang Z, Ding M, Hu H, Zhai B. Technical safety and efficacy of a blunt-tip microwave ablation electrode for ct-guided ablation of pulmonary ground-glass opacity nodules. *Eur Radiol* (2021) 31(10):7484–90. doi: 10.1007/s00330-021-07774-4

21. Hertzanu Y, Ye X. Computed tomography-guided percutaneous microwave ablation: A new weapon to treat ground-glass opacity-lung adenocarcinoma. *J Cancer Res Ther* (2019) 15(2):265–6. doi: 10.4103/jcrt.JCRT_65_19

22. Huang G, Yang X, Li W, Wang J, Han X, Wei Z, et al. A feasibility and safety study of computed tomography-guided percutaneous microwave ablation: A novel therapy for multiple synchronous ground-glass opacities of the lung. *Int J Hyperthermia* (2020) 37(1):414–22. doi: 10.1080/02656736.2020.1756467

23. Xue G, Li Z, Wang G, Wei Z, Ye X. Computed tomography-guided percutaneous microwave ablation for pulmonary multiple ground-glass opacities. *J Cancer Res Ther* (2021) 17(3):811–3. doi: 10.4103/jcrt.jcrt_531_21

24. Yang X, Ye X, Lin Z, Jin Y, Zhang K, Dong Y, et al. Computed tomography-guided percutaneous microwave ablation for treatment of peripheral ground-glass opacity-lung adenocarcinoma: A pilot study. *J Cancer Res Ther* (2018) 14(4):764–71. doi: 10.4103/jcrt.JCRT_269_18

25. Available at: https://publications.iarc.fr/Book-And-Report-Series/Who-Classification-Of-Tumours/Thoracic-Tumours-2021.

26. Wei Z, Yang X, Feng Y, Kong Y, Yao Z, Ma J, et al. Could concurrent biopsy and microwave ablation be reliable? concordance between frozen section examination and final pathology in ct-guided biopsy of lung cancer. *Int J Hyperthermia: Off J Eur Soc For Hyperthermic Oncology North Am Hyperthermia Group* (2021) 38(1):1031–6. doi: 10.1080/02656736.2021.1947528

27. Wang J, Ni Y, Yang X, Huang G, Wei Z, Li W, et al. Diagnostic ability of percutaneous core biopsy immediately after microwave ablation for lung ground-glass opacity. *J Cancer Res Ther* (2019) 15(4):755–9. doi: 10.4103/jcrt.JCRT_399_19

28. Zhang P, Liu JM, Zhang YY, Hua R, Xia FF, Shi YB. Computed tomography-guided lung biopsy: A meta-analysis of low-dose and standard-dose protocols. *J Cancer Res Ther* (2021) 17(3):695–701. doi: 10.4103/jcrt.JCRT_1274_20

29. Ni Y, Peng J, Yang X, Wei Z, Zhai B, Chi J, et al. Multicentre study of microwave ablation for pulmonary oligorecurrence after radical resection of non-Small-Cell lung cancer. *Br J Cancer* (2021) 125(5):672–8. doi: 10.1038/s41416-021-01404-y

30. Wei Z, Yang X, Ye X, Feng Q, Xu Y, Zhang L, et al. Microwave ablation plus chemotherapy versus chemotherapy in advanced non-small cell lung cancer: A multicenter, randomized, controlled, phase iii clinical trial. *Eur Radiol* (2020) 30 (5):2692–702. doi: 10.1007/s00330-019-06613-x

31. Yang X, Ye X, Zheng A, Huang G, Ni X, Wang J, et al. Percutaneous microwave ablation of stage I medically inoperable non-small cell lung cancer: Clinical evaluation of 47 cases. *J Surg Oncol* (2014) 110(6):758–63. doi: 10.1002/jso.23701

32. Gonzalez D, Paradela M, Garcia J, Dela Torre M. Single-port video-assisted thoracoscopic lobectomy. *Interact Cardiovasc Thorac Surg* (2011) 12(3):514–5. doi: 10.1510/icvts.2010.256222

33. Wang H, Zhou X, Xie D, Jiang S, Ding H, Gonzalez D, et al. Uniportal video-assisted thoracic surgery-the experiences of shanghai pulmonary hospital. *J Vis Surg* (2016) 2:56. doi: 10.21037/jovs.2016.03.06

34. Yim AP, Izzat MB, Liu HP, Ma CC. Thoracoscopic major lung resections: An Asian perspective. *Semin Thorac Cardiovasc Surg* (1998) 10(4):326–31. doi: 10.1016/s1043-0679(98)70035-8

35. [Clinical practice guidelines : Image-guided thermal ablation of primary and metastatic lung tumors (2021 edition)]. *Zhonghua Nei Ke Za Zhi* (2021) 60 (12):1088–105. doi: 10.3760/cma.j.cn112138-20210814-00554

36. Ye X, Fan W, Wang H, Wang J, Wang Z, Gu S, et al. Expert consensus workshop report: Guidelines for thermal ablation of primary and metastatic lung tumors (2018 edition). *J Cancer Res Ther* (2018) 14(4):730–44. doi: 10.4103/jcrt.JCRT_221_18

37. Eisenhauer EA, Therasse P, Bogaerts J, Schwartz LH, Sargent D, Ford R, et al. New response evaluation criteria in solid tumours: Revised recist guideline (Version 1.1). *Eur J Cancer* (2009) 45(2):228–47. doi: 10.1016/j.ejca.2008.10.026

38. Chen W, Yu Z, Zhang Y, Liu H. Comparison of cost effectiveness between video-assisted thoracoscopic surgery (Vats) and open lobectomy: A retrospective study. *Cost Eff Resour Alloc* (2021) 19(1):55. doi: 10.1186/s12962-021-00307-2

39. Bendixen M, Kronborg C, Jorgensen OD, Andersen C, Licht PB. Cost-utility analysis of minimally invasive surgery for lung cancer: A randomized controlled trial. *Eur J Cardiothorac Surg* (2019) 56(4):754–61. doi: 10.1093/ejcts/ezz064

40. Cowper PA, Feng L, Kosinski AS, Tong BC, Habib RH, Putnam JBJr., et al. Initial and longitudinal cost of surgical resection for lung cancer. *Ann Thorac Surg* (2021) 111(6):1827–33. doi: 10.1016/j.athoracsur.2020.07.048

41. Medbery RL, Fernandez FG, Kosinski AS, Tong BC, Furnary AP, Feng L, et al. Costs associated with lobectomy for lung cancer: An analysis merging sts and Medicare data. *Ann Thorac Surg* (2021) 111(6):1781–90. doi: 10.1016/j.athoracsur.2020.08.073

42. Ahmed M, Solbiati L, Brace CL, Breen DJ, Callstrom MR, Charboneau JW, et al. Image-guided tumor ablation: Standardization of terminology and reporting criteria–a 10-year update. *Radiology* (2014) 273(1):241–60. doi: 10.1148/radiol.14132958

43. Filippiadis DK, Binkert C, Pellerin O, Hoffmann RT, Krajina A, Pereira PL. Cirse quality assurance document and standards for classification of complications: The cirse classification system. *Cardiovasc Intervent Radiol* (2017) 40(8):1141–6. doi: 10.1007/s00270-017-1703-4

44. Dindo D, Demartines N, Clavien PA. Classification of surgical complications: A new proposal with evaluation in a cohort of 6336 patients and results of a survey. *Ann Surg* (2004) 240(2):205–13. doi: 10.1097/01.sla.0000133083.54934.ae

45. Swanson SJ, Herndon JE, D'Amico TA, Demmy TL, McKenna RJ, Green MR, et al. Video-assisted thoracic surgery lobectomy: Report of calgb 39802–a prospective, multi-institution feasibility study. *J Clin Oncol* (2007) 25(31):4993–7. doi: 10.1200/JCO.2007.12.6649

46. Kim HK. Video-assisted thoracic surgery lobectomy. *J Chest Surg* (2021) 54 (4):239–45. doi: 10.5090/jcs.21.061

47. Manerikar A, Querrey M, Cerier E, Kim S, Odell DD, Pesce LL, et al. Comparative effectiveness of surgical approaches for lung cancer. *J Surg Res* (2021) 263:274–84. doi: 10.1016/j.jss.2020.10.020

48. McKenna RJJr., Houck W, Fuller CB. Video-assisted thoracic surgery lobectomy: Experience with 1,100 cases. *Ann Thorac Surg* (2006) 81(2):421–5. doi: 10.1016/j.athoracsur.2005.07.078

49. Montagne F, Guisier F, Venissac N, Baste JM. The role of surgery in lung cancer treatment: Present indications and future perspectives-state of the art. *Cancers (Basel)* (2021) 13(15):3711. doi: 10.3390/cancers13153711

50. Chi J, Ding M, Wang Z, Hu H, Shi Y, Cui D, et al. Pathologic diagnosis and genetic analysis of sequential biopsy following coaxial low-power microwave thermal coagulation for pulmonary ground-glass opacity nodules. *Cardiovasc Intervent Radiol* (2021) 44(8):1204–13. doi: 10.1007/s00270-021-02782-9

51. Bao F, Yu F, Wang R, Chen C, Zhang Y, Lin B, et al. Electromagnetic bronchoscopy guided microwave ablation for early stage lung cancer presenting as ground glass nodule. *Transl Lung Cancer Res* (2021) 10(9):3759–70. doi: 10.21037/tlcr-21-474

52. Wang Y, Liu B, Cao P, Wang W, Wang W, Chang H, et al. Comparison between computed tomography-guided percutaneous microwave ablation and thoracoscopic lobectomy for stage I non-small cell lung cancer. *Thorac Cancer* (2018) 9(11):1376–82. doi: 10.1111/1759-7714.12842

53. Qu R, Tu D, Hu S, Wang Q, Ping W, Hao Z, et al. Electromagnetic navigation bronchoscopy-guided microwave ablation combined with uniportal video-assisted thoracoscopic surgery for multiple ground glass opacities. *Ann Thorac Surg* (2022) 113(4):1307–15. doi: 10.1016/j.athoracsur.2021.04.061

54. Liu S, Liang B, Li Y, Xu J, Qian W, Lin M, et al. CT-guided percutaneous cryoablation in patients with lung nodules mainly composed of ground-glass opacities. *J Vasc Interv Radiol* (2022) 33(8):942–8. doi: 10.1016/j.jvir.2022.04.021

55. Liu S, Zhu X, Qin Z, Xu J, Zeng J, Chen J, et al. Computed tomography-guided percutaneous cryoablation for lung ground-glass opacity: A pilot study. *J Cancer Res Ther* (2019) 15(2):370–4. doi: 10.4103/jcrt.JCRT_299_18

frontiers | Frontiers in Oncology

TYPE Original Research
PUBLISHED 31 October 2022
DOI 10.3389/fonc.2022.955778

OPEN ACCESS

EDITED BY
Xin Ye,
Qianfoshan Hospital, Shandong University, China

REVIEWED BY
Weijun Fan,
Sun Yat-sen University Cancer Center (SYSUCC), China
Nuo Yang,
Guangxi Medical University, China

*CORRESPONDENCE
Yong Jin
jinyong@suda.edu.cn

†These authors have contributed equally to this work

SPECIALTY SECTION
This article was submitted to Thoracic Oncology, a section of the journal Frontiers in Oncology

RECEIVED 29 May 2022
ACCEPTED 12 October 2022
PUBLISHED 31 October 2022

CITATION
Ni Y, Zhong Y, Zhang Y, Tao Y, Pan J, Zhao Y, Zhang Z and Jin Y (2022) Single ultrasound-guided thoracic paravertebral block with a large volume of anesthetic for microwave ablation of lung tumors.
Front. Oncol. 12:955778.
doi: 10.3389/fonc.2022.955778

Single ultrasound-guided thoracic paravertebral block with a large volume of anesthetic for microwave ablation of lung tumors

Yong Ni[1†], Yulong Zhong[1,2†], Yue Zhang[1], Yifei Tao[1], Jiang Pan[1], Yiming Zhao[1], Zhicheng Zhang[1] and Yong Jin[3*]

[1]Pain Department, The Second Affiliated Hospital of Soochow University, Suzhou, China, [2]Anesthesia Department, Sichuan Science City Hospital, Mianyang, China, [3]The Interventional Therapy Department, The Second Affiliated Hospital of Soochow University, Suzhou, China

Objective: To compare single ultrasound-guided thoracic paravertebral block (TPVB) using a large volume of anesthetic with local anesthesia (LA) in computed tomography (CT)-guided pulmonary microwave ablation.

Subjects and methods: Eighty patients who underwent CT-guided microwave ablation of pulmonary tumors were randomly divided into the TPVB group and the LA group. Patients of the TPVB group were anesthetized with a single injection of a large volume (40 ml) of 0.375% ropivacaine injection at T4, and those of the LA group had local infiltration by the surgeon at the puncture site, and emergency rescue with propofol injection was administered when the patient could not tolerate pain in either group. The following variables were recorded in both groups: general conditions; volume of propofol injection for emergency rescue during ablation; visual analog scale (VAS) scores during ablation and at 0, 2, 12, and 24 h after ablation; the need to use analgesics for rescue within 24 h after ablation; number of ablations; number of punctures performed by the surgeon; patient's movements during puncturing; and puncturing-associated complications.

Results: Compared with the TPVB group, the amount of emergency use of propofol injection was significantly more in the LA group ($P < 0.05$). There were no significant differences in the VAS scores recorded intraoperatively and at 0, 2, 12, and 24 h after ablation between the two groups ($P > 0.05$). There was a significant difference in the patient's movements upon puncturing between the two groups ($P < 0.05$), but there were no significant differences in the numbers of punctures and ablations between the two groups ($P > 0.05$). The number of patients using analgesics within 24 h after the operation was also more in the LA group than in the TPVB group, and the difference between the two groups was statistically significant ($P < 0.05$).

Conclusion: Single ultrasound-guided TPVB with a large volume of anesthetic offers effective analgesia for microwave ablation of lung tumors, helping the patient cooperate with the operating surgeon to reduce injury from multiple lung punctures. Further studies are recommended to validate these findings.

KEYWORDS

ultrasound, thoracic paravertebral block, microwave ablation, nerve block, lung cancer

1. Introduction

Microwave ablation (MWA) is the application of electromagnetic waves with frequencies ≥9.2 × 10^8 Hz to treat solid tumors. By causing oscillation of polar water molecules, microwaves produce frictional heating and ultimately induce cellular death *via* coagulation necrosis. In recent years, MWA has become the preferred thermal ablation method (1), and MWA of lung tumors has shown good efficacy in lung metastases from colorectal cancer (2, 3) and thyroid cancer (4), in percutaneous pulmonary ablation for multiple pulmonary nodules (5), and in non-small cell lung cancer (6, 7) (Figure 1). However, MWA of lung tumors causes pain and discomfort during and after ablation; thus, the selection of an anesthetic modality is important. For MWA of lung tumors, the common anesthetic modalities include general anesthesia, local infiltration anesthesia, and nerve block. General anesthesia is an effective analgesic but also has some disadvantages. For instance, under general anesthesia, the patient cannot cooperate with the surgeon, which causes inconvenience to the surgeon.

Since Hara et al. reported ultrasound-guided thoracic paravertebral nerve block (TPVB) in 2007 (8), it has been widely used in thoracic surgery such as in thoracoscopic lung surgery (9), breast surgery (10), rib surgery, and mediastinal surgery and thoracotomies. TPVB has a good analgesic effect in these surgeries. In 2018, Ruscio et al. (11) reported the use of TPVB in computed tomography (CT)-guided percutaneous radiofrequency ablation of lung metastases, with the anesthesiologist performing CT-guided TPVB using 20 ml of 0.375% ropivacaine injection and 2.7 μg/ml of iodixanol. It was concluded that CT-guided TPVB was an effective, low-risk strategy that provided high-quality analgesia. However, CT-guided thoracic paravertebral block is not convenient and only used for analgesia in this study, and patients still need to complete the operation under general anesthesia, which makes patients still unable to cooperate with the surgeon during the operation.

Therefore, we hypothesized that TPVB alone could potentially keep the patient awake to cooperate with the surgeon and also achieve analgesia in MWA of lung tumors. Based on this hypothesis, the current study aimed to compare the intra- and postoperative pain in patients under ultrasound-guided TPVB using a single injection of 40 ml of local anesthetic administered at the T4 level with that of local infiltration anesthesia. This would provide a basis for TPVB alone to be

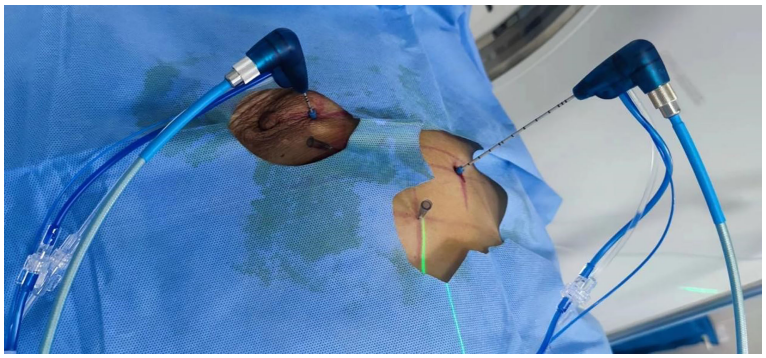

FIGURE 1
CT-guided microwave ablations of lung tumor.

used in MWAs of lung tumors and provide an effective and convenient anesthetic modality for the surgeon and patient.

2. Methods

2.1 Study design, settings, and participants

In accordance with the Declaration of Helsinki (National Health Council Resolution 196/96), written informed consent was obtained from all patients prior to participation in this randomized, parallel-group, clinical trial, and the trial was approved by the Ethics Committee of the Second Affiliated Hospital of Suzhou University (Ethics Committee JD-LK-2022-042-01). A total of 80 patients who underwent CT-guided MWA of lung tumor [age 29–88 years, body mass index (BMI) 16.61–29.38 kg/m^2, American Society of Anesthesiologists (ASA) class I–III] were enrolled in the Interventional Department of the Second Affiliated Hospital of Suzhou University.

The inclusion criteria were as follows: 1) patients intended to undergo CT-guided MWA of lung tumor nodules or tumors, 2) age ≥18 years, and 3) ASA class I–III. The exclusion criteria include the following: 1) allergy to anesthetics, 2) long-term opioid use, 3) puncture site infection, 4) difficulty in communication, and 5) allergy to iodinated contrast media. The elimination criteria were 1) subjects who failed to comply with the established study protocol and 2) subjects with incomplete study data.

2.2 Sample size justification

The sample size for this study was determined according to the results of a pilot study. This study was a randomized, double-blind, controlled parallel-group trial. The intervention group was the TPVB group, while the control group was the LA group. The primary outcome was the volume of propofol injection used for emergency rescue during ablation. Based on the results of the pilot study, the volume of propofol injection used was 96 ± 35.777 ml in the LA group and 50 ± 70.711 ml in the TPVB group. The following statistics were adopted: $\alpha = 0.05$ (bilateral), power = 0.90, and N1 = N2. The sample size was calculated by using PASS 15 software to be N1 = N2 = 33. Assuming a rate of loss to follow-up of 10%, a sample size of N1′ = N2′= 33 ÷ 0.9 = 37 was required. A total of 80 patients were finally enrolled in the two groups.

2.3 Randomization

A patient was assigned to the TPVB group or the LA group by using a computerized random-number generator. Opaque envelopes containing a set of materials for either group were prepared prior to subject enrollment, which were sealed and numbered sequentially. After a participant agreed to participate in the trial, the next envelope in the sequence was opened by the coordinator who was not involved in the patient intervention.

2.4 Blinding

To control for possible measurement bias and high placebo effect due to active treatment in this study, the following measures were taken: 1) patients discussed their relevant treatment strategies with their treating doctor only, but not with the investigator; 2) two licensed anesthesiologists managed the anesthetic process for the patient; 3) two independent assessors instructed the patient on and administered VAS scoring in the trial; 4) two independent assessors tested the levels of skin hypoesthesia in patients who were intervened; and 5) two investigators who did not participate in the patient assessment were responsible for the blinding and randomization processes.

2.5 Interventions

2.5.1 Ultrasound-guided TPVB localization and puncturing

The patient was placed in the prone position. Ribs 1 to 4 were identified from top to bottom by using a low-frequency ultrasound probe (Vinno Technology, Suzhou, China) placed next to the spine, and the fourth rib was marked with a marker pen.

2.5.2 Puncturing

At the fourth rib, the low-frequency ultrasound probe was paralleled to the short axis of the body, and the transverse process and pleura were located and identified in this plane. Using the planar technique, the needle was inserted from the lateral side to the medial side and advanced until it entered the triangle formed by the parietal pleura (anterior), the intercostal membrane, and the intercostal innermost muscle (posterior) Figure 2. The needle tip and puncture path were clearly displayed during the puncturing process. The puncture needle was advanced to the vicinity of the pleura. The water separation technique was used to observe the pressure beneath the pleura, and the syringe plunger was withdrawn if pressure was present beneath the pleura. If no air or blood was drawn, 40 ml of 0.375% ropivacaine was injected. If there was no pressure beneath the pleura, the puncture needle was adjusted until pressure beneath the pleura was observed; the remaining steps were then performed Figure 3.

To ensure the consistency of the puncturing procedure throughout the trial, ultrasound-guided TPVB was performed by one anesthesiologist experienced in nerve block.

2.6 Supplementary analgesic use

Rescue with propofol injection for anesthesia and analgesic use for pain relief were allowed after ablation in all patients. Analgesics were used in the following order: non-steroidal anti-inflammatory analgesics, weak opioids, and strong opioids. The use of any analgesics within 24 h after ablation was recorded.

2.7 Instruments and assessments

The visual analog scale (VAS) employed in this study has been widely used clinically. Two independent assessors trained the patient on VAS scoring. Two other independent assessors were trained in testing the plane of skin hypoesthesia after ultrasound-guided TPVB.

2.8 Outcomes

2.8.1 Primary outcomes

The volume of propofol injection is required for emergency intraoperative intravenous rescue. Propofol injection at a dose of 1–2 mg/kg was given intraoperatively when the VAS score was ≥4 points to keep the patient unconscious until the end of ablation.

2.8.2 Secondary outcomes

Pain intensity was measured by using a 10-cm VAS. The VAS score ranges from no pain (0) to worst pain (10). The VAS scores were recorded intraoperatively and at 0, 2, 12, and 24 h postoperatively. Intraoperative VAS scoring helped determine the intensity of pain and whether emergency intravenous rescue was required. The VAS scores at 0, 2, 12, and 24 h postoperatively revealed the intensity and duration of pain following ablation and helped analyze the intensity and influencing factors of postoperative pain.

2.8.3 The patient's reactions to intraoperative puncturing through the pleura

The surgeon required the patient to remain immobile during ablation to reduce lung injury from punctures. The disappearance of this reaction may reduce the number of punctures and indirectly reduce lung injury.

2.8.4 Puncturing-associated complications

These included pneumothorax, bleeding, and local anesthetic poisoning.

2.9 Statistical analysis

Statistical analyses were performed by using SPSS 25.0. Data of normal distribution are expressed as mean ± standard deviation. Measurement data were compared by *t*-test. Paired *t*-tests were performed for intragroup comparison. Chi-square tests were conducted to compare enumeration data. Rank-sum tests were performed to compare measurement data of non-normal distribution and ranked data. A *P*-value <0.05 was deemed statistically significant.

3. Results

3.1 General data

Eighty patients with lung tumors were enrolled and randomized into two groups. Demographic data (age and sex), BMI, and ASA classification are presented in Table 1.

3.2 Primary outcomes

All 40 patients in the LA group received an emergency rescue with propofol injection (1–2 mg/kg) for intolerable intraoperative pain due to ablation, while only 7 patients in the TPVB group received emergency sedation with propofol injection (Table 2).

Intraoperative VAS scoring indicated severe pain in 9 patients, moderate pain in 8 patients, and mild or no pain in 23 patients in the LA group and severe pain in 5 patients, moderate pain in 10 patients, and mild or no pain in 25 patients in the TPVB group. VAS scoring immediately after ablation indicated severe pain in 1 patient, moderate pain in 2 patients, and mild or no pain in 37 patients in the LA group and severe pain in 3 patients, moderate pain in 6 patients, and mild or no pain in 31 patients in the TPVB group. VAS scoring at 2 h after ablation indicated severe pain in 1 patient, moderate pain in 1 patient, and mild or no pain in 38 patients in the LA group and severe pain in 0 patients, moderate pain in 2 patients, and mild or no pain in 38 patients in the TPVB group. VAS scoring at 12 h after ablation indicated severe pain in 1 patient, moderate pain in 3 patients, and mild or no pain in 36 patients in the LA group and severe pain in 3 patients, moderate pain in 0 patients, and mild or no pain in 37 patients in the TPVB group. VAS scoring at 24 h after ablation indicated severe pain in 0 patients, moderate pain in 2 patients, and mild or no pain in 38 patients in the LA group and severe pain in 2 patients,

TABLE 1 Age, sex, BMI, and ASA classification of the patients.

Variable	LA group	TPVB group	*P*-value
Age (years)	57.33 ± 13.96	57.13 ± 14.69	0.732
BMI (kg/m^2)	22.47 ± 3.45	22.64 ± 3.09	0.310
ASA (I/II/III)	12/24/4	19/16/5	0.193
Sex (F/M)	17/23	22/18	0.263

10.3389/fonc.2022.955778

TABLE 2 Comparison of propofol volume, VAS scores, and use of analgesics within 24 h after ablation between the two groups.

Primary outcome variable	LA group	TPVB group	*P*-value
Volume of propofol (ml)	100 (80)	0 (0)	<0.001
Intraoperative VAS score	1 (6)	2 (5)	0.61
VAS score 0 h after ablation	1 (1)	1 (3)	0.264
VAS score 2 h after ablation	1 (1)	1 (2)	0.425
VAS score 12 h after ablation	0 (1)	0 (1)	0.287
VAS score 24 h after ablation	0 (1)	0 (1)	0.333
Use of analgesics within 24 h after ablation (Y/N)	32/8	6/34	<0.001
Patient's movements during puncturing (N/Y)	0/40	38/2	<0.001

Values outside the parenthesis: median; values in parenthesis: interquartile spacing.

moderate pain in 0 patients, and mild or no pain in 38 patients in the TPVB group. There were no significant differences in the VAS scores recorded intraoperatively and at 0, 2, 12, and 24 h after ablation between the two groups ($P > 0.05$) (Table 2).

Thirty-two patients in the LA group and 6 patients in the TPVB group received analgesic rescue within 24 h after ablation, and there was a significant difference between the two groups ($P < 0.05$) (Table 2).

Upon puncturing through the pleura, movement was recorded in all 40 patients in the LA group but in only 2 patients in the TPVB group, and this difference between the two groups was significant ($P < 0.05$) (Table 3).

The number of nodules ablated per patient differed insignificantly between the LA group and the TPVB group [1 (1) *vs.* 1 (1)] ($P > 0.05$) (Table 3).

There were no significant differences in the number of punctures between the LA group and the TPVB group [9 (9) *vs.* 8 (6)] ($P > 0.05$) (Table 3).

In the LA group, there were 63 puncture sites across C7 to T9, and 1 patient had an ablation site close to the diaphragm. In the TPVB group, there were 57 puncture sites, and 2 patients had an ablation site close to the pleura (Table 4).

There was skin hypoesthesia in a minimum of 1 segment and a maximum of 10 segments (an average of 4.625 segments) following ultrasound-guided TPVB (Figure 4).

TABLE 3 Comparison of patient's movements, number of nodules ablated, and number of punctures between the two groups.

Secondary outcome variable	LA group	TPVB group	*P*-value
Patient movement upon puncturing (N/Y)	0/40	38/2	<0.001
Number of nodules ablated	1 (1)	1 (1)	0.542
Number of punctures	9 (9)	8 (6)	0.321

Values outside the parenthesis: median; values in parenthesis: interquartile spacing.

No puncturing-associated complications occurred in 40 patients following ultrasound-guided TPVB.

4. Discussion

Pain during MWA of lung tumors predominantly stems from 1) local skin puncture (12); 2) heat transferred to the surrounding tissues during ablation (7); 3) intercostal neuralgia caused by ablation near the pleura, especially near the intercostal nerve (7); and 4) phrenic nerve injury from ablation near the mediastinum or phrenic nerve or referred pain of the shoulder caused by hampered conduction of the phrenic nerve (13). Determining the underlying causes of pain in MWA of lung tumors helps with the selection of appropriate anesthetic modalities and facilitates both intra- and postoperative analgesia. The puncture sites for MWA of lung tumors spanned widely from C7 to T9, and one patient even had more than two MWAs of lung tumor sites; hence, a large volume of ropivacaine (40 ml) was injected at a single site.

There is evidence of some experiences with anesthesia for pulmonary MWA. Kashima et al. used 0.5%–1% lidocaine hydrochloride injection for local infiltration anesthesia in combination with 0.1–0.2 mg of fentanyl for analgesia (14). Hoffman et al. compared general anesthesia with conscious sedation and found that general anesthesia was better for anxious, restless patients and for those unable to hold their breath during needle positioning (15). Ruscio et al. reported the use of ultrasound-guided TPVB in CT-guided pulmonary percutaneous radiofrequency ablations and found that ultrasound-guided TPVB was an effective, low-risk, high-quality modality of analgesia (11). García et al. further demonstrated the advantages of ultrasound-guided TPVB in a case report of pulmonary radiofrequency ablation, suggesting that a single ultrasound-guided TPVB was an effective and safe technique that led to high patient satisfaction and low complication rates. TPVB enables better cooperation between the patient and surgeon while providing good analgesia, which minimizes the risk of pneumothorax by maintaining spontaneous ventilation and has a low failure rate (estimated at 1.98%) (6). In the current study, the volume of intraoperative propofol injection required for emergency rescue was significantly smaller in the TPVB group compared with that in the LA group, which directly indicated that more patients in the TPVB group remained awake during ablation and were better able to cooperate with the surgeon to hold their breath during puncturing (15). Furthermore, compared with the LA group, significantly fewer patients in the TPVB group received emergency analgesic rescue within 24 h after ablation. There were no differences in the VAS scores recorded intraoperatively and at 0, 2, 12, and 24 h after ablation, which were mainly related to the emergency rescue with propofol injection if the intraoperative VAS scores were 4 or more points and to the

10.3389/fonc.2022.955778

TABLE 4 Puncture sites and ablation sites close to the pleura or diaphragm.

LA group	Puncture site	Close to the diaphragm?	Close to the pleura?	TPVB group	Puncture site	Close to the diaphragm?	Close to the pleura?
1	T5, T5, T2, T4	No	No	1	T10	No	No
2	T3	No	No	2	T6	No	No
3	T1	No	No	3	T8, T8	No	No
4	T1, T2	No	No	4	T3	No	No
5	T6, T7	No	No	5	T3	No	No
6	T4	No	No	6	T8	No	No
7	C7	No	No	7	T1	No	No
8	T2	No	No	8	T7	No	No
9	T4, T8	No	No	9	T2, T2	No	No
10	T1	No	No	10	T2	No	No
11	T3	No	No	11	T9	No	No
12	T1	No	No	12	T4	No	No
13	T2, T7	No	No	13	T10	No	No
14	T6	No	No	14	T5	No	No
15	T4	No	No	15	T3, T3, T3	No	No
16	T6, T6	No	No	16	T1	No	No
17	T6	No	No	17	T8, T4	No	No
18	T6, T7	No	No	18	T3	No	No
19	T1, T1	No	No	19	T7	No	No
20	T4, T4	No	No	20	T7, T7	No	No
21	T9	Yes	No	21	T7	No	No
22	T2	No	No	22	T4	No	No
23	T8	No	No	23	T4, T4	No	No
24	T2, T3	No	No	24	T3	No	No
25	T5, T5	No	No	25	T2	No	No
26	T6	No	No	26	T3, T4	No	No
27	T8	No	No	27	T2, T2	No	No
28	T5, T7	No	No	28	T9	No	No
29	T3, T6, T8	No	No	29	T2, T2	No	No
30	T3	No	No	30	T1, T4	No	No
31	T3, T7	No	No	31	T1	No	No
32	T1	No	No	32	T5, T3	No	Yes
33	T6, T8, T9	No	No	33	T1, T2	No	No
34	T3	No	No	34	T2, T6	No	Yes
35	T4	No	No	35	T5	No	No
36	T3, T3, T3	No	No	36	T1, T4	No	No
37	T7	No	No	37	T2, T3	No	No
38	T2, T3	No	No	38	T4	No	No
39	T3	No	No	39	T1, T3	No	No
40	T5, T5	No	No	40	T3	No	No

postoperative analgesic rescue with analgesics. The primary objective of both rescues was to relieve the patient's pain.

In the present study, no puncturing-associated complications occurred in the 40 patients receiving ultrasound-guided TPVB, which may relate to the skillfulness of the operator and may also relate to the small number of cases. This requires verification by studies with larger sample sizes.

This study does have some limitations. Firstly, a large volume (40 ml) of ropivacaine was injected at a single site on the T4 level. Surgeons select the puncture site according to the location of the patient's tumor, several sites of the same patient can be punctured at the same time, and different body positions will affect the selection of the ultrasound-guided thoracic paravertebral puncture site. Improvements will be made in future studies to

FIGURE 2
Ultrasound-guided paravertebral puncturing.

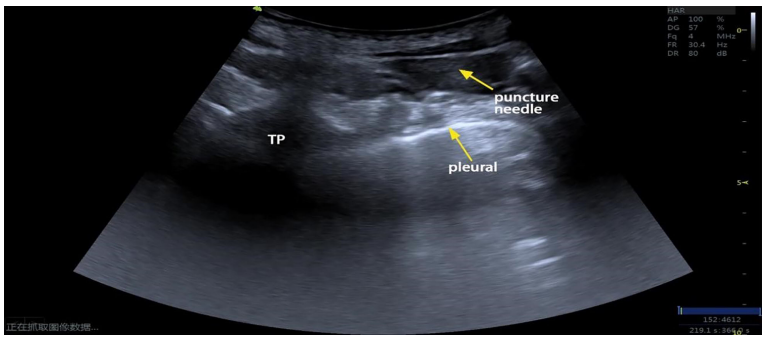

FIGURE 3
Echocardiography of ultrasound-guided TPVB (TP, transverse process).

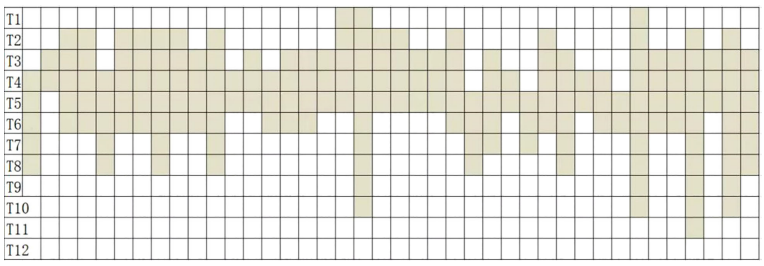

FIGURE 4
Skin hypoesthesia in 40 patients following ultrasound-guided TPVB.

adjust the puncture site for TPVB based on the surgical site and to observe the effect of the surgeon's puncture site and the puncture site for ultrasound-guided TPVB on the control of ablation-induced pain. Secondly, when lung ablation was in the vicinity of the diaphragm, the pain could not be completely controlled. This is because phrenic nerve block has a certain probability of diaphragm inhibition, and phrenic nerve inhibition will affect the patient's respiration to some extent. Thirdly, no sedatives were routinely administered in this study. In future studies, consideration will be given to how the use of sedatives can ensure that the patient can cooperate with the surgeon during the procedure.

5. Conclusion

Single ultrasound-guided TPVB with a large volume of anesthetic can provide effective analgesia for most MWAs of lung tumors, and patients can better cooperate with the surgeon to reduce injury from multiple lung punctures. Multicenter clinical studies with larger sample sizes are required in the future to validate the findings of the current study.

Data availability statement

The original contributions presented in the study are included in the article/Supplementary Material. Further inquiries can be directed to the corresponding author.

Ethics statement

The studies involving human participants were reviewed and approved by Ethics Committee of the Second Affiliated Hospital of Soochow University. The patients/participants provided their written informed consent to participate in this study. Written informed consent was obtained from the individual(s) for the publication of any potentially identifiable images or data included in this article.

Author contributions

YN and YLZ were responsible for collecting the data and writing the article. YZ was responsible for touching up the article. YT, JP, YMZ and ZZ contributed equally to the writing of the article. YJ was responsible for the overall analysis as well as for reviewing the article. All authors contributed to the article and approved the submitted version.

Conflict of interest

The authors declare that the research was conducted in the absence of any commercial or financial relationships that could be construed as a potential conflict of interest.

Publisher's note

References

1. Hartley-Blossom ZJ, Healey TT. Percutaneous thermal ablation for lung cancer: An update. *Surg Technol Int* (2019) 34:359–64.

2. Zhou X, Li H, Qiao Q, Pan H, Fang Y. Ct-guided percutaneous minimally invasive radiofrequency ablation for the relief of cancer related pain from metastatic non-small cell lung cancer patients: A retrospective study. *Ann Palliat Med* (2021) 10(2):1494–502. doi: 10.21037/apm-19-474

3. Lee VTY, Lin YH, Glenn D, Lodh S, Morris DL. Long term survival after multiple microwave ablations for colorectal cancer lung metastases: A case report. *Radiol Case Rep* (2022) 17(6):2038–42. doi: 10.1016/j.radcr.2022.03.059

4. Bonichon F, de Baere T, Berdelou A, Leboulleux S, Giraudet AL, Cuinet M, et al. Percutaneous thermal ablation of lung metastases from thyroid carcinomas. a retrospective multicenter study of 107 nodules. on behalf of the tuthyref network. *Endocrine* (2021) 72(3):798–808. doi: 10.1007/s12020-020-02580-2

5. Xue G, Li Z, Wang G, Wei Z, Ye X. Computed tomography–guided percutaneous microwave ablation for pulmonary multiple ground–glass opacities. *J Can Res Ther* (2021) 17 (3):811–3. doi: 10.4103/jcrt.jcrt_531_21

6. García FJS, Aragón EM, Alvarez SA, Caravajal JMG, Fayos JJ, Guerrero ME, et al. Ultrasound-guided thoracic paravertebral block for pulmonary radiofrequency ablation. *J Cardiothorac Vasc Anesth* (2022) 36(2):553–6. doi: 10.1053/j.jvca.2021.03.042

7. Vogl TJ, Nour-Eldin NA, Albrecht MH, Kaltenbach B, Hohenforst-Schmidt W, Lin H, et al. Thermal ablation of lung tumors: Focus on microwave ablation. *Rofo* (2017) 189(9):828–43. doi: 10.1055/s-0043-109010

8. Hara K, Sakura S, Nomura T. Use of ultrasound for thoracic paravertebral block. *Masui Japanese J Anesthesiology* (2007) 56(8):925–31.

9. Jo Y, Park S, Oh C, Pak Y, Jeong K, Yun S, et al. Regional analgesia techniques for video assisted thoracic procedure: A frequentist network meta-analysis. *Korean J Anesthesiol* (2021) 75(3):231–44. doi: 10.4097/kja.21330

10. Hou X, Zhuang X, Zhang H, Wang K, Zhang Y. Artificial pneumothorax: A safe and simple method to relieve pain during microwave ablation of subpleural lung malignancy. *Minim Invasive Ther Allied Technol* (2017) 26(4):220–6. doi: 10.1080/13645706.2017.1287089

11. Ruscio L, Planche O, Zetlaoui P, Benhamou D. Percutaneous radiofrequency ablation of pulmonary metastasis and thoracic paravertebral block under computed tomographic scan guidance: A case report. *A A Pract* (2018) 11(8):213–5. doi: 10.1213/xaa.0000000000000784

12. Chin KJ, Versyck B, Elsharkawy H, Rojas Gomez MF, Sala-Blanch X, Reina MA. Anatomical basis of fascial plane blocks. *Reg Anesth Pain Med* (2021) 46 (7):581–99. doi: 10.1136/rapm-2021-102506

13. Bolser DC, Hobbs SF, Chandler MJ, Ammons WS, Brennan TJ, Foreman RD. Convergence of phrenic and cardiopulmonary spinal afferent information on cervical and thoracic spinothalamic tract neurons in the monkey: Implications for referred pain from the diaphragm and heart. *J Neurophysiol* (1991) 65(5):1042–54.

14. Kashima M, Yamakado K, Takaki H, Kodama H, Yamada T, Uraki J, et al. Complications after 1000 lung radiofrequency ablation sessions in 420 patients: A single center's experiences. *AJR Am J Roentgenol* (2011) 197(4):W576–80. doi: 10.2214/ajr.11.6408

15. Hoffmann RT, Jakobs TF, Lubienski A, Schrader A, Trumm C, Reiser MF, et al. Percutaneous radiofrequency ablation of pulmonary tumors–is there a difference between treatment under general anaesthesia and under conscious sedation? *Eur J Radiol* (2006) 59(2):168–74. doi: 10.1016/j.ejrad.2006.04.010

frontiers | Frontiers in Oncology

TYPE Case Report
PUBLISHED 14 December 2022
DOI 10.3389/fonc.2022.1026087

OPEN ACCESS

EDITED BY
Yuliang Li,
The Second Hospital of Shandong University, China

REVIEWED BY
Phurich Janjindamai,
Prince of Songkla University, Thailand
Hitoshi Takeuchi,
Fukujuji Hospital, Japan

*CORRESPONDENCE
Xiao Han
hxzbb1983@163.com
Yingtao Meng
mengyt20210816@163.com

†These authors have contributed equally to this work

SPECIALTY SECTION
This article was submitted to Thoracic Oncology, a section of the journal Frontiers in Oncology

RECEIVED 23 August 2022
ACCEPTED 29 November 2022
PUBLISHED 14 December 2022

CITATION
Zhou S, Zhang J, Meng X, Meng Y and Han X (2022) Case Report: Bronchial artery embolization and chemoradiotherapy for central squamous cell lung carcinoma with rapid regression.
Front. Oncol. 12:1026087.
doi: 10.3389/fonc.2022.1026087

Case Report: Bronchial artery embolization and chemoradiotherapy for central squamous cell lung carcinoma with rapid regression

Siqi Zhou[1,2], Jianxin Zhang[2], Xue Meng[2], Yingtao Meng[2*†] and Xiao Han[2*†]

[1]Department of Oncology, Shandong First Medical University and Shandong Academy of Medical Sciences, Jinan, Shandong, China, [2]Department of Radiation Oncology, Shandong Cancer Hospital and Institute, Shandong First Medical University and Shandong Academy of Medical Sciences, Jinan, Shandong, China

Background: Interventional embolization is a common treatment for hemoptysis, one of the complications of lung cancer. However, there are no official guidelines for the use of this method in antitumor therapy.

Case Description: Herein, we describe a case of a patient who was pathologically diagnosed as central squamous cell lung cancer. The patient received chemotherapy, interventional embolization and radiotherapy successively. The tumor regressed rapidly within 48 hours of receipt of interventional embolization. Furthermore, the tumor decreased by more than 50% in size within 7 days during radiotherapy. Unfortunately, the patient has since developed lymph node metastases and remains under treatment.

Conclusions: Thus, finding the suitable blood vessel embolized may be a suitable option to reduce the local tumor load and can be considered as antitumor therapy in combination with other treatments. The patient's theoretical hypoxia state after interventional therapy still produced a good tumor regression after radiotherapy. However, so far, no related studies have reported the changes of tumor immune microenvironment in human body after intervention and radiotherapy.

KEYWORDS

lung cancer, hemoptysis, interventional embolization, combined treatment, case report

Abbreviations: BAE, Bronchial artery embolization; CT, Computed tomography; IMRT, Intensity-modulated radiation therapy; SCC, Squamous cell carcinoma; MDT, Multidisciplinary team; NSCLC, Non-small cell lung cancer; PVA, Poly vinyl alcohol.

Introduction

Interventional embolization is a minimally invasive treatment that aims at blocking blood flow by placing embolic materials to achieve the purpose of treatment. It is often used to treat patients with hemoptysis (1, 2) but is rarely used as an antitumor therapy. However, based on its mechanism of action, bronchial arterial embolization (BAE) as an auxiliary means of local antitumor therapy may be capable of providing a good response (3–8). Here, we report a case of tumor remission achieved through this intervention when used in combination with other treatments. Although it is not a conventional clinical treatment, considerable therapeutic effect was seen in this case. We present the following case in accordance with the CARE reporting checklist.

Case presentation

A 57-year-old Chinese man was admitted to the respiratory department at a regional hospital owing to hemoptysis and cough, no obvious cause was identified, and the patient denied having chest pain, fever, shiver, and other concomitant symptoms. The patient's social history was as follows: 60-pack years and 30 years of significant alcohol intake; however, he had been sober for 10 years. There was no other relevant medical history of note, and the patient revealed no genetic, congenital, or developmental abnormalities. Unfortunately, the family genetic history was not provided. The patient had not received any prior treatment for these symptoms. Physical examination revealed that the superficial lymph nodes of the whole body were not palpable or enlarged. The breathing sounds of both lungs were clear, and no coarse or fine crackles were heard. Computed tomography (CT) scan revealed an irregular large soft tissue mass in the right hilar region, invading the right main bronchus, narrowing, and truncating with atelectasis. The tumor diameter was 52.85 mm (mediastinal window images were uniformly used for measurement and comparison) with atelectasis (Figure 1A). Histological examination of a transbronchial specimen confirmed that the tumor was a squamous cell carcinoma (SCC). No lymph node metastases or distant organ metastases were identified. Based on the 8th Edition Lung Cancer Stage Classification, it was diagnosed as right central lung SCC with right upper lobe atelectasis (stage cT3N0M0, IIB) (9).

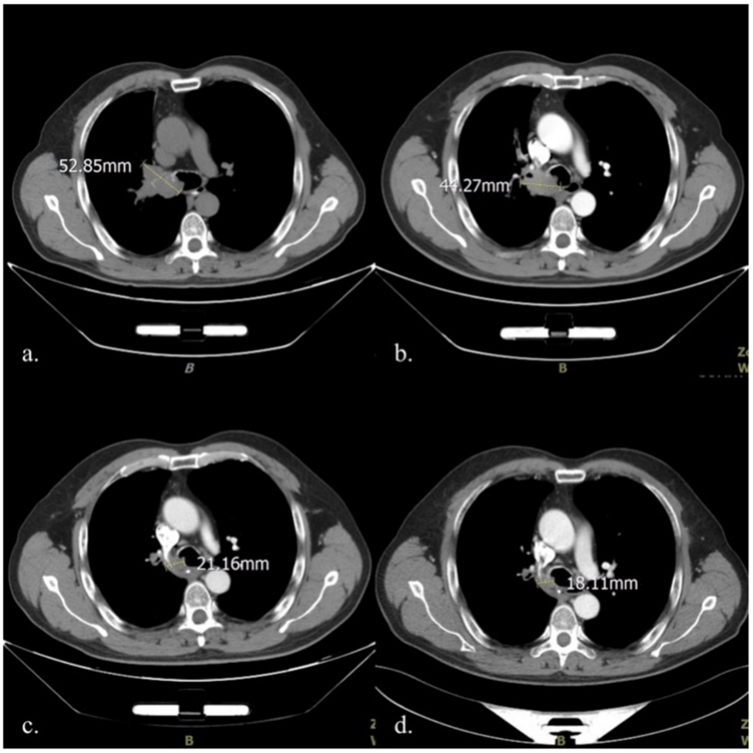

FIGURE 1
Comparison of mediastinal window CT images in four different periods: **(A)** Before treatment initiation (2020-10-12); **(B)**. After two cycles of chemotherapy (2020-11-25); **(C)** At the end of the 5th fractionation of radiotherapy (2020-12-9); **(D)** At the end of the 10th fractionation of radiotherapy (2020-12-16). CT, computed tomography.

As the tumor was close to the carina, a multidisciplinary team (MDT) consultation was undertaken; the team consisted of a medical oncologist, a thoracic surgeon, a radiologist, and a pathologist. As the MDT concluded that the risks associated with the surgical resection of the tumor were very high, it was not considered at the time. A treatment plan was developed for induction chemotherapy with sequential thoracic radiotherapy since the large diameter of the tumor and vascular invasion. Paclitaxel (albumin-bound) 400 mg D1 combined with carboplatin 500 mg D1 on a 21-day cycle was used for induction chemotherapy. The first treatment cycle began on October 16, 2020, and the two-cycle efficacy was evaluated as stable disease (Figure 1B).

At the end of the first round of chemotherapy, the patient again presented with cough with hemoptysis in the early morning of the 3rd day; the blood was dark red and of approximately 10-15 ml. Routine blood test revealed that the bleeding was not caused by thrombocytopenia, a common adverse reaction to chemotherapy. Bronchial artery embolization was performed twice during chemotherapy to address the symptoms. The first embolization was performed on October 19, 2020. The interventional doctor injected the contrast medium into the thickened artery— the trunk of the right middle and lower lobe bronchial artery; this helped to clearly stain the tumor, and the staining disappeared after poly vinyl alcohol (PVA) microspheres measuring 300–500 mm in diameter was injected into the arteries. However, the results were unsatisfactory, and the patient's hemoptysis did not reduce in intensity following the procedure. A second embolization was performed 6 weeks later (December 2, 2020). The PVA microspheres with a diameter of 100-300mm and two coils with diameter 2cm/crimp diameter 2cm (2-2) were injected into the right upper lobe bronchial artery; and four coils with diameter 2cm/crimp diameter 2cm (2-2) were injected into the right middle lobe bronchial artery. The patient's hemoptysis disappeared; no chemotherapeutic drugs were used in either procedure. The patient tolerated the intervention, and there were no adverse reactions, such as fever, headache, nausea, or vomiting. On the second day after embolization, intensity-modulated radiation therapy (IMRT) was initiated at a dose of 60 Gy for 30 fractions. On December 9, 2020, enhanced CT performed during radiotherapy to reposition the patient revealed that the tumor had significantly reduced in size to 21.16 mm (Figure 1C). On December 16, 2020, after the 10th radiotherapy fractionation, an enhanced CT scan revealed that the tumor had reduced to 18.11 mm in size. It remained this size for 4 months (Figure 1D). Unfortunately, the patient has since developed lymph node metastases (occurred 3 months after radiotherapy) and remains under treatment. The patient provided informed consent for publication of this case report.

Discussion

In this case, the SCC of the lung markedly reduced after interventional therapy. Albumin-bound paclitaxel-carboplatin combination is a standard chemotherapy regimen for SCC of the lung. The patient first received two cycles of this regimen as induction chemotherapy, with resultant stabilization of disease (10). The hemoptysis symptoms worsened during chemotherapy, indicating that the tumor was not satisfactorily controlled; two BAEs were therefore performed. Different blood vessels were used in both embolization processes. The first embolization was performed on the right lower lobe bronchial artery. Although the interventional doctor identified the responsible vessels on injection of contrast media before and after embolization, the hemoptysis was not completely relieved. Angiography of the tumor and its vasculature was repeated; it was noted that the tumor was located at the junction of the upper and middle lobes of the right lung (Figure 2). Therefore, the small right upper lobe bronchial artery was embolized the second time, and the embolization of the middle lobe bronchial artery was improved. On the second day after the surgery, the patient expectorated soft, grayish-red tissue (December 4, 2020). This was pathologically confirmed as SCC, and it was reported as being necrotic and friable. This suggests that the rapid reduction of the tumor likely occurred within 48 hours after the interventions discussed in this case study. Successive imaging during radiotherapy also confirmed this.

The maximum diameter of the tumor decreased by more than half (from 44.27 mm to 21.16 mm) on day 7 after therapeutic intervention following the administration of only 5 fractions of radiation (cumulative dose: 10 Gy), considerably less than the current, effective antitumor dose recommended (11). Therefore, we hypothesize that the short-term effect on the tumor is related to bronchial artery embolization. Vascular occlusions are caused by placing embolic material upstream of the target blood vessels to occlude it and prevent hemoptysis. In fact, interrupting the blood supply can block the supply of nutrients necessary for tumor growth and enable necrosis. However, it is difficult to block the blood supply entirely in the clinical setting. Thus, embolization is typically used as a treatment for hemoptysis, and it is rarely used in local antitumor therapy.

Tumors can develop new vascular branches when the primary blood supply is blocked. These new branches are often very small and difficult to observe with the current imaging techniques. Even if a blood vessel is identified, its small lumen diameter makes the surgical procedure challenging. In a study by Fujita et al. (7), bleeding did not stop immediately in 18% patients with hemoptysis who received BAE. This was due to the incomplete embolization of the contributory vessels. Some large tumors invade the mediastinum and the thoracic wall, precluding complete embolization of the contributory arteries (7).

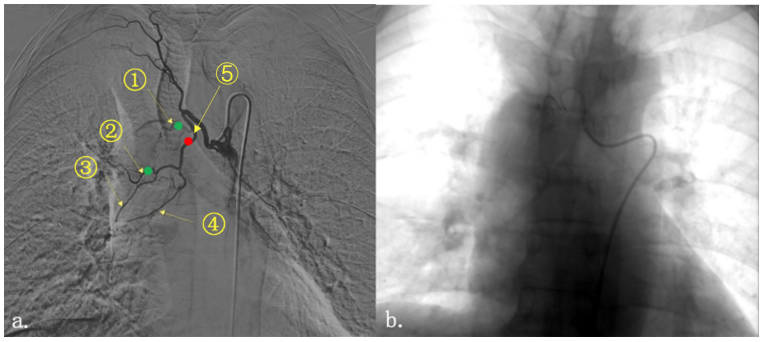

FIGURE 2
Imaging of tumor under contrast medium perfusion. Right bronchial artery angiography showed that the tumor at the right hilum was mainly supplied by two blood vessels **(A)**. They are (1) the right upper lobe bronchial artery; (2) the right middle lobe bronchial artery; (3) the right bronchial artery flowing through part of the middle lobe and lower lobe; (4) the right inferior lobe bronchial artery; and (5) the trunk of the right middle and lower lobe bronchial artery. The red dot represented the general location of the first embolization; and the green dot represented the location of the second one. **(B)** The bronchial artery was embolized by injection of microspheres and coils until the vascular enhancement image disappeared.

Furthermore, it is challenging to choose the appropriate embolus. Arteries are elastic, and if the embolization procedure is not secure, blood may flow through, resulting in embolization failure. Many types of embolic agents are clinically used, each with distinct properties. Because of its small diameter, ethiodized oil injection can cause complications, such as spinal cord injury and cerebral embolism. There is also the disadvantage of incomplete embolization. Gelatin sponge particles have good flexibility, excellent transport ability, and better fusion with the target vessels; thus, embolization is thorough. However, due to their biodegradability, blood flow is easily restored (12, 13), necessitating multiple interventional therapies to be performed (14, 15).

In China, some physicians perform palliative treatment through interventional therapy combined with chemoembolization by administering chemotherapeutic drugs directly into the tumor-feeding artery. This can significantly increase the local drug concentration in the tumor and reduce systemic adverse reactions (16). Zhao RF et al. (17) studied 50 patients with lung carcinoma who were administered chemotherapeutic drugs with Embosphere® Microspheres (Merit Medical, Utah, USA) into target vessels. The efficacy of the intervention was evaluated one month after the third treatment. An overall effective rate of 88% was observed—9 patients (18%) had complete responses, 35 (70%) had partial responses, and 6 (12%) had no change. A prospective study also achieved good responses. Liu S et al. (18) used CalliSpheres drug-eluting beads-bronchial artery chemoembolization embolization (DEB-BACE) to treat 21 refractory non-small cell lung cancer (NSCLC). After treatment the quality of life was significantly improved, and no serious adverse events such as spinal cord injury and cerebral embolism during the perioperative period. However, in the current case, the patient was significantly relieved only by simple embolization, which suggests that finding specific target vessels is of vital importance for killing tumors. Combined chemotherapy can achieve the effect of icing on the cake.

In addition, the patient received IMRT on day 2 following the intervention, and the tumor continued to regress during radiotherapy. After the 10th radiotherapy session, the maximum diameter of the tumor was 20 mm. Theoretically, tumor cell hypoxia is exacerbated by embolization, which could promote the development of dormant carcinoma stem cells, sustain their potential for proliferation and differentiation, and reduce tumor sensitivity to radiotherapy. Further research is required to explore the process of continuous tumor regression in patients undergoing radiotherapy and how embolization alters the tumor microenvironment (19).

Although BAE is not a routine treatment per the National Comprehensive Cancer Network Guidelines for non-small cell lung cancer, its anticancer effect could be underestimated. Local interventional embolization combined with systemic therapy could be an excellent strategy to control the overall tumor load. The selection of suitable blood vessels is imperative. The timing of embolization and the mode of combination of constituents are topics for further research.

Data availability statement

The original contributions presented in the study are included in the article/Supplementary Material. Further inquiries can be directed to the corresponding authors.

Ethics statement

The studies involving human participants were reviewed and approved by the Ethics Committee of Shandong Cancer

Hospital and Institute. The patient provided his written informed consent to participate in this study. Written informed consent was obtained from the individual(s) for the publication of any potentially identifiable images or data included in this article.

Author contributions

XH and YM contributed to conception and design of the report. SZ wrote the first draft of the manuscript. JZ, XM, XH and YM wrote sections of the manuscript. All authors contributed to the article and approved the submitted version.

Funding

This work was supported by the National Natural Science Foundation of China [grant numbers 82172720 and 81972864].

Acknowledgments

Thanks to Editage Inc. for English language editing.

Conflict of interest

The authors declare that the research was conducted in the absence of any commercial or financial relationships that could be construed as a potential conflict of interest.

The handling editor YL declared a shared parent affiliation with the authors JZ, XM, YM, XH at the time of review.

Publisher's note

Supplementary material

The Supplementary Material for this article can be found online at: https://www.frontiersin.org/articles/10.3389/fonc.2022.1026087/full#supplementary-material

References

1. Kalva SP. Bronchial artery embolization. *Tech Vasc Interv Radiol* (2009) 12:130–8. doi: 10.1053/j.tvir.2009.08.006

2. Chun JY, Morgan R, Belli AM. Radiological management of hemoptysis: a comprehensive review of diagnostic imaging and bronchial arterial embolization. *Cardiovasc Intervent Radiol* (2010) 33(2):240–50. doi: 10.1007/s00270-009-9788-z

3. Hayakawa K, Tanaka F, Torizuka T, Mitsumori M, Okuno Y, Matsui A, et al. Bronchial artery embolization for hemoptysis: immediate and long-term results. *Cardiovasc Intervent Radiol* (1992) 15(3):154–8; discussion 158. doi: 10.1007/BF02735578

4. Park HS, Kim YI, Kim HY, Zo JI, Lee JH, Lee JS. Bronchial artery and systemic artery embolization in the management of primary lung cancer patients with hemoptysis. *Cardiovasc Intervent Radiol* (2007) 30(4):638–43. doi: 10.1007/s00270-007-9034-5

5. Wang GR, Ensor JE, Gupta S, Hicks ME, Tam AL. Bronchial artery embolization for the management of hemoptysis in oncology patients: utility and prognostic factors. *J Vasc Interv Radiol* (2009) 20(6):722–9. doi: 10.1016/j.jvir.2009.02.016

6. Garcia-Olivé I, Sanz-Santos J, Centeno C, Andreo F, Muñoz-Ferrer A, Serra P, et al. Results of bronchial artery embolization for the treatment of hemoptysis caused by neoplasm. *J Vasc Interv Radiol* (2014) 25(2):221–8. doi: 10.1016/j.jvir.2013.09.017

7. Fujita T, Tanabe M, Moritani K, Matsunaga N, Matsumoto T. Immediate and late outcomes of bronchial and systemic artery embolization for palliative treatment of patients with nonsmallcell lung cancer having hemoptysis. *Am J Hosp Palliat Care* (2014) 31(6):602–7. doi: 10.1177/1049909113499442

8. Xie K, Wang YL, Chen L, Peng ZQ, Liu Q. Clinical comparative analysis of two embolization methods in interventional treatment of hemoptysis. *Lin Chuang Fang She Xue Za Zhi* (2018) 6:1034–9. doi: 10.13437/j.cnki.jcr.2018.06.039

9. Detterbeck FC, Boffa DJ, Kim AW, Tanoue LT. The eighth edition lung cancer stage classification. *Chest.* (2017) 151:193–203. doi: 10.1016/j.chest.2016.10.010

10. Aupérin A, Le Péchoux C, Pignon JP, Koning C, Jeremic B, Clamon G, et al. Concomitant radio-chemotherapy based on platin compounds in patients with locally advanced non-small cell lung cancer (NSCLC): A meta-analysis of individual data from 1764 patients. *Ann Oncol* (2006) 17(3):473–83. doi: 10.1093/annonc/mdj117

11. Bezjak A, Temin S, Franklin G, Giaccone G, Govindan R, Johnson ML, et al. Definitive and adjuvant radiotherapy in locally advanced non-small-cell lung cancer: American society of clinical oncology clinical practice guideline endorsement of the American society for radiation oncology evidence-based clinical practice guideline. *J Clin Oncol* (2015) 33(18):2100–5. doi: 10.1200/JCO.2014.59.2360

12. Seki A, Hori S, Sueyoshi S, Hori A, Kono M, Murata S, et al. Transcatheter arterial embolization with spherical embolic agent for pulmonary metastases from renal cell carcinoma. *Cardiovasc Intervent Radiol* (2013) 36(6):1527–35. doi: 10.1007/s00270-013-0576-4

13. White RIJr. Bronchial artery embolotherapy for control of acute hemoptysis: analysis of outcome. *Chest* (1999) 115(4):912–5. doi: 10.1378/chest.115.4.912

14. Han K, Yoon KW, Kim JH, Kim GM. Bronchial artery embolization for hemoptysis in primary lung cancer: A retrospective review of 84 patients. *J Vasc Interv Radiol* (2019) 30(3):428–34. doi: 10.1016/j.jvir.2018.08.022

15. Zhao GS, Liu Y, Zhang Q, Li C, Zhang YW, Ren ZZ, et al. Transarterial chemoembolization combined with huaier granule for the treatment of primary hepatic carcinoma: Safety and efficacy. *Med (Baltimore)* (2017) 96(29):e7589. doi: 10.1097/MD.0000000000007589

16. Seki A, Shimono C. Transarterial chemoembolization for management of hemoptysis: initial experience in advanced primary lung cancer patients. *Jpn J Radiol* (2017) 35(9):495–504. doi: 10.1007/s11604-017-0659-2

17. Zhao RF, Cheng LZ, Wang D, Zhao ZJ. Application value of embolization with embosphere microspheres in bronchogenic carcinoma. *Zhong Guo Yi Yao Ke Xue* (2021) 10:199–202. doi: 10.3969/j.issn.2095-0616.2021.10.051

18. Liu S, Wang QD, Li Q, Yu GJ, Xu HC. CalliSpheres drug-eluting beads trans-bronchial artery chemoembolization for 21 cases of refractory non-small cell lung cancer. *Zhong Guo Lin Chuang Yan Jiu* (2021) 01):56–60. doi: 10.13429/j.cnki.cjcr.2021.01.012

19. Jarosz-Biej M, Smolarczyk R, Cichoń T, Kułach N. Tumor microenvironment as a "game changer" in cancer radiotherapy. *Int J Mol Sci* (2019) 20(13):3212. doi: 10.3390/ijms20133212

Frontiers in Oncology

Advances knowledge of carcinogenesis and tumor progression for better treatment and management

The third most-cited oncology journal, which highlights research in carcinogenesis and tumor progression, bridging the gap between basic research and applications to imrpove diagnosis, therapeutics and management strategies.

Discover the latest Research Topics

See more →

Frontiers

Avenue du Tribunal-Fédéral 34
1005 Lausanne, Switzerland
frontiersin.org

Contact us

+41 (0)21 510 17 00
frontiersin.org/about/contact